# IDENTIFICATION OF MOLECULAR TARGETS IN THE PATHOGENESIS OF MULTIPLE MYELOMA

**IVYNA BONG PAU NI**

**FACULTY OF SCIENCE**
**UNIVERSITY OF MALAYA**
**KUALA LUMPUR**

**2017**

# IDENTIFICATION OF MOLECULAR TARGETS IN THE PATHOGENESIS OF MULTIPLE MYELOMA

**IVYNA BONG PAU NI**

**THESIS SUBMITTED IN FULFILMENT OF THE REQUIREMENTS FOR THE DEGREE OF DOCTOR OF PHILOSOPHY**

**FACULTY OF SCIENCE**
**UNIVERSITY OF MALAYA**
**KUALA LUMPUR**

**2017**

**UNIVERSITY OF MALAYA**
**ORIGINAL LITERARY WORK DECLARATION**

Name of Candidate: IVYNA BONG PAU NI

Matric No: SHC120087

Name of Degree: THE DEGREE OF DOCTOR OF PHILOSOPHY

Title of Project Paper/Research Report/Dissertation/Thesis ("this Work"):

IDENTIFICATION OF MOLECULAR TARGETS IN THE PATHOGENESIS OF MULTIPLE MYELOMA

Field of Study: GENETICS AND MOLECULAR BIOLOGY

I do solemnly and sincerely declare that:

(1) I am the sole author/writer of this Work;
(2) This Work is original;
(3) Any use of any work in which copyright exists was done by way of fair dealing and for permitted purposes and any excerpt or extract from, or reference to or reproduction of any copyright work has been disclosed expressly and sufficiently and the title of the Work and its authorship have been acknowledged in this Work;
(4) I do not have any actual knowledge nor do I ought reasonably to know that the making of this work constitutes an infringement of any copyright work;
(5) I hereby assign all and every rights in the copyright to this Work to the University of Malaya ("UM"), who henceforth shall be owner of the copyright in this Work and that any reproduction or use in any form or by any means whatsoever is prohibited without the written consent of UM having been first had and obtained;
(6) I am fully aware that if in the course of making this Work I have infringed any copyright whether intentionally or otherwise, I may be subject to legal action or any other action as may be determined by UM.

Candidate's Signature Date:

Subscribed and solemnly declared before,

Witness's Signature Date:

Name:

Designation:

## ABSTRACT

Multiple myeloma (MM) is a cancer of plasma cells. It is a highly heterogenous disease composed of numerous molecularly defined subtypes, each with varying clinicopathological features and disease outcomes. In the present study, we performed array comparative genomic hybridisation (aCGH) to identify common copy number variations (CNVs) in 63 MM patients. Our findings revealed CNVs in 100% of patients analysed. Common copy number gains were detected in 1q, 2q, 3p, 3q, 4q, 5q, 6q, 7q, 8q, 9q, 10q, 11q, 13q, 14q, 15q, 21q and Xq while common copy number loss in 14q. Gain of 7q22.3 was the most common CNV (92%) and *NAMPT* is localised in this region. The *CTSS*, *LYST*, *CLK1*, *ACSL1* and *NFκBIA* are genes localised within the CNVs and they represent novel information that have never been previously described in MM. Interestingly, *CTSS* is localised in 1q21.2, a frequently gain region which is associated with poor prognosis in MM. Two CNVs (1q42.3 and 7q22.3) were verified by qPCR. By using different cohort of samples, we performed global mRNA and miRNA expression profiling of 27 MM samples (19 clinical specimens and 8 myeloma cell lines) and 3 normal controls by microarray. Both the mRNA and miRNA expressional profiles in the normal and MM were compared to identify potential mRNAs and miRNAs involved in the pathogenesis of MM. The differential miRNA-target was also identified by databases prediction and inverse correlation analysis of the matched miRNA and mRNA expression profiles. A total of 348 differentially expressed mRNAs (≥2.0 fold change; $p<0.01$) and 1781 miRNAs (≥2.0 fold change; $p<0.05$) were identified. The reliability of the microarray data was verified for 4 mRNAs (*CCNA2*, *RAD54L*, *RASGRF2* and *HKDC1*) and 2 miRNAs (miR-150-5p and miR-4430). Majority of the differentially expressed genes are involved in cell cycle and cell cycle checkpoints, DNA repair, mitotic/ spindle checkpoints, cell proliferation, mismatch repair pathway and kinetochore and microtubule attachment. The *HIST2H3A*, *CYSLTR2*

and *AURKB* were 3 most significant differentially expressed genes, which are localised in the frequently altered chromosomal regions, namely 1q21, 13q14.2 and 17p13.1, respectively. Apart from that, the miR-150 and miR-125b were 2 differentially expressed miRNAs, which are closely related to B cell differentiation and therefore highlighted their critical roles in MM development. The miRNA-target integrative analysis revealed inverse correlation between 5 putative target genes and 15 miRNAs ($p<0.05$). Interestingly, all 5 target genes, namely *RAD54L*, *CCNA2*, *CYSLTR2*, *RASGRF2* and *HKDC1* play critical functions in oncogenesis. Apart from that, the biological function of *NAMPT* in RPMI-8226 myeloma cell line was determined by RNAi approach. The RNAi findings revealed that silencing of *NAMPT* significantly reduced the mRNA ($p<0.05$) and protein expression levels ($p<0.01$) in RPMI-8226 myeloma cells. These scenarios indicated that *NAMPT*-mediated gene silencing inhibited cell proliferation and induced apoptosis in RPMI-8226 ($p<0.05$). The present study has expanded our knowledge on the genomic and epigenetic mechanisms underlying the molecular pathogenesis of MM and also opens up clues and avenues for future investigation of myelomagenesis

## ABSTRAK

Multiple myeloma (MM) adalah kanser sel-sel plasma. Ia adalah penyakit yang sangat heterogen yang terdiri daripada pelbagai sub-jenis molekul yang ditakrifkan, masing-masing dengan pelbagai ciri klinikopatologi dan hasil penyakit. Dalam kajian ini, kami menjalankan penghibridan genomik perbandingan (aCGH) untuk mengenalpasti variasi bilangan salinan biasa (CNVs) dalam 63 pesakit MM. Penemuan kami menunjukkan CNVs dalam 100% pesakit yang dianalisis. Penambahan kromosom biasa dikesan di kawasan 1q, 2q, 3p, 3q, 4q, 5q, 6q, 7q, 8q, 9q, 10q, 11q, 13q, 14q, 15q, 21q and Xq manakala pengurangan kromosom biasa dikenalpasti di kawasan 14q. Penambahan 7q22.3 adalah CNV paling biasa (92%) dan *NAMPT* dikenalpasti di kawasan ini. *CTSS*, *LYST*, *CLK1*, *ACSL1* dan *NFκBIA* adalah gen-gen yang terletak dalam CNVs dan mereka mewakili maklumat baru yang tidak pernah ditemui dalam MM. Menariknya, *CTSS* terletak di 1q21, kawasan yang berkait-rapat dengan prognosis buruk di MM. Dua CNV telah disahkan oleh kuantitatif PCR (1q42.3 and 7q22.3). Dengan menggunakan kohort sampel yang berbeza, kami melakukan global mRNA dan miRNA profil ekspresi daripada 27 sampel MM (19 spesimen klinikal dan 8 titisan sel myeloma) dan 3 kawalan normal dengan menggunakan microatur. Kedua-dua profil ekspresi mRNA dan miRNA dalam kawalan normal dan MM telah dibandingkan untuk mengenalpasti mRNA dan miRNA berpotensi yang terlibat dalam patogenesis MM. Gen-gen sasaran bagi pengkamiran miRNA juga dikenalpasti dengan pangkalan data ramalan dan analisis korelasi songsang bagi profil ekspresi miRNA dan mRNA yang sepadan. Sebanyak 348 mRNAs pengkamiran (perubahan ekspresi ≥2.0 ganda; $p<0.01$) dan 1781 miRNAs prob pengkamiran (perubahan ekspresi ≥2.0 ganda; $p<0.05$) telah dikenalpasti dan kesahihan data microatur telah disahkan untuk 4 mRNAs (*CCNA2*, *RAD54L*, *RASGRF2* and *HKDC1*) dan 2 miRNAs (miR-150-5p and miR-4430). Majoriti pengkamiran gen terlibat dalam kitaran sel dan pusat pemeriksaan kitaran sel,

pembaikan DNA, pusat pemeriksaan mitosis/ spindle, percambahan sel , pembaikan tidak sepadan laluan dan kinetokor dan lampiran microtubule. *HIST2H3A*, *CYSLTR2* dan *AURKB* adalah 3 gen pengkamiran paling penting yang terletak di kawasan-kawasan kromosom kerap diubah, iaitu masing-masing di 1q21, 13q14.2 and 17p13.1. Selain itu, miR-150 and miR-125b adalah 2 miRNAs pengkamiran yang berkait rapat dengan pembezaan sel B dan oleh itu menekankan peranan kritikal mereka dalam perkembangan MM. Analisis miRNA-mRNA integratif mendedahkan hubungan songsang antara 5 gen sasaran dan 15 miRNAs ($p<0.05$). Menariknya, semua 5 gen sasaran, iaitu *RAD54L*, *CCNA2*, *CYSLTR2*, *RASGRF2* dan *HKDC1* memainkan fungsi penting dalam onkogenesis. Selain itu, fungsi biologi *NAMPT* dalam RPMI-8226 titisan sel myeloma juga dikaji dengan kaedah RNAi. Keputusan RNAi menunjukkan bahawa dengan menyenyapkan *NAMPT* boleh mengurangkan mRNA ($p<0.05$) dan tahap ekspresi protein ($p<0.01$) dalam RPMI-8226 sel myeloma. Penemuan ini menunjukkan bahawa dengan menyenyapkan *NAMPT* akan menghalang proliferasi sel dan merangsang kematian sel terprogram dalam RPMI-8226 ($p<0.05$). Kajian ini bukan sahaja mengembangkan pengetahuan terhadap acara-acara genomik dan epigenetik asas dalam patogenesis molekul MM tetapi juga membuka petunjuk dan jalan untuk siasatan myelomagenesis pada masa depan.

## ACKNOWLEDGEMENTS

First and foremost, I would like to express my deepest gratitude to my supervisor, Assoc. Prof. Dr Ng Ching Ching for giving me the opportunity to conduct this research. I am extremely thankful for her continuous expert, valuable guidance and encouragement extended to me.

I am highly indebted to Ministry of Health and Director of Institute for Medical Research for providing fund and all the necessary facilities to carry out this study. I am grateful to the Head of Cancer Research Centre, Dr Zubaidah Zakaria for her help and support in dealing with sampling, facilities and fund.

My sincere thanks to all the voluntary participants, clinicians and medical laboratory technologies in this project who have helped in successful procurement of the samples. I greatly appreciate Ms. Ten Sew Keoh and Dr Chin Yuet Ming for reviewing my manuscripts. Their comments and corrections have substantially improved my manuscripts.

Finally, a special gratitude goes to my beloved family and friends for their support and encouragement throughout the completion of this study. Thanks for their continuous love, support and understanding during the most difficult times in my study.

## TABLE OF CONTENTS

## LIST OF FIGURES

## LIST OF TABLES

## LIST OF SYMBOLS AND ABBREVIATIONS

| | | |
|---|---|---|
| > | : | More than |
| < | : | Less than |
| ≥ | : | More than and equal to |
| ≤ | : | Less than and equal to |
| % | : | Percentage |
| °C | : | Degree Celcius |
| κ | : | Kappa |
| λ | : | Lambda |
| Δ | : | Delta |
| ACGH | : | Array comparative genomic hybridization |
| ACSL1 | : | Acyl-CoA Synthetase Long-Chain Family Member 1 |
| ADM2 | : | Adaptive discontinuity meshing 2 |
| AF10 | : | Acute lymphoblastic leukaemia 1-fused 10 |
| AGO | : | Argonaut |
| AGO2 | : | Argonaute 2 |
| AGTPBP1 | : | ATP/GTP Binding Protein 1 |
| Akt | : | Protein kinase B |
| ALDH4A1 | : | Aldehyde dehydrogenase 4A1 |
| AML | : | Acute myeloid leukemia |
| ANLN | : | Anillin, actin binding protein |
| ANP32E | : | Acidic leucine-rich nuclear phosphoprotein 32 family member E |
| APITD1 | : | Apoptosis-inducing, TAF9-like domain 1 |
| APITD1 | : | Apoptosis-inducing, TAF9-like domain 1 |
| ARRDC3 | : | Arrestin Domain Containing 3 |
| ASF1B | : | Anti- silencing function 1B |

| | | |
|---|---|---|
| ASPM | : | Abnormal spindle protein homolog |
| ATCC | : | American Type Culture Collection |
| ATF1 | : | Activating transcription factor 1 |
| ATP | : | Adenosine triphosphate |
| ATP8B4 | : | ATPase, Class I, Type 8B, Member 4, |
| AUNIP | : | Aurora kinase A and ninein interacting protein |
| AURKB | : | Aurora kinase B |
| BCA | : | Bicinchoninic acid |
| Bcl-2 | : | B-cell CLL/ lymphoma 2, |
| Bcl-XL | : | B-cell lymphoma-extra large |
| bFGF | : | Basic fibroblast growth factor |
| BIK | : | BCL2-interacting killer |
| Bim | : | BCL2-like 11 |
| BIRC2 | : | Baculoviral IAP repeat containing 2 |
| BIRC3 | : | Baculoviral IAP repeat containing 3 |
| BIRC5 | : | Baculoviral IAP repeat containing 5 |
| Blimp1 | : | B-lymphocyte-induced maturation protein 1 |
| BMI-1 | : | B lymphoma Mo-MLV insertion region 1 homolog |
| BMSCs | : | Bone marrow stromal cells |
| BNIP2 | : | BCL2/adenovirus E1B 19 kd-interacting protein |
| BOK | : | Bcl-2 related ovarian killer |
| BRAF | : | v-raf murine sarcoma viral oncogene homolog B1 |
| BUB1 | : | BUB1 mitotic checkpoint serine/threonine kinase |
| BUB1B | : | BUB1 mitotic checkpoint serine/threonine kinase B |
| CA6 | : | Carbonic anhydrase VI |
| CCNA2 | : | Cyclin A2 |

| | | |
|---|---|---|
| CCNB1 | : | Cyclin B1 |
| CCNB2 | : | Cyclin B2 |
| CCND1 | : | Cyclin D1 |
| CCND2 | : | cyclin D2 |
| CCNL1 | : | Cyclin L1 |
| CD1C | : | CD1c molecule |
| CD40 | : | Cluster of differentiation |
| CD40L | : | CD40 ligand |
| CDC20 | : | Cell division cycle 20 |
| CDC25C | : | Cell division cycle 25C |
| CDCA8 | : | Cell division cycle associated 8 |
| CDK1 | : | Cyclin-dependent kinase 1 |
| CDK6 | : | Cyclin dependent kinase 6 |
| cDNA | : | Copy deoxyribonucleic acid |
| CENPA | : | Centromere protein A |
| CENPF | : | Centromere protein F |
| CGH | : | Comparative genomic hybridization |
| CHEK1 | : | Checkpoint kinase 1 |
| CKAP2L | : | cytoskeleton associated protein 2-like |
| CKS1B | : | Cyclin-dependent kinases regulatory subunit 1B |
| CLK1 | : | CDC-Like Kinase 1 |
| c-MET | : | Hepatocyte growth factor receptor |
| c-Myb | : | v-myb avian myelocytomatosis viral oncogene homolog |
| c-myc | : | v-myc avian myelocytomatosis viral oncogene homolog |
| COBRA-FISH | : | Combined binary ratio labelling-fluorescence in situ hybridization |

| | | |
|---|---|---|
| Cot1 | : | Cotyledon trichome 1 |
| CRAB | : | calcium, renal insufficiency, anaemia, or bone lesions |
| CREB1 | : | cAMP responsive element binding protein 1 |
| CT | : | Computed tomography |
| Ct | : | Cycle threshold |
| CTA | : | Cancer testis antigens |
| CTBS | : | Chitobiase, di-N-acetyl |
| CTNNAL1 | : | Catenin (cadherin-associated protein), alpha-like 1 |
| CTP | : | Cytidine triphosphate |
| CTSS | : | Cathepsin S |
| Cy | : | Cyanine |
| CyLD | : | Cylindromatosis |
| DEPDC1 | : | DEP domain containing 1 |
| DIAPH3 | : | Diaphanous-related formin 3 |
| DMTF1 | : | Cyclin D binding myb-like transcription factor 1 |
| DMXL2 | : | Dmx-Like 2 |
| DNA | : | Deoxyribonucleic acid |
| DNMT3A/3B | : | DNA methytransferase 3A/3B |
| dNTP | : | Deoxynucleoside triphosphate |
| DTL | : | Denticleless E3 ubiquitin protein ligase homolog |
| DTT | : | Dithiothreitol |
| dUTP | : | 2'-Deoxyuridine 5'-Triphosphate |
| E2F1 | : | E2F transcription factor 1 |
| E2F7 | : | E2F transcription factor 7 |
| E2F8 | : | E2F transcription factor 8 |
| EDTA | : | Ethylenediaminetetraacetic acid |

| | | |
|---|---|---|
| ELISA | : | Enzyme-linked immunosorbent assay |
| ERK | : | Extracellular signal-regulated kinases |
| ETV1 | : | ETS translocation variant 1 |
| EXO1 | : | Exonuclease 1 |
| EZH2 | : | Enhancer of zeste homolog 2 |
| FACS | : | Fluorescence-activated cell sorter |
| FAS | : | Fas cell surface death receptor |
| FCRL3 | : | Fc receptor-like 3 |
| FGFR3 | : | Fibroblast growth factor receptor 3 |
| FHL1 | : | Four and a half LIM domains 1 |
| FISH | : | Fluorescent in situ hybridization |
| FITC | : | Fluorescein isothiocyanate |
| FOXO | : | Forkhead box O1 |
| FZD5 | : | Frizzled class receptor 5 |
| GAPDH | : | Glyceraldehyde 3-phosphate dehydrogenase |
| GEO | : | Gene Expression Omnibus |
| GO | : | Gene Ontology |
| HDACs | : | Histone deacetylases |
| HIF-1a | : | Hypoxia-inducible factor 1-alpha |
| HIPK3 | : | Homeodomain interacting protein kinase 3 |
| HIST2H3A | : | Histone cluster 2, H3a |
| HKDC1 | : | Hexokinase domain containing 1 |
| HMGA2 | : | High mobility AT-hook 2 |
| H-MM | : | Hyperdiploid |
| HOXA9 | : | Homeobox A9 |
| HSP76 | : | Heat shock 70 kDa protein 6 |

| | | |
|---|---|---|
| HY | : | Hyperdiploid cluster |
| IFNG | : | Interferon gamma |
| Ig | : | Immunoglobulin |
| IgA | : | Immunoglobulin alpha |
| IgD | : | Immunoglobulin delta |
| IgE | : | Immunoglobulin epsilon |
| IGF-1 | : | Insulin-like growth factor 1 |
| IGF1R | : | Insulin-like growth factor 1 receptor |
| IgG | : | Immunoglobulin gamma |
| IgH | : | Immunoglobulin heavy chain |
| IgM | : | Immunoglobulin mu |
| IL1B | : | Interleukin 1B |
| IL1B | : | Interleukin 1B |
| IL-4 | : | Interleukin 4 |
| IL-6 | : | Interleukin 6 |
| IL-17 | : | Interleukin 17 |
| ING | : | Inhibitor of growth |
| IP6K2 | : | Inositol hexakisphosphate kinase 2 |
| IRF2 | : | Interferon regulatory factor 2 |
| IRF4 | : | Interferon regulatory factor 4 |
| ISS | : | International staging system |
| IκBKB | : | Inhibitor of kappa light polypeptide gene enhancer in B-cells, kinase beta |
| JAK | : | Janus kinase |
| JCRB | : | Japanese Collection of Research Bioresources |
| KCTD3 | : | Potassium channel tetramerization domain containing 3 |

| | | |
|---|---|---|
| KIF11 | : | Kinesin family member 11 |
| KIF14 | : | Kinesin family member 14 |
| KIF15 | : | Kinesin family member 15 |
| KIF20A | : | Kinesin family member 20A |
| KIF28 | : | Kinesin family member 28 |
| KIF2C | : | Kinesin family member 2C |
| KIF2C | : | Kinesin family member 2C |
| KRAS | : | Kirsten rat sarcoma viral oncogene homolog |
| LAMP2 | : | Lysosomal associated membrane protein-2 |
| LB | : | Low percentage of bone disease |
| LBR | : | Lamin B receptor |
| LYST | : | Lysosomal Trafficking Regulator |
| MAF | : | V-Maf Avian Musculoaponeurotic Fibrosarcoma Oncogene Homolog |
| MAPK | : | Mitogen-activated protein kinase |
| Mcl-1 | : | Induced myeloid leukemia cell differentiation protein |
| MCL-1 | : | Myeloid cell leukaemia 1 |
| MDM2 | : | Mouse Double Minute 2 Homolog |
| MEIS1 | : | Meis homeobox 1 |
| MEK | : | Mitogen-activated protein kinases |
| M-FISH | : | Multiplex-fluorescence in situ hybridization |
| MGUS | : | Monoclonal gammopathy of undetermined significance |
| miRISC | : | Micro ribonucleic acids-induced silencing complex |
| MIRNA | : | Micro ribonucleic acids |
| MLL | : | Mixed-Lineage Leukemia |
| MM | : | Multiple myeloma |

| | | |
|---|---|---|
| MM | : | Multiple myeloma |
| MMSET | : | Multiple myeloma SET domain |
| MnSOD | : | Manganese superoxide dismutase |
| M-protein | : | Monoclonal-protein |
| MREC | : | Medical Research & Ethics Committee |
| MRI | : | Magnetic resonance imaging |
| mRNA | : | Messenger ribonucleic acid |
| MTT | : | 3-(4,5-dimethyl-2-thiazolyl)-2,5-diphenyl-2h-tetrazolium |
| N4BP2L2 | : | NEDD4 Binding Protein 2-Like 2 |
| NAD | : | Nicotinamide adenine dinucleotide |
| NAM | : | Nicotinamide |
| NAMPT | : | Nicotinamide phosphoribosyl transferase |
| NBN | : | Nibrin |
| NEK2 | : | NIMA-related kinase 2 |
| NF-κB | : | Nuclear factor kappa-light-chain-enhancer of activated B cells |
| NFκBIA | : | Nuclear factor kappa B inhibitor A |
| NH-MM | : | Non-hyperdiploid |
| NMN | : | Nicotinamide mononucleotide |
| NMNAT | : | Nicotinamide-nucleotide adenylyltransferase |
| NOTCH1 | : | Notch homolog 1 |
| NRAS | : | Neuroblastoma RAS viral (v-ras) oncogene homolog |
| NUF2 | : | NDC80 kinetochore complex component |
| Oct-1 | : | Organic cation transporter 1 |
| OD | : | Optical density |
| OPG | : | Osteoprotegerin |
| OR4K1 | : | Olfactory receptor 4K1 |

| | | |
|---|---|---|
| OR4K2 | : | Olfactory receptor 4K2 |
| OR4K5 | : | Olfactory receptor 4K5 |
| OR4M1 | : | Olfactory receptor 4M1 |
| OR4N2 | : | Olfactory receptor 4N2 |
| ORC1 | : | Origin recognition complex, subunit 1 |
| OSCP1 | : | Organic solute carrier partner 1 |
| p27kip1 | : | P27 kip1 |
| p300 | : | E1A Binding Protein P300 |
| PARP1 | : | Poly-(ADP-ribose) polymerase 1 |
| PBEF | : | Pre-B cell colony-enhancing factor 1 |
| PCA | : | Principle component analysis |
| PCNA | : | Proliferating cell nuclear antigen |
| PCOLCE2 | : | procollagen C-endopeptidase enhancer 2 |
| PDCD4 | : | programmed cell death 4 |
| PET-CT | : | Positron emission tomography–computed tomography |
| PGC-1α | : | Peroxisome proliferator-activated receptor gamma coactivator 1-alpha |
| PI | : | Propidium iodide |
| PI3K | : | Phosphatidylinositol-3-Kinase |
| PICALM | : | Phosphatidylinositol Binding Clathrin Assembly |
| Pim-1 | : | Pim-1 Proto-Oncogene, Serine/Threonine Kinase |
| PKC | : | Protein kinase C |
| PLK1 | : | Polo-like kinase 1 |
| PMAIP1 | : | Phorbol-12-myristate-13-acetate-induced protein 1 |
| pmaxGFP | : | pmax green fluorescent protein |
| PP2A | : | Protein phosphatase 2A |

| | | |
|---|---|---|
| PPARγ | : | peroxisome proliferator-activated receptor gamma |
| PPP2R4 | : | Protein phosphatase 2A activator, regulatory subunit 4 |
| PR | : | Proliferation-associated genes |
| PR 53 | : | Protein phosphatase 2A regulatory subunit B |
| pre-miRNAs | : | Precursor micro ribonucleic acids |
| pri-miRNAs | : | Primary micro ribonucleic acids |
| PRL | : | Protein tyrosine phosphatases |
| PRL-3 | : | Protein tyrosine phosphatases 3 |
| PSCDBP | : | Assignment of the human B3-1 gene |
| PSMD10 | : | Proteasome (prosome, macropain) 26S subunit, non-ATPase 10 |
| PSMD4 | : | Proteasome (prosome, macropain) 26S subunit, non-ATPase 4 |
| PTEN | : | Phosphatase and tensin homolog |
| PTGS2 | : | Prostaglandin-endoperoxide synthase 2 |
| PTPRE | : | Protein tyrosine phosphatase epsilon |
| PTPRZ1 | : | Protein tyrosine phosphatase receptor-type Z polypeptide 1 |
| PUMA | : | p53 up-regulated modulator of apoptosis |
| qPCR | : | Quantitative polymerase chain reaction |
| RAB34 | : | RAB34, Member RAS Oncogene Family |
| RABGAP1L | : | RAB GTPase activating protein 1-like |
| RAD51AP1 | : | RAD51 associated protein 1 |
| RAD54L | : | RAD54-like (S. cerevisiae) |
| RALA | : | Ras-related protein Ral-A precursor |
| RANKL | : | Receptor activator of NF-κB ligand |
| Ras | : | Rat sarcoma |
| RASGRF2 | : | Ras protein-specific guanine nucleotide-releasing factor 2 |
| RB1 | : | Retinoblastoma 1 |

| | | |
|---|---|---|
| REL | : | REL proto-oncogene, NFκB subunit |
| RELA | : | V-rel avian reticuloendotheliosis viral oncogene homolog A |
| RHCE | : | CcEe antigens |
| RIN | : | Ribonucleic acid integrity number |
| RNA | : | Ribonucleic acid |
| RNAi | : | Ribonucleic acid interference |
| RNase | : | Ribonuclease |
| RNU6 | : | Ribonucleic acid U6 |
| ROCK1 | : | Rho-associated, coiled-coil containing protein kinase 1 |
| ROTI | : | No related organ or tissue impairment |
| RPS6KA5 | : | Ribosomal protein S6 kinase A5 |
| RT-PCR | : | Reverse transcriptase polymerase chain reaction |
| RT-qPCR | : | Real-time quantitative polymerase chain reaction |
| SAMSN1 | : | SAM Domain, SH3 Domain And Nuclear Localization Signals 1 |
| SD | : | Standard deviation |
| SHCBP1 | : | SH2-domain binding protein 1 |
| SHCBP1 | : | SHC SH2-domain binding protein 1 |
| siRNA | : | Small interfering RNA |
| SIRT1 | : | Sirtuin-1 |
| SKA1 | : | Spindle and kinetochore associated complex subunit 1 |
| SKA3 | : | Spindle and kinetochore associated complex subunit 3 |
| SKY | : | Spectral karyotyping |
| SLC6A9 | : | Solute carrier 6 (neurotransmitter transporter, glycine) 9 |
| Smad3 | : | Smad family member 3 |
| Smad4 | : | Smad family member 4 |
| SNALPs | : | Stable nucleic acid lipid particles |

| | | |
|---|---|---|
| SNORD75 | : | Small nucleolar RNA, C/D box 75 |
| SNP | : | Single nucleotide polymorphism array |
| SOCS1 | : | Suppressor of cytokine signaling 1 |
| SOCS3 | : | Suppressor of cytokine signaling 3 |
| SOD2 | : | Superoxide Dismutase 2 |
| SOX9 | : | Sex-Determining Region Y- box 9 |
| SP1 | : | Specificity protein 1 |
| STAT1 | : | Signal transducer and activator of transcription 1 |
| STAT3 | : | Signal transducer and activator of transcription 3 |
| STAT6 | : | Signal transducer and activator of transcription 6 |
| STIM1 | : | Stromal interaction molecule 1 |
| STK17B | : | Serine/Threonine Kinase 17b |
| TACC3 | : | Transforming, acidic coiled-coil containing protein 3 |
| TAMs | : | Tumour associated macrophages |
| TERT | : | Telomerase reverse transcriptase |
| TGF-β | : | Transforming growth factor beta |
| TK1 | : | Thymidine kinase 1 |
| TMEM56 | : | Transmembrane protein 56 |
| TNF | : | Tumour necrosis factor |
| TNF | : | Tumour necrosis factor |
| TNFAIP3 | : | Tumour necrosis factor alpha-induced protein 3 |
| TNFRSF10D | : | Tumour necrosis factor receptor superfamily member 10d |
| TNFα | : | Tumour necrosis factor alpha |
| TOP2A | : | Topoisomerase (DNA) II alpha |
| TOP2B | : | Topoisomerase (DNA) II Beta |
| TP53/ P53 | : | Tumour protein p53 |

| | | |
|---|---|---|
| TPX2 | : | TPX2, microtubule-associated |
| TRAF3 | : | TNF Receptor-Associated Factor 3 |
| TRAIL | : | TNF-related apoptosis-inducing ligand |
| TTK | : | TTK protein kinase |
| TWIST | : | Twist family bHLH transcription factor |
| UBE2S | : | Ubiquitin-conjugating enzyme E2S |
| UBE2T | : | Ubiquitin-conjugating enzyme E2T |
| ULS | : | Universal licensing system |
| UPD | : | Uniparental disomy |
| VEGF | : | Vascular endothelial growth factor |
| WHSC1 | : | Wolf-Hirschhorn Syndrome Candidate 1 |
| WWOX | : | WW domain-containing oxidoreductase |
| ZEB2 | : | Zinc Finger E-Box Binding Homeobox 2 |
| ZWINT | : | ZW10 interacting kinetochore protein |

## LIST OF APPENDICES

# CHAPTER 1: INTRODUCTION

Multiple myeloma (MM) is a cancer of plasma cells. It is the second most common haematological malignancies in the world (de Mel *et al*., 2014). MM is unevenly distributed in different geographic origins in the world, with the highest incidence rate in blacks compared to whites (Waxman *et al*., 2010). The incidence rates increase with age and it is higher in males than females (Renshaw *et al*., 2010; Tuchman *et al*., 2014). In Malaysia, more than 50% of myeloma patients are diagnosed at the late stage of the disease and it is likely to be equally distributed across Malays, Chinese and Indians (Omar and Ibrahim Tamin *et al*., 2011). The etiology of MM are not well established, several risk factors such as age, gender, family history, chromosomal, genetic and epigenetic abnormalities are believed to be contributed in the oncogenesis of MM (Koura and Langston, 2013).

Although numerous chromosomal copy number changes, genetic and epigenetic abnormalities have been reported, the actual molecular mechanism involved in the pathogenesis of MM is not fully understood. Identification of molecular targets of MM is crucial for improving our understanding of biology and molecular events involved in the pathogenesis of MM.

Genome wide screening of chromosomal copy number change, gene and miRNA expression of MM in Malaysian is still lacking and only one association study had been published so far (Yusnita *et al*., 2012). In the present study, microarray was performed to identify potential molecular targets underlying the pathogenesis of MM. Chromosomal copy number variations (CNVs) was evaluated in 63 MM patients using aCGH. By using different sample sets, differentially expressed genes and miRNAs of 27 MM samples (19 clinical specimens and 8 cell lines) were evaluated using

microarray. Apart from that, miRNA-target was identified by databases prediction and inverse correlation analysis of matched miRNA and mRNA expression profiles.

Besides that, the biological function of nicotinamide phosphoribosyltransferase (*NAMPT*) on growth and survival of RPMI-8226 myeloma cells was evaluated by using RNA interference (RNAi) approach. We performed functional study of *NAMPT* because the chromosomal region 7q22.3 where *NAMPT* gene (7q22.3) is localised was amplified in 92% of MM patients in aCGH study.

Overall, this study describes information on the CNVs, differentially expressed genes/ miRNAs, and miRNA-targets, which are potentially involved in the molecular pathogenesis of MM. Some of these CNVs, genes and miRNAs represent new information that has never been reported in association with MM oncogenesis.

This project was aimed to identify potential molecular targets in the pathogenesis of MM.

The specific objectives of this study are listed below:

- To identify copy number variations in MM patients by genome-wide aCGH approach.
- To identify potential mRNAs and miRNAs involved in the pathogenesis of MM by microarrays.
- To predict miRNA-target interaction based on the integrated analysis of matched miRNA and mRNA expression profiles.
- To investigate the function of *NAMPT*-mediated gene silencing in human RPMI-8226 myeloma cells by RNAi approach.

# CHAPTER 2: LITERATURE REVIEW

## 2.1 MULTIPLE MYELOMA (MM)

Under normal condition, B cells defend the body against infection by the viruses and microbial toxins. When B cells respond to an infection, they differentiate into plasma cells and produce antibodies/ immunoglobulins (Igs) specific to the foreign substance to fight the disease and infection (Nutt *et al*., 2015). Types of Igs produce by plasma cells are gamma (IgG), alpha (IgA), mu (IgM), delta (IgD) or epsilon (IgE) or Bence-jones protein (free monoclonal κ and λ light chains) (Gertz and Greipp, 2003).

Multiple myeloma (MM) is the malignancy of terminally differentiated B lymphocytes characterised by clonal expansion of plasma cells in the bone marrow (Johnson *et al*., 2016). These malignant cells do not function properly and their increased in numbers produce excess Igs of a single type (M-protein) but reduce in the amounts of normal Igs (Figure 2.1). In MM, IgG is the most commonly produced Ig, followed in frequency by IgA, IgD and extremely rarely IgE (Attaelmannan and Levinson, 2000; Raeve and Vanderkerken, 2005).

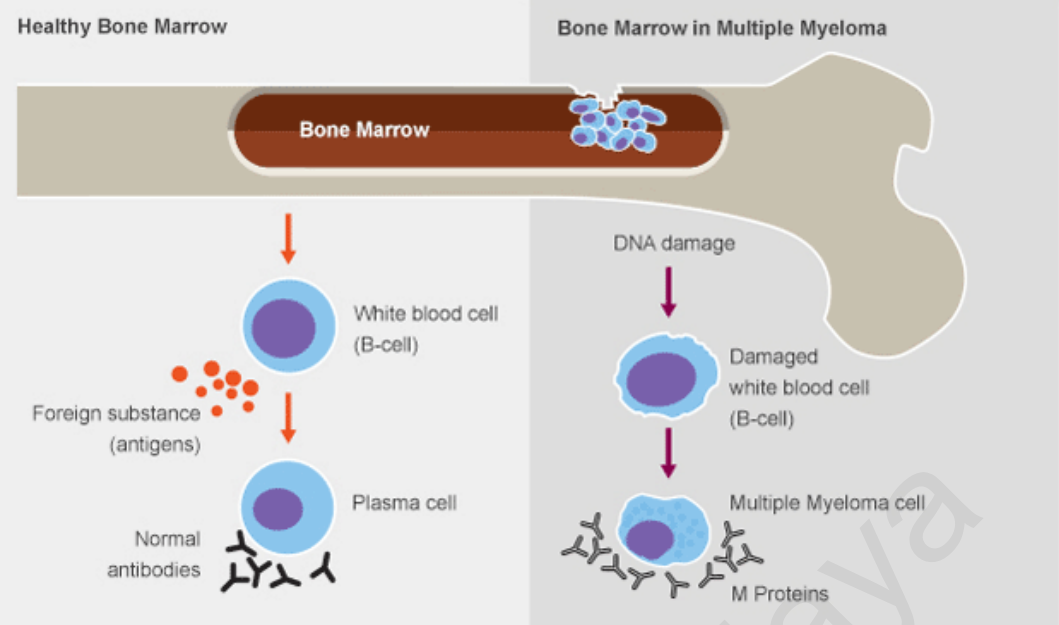


**Figure 2.1:** Healthy bone marrow vs bone marrow in multiple myeloma (Adapted from Devita *et al*., 1997).

### 2.1.1 Classification of MM

Classification of MM is important in clinical basis to find out how much the cancer has advanced. It is useful in determining prognosis and treatment options for the patients with MM. Current staging system and diagnostic criteria for MM are described below.

#### 2.1.1.1 International staging system (ISS)

The international staging system (ISS) is the current standard used internationally in the classification and stratification of MM. The ISS provides useful prognostic groupings in a variety of situations. It classified MM correctly regardless of patient's age, geographic origin and treatment (Greipp *et al*., 2005). According to ISS, MM is classified into 3 stages as shown in Table 2.1.

Recently, the revised ISS has been proposed in which the ISS is combined with chromosomal abnormalities (translocation t(4;14)(p16;q32) and deletion of chromosome 17p) and serum lactate dehydrogenase to facilitate diagnosis, prognostic and risk stratification of myeloma patients (Palumbo *et al*., 2015). However, the revised ISS has yet to be used in routine clinical practice in most of the laboratories.

**Table 2.1:** International staging system (ISS) for multiple myeloma (Greipp *et al*., 2005)

| Stage | Criteria | Median survival (months) |
|---|---|---|
| Stage I | Serum β-2 microglobulin < 3.5 mg/ L and serum albumin ≥ 3.5 g/ dL | 62 |
| Stage II | Neither stage I nor stage III | 44 |
| Stage III | Serum β-2 microglobulin ≥ 5.5 mg/L | 29 |

(Greipp *et al*., 2005)

#### 2.1.1.2 International Myeloma Working Group diagnostic criteria

The ISS is combined with International Myeloma Working Group diagnostic criteria to facilitate the clinical diagnostic and prognostic prediction of MM. The diagnostic criteria of MM are shown in Table 2.2.

**Table 2.2:** International Myeloma Working Group diagnostic criteria

| Disease | Criteria |
|---|---|
| Monoclonal gammopathy of undetermined significance (MGUS) | • monoclonal protein (M-protein) is <30 g/ l<br>• bone marrow clonal cells <10% with no evidence of MM, other B-cell proliferative disorders or amyloidosis |
| Asymptomatic (smouldering) myeloma | • M-protein is ≥30 g/ l or urinary monoclonal protein ≥500mg per 24 h and/or bone marrow clonal plasma cells 10-60%<br>• no related organ or tissue impairment (ROTI) (end-organ damage), which is typically manifested by increased calcium, renal insufficiency, anaemia, or bone lesions (CRAB) |
| Symptomatic myeloma | • Similar with asymptomatic myeloma but with evidence of ROTI<br>• Any one or more of the following biomarkers of malignancy: (i) bone marrow clonal plasma cells ≥60% (ii) involved:uninvolved serum free light chain ratios ≥100 (iii) >1 focal lesions on MRI analysis |
| Non-secretory myeloma | • Absence of M-protein in the serum and urine, bone marrow plasmacytosis and ROTI. |

(International Myeloma Working Group, 2003; Rajkumar *et al*., 2014)

### 2.1.2 Incidence of MM

Multiple myeloma is the second most common haematologic cancer, representing 1% of all cancer diagnoses and 2% of all cancer deaths (Zweegman *et al*., 2014). This disease is unevenly distributed in different geographic origins in the world. The highest incidence of MM is found in the industrialised regions of Australia or New Zealand, Europe and North America. In Asian countries, the incidence and mortality is stable over the decades (Becker, 2011). GLOBOCAN2012 estimated a total of 114251 MM cases and 80019 deaths in 2012 (Ferlay *et al*., 2013). It is more prevalence in males (62469 cases) than in females (51782 cases) and the incidence rate increases with age in both genders (Ferlay *et al*., 2013). The MM is considered rare in most of the countries, the age-standardised rates (ASR) for MM incidence and mortality are 1.5 and 1.0 per 100,000 population, respectively (Ferlay *et al*., 2013). Although MM occurs twice as frequently in the blacks compared to the whites, the incidence is slowly increasing among whites in the western countries over the past few years (Waxman *et al*., 2010; Becker, 2011). In Malaysia, approximately 50% of MM patients are diagnosed at the advanced stages of the disease and it occurred more commonly in men compared to women (Omar and Ibrahim Tamin *et al*., 2011). MM is likely to be distributed equally among different ethnicities in Malaysia (Malays, Chinese and Indians) (Omar and Ibrahim Tamin *et al*., 2011).

### 2.1.3 Etiology of MM

The etiology of MM remains obscure. Various risk factors have been implicated as potential etiologic of MM but most of them are not established risk factors. Previous studies showed that genetic and environmental risk factors are important in the development of MM and its precursor state such as MGUS (Kristinsson *et al*., 2009). Several important risk factors for MM development are discussed below.

#### a. Age and gender

Multiple myeloma is a disease of the elderly reflected by a median age at diagnosis of approximately 70 years, with 35–40% of the patients being older than 75 years (Palombo *et al*., 2011). It is rarely diagnosed in people younger than 40 years (Palombo *et al*., 2011). With the ageing of the population, the number of elderly adult diagnosed with MM would be increased by approximately 80% in the next two decades (Wildes *et al*., 2014). Besides age factor, MM is more commonly occurred in men than in women (Renshaw *et al*., 2010; Tuchman *et al*., 2014).

#### b. Race

Myeloma is about twice as common in African-Caribbean people than in white people (Landgren *et al*., 2006). According to the latest statistics, age-standardised incidence rate (per 100 000) is higher in the black ethnic category at 15.0 compared to the South Asians (5.45) or the White group (6.11) (Samy *et al*., 2015).

### c. Dietary and nutrition factors

High consumption of fruits and vegetables, which are rich in Vitamin C is shown to decrease the risk of MM. This is proven in a population based control study by Brown *et al*. (2001). Brown *et al*. (2001) reported that frequent intake of vitamin C is associated with a protective effect in whites. Another studied postulated that diet high in fish may reduce the risk of MM development (Fritschi *et al*., 2004).

### d. Family history

Potential family predisposition to MM was reported for the first time in 1925 (Meyerding, 1925). More cases of MM with family history were reported after that (Geschickter and Copeland, 1928; Alexander and Benninghoff, 1965; Mandema and Wildervanck, 1954). The latest findings showed that the occurrence of this disease has moved towards at an earlier age in later generation (Lynch *et al*., 2005; Jain *et al*., 2009). Studies have shown that first degree relatives of people with MM had a higher risk of developing MM (Kristinsson *et al*., 2009). To date, over 100 families with multiple affected members with myeloma or other plasma cell dyscrasias have been described and these provide strong evidence for the existence of inherited risk factor for MM (Koura and Langston, 2013).

### e. Prevalence of monoclonal gammopathy of undetermined significance (MGUS)

There are two types of MGUS phenotypes. First type is referring to the MGUS that secretes IgM or also known as lymphoid MGUS has higher risk to progress into Waldenstrom macroglobulinemia, lymphoma or other lymphoidproliferative disorder. Second type of MGUS is non-IgM (IgG, IgA, IgD, IgE and Ig light chain only) has a plasma cell phenotype and it has higher risk of progresssion into MM or other plasma cell disorders (Landgren, 2013). The overall risk of progression from MGUS to a malignant condition is 10% per year for the first 5 years, approximately 3% per year for the next 5 years, and 1-2% per year for the following 10 years (Kyle *et al*., 2011). The risk level of malignant progression is depends on numerous factors such as the type of M protein, the size of M protein and the percentage of abnormal plasma cells in the bone marrow (Kyle *et al*., 2011). Landgren *et al*. (2009) reported that virtually all 71 healthy individuals who had diagnosed with MGUS developed MM during a 10-year follow-up study. Another study performed by Weiss *et al*. (2009) showed similar findings in which 27 out of 30 MM patients arose from MGUS.

### f. Genetic factors

High prevalence of MM in blacks compared to whites suggests that genetic factors play a pivotal role in the development of MM. Genomic aberrations in MM including hyperdiploidy, chromosomal translocations, loss of chromosome 13, amplification of chromosome 1q and deletion of chromosome 17p (Segges and Braggio, 2011). Apart from that, identification of 70 gene signatures for the prediction of disease progression and prognostic significance in MM suggest the involvement of gene expression changes in the transition of normal plasma cells to malignant cells (Shaughnessy *et al*., 2007). Besides abnormalities involving chromosomal amplification/ deletions, translocations

and changes in gene expression, epigenetic abnormalities such as DNA methylation, histone modifications and non-coding RNAs also contribute to the pathogenesis of MM (Dimopoulos *et al*., 2014).

### 2.1.4 Symptoms, diagnostic and treatment of MM

MM may not cause any signs or symptoms at the very early stage of the disease. The symptoms often develop slowly over time and usually appear when the disease reaches an advanced stage. The most common symptom of MM is bone disease such as bone pain and osteolytic bone lesions (Ise and Takagi, 2007). Bone disease is observed in almost 80% of newly diagnosed MM patients (Tosi, 2013). Other symptoms include fatigue due to low red blood cells, frequent urination, constipation, high blood calcium levels or hypercalcemia (Firkin, 2009). Fever and repeated infection are also common in the patients when the disease affects the immune system in the body (Hussein, 2007). Some patients may experience weight loss, shortness of breath, tiredness and swollen ankles, feet and hands due to impair kidney function (Hussein, 2007). Unusual bleeding of the nose and gums and heavy period can be signs of MM when abnormal platelets counts are persist in the patient (Eby, 2007). Neurological symptoms such as numbness or tingling sensation, pain or muscle weakness may occur when the plasma cells grow out of control and increase pressure on the nerve roots and spinal cord (Velasco and Bruna, 2012).

The MM is diagnosed based on signs and symptoms, medical history, physical examination, laboratory and imaging tests. Individual with abnormal red and white cell count, high calcium level and abnormal total protein in the blood test will be subjected for further testing. Patients will be tested for the presence of M proteins using a combination of tests that include serum protein electrophoresis, serum immunofixation

and serum-free light chain assay (Katzmann *et al*., 2006; Jenner, 2014). When MM is suspected, bone marrow aspiration and biopsy examination is needed to confirm there is >10% of clonal plasma cells in the bone marrow and to what extend the abnormal plasma cells have affected the production of normal white blood cells, red blood cells, and platelets (Kumar *et al*., 2009). Other bone marrow examination tests include conventional karyotyping or fluorescent in situ hybridisation (FISH) to evaluate the chromosomal abnormalities in the patients (Zhou *et al*., 2009; Rajan & Rajkumar, 2015). Other non-laboratory tests such as plain radiograph of the skeleton, computed tomography (CT), positron emission tomography–computed tomography (PET-CT) and magnetic resonance imaging (MRI) are required to diagnose, stage, and evaluate the extent of bone damage, and the number and size of tumours in the bones (O'Sullivan *et al*., 2015). Evidence of amount of plasma cells in the bone marrow, end-organ damage, levels of β-2 microglobulin, albumin, creatinine and calcium are important in myeloma staging (Kyle and Rajkumar, 2009). Gene expression profiling is not a routine diagnostic test for MM but it is useful for prognostic measurement and risk stratification of the patients (Zhou *et al*., 2009; Kuiper *et al*., 2015; Hermansen *et al*., 2016).

At this time, MM is still incurable. Treatment is given to the patients to improve their overall survival, slow down the disease progression, and eliminate symptoms and complications. Chemotherapy, immunomodulating agents, proteasome inhibitor and stem cell transplantation are available treatment options. They are given to MM patients, either single or in combination, depending on the stage and aggressiveness of the disease. Currently, thalidomide, lenalidomide and pomalidomide are 3 immmunomodulating agents, which are widely used in the treatment of MM (Chang *et al*., 2014). Bortezomib is the proteasome inhibitor used in stopping enzyme complexes (proteasomes) in cells from breaking down proteins, which are important in controlling cell division (Rajkumar *et al*., 2004; Kumar *et al*., 2008). Another treatment option is

stem cell transplantation, it can be given either at the time of initial diagnosis or at relapse. Stem cell transplantation is usually given to patients younger than 70 years old. Autologous stem cell transplantation is thought to improve the median overall survival by approximately 12 months (Child *et al*., 2003; Rajkumar, 2012).

## 2.2 MOLECULAR BIOLOGY IN THE DEVELOPMENT AND PROGRESSION OF MM

The transformation and progression of normal plasma cells into the benign plasma cell neoplasm MGUS, smouldering MM, intramedullary and extramedullary MM are consist of multistep initiating and secondary oncogenic events. Primary oncogenic events such as translocation resulted from abnormal B cell differentiation and hyperdiploidy usually initiate the development of MM. Secondary translocations, over-expression Kirsten rat sarcoma viral oncogene homolog (*KRAS*) and neuroblastoma RAS viral (v-ras) oncogene homolog (*NRAS*) mutations and deletion of *p53* gene are usually occur at later stage of disease onset and may be associated with disease progression in MM (Bergsagel *et al*., 2005). The important molecular biology contributing to the development and progression of MM are discussed below.

### 2.2.1 Abnormal B cell differentiation

The differentiation of pro-B cells into pre-B cells and then immature B cells is an antigen independent processes and it occurs within the bone marrow (Shapiro-Shelef and Calame, 2005). The differentiation of pro-B cells into immature B cells involves the rearrangements of the immunoglobulin (Ig) gene (Corre *et al*., 2015). These immature B cells will then migrate from the bone marrow to the secondary lymphoid tissues to continue their maturation, and at this stage the maturation steps are dependent on

antigen pressure (Corre *et al*., 2015). Following stimulation of antigen, B cells differentiate into antibody secreting plasma cells. These plasma cells may enter a short-lived plasma cell population that reside primarily in the non-lymphoid area of the spleen or lymph nodes, or migrate to the bone marrow where the majority of them enter a long-lived population of plasma cells (Bortnick and Allman, 2013). Oncogenic transformation is thought to occur at the germinal centers of the secondary lymphoid tissues during B cells differentiation through molecular rearrangement processes known as somatic hypermutation and class switch recombination (Corre *et al*., 2015). The DNA damage can also occur at the very early stage of the B cell differentiation in the bone marrow during the immunoglobulin heavy chain (IgH) rearrangements (Walker *et al*., 2013).

### 2.2.2 Bone marrow microenvironment and cellular pathways in MM

Myeloma cell growth and survival is facilitated by the interaction between the malignant plasma cells and the bone marrow microenvironment. Bone marrow microenvironment is thought to play a pivotal role in differentiation, migration, proliferation, survival, and drug resistance of the malignant plasma cells (Ghobrial, 2012).

Malignant plasma cells adhere to bone marrow stromal cells (BMSCs) and extracellular matrix into the bone marrow. The interaction between BMSCs and myeloma cells activate nuclear factor kappa-light-chain-enhancer of activated B cells (NF-κB) signaling pathway and interleukin 6 (*IL-6*) secretions in BMSCs. Activation of NF-κB signaling pathway induces the production of *IL-6*, which support the growth and survival of myeloma cells. Besides NF-κB signaling pathway, *IL-6* also triggers mitogen-activated protein kinase (MEK/MAPK), Janus kinase/ signal transducer and

activator of transcription 3 (JAK/STAT3), and phosphatidylinositol-3-kinase/ protein kinase B (PI3K/Akt) signaling pathways (Hideshima *et al*., 2007; Wang *et al*., 2014). Myeloma cells continue to proliferate through the *IL-6* induces inhibition of cyclin dependent kinases inhibitors in PI3K/Akt signaling pathway and activation of MEK/MAPK signaling pathway (Hideshima *et al*., 2001; Wang *et al*., 2014). By activating JAK/STAT3 pathway, *IL-6* enhances myeloma cell survival through the activation of anti-apoptotic genes such as myeloid leukaemia cell differentiation protein (*Mcl-1*), B-cell lymphoma extra large (*Bcl-XL*) and *c-Myc* proto-oncogene (Manier *et al*., 2012).

Apart from *IL-6*, Insulin-like growth factor *1* (*IGF-1*) is secreted as a result of the interaction between BMSCs and myeloma cells. The *IGF-1* production promotes myeloma cell growth, survival and migration through activation of PI3K/Akt pathway. *IGF-1*-mediated activation of PI3K/Akt pathway suppresses the apoptotic effect of BCL2-like 11 (*Bim*) and induces anti-apoptotic genes *Bcl-XL* and B-cell CLL/lymphoma 2 (*Bcl-2*) (De Bruyne *et al*., 2010).

Vascular endothelial growth factor (*VEGF*) is a primary growth and survival factor for endothelial cells and it is essential for vascular development. It is secreted by BMSCs and MM upon stimulation of cytokines and growth factors such as *IL-6*, basic fibroblast growth factor (*bFGF*), transforming growth factor beta (*TGF-β*) or tumour necrosis factor alpha (*TNFα*). The expression of *VEGF* induces angiogenic activity of myeloma cells and activates several oncogenic signaling pathways, the Ras GTPase activating protein (RAS GAP), PI3-kinase/Akt, MEK and STAT, for instance (Podar and Anderson, 2005; Giuliani *et al*., 2011).

Osteoclasts and osteoblasts are two main cellular components in the bone marrow, which may contribute to the pathogenesis of MM. Increase osteoclastogenesis in MM activates receptor activator of NF-κB ligand (*RANKL*), which would inhibit the osteoclasts apoptosis and induce cell differentiation through NF-κB and JunN-terminal kinase pathways (Roodman, 2002). In contrast, osteoblasts are strongly reduced when MM cells adhere to the BMSCs. Reduction in osteoblasts levels decrease the amount of osteoprotegerin (*OPG*), a receptor for *RANKL*, which is secreted by osteoblasts (Pitari *et al*., 2015). This scenario would affect the balance between osteoclasts and osteoblasts (*RANKL*/*OPG* balance) in MM. As a result, bone resorption by osteoclasts is increased and exceeded bone reformation by osteoblasts (Pitari *et al*., 2015). The increase in bone resorption results in bone fractures, hypercalcemia and spinal cord compression in patients with MM.

Due to the importance of bone marrow microenvironment in the development and disease progression of MM, new therapeutic agents, which not only targeting the MM cell clones but also the bone marrow milieu, pro-angiogenic molecules and pathways involved are urgently needed to prevent the disease progression.

### 2.2.3 Chromosomal translocations in MM

Chromosomal translocations account for 40–50% of primary events in myeloma and strongly influence disease phenotype (Prideaux *et al*., 2014). Secondary translocations, not associated with aberrant somatic hypermutation and class switch recombination during B cell differentiation occur later in disease and are likely to represent progression events. In MM, translocations involving the IgH locus are present in about 60% of patients diagnosed with MM (Dib *et al*., 2008). Translocations of the IgH alleles at chromosome 14q32 with various partner chromosomes (4, 8, 11, 16) are the most

recurrent translocations in MM (Chng *et al*., 2005; Fonseca *et al*., 2003; Smadja *et al*., 2003; Prideaux et al., 2014). Recurrent primary translocations and secondary translocation are discussed below.

#### 2.2.3.1 t(4;14)(p16;q32) in MM

The t(4;14) is found in approximately 15% of primary MM (Mirabella *et al*., 2013). This translocation is cryptic because of the telomeric localisation of both chromosomal partner domains (Keat *et al*., 2003). Thus, it is undetectable by conventional cytogenetics. It can only be detected by FISH and reverse transcription polymerase chain reaction (RT-PCR). The t(4;14) affects the telomeric portion of chromosome 4p leading to the dysregulation of two proto-oncogenes, namely fibroblast growth factor receptor 3 (*FGFR3*) in derivate chromosome 14 (der14) and multiple myeloma SET domain (*MMSET*) in derivative chromosome 4 (der4) (Kalff and Spencer, 2012). The t(4;14) is associated with more aggressive MM and some findings have shown decrease of overall survival rate in the patients carrying t(4;14) (Sibley *et al*., 2002; Moreau *et al*., 2002). In addition, research findings also suggest a significant correlation between poor prognostic/ overall survival and t(4;14) independent of *FGFR3* over-expression (Keat *et al*., 2003; Xie and Chng, 2014).

#### 2.2.3.2 t(14;16)(q32;q23) and t(14;20)(q32;q11) in MM

Translocation t(14;16) is rare, it is found in 5–7% of all MM cases (Fonseca *et al*., 2003; Chng *et al*., 2007). It is characterised by up-regulation of V-Maf Avian Musculoaponeurotic Fibrosarcoma Oncogene Homolog (*MAF*), which plays a pivotal role in oncogenic transformation of MM (Avet-Loiseau *et al*., 2011). Translocations involving *MAF* in MM include the t(14;16) and t(14;20). Translocation t(14;16) is associated with up-regulation of *c-MAF* while t(14;20) with *MAF-B*. Both t(14;16) and t(14;20) are rare in myeloma and associated with poor prognosis (Fonseca *et al*., 2003; Attal *et al*., 2006;). Nevertheless, latest finding on t(14;16) postulated that it is not significantly correlated with the prognostic and overall survival in MM (Avet-Loiseau *et al*., 2011). The t(14;16) and t(14;20) are not the established prognostic markers in routine cytogenetic analysis due to the low prevalence of the translocations in MM.

#### 2.2.3.3 t(11;14)(q13;q32) in MM

Translocation t(11;14) is seen at the very early stages of MM (Fenton *et al*., 2004). The t(11;14)(q13;q32) resulted in the up-regulation of *CCND1* and is the most common translocation detected in MM (15-20%) (Chang *et al*., 2005; Fonseca *et al*., 2002). Patients harbour translocation t(11;14) are conferred to have a favourable prognosis. However, t(11;14) alone is not a sufficient marker to predict patient's survival, other genetic abnormalities should be taken into consideration (Chang *et al*., 2005). For instances, the presence of *K-RAS* mutations and other primary IgH translocations (Chng *et al*., 2008). Translocation t(11;14) is an indicator for poor prognostic for autologous stem cell transplantation in MM with extramedullary plasmacytoma (Shin *et al*., 2015).

#### 2.2.3.4 Secondary translocation in MM

Unlike translocations t(4;14), t(14;16), t(14;20) and t(11;14), which are considered as the most recurrent primary translocations in MM, the t(8;14)(q24;q32) is the most frequent secondary translocation in MM. The t(8;14) translocation is independent of somatic hypermutation and class switch recombination events (Prideaux *et al*., 2014). This translocation is usually observed at the advanced stages of the disease (Prideaux *et al*., 2014). It is occurs in approximately 15% of MM and 50% of advanced disease (Avet-Loiseau *et al*., 2001; Gabrea *et al*., 2008). It promotes myeloma cell proliferation by up-regulating *MYC* oncogene (Avet-Loiseau *et al*., 2001; Gabrea *et al*., 2008). Over-expression of *MYC* in MM is an indication of poor prognosis in the patients (Tomas *et al*., 2015).

### 2.2.4 Copy number variations (CNVs) in MM

Copy number variations (CNVs) resulted from gains or losses of DNA are common events in MM. The CNVs can involve the whole chromosome arm or just small region of the chromosome. Generally, losses of DNA region contribute to the malignancy through loss of tumour suppressor genes while gains are oncogenic through activation of proto-oncogenes. Frequent CNVs in MM are described below.

#### 2.2.4.1 Hyperdiploidy

In general, MM is divided into 2 genetic subtypes, namely the hyperdiploid and non-hyperdiploid subtypes. The hyperdiploid subtype can be defined by the gain of odd-numbered chromosomes 3, 5, 7, 9, 11, 15, 19, and 21 and a lower prevalence of primary translocations involving the IgH locus at 14q32 (Prideaux *et al*., 2014). Hyperdiploid accounts for approximately 50–60% of MM (Fonseca *et al*., 2003; Smadja *et al*., 2001; Prideaux *et al*., 2014). The overall survival is higher in patients with hyperdiploidy characteristic although a minority of them exhibits a more aggressive variant of the disease (Chng *et al*., 2006; Carrasco *et al*., 2006).

#### 2.2.4.2 Chromosome 1

Genomic aberration in chromosome 1 is a frequent event in MM. It accounts for nearly 50% of MM cases. The short arm of chromosome 1 commonly involved in deletions (1p) while the long arm in gains (1q) (Marzin *et al*., 2006). Band 1p21 is frequently deleted in MM suggested that 1p deletion could lead to hemizygosity of at least 1 tumour suppressor gene. In contrast, two regions of 1q show preferential gains, they are q12-q22 and q31-q42, with 1q21 being the most commonly gain region in chromosome 1. Gain of chromosome 1q21 is associated with poor prognosis and shorter survival in MM (Sonneveld, 2006; Bergsagel *et al*., 2013). Gain of 1q21 is observed in >40% of patients diagnosed with smouldering MM and MM while it is rarely seen in MGUS suggested that gain of 1q21 is associated with disease progression (Rajan and Rajkumar, 2015). Amplification at 1q21 induces the overexpression of 1 or more oncogenes (Marzin *et al*., 2006). Potential targets of gain in chromosome 1q21 include CDC28 protein kinase regulatory subunit 1B (*CKS1B*) and proteasome (prosome, macropain) 26S subunit, non-ATPase 4 (*PSMD4*) genes, which play a pivotal role in mediating cell

cycle progression and inducing drug resistance to bortezomib, respectively (An *et al*., 2014). Apart from that, study on chromosome 1q aberrations in MM revealed that majority of patients having relapsed and refractory of MM display whole arm 1q gain (Balćarková *et al*., 2009).

#### 2.2.4.3 Deletion of chromosome 13

Chromosome 13 deletions present in approximately 30–50% of total myeloma population (Barlogie *et al*., 1997; Avet-Loiseau *et al*., 1999; Zojer *et al*., 2000; Facon *et al*., 2001; Fonseca *et al*., 2002). Abnormalities in chromosome 13 frequently involve complete monosomy, which is associated with poor prognosis (Munshi and Avet-Loiseau, 2011). The minimal common deleted region of approximately 350 Kb has been identified in 13q14 [1.5 Mb telomerically to the retinoblastoma 1 (*RB1*) tumour suppressor gene] (Avet-Loiseau *et al*., 1999; Fonseca *et al*., 2001; Elnenaei *et al*., 2003; Munshi and Avet-Loiseau, 2011). Such losses suggested the possible inactivation of a putative tumour suppressor gene that is localisd in this region.

#### 2.2.4.4 Deletion of chromosome 17p

The deletion of chromosome 17p13 is an independent prognostic marker in MM. The deletion is generally monoallelic and involves inactivation of tumour protein p53 (TP53). The loss of TP53 protein, turning off the activity of TP53 networks and resulted in inactivation of various anti-proliferative and apoptotic genes in its downstream signaling (Drach *et al*., 1998; Chng *et al*., 2007; Lodé *et al*., 2010). The *TP53* gene is deleted in only 5-10% of newly diagnosed MM cases but 40% of advanced MM (Gozzetti *et al*., 2014). The incidence of deletion of 17p increases as the stage of disease advances suggesting its essential role in myeloma disease progression (Gozzetti *et al*.,

2014). Recent study showed that MM patients with deletion in chromosome 17p are normally resistant to standard therapy. In such patient, alternative therapies such as *p53* reactivating agents can be added in order to restore p53 tumour suppressive abilities (Teoh and Chng, 2014). This observation implied that deletion of chromosome 17p is not only used as prognostic marker but also important in therapeutic decision making in MM patients.

#### 2.2.4.5 Other chromosomal losses

Apart from frequently altered chromosomes described above, other chromosomal losses involving inactivation or losses of tumour suppressor genes also detected in MM. They are also known as "passenger lesions" because of their lower frequency in myelomagenesis. Deletion of 11q is occurs in approximately 7% of MM cases, and this region harbours two important tumour suppressor baculoviral IAP repeat-containing protein 2 (*BIRC2*) and baculoviral IAP repeat-containing protein 3 (*BIRC3*) genes (Walker *et al*., 2010). Besides that, deletion of 14q and 16q are found in 38% and 35% of MM, respectively. Deletion of 14q is associated with the loss of TNF Receptor-Associated Factor 3 (*TRAF3*) gene while 16q involves the loss of cylindromatosis (*CYLD*) and WW domain-containing oxidoreductase (*WWOX*) genes (Gazitt *et al*., 1999). *TRAF3* and *CYLD* are two critical genes in NFκB signaling pathway (Gazitt *et al*., 1999). Apart from that, deletion of 8p implies the loss of TNF-related apoptosis-inducing ligand (*TRAIL*) receptor gene, thereby facilitates myeloma cell growth by reducing *TRAIL*-mediated apoptosis in MM. Deletion of 8p is associated with poor prognosis in MM (Gazitt *et al*., 1999).

### 2.2.5 Gene expression changes in MM

Transcriptomic changes are important factors contributing to the development and progression of MM. As discussed above, primary translocations in MM often resulted in the upregulation of proto-oncogenes such as *CCND1*, *MMSET* and *MAF*. Besides that, chromosomal alterations also resulted in the inactivation and activation of various tumour suppressor and oncogenes, respectively. Gene expression changes therefore are useful in molecular classification of disease subtypes, risk assessment, prognostic measurement, predicting survival and treatment decision making in MM. Herein, some of the important findings on gene expression changes in MM are discussed.

Gene expression changes play a critical role in the transformation of normal plasma cells to neoplastic cells. It has been proven that normal plasma cells can be distinguished from the myeloma cells on the basis of the gene expression patterns (Zhan *et al*., 2002). Zhan *et al*. (2002) and his team had identified 4 distinct subgroups of MM by using gene expression method. They found that MGUS is more similar to normal plasma cells whereas MM is similar to myeloma cell lines. They also found that various genes involved in the cell cycle and DNA metabolism are up-regulated in MM when compared to the normal controls. Their findings postulated that gene expression changes is involved in different clinicopathological subtypes of MM. Apart from that, De Vos *et al*. (2002) had studied gene expression profiles of a total of 25 samples (9 MM clinical specimens, 8 myeloma cell lines and 8 non-malignant plasma cells). The samples are clustered into 2 distinct subgroups (malignant plasma cell cluster and normal plasma cluster) by unsupervised clustering algorithms. Significant differentially expressed genes identified in their study include the cell cycle genes, oncogenes and tumour suppressor genes such as Cyclin D1 (*CCND1*), v-myc avian myelocytomatosis viral oncogene homolog (*c-myc*), B lymphoma Mo-MLV insertion region 1 homolog (*BMI-1*) and retinoblastoma (*RB*). Pre-B cell proliferation enhancers, namely stromal

interaction molecule 1 (*STIM1*) and pre-B cell colony-enhancing factor 1 (*PBEF/ NAMPT*) are also up-regulated in myeloma group. Other important genes such as BCL2-interacting killer (*BIK*) and B-cell lymphoma 2 (*BCL2*) are significantly down-regulated and up-regulated in the myeloma group, respectively.

In 2007, a group of scientists had revealed 70 genes signature for survival and outcome prediction of MM patients known as UAMS70 (Shaughnessy *et al*., 2007). Majority of the 70 genes signature are mapped to chromosome 1. They found that most of the up-regulated genes and down-regulated genes are mapped to chromosome 1q and 1p, respectively. Their findings are expected as chromosome 1q and 1p is frequently amplified and deleted, respectively at chromosomal level (Marzin *et al*., 2006). Their findings suggested that gene copy number influences mRNA expression levels (Hastings *et al*., 2009). Further, they showed that a 17 genes model could be used to predict high risk myeloma. These 70 genes include cyclin-dependent kinases regulatory subunit 1B (*CKS1B*), chitobiase, di-N-acetyl (*CTBS*), abnormal spindle protein homolog (*ASPM*) and kinesin family member 14 (*KIF14*).

Another group of scientists showed that gene expression profiles are useful in risk factor prediction of MM (Decaux *et al*., 2008). They found that high risk patients constitute a homogeneous biologic entity characterised by over-expression of cell cylce progression genes whereas low-risk patients are heterogeneous and displayed hyperdiploid signatures. Other results showed that hypodiploid and non-hyperdiploid subtypes are very similar in term of gene expression changes, except that hypodiploid subtype is highlighted by over-expression of several oncogenes such as cyclin D2 (*CCND2*), Wolf-Hirschhorn syndrome candidate 1 *(WHSC1/MMSET*) and fibroblast growth factor receptor 3 (*FGFR3*), which are associated with poorer outcome and disease progression in MM (Van Wier *et al*., 2013).

By analysing gene expression profiles of newly diagnosed MM cases, several MM clusters had been proposed by Broyl *et al*. (2010). They found that MM is not only can be classified based on 7 unique characteristics, namely the translocation clusters MMSET [t(4;14)], MAF [t(14;16)/ t(14;20)], and Cyclin D1 [t(11;14)], Cyclin D2 [t(6;14)], hyperdiploid cluster (HY), a cluster with proliferation-associated genes (PR), and a cluster mainly characterised by a low percentage of bone disease (LB), they can be further characterised by over-expression of cancer testis antigens (CTA), genes involved in NFκB pathway [tumour necrosis factor alpha-induced protein 3 (*TNFAIP3*) and cluster of differentiation (*CD40*)], and over-expression of protein tyrosine phosphatases (PRL) [protein tyrosine phosphatases 3 (*PRL-3*) and protein tyrosine phosphatase receptor-type Z polypeptide 1 (*PTPRZ1*) as well as suppressor of cytokine signaling 3 (*SOCS3*)].

In additional to the identification of 70 gene signature for survival and risk stratification of MM patients, a EMC-92 gene signature is developed to better discriminate patients with high and standard risk MM, irrespective of treatment regime, age and relapse setting (Kuiper *et al*., 2012). Apoptosis and cell cycle related genes, baculoviral IAP repeat containing 5 (*BIRC5*) and *FGFR3* are two important genes in the signature. Signal transducer and activator of transcription 1 (*STAT1*), a component of the JAK/ STAT signaling pathway is also identified as one of the crucial gene in the EMC-92 gene signature. Recently, Kuiper *et al*. (2015) combined EMC-92, UAMS70, ISS and FISH markers [t(4;14) and deletion of 17p] to identify novel risk classification in MM. Their findings revealed that EMC-92 and ISS combination is the strongest predictor for overall survival in MM.

The advances in molecular cytogenetics allowed us to classified MM into several groups based on their biological features such as ploidy status, translocations and copy number changes. MM can now further defined into distinct subtypes on the basis of their gene expression patterns on a subset of genes such as those involved in the cell cycle regulation, apoptosis and oncogenic signaling pathways. For example, Li *et al*. (2013) had recently developed and validated a new method known as K-nearest neighbour method to classify hyperdiploid and non-hyperdiploid MM based on gene expression profiles. Apart from using gene expression profiles for molecular classification of MM, patients' survival rate and prognostic value can also be predicted based on the gene expression patterns (van Laar *et al*., 2014; Kuiper *et al*., 2015). Gene expression profiling could also be used to search for novel potential therapeutic markers in MM (Alexandra *et al*., 2015). In summary, gene expression profiling, alone or in combination with other molecular cytogenetic analysis such as FISH and aCGH has emerged as a powerful tool in clinical diagnostic, prognostic assessment, risk stratification and treatment decision making of MM patients (Segges and Braggio, 2011).

### 2.2.6 MicroRNA (miRNA) changes in MM

Apart from central role of genetic changes, epigenetic abnormalities arise as important factors in the development and progression of MM. Genetic and epigenetic abnormalities are tightly connected and affect each other. Epigenetic changes in MM such as DNA methylations, histone modifications and non-coding RNAs lead to changes in cell cycle, apoptosis and signalling pathways, which facilitate the growth and survival of myeloma cells (Dimopoulos *et al*., 2014).

Non-coding small RNAs or microRNAs (miRNAs) consist of 18-22 nt in length originated from either intragenic or intergenic DNA loci. They are known to regulate gene expression at post-transcriptional level (Bartel, 2009). Intergenic miRNAs is mediated by RNA polymerase II into primary miRNAs (pri-miRNAs), which will then process by RNase III type enzyme Drosha to form -70nt precursor molecules (pre-miRNAs). This process is also known as canonical miRNA biogenesis. In non-canonical miRNA biogenesis, intragenic miRNAs is mediated by RNA polymerase II together with the mRNA molecule of their host gene, and pre-miRNAs are produced either by Drosha processing or splicing. Pre-miRNAs are then transported from the nucleus to cytoplasm by protein Exportin-5. The enzyme Dicer cleaves the loop of the hairpin structure of pre-miRNAs to form mature miRNAs-3p and miRNAs-5p duplexes. One strand of the miRNA is degraded and the other strand is loaded on an Argonaut (AGO) protein to form the miRNA-induced silencing complex (miRISC) (Figure 2.2) (Krol *et al*., 2010). Binding of miRNA to their target mRNA resulted in translational repression or mRNA degradation. The canonical and non-canonical biogenesis of miRNA is illustrated in Figure 2.2.

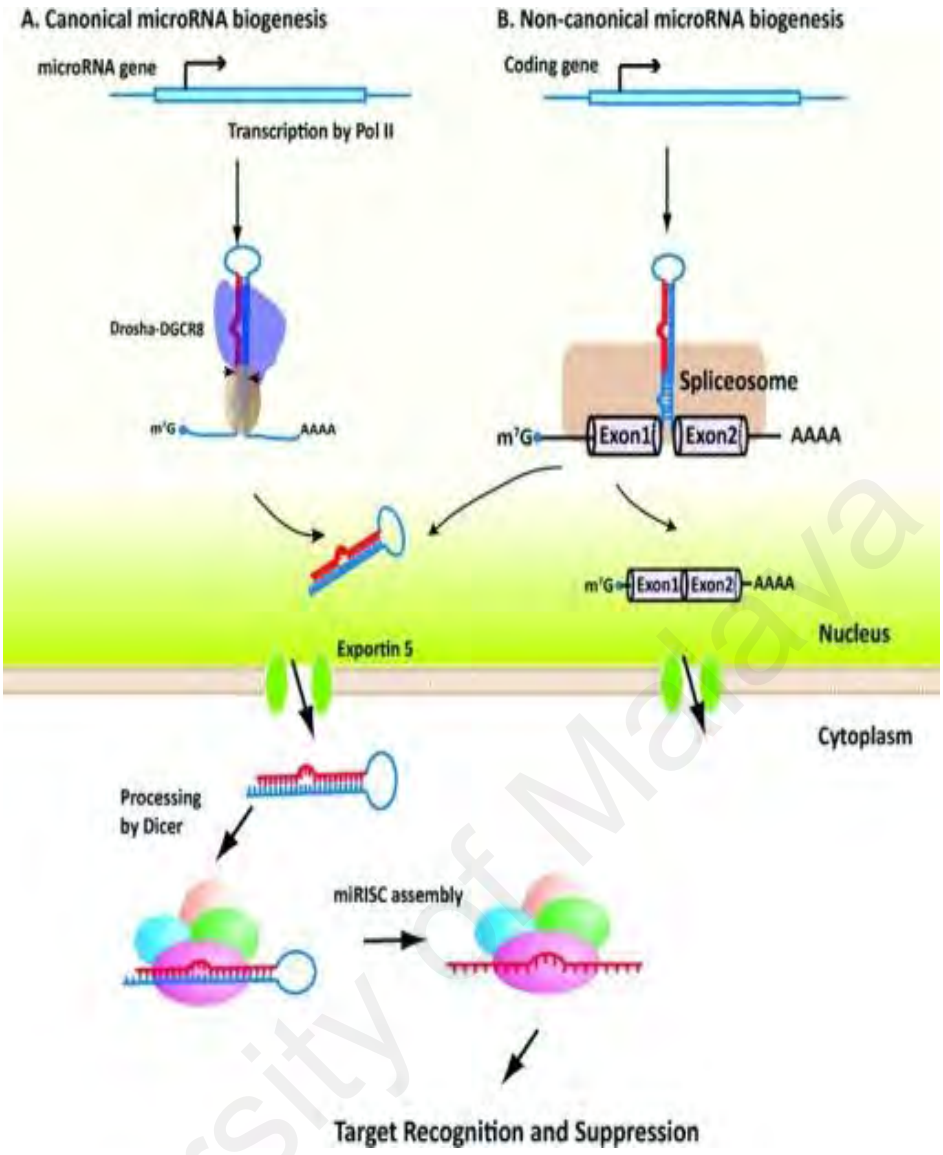


**Figure 2.2:** Canonical and non-canonical biogenesis of miRNAs (adapted from Li and Rana, 2012).

The miRNAs are important components of gene regulatory networks. Numerous studies on miRNA expression profiling were carried out by the researchers to identify potential miRNAs in the pathobiology, prognosis and therapy of MM. They were studies reported differential expression of miRNAs in different stages of MM. Others correlates dysregulation of miRNAs with different molecular subtypes of MM. Pichiorri *et al*. (2008) performed clustering on 5 MGUS, 10 MM and 4 controls based on the miRNA expression patterns. Their results showed that majority of the aberrant miRNAs are similar in MGUS and MM, except miR-32 and miR-17–92 are unique to overt MM but not MGUS. Another studied on the analysis of global miRNA expression in MM revealed that normal samples can be distinguished from MM or MGUS but MM and MGUS are not separate into clear clusters (Chi *et al*., 2011).

Several groups of researchers had identified miRNAs, which might contribute to the pathogenesis of specific molecular subtype in MM using miRNA microarray. Down-regulation of 16 miRNAs including miR-425, miR-152, and miR-24 are observed in hyperdiploid but not non-hyperdiploid MM (Rio-Machin *et al*., 2013). Intriguingly, down-regulation of these miRNAs are accompanied by a concomitant up-regulation of their targets *CCND1*, transforming, acidic coiled-coil containing protein 3 (*TACC3*), *MAFB*, *FGFR3*, and *MYC*. Their findings suggested that miRNA dysregulation could be the mechanism behind cyclin D as a unifying feature in both non-hyperdiploid and hyperdiploid MM. As mentioned earlier, deletion of *p53* gene in MM is associated with advanced MM and poor outcome in the patients. Pichiorri *et al*. (2008) observed that lower expression of miR-192, miR-194, and miR-215 in MM cell lines are most likely correlated with mutation in *p53*. Apart from that, Agnelli *et al*. (2005) showed that up-regulation of miR-99b, miR-125a-5p, and let-7e are associated with translocation involving *FGFR3* whereas miR-99a, let-7c, and miR-125b-2 are related with translocations involving *MAF* gene loci. Chi *et al*. (2011) described specific

miRNA signatures associated with the most common IgH translocations t(4;14) and t(11;14), and deletion in chromosome 13q. They also identified aberrant miRNAs associated with light chain myeloma, as well as IgG and IgA type MM.

Based on the data obtained from global miRNA expression studies as discussed above, thousands of aberrant miRNAs have been identified as potential targets in myelomagenesis. The miRNAs can function as oncomiRs or tumour suppressor miRs in MM. For instance, expression of miR-21, miR-17–92 cluster, miR-221/222 and miR-125a are normally up-regulated in MM cells while miR-15a/16 cluster, miR-29b, miR-34, miR-125b and miR-199a are frequently down-regulated in MM cells (Dimopoulos *et al*., 2013; Rossi *et al*., 2015). Here, the key dysregulated miRNAs, which are involved in oncogenic transformation of MM are discussed.

**a. miR-21**

The miR-21 is commonly up-regulated in MM and its dysregulation leads to inhibition of apoptosis in myeloma cells. The miR-21 is up-regulated through *IL-6*-mediated STAT3 pathway upon adherence of malignant plasma cells with the BMSCs (Löffler *et al*., 2007). Its up-regulation is not only suppresses apoptosis but strongly associated with melphalan resistance in MM. Silencing of miR-21 increases drug sensitivity, which suggested that miR-21 could be a possible therapeutic target in MM (Wang *et al*., 2011). Tumour suppressor phosphatase and tensin homolog (*PTEN)* is identified as the most critical miR-21 target in the pathogenesis of MM. Inhibition of miR-21 expression is thought to induce *PTEN* and inhibit MM cell proliferation through activation of oncogenic PI3K/Akt pathway (Leone *et al*., 2013; Xi and Chen, 2015).

**b. miR-17-92 cluster**

The miR-17-92 cluster encodes for six miRNAs, namely miR-17, miR-18a, miR-19a, miR-20a, miR-19b-1 and miR-92a-1. Over-expression of miR-17-92 cluster causes down-regulation of pro-apoptotic genes, *Bim* and suppressor of cytokine signaling 1 (*SOCS1*) in MM (Pichiorri *et al*., 2008). Chen *et al*. (2011) further confirmed that silencing of *c-Myc* causes down-regulation of miR-17-92 cluster and up-regulation of *Bim*. Their findings suggested that miR-17-92 cluster plays as an oncomiR in the pathogenesis of MM and inhibitors targeting miR-17-92 families could be a potential therapeutic target in myeloma patients.

**c. miR-221/ 222 cluster**

The miR-221/222 cluster is shown to act as oncogenic driver in MM. Their up-regulation is associated with poor prognosis in MM (Di Martino *et al*., 2014). *In vitro* and *in vivo* study of miR-221/222 suggested that they play a critical role in growth, survival as well as drug resistance in myeloma patients (Zhao *et al*., 2015). The main targets of miR221/222 is the cell cycle regulator p27 kip1 (*p27kip1*) gene and pro-apoptotic gene, p53 up-regulated modulator of apoptosis (*PUMA*) (Di Martino 2013 & 2014; Zhao *et al*., 2015). By using a 13-mer locked nucleic acid form of miR221 inhibitor is shown to restore drug resistance in preclinical models of MM implicated that miR-221 inhibitor is a potential drug sensitising agent that can be used to improve treatment outcome in myeloma patients (Gullà *et al*., 2016).

**d. miR-125a and miR-125b**

The adherent of MM cells to BMSCs induces expression of miR-125a. The miR-125a is involved in regulating p53 pathway related genes. Over-expression of miR-125a led to the suppression of *p53* and other tumour suppressor miRs such as miR-192 and miR-194. Over-expression of miR-125a impairs tumour cell proliferation and migration while promoting apoptosis in MM cells (Leotta *et al*., 2014).

Lately, Morelli *et al*. (2015) reported the potential role of miR-125b in the pathogenesis of MM. They claimed that miR-125b is commonly down-regulated in MM patients carrying translocations involving the up-regulation of *CCND2* and *CCND3* genes. Furthermore, Morelli *et al*. (2015) demonstrated that delivery of miR-125b mimics into human MM xenografts could inhibit growth and survival of MM cells while trigger apoptotic and autophagy cell death in MM cells. This anti-cancer activity demonstrated by miR-125b mimics is possibly caused by reduced expression of interferon regulatory factor 4 (*IRF4*), which in turn deactivated *c-MYC* and *BLIMP-1* expression. The transcription factor *BLIMP-1* is important in regulating plasma cell function and differentiation (Gururajan *et al*., 2010).

**e. miR-15a/ miR-16**

The miR-15a/ miR-16 is frequently down-regulated in MM. The miR-15a/ miR-16 cluster is a negative regulator of *VEGF*, an important growth factor which is produced upon interaction of MM cells and BMSCs (Sun *et al*., 2013). Thus, down-regulation of miR-15a/ miR-16 cluster promotes MM cell growth and survival through *VEGF*-mediated angiogenesis (Li *et al*., 2016). Besides *VEGF*, down-regulation of miR-15a/ miR-16 also induces cell proliferation and suppresses apoptosis through activation of *Bcl-2* (Aqeilan *et al*., 2010; Li *et al*., 2016). Other critical targets of miR-15a/ miR-16

are *CCND1* and interleukin 17 (*IL-17*) (Aqeilan *et al*., 2010; Li *et al*., 2016). *In vitro* studied of miR-15a/ miR-16 has confirmed that restoration of miR-15a/ miR-16 increases apoptosis event in MM cell lines (Hao *et al*., 2011).

**f. miR-29b**

The miR-29b is long recognised as a tumour suppressor miR involved critically in the pathogenesis of MM. Its restoration is thought to suppress myeloma cell proliferation and induce apoptosis by targeting cyclin dependent kinase 6 (*CDK6*) and myeloid cell leukaemia 1 (*MCL-1*) (Zhang *et al*., 2011; Amodio *et al*., 2012). It is believed that miR-29b targets anti-apoptotic gene *MCL-1* via activation of caspase 3 (Zhang *et al*., 2011; Amodio *et al*., 2012). Other important function of miR-29b in myelomagenesis includes reducing global DNA methylation via suppression of DNA methytransferase 3A/3B (*DNMT3A/3B*) gene (Yan *et al*., 2015). The tumour suppressor *SOCS-1* gene is commonly methylated in MM. The restoration of miR-29b causes demethylation of *SOCS-1* and inhibition of MM and epithelial cell migration in MM (Amodio *et al*., 2013). The most recent finding on miR-29b in MM confirmed that miR-29b targets histone deacetylases (*HDACs*) gene. Silencing of *HDACs* in MM induces miR-29b expression through promoter hyperacetylation, this in turn reduces the expression of transcription factor, specificity protein 1 (*SP1*) and anti-apoptotic *MCL-1* gene (Amodio *et al*., 2016). Taken together, miR-29b restoration is a promising therapeutic strategy that could be used to control the survival and proliferation of MM cells at epigenetic level.

### g. miR-34 family

Another key miRNA, namely miR-34 family (miR-34a, miR-34b and miR-34c) is also important in cell control and apoptosis of MM (Hermeking, 2010). The miR-34 is a direct target of *p53* and its expression is associated with *c-Myc*, *CDK6* and hepatocyte growth factor receptor (*c-MET*) and Notch homolog 1 (*NOTCH1*) (Christoffersen *et al*., 2010; ). Lastest findings shows successful delivery of miR-34a mimics into animals using stable nucleic acid lipid particles (SNALPs) and chitosan/ PLGA nanoplexes approaches and they are able to inhibit MM cell growth and improve survival of the treated animals (Di Martino *et al*., 2014; Cosco *et al*., 2015). This evidence implicated that miR-34a mimics is another promising therapeutic agent for anti-tumour treatment in MM.

### h. miR-199a

The miR-199a is another newly discovered tumour suppressor miR, which is related to angiogenic activity in MM. It is frequently down-regulated in MM and its down-regulation promotes angiogenesis in MM through over-expression of hypoxia-inducible factor 1-alpha (*HIF-1a*) under hypoxic condition (Raimondi *et al*., 2016). Replacement of miR-199a in MM cells suppresses *HIF-1a* and resulted in the reduction of *VEGF* and *IL-8*, which are essential growth factor/ cytokine involved in angiogenic activity of MM (Raimondi *et al*., 2014). Thus, miR-199a replacement therapy is a potential treatment strategy to overcome hypoxic microenvironment in MM.

## 2.3 MICRORNA-TARGET INTERACTIONS IN MM

Although abundant altered miRNAs are found to be associated with MM development and disease progression, the classical identification method fails to consider the structural information of pathways and the regulation of miRNAs simultaneously. The main challenge is that a single miRNA can control hundreds of genes and a gene is controls by several miRNAs. Generally, most of the miRNA-target predictions are solely based on the sequence matching information generated from the computational target prediction algorithms such as TargetScan and PicTar, which unavoidably have high false detection rates. However, the best way to understand the regulatory effects of miRNAs is the reliable prediction of their target mRNAs. Integrative approach is a reliable and powerful way to predict miRNA-targets in order to improve our comprehensive understanding of gene regulation in the disease. Integrative approach can be performed by integrating matched expression profiles of mRNA and miRNA from the same samples (Su *et al*., 2013). Besides that, gene-specific experimental validation with the well-established techniques of RT–qPCR, luciferase reporter assays and western blot are also useful in identifying individual miRNA-target interactions (Thomson *et al*., 2011).

To date, the information obtained on the integrated analysis of matched miRNA and mRNA expression profiles of MM are very limited. In 2009, Lionetti and co-workers had described miRNA-target by using integrative analysis of differential miRNA and mRNA expression in t(4;14) MM signature. Their findings revealed that let-7e targets protein tyrosine phosphatase epsilon (*PTPRE*), a critical component in *IL-6*-induced JAK-STAT signaling pathway (Tanuma *et al*., 2001). Interestingly, they found that miR-221 may regulate programmed cell death 4 (*PDCD4*), a tumour suppressor gene, in which its expression is regulated by *MMSET*. The *MMSET* is commonly up-regulated in t(4;14) MM subtype (Brito *et al*., 2009; Lankat-Buttgerei and

Goke, 2009). Apart from that, they reported that tumour suppressor genes, namely inhibitor of growth (*ING*) and cyclin D binding myb-like transcription factor 1 (*DMTF1*) as targets of miR-365 and miR-133a, respectively. The *ING* functions in controling angiogenesis and it is frequently down-regulated and mutated in MM (Kim, 2005; Colla *et al*., 2007). The *DMTF1* is involved in regulating cell cycle arrest and apoptosis in MM via ARF-p53 pathway (Inoue *et al*., 2007). In addition, Lionetti *et al*. (2009) also found that miR-361-3p and miR-30e* target phosphotyrosyl phosphatase activator, protein phosphatase 2A regulatory subunit B (PR 53) (*PPP2R4*) in MM exhibited t(11;14) signature. Protein phosphatase 2A activator, regulatory subunit 4 (*PPP2R4*) is an activator subunit of protein phosphatase 2A (*PP2A*), which control the survival and growth of MM cells through *IL-6*-mediated signaling pathway (Lionetti *et al*., 2009).

Besides that, Zhou *et al*. (2010) correlated analysis between miRNA expression profiles and a validated mRNA-based risk stratification score, proliferation index, and predefined gene sets. Their findings revealed that expression of *MYC* is positively associated with expression levels of miR-17–5p, miR-18a, miR-19b, and miR-20a. Moreover, they found that *p53* expression is not significantly correlated with miR-34a, miR-29a, miR-29b, miR15a, and miR-16 expression. More importantly, Zhou and his team (2010) showed that the silencing of protein argonaute 2 (*AGO2*), a critical component in miRNA biogenesis and B cell differentiation is not significantly associated with global increased in miRNA expression (Zhou *et al*., 2010; Bronevetsky and Ansel, 2013). This observation suggested that *AGO2* is not the only regulator that led to the global up-regulation of miRNAs in high-risk MM but other factors might contribute to this circumstance. Other findings showed that *AGO2* expression is involved in the regulation of some angiogenic miRNAs such as miR-17a and miR-92-1, and anti-angiogenic miRNAs such as miR-145 and miR-361 (Wu *et al*., 2014).

Recently, Zhang *et al*. (2015) evaluated the miRNA-target interaction in different clinicopathological subtypes of MM. Their findings indicated a subset of miRNAs and mRNAs, which are specific in MM that carrying deletion of *RB* gene and translocation t(4;14). Deletion of *RB* is one of the important indicators of poor outcome and shorter survival in MM patients (Zojer *et al*., 2000). Zhang *et al*. (2015) had identified 6 miRNAs and 52 genes, which were important in the *RB* deletion subtype. These aberrant miRNAs include miR-335, miR-17-5p, miR-451 and miR-301. These miRNA are commonly altered in cancers and leukaemia (Mi *et al*., 2007; Zhang *et al*., 2009; Serpico *et al*., 2014; Wang *et al*., 2014). Out of 52 genes, BCL2/adenovirus E1B 19 kd-interacting protein (*BNIP2*), CD44 molecule (Indian blood group) (*CD44*), homeodomain interacting protein kinase 3 (*HIPK3*), inositol hexakisphosphate kinase 2 (*IP6K2*), interleukin 1B (*IL1B*), Phorbol-12-myristate-13-acetate-induced protein 1 (*PMAIP1*), Rho-associated, coiled-coil containing protein kinase 1 (*ROCK1*), and tumour necrosis factor receptor superfamily member 10d (*TNFRSF10D*) are key components in apoptosis mechanisms (Zhang *et al*., 2015). In addition, they also identified 36 miRNAs and 382 mRNAs related to the translocation t(4;14) subtype. These subsets of miRNAs include let-7a, miR-125a, miR-193b, miR-25, and miR-181c. A potential mRNA identified in t(4;14) group is Ras-related protein Ral-A precursor (*RALA*), a component in oncogenic RALA and MAPK/ERK signal transduction pathways (Lim *et al*., 2005). Inhibition of RALA pathway has been implicated as a potential therapeutic intervention in non-small cells lung cancer and hepatocellular carcinoma but it has not been investigated in MM (Male *et al*., 2012; Ezzeldin *et al*., 2014).

## 2.4 ROLE OF NICOTINAMIDE PHOSPHORIBOSYL TRANSFERASE (*NAMPT*) IN MM

Nicotinamide phosphoribosyl transferase (*NAMPT*) is a key enzyme involved in the nicotinamide adenine dinucleotide ($NAD^+$) salvage pathway (Revollo *et al*., 2004). *NAMPT* is elevated in many different kinds of cancers, for examples ovarian, breast, colorectal, gastric, prostate, well-differentiated thyroid and endometrial carcinomas, melanoma, astrocytoma, lymphoma and MM (Shackelford *et al*., 2013). MM cells obtained sufficient energy for proliferation from increase activity of NAD resynthesis, which is triggers by elevated expression of *NAMPT* gene (Chiarugi *et al*., 2012). MM cell death is thought to increase by silencing the *NAMPT* gene (de la Puente *et al*., 2014; Prideaux *et al*., 2014). Inhibition of *NAMPT* by using small molecule inhibitor, APO866 reduces osteoclastogenesis/ bone resorption through suppression of NFκB pathway (Venkateshaiah *et al*., 2013).

The $NAD^+$ is a pivotal signaling molecule, which is involved in maintaining the functions of a wide variety of $NAD^+$-dependent enzymes in the cytoplasm and nucleus. *NAMPT* and nicotinamide-nucleotide adenylyltransferase (*NMNAT*) are two key enzymes involved in the $NAD^+$ salvage pathway (Rongvaux *et al*., 2013). *NAMPT* catalyses the conversion of nicotinamide (*NAM*) to nicotinamide mononucleotide (*NMN*), which is then converts to $NAD^+$ by *NMNAT* (Zhang *et al*., 2009). In humans, normal *NAMPT* expression is required during early embryo development, lymphocyte differentiation, muscle cell differentiation, maturation, and senescence (van der Veer *et al*., 2005 & 2007; Revollo *et al*., 2007; Fulco *et al*., 2008; Rongvaux *et al*., 2008). In cancer cells, more $NAD^+$ is required to generate adenosine triphosphate (ATP) to supply energy for cell growth and survival (Cea *et al*., 2012). Therefore, the expression of *NAMPT* gene is usually high in MM. Over-expression of NAD regulates the transcription activity of two important $NAD^+$ dependent enzymes, namely the protein deacetylase sirtuin-1 (*SIRT1*) and poly-(ADP-ribose) polymerase 1 (*PARP1*) (Figure

2.3). These two $NAD^+$ dependent enzymes play key functions in tumourigenesis (Zhang *et al*., 2009). Gene transcription and chromatin structure is controlled by *SIRT1* through histone modifications, transcription factors and co-regulators. The tumour protein p53, NFκB, forkhead box O1 (FOXO) proteins, estrogen receptor α, liver X receptor, Sex determining region Y- box 9 (SOX9), peroxisome proliferator-activated receptor gamma coactivator 1-alpha (PGC-1α) and E1A Binding Protein P300 (p300) coactivator are all parts of critical down-stream targets of *SIRT1* (Kim *et al*., 2006; Michan and Sinclair, 2007; Dvir-Ginzberg *et al*., 2008; Feige *et al*., 2008). In addition, *PARP1* is not only function in chromatin remodeling and transcription factor regulation, it also plays an important role in DNA repair (Schiewer *et al*., 2012). *PARP1* is involved in the transcription regulation of octamer transcription factor 1 (Oct-1), peroxisome proliferator-activated receptor gamma (PPARγ), specificity protein 1 (SP1), Smad family member 3 or 4 (Smad3/Smad4), sex determining region Y-box 2 (Sox2), NFκB, and p300 (Ko and Ren, 2012). Some of these genes for instance, NFκB, p53, FOXO, and p300 are critical components in the initialtion and progression of MM (Zhou *et al*., 2008; Abdi *et al*., 2013; Dimopoulos *et al*., 2014; Teoh and Chng, 2014).

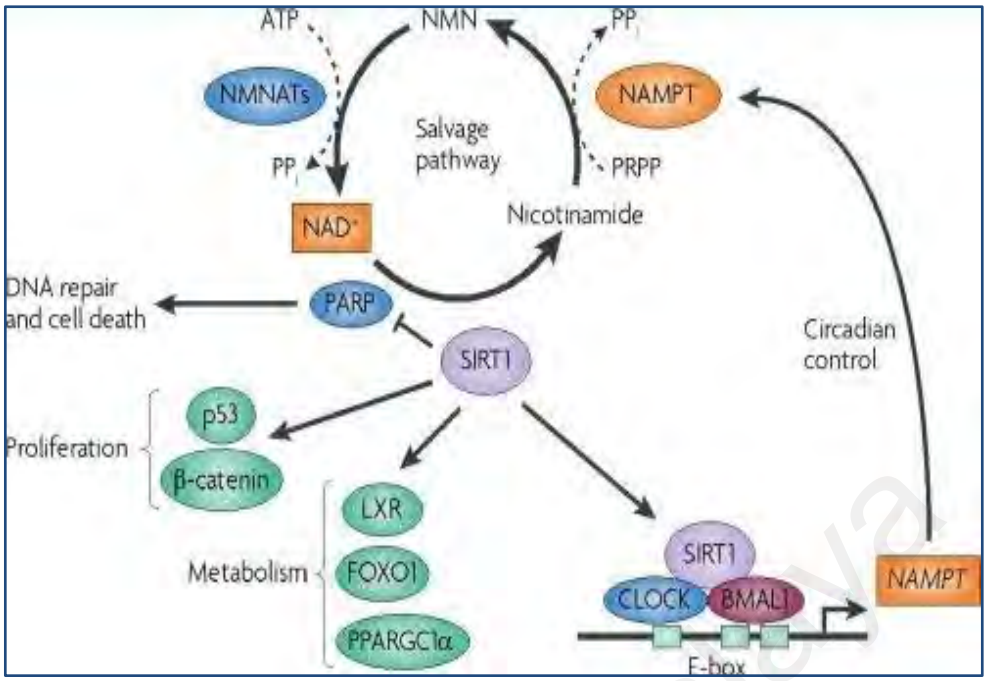


**Figure 2.3:** $NAD^+$ salvage pathway (adapted from Sahar and Sassone-Corsi, 2009).

# CHAPTER 3: MATERIALS AND METHODS

## 3.1 COPY NUMBER VARIATION STUDY OF MM

Copy number variation study was carried out by using genome wide array comparative genomic hybridisation (aCGH) approach. The MM samples and controls were labeled with Agilent two color labeling system and hybridised onto Agilent Human Genome CGH Microarray Kit 244k. Microarray data was analysed by Agilent DNA Analytics software (v4.0). Chromosomal aberrations were identified by comparing the copy number profiles of MM patients with normal controls. The microarray data have been submitted to the Gene Expression Omnibus (GEO) and assigned with an accession number GSE44745.

### 3.1.1 Study subjects

Sixty-three archival bone marrow cell suspensions diagnosed from year 2007-2010 were recruited for aCGH study (Samples were designated as M4, M5, M6, M7, M9, M11, M16, M17, M18, M19, M20, M21, M22, M23, M24, M27, M28, M30, M31, M32, M33, M34, M35, M38, M39, M41, M42, M43, M45, M47, M48, M49, M51, M52, M54, M55, M56, M62, M63, M65, M68, M69, M70, M71, M73, M74, M76, M80, M81, M84, M86, M89, M91, M94, M95, M96, M98, M100, M101, M102, M103, M104, M105). The age of these patients ranged between 15-77 years with a mean and median age of 57 and 58 years, respectively. Only newly diagnosed patients with plasma cell infiltration >10% were included in this study. Patients' characteristics were summarised in Table 3.1. Apart from that, a total of 60 normal whole blood were collected with the help of National Blood Centre Malaysia. They were used as normal controls in aCGH study. Normal controls were divided into 6 groups, in which each group was pooled

from 10 gender and ethnicity matched individuals: male Malays (N1), female Malays (N2), male Chinese (N3), female Chinese (N4), male Indians (N5) and female Indians (N6). The mean age for each control group was: male Malays, 47 years; female Malays, 34 years; male Chinese, 45 years; female Chinese, 41 years; male Indians, 48 years and female Indians, 34 years. This study had been approved by the Medical Research & Ethics Committee (MREC), Ministry of Health, Malaysia (NMRR-09-731-4537). Written informed consent was obtained from all patients for being included in the study.

### 3.1.2 Genomic DNA extraction

Genomic DNAs were extracted from bone marrow cells and whole blood by using Qiagen DNA mini kit according to manufacturer's recommendation. Briefly, 20 µl of Proteinase K was added into a microcentrifuge tube. Then, 200 µl of whole blood or cells in PBS buffer was transferred to the microcentrifuge tube. Two hundred microliter of buffer AL was then added to the tube and the mixture was incubated in a waterbath at 56 ºC for 10 min. After cells lysed, 200 µl of absolute ethanol was added to the tube and mixed by gently vortexing for 15 s. This was followed by transferring all the mixture into a spin column and centrifuged at 6000 x *g* for 1 min in a microcentrifuge. The spin column was washed by adding 500 µl of Buffer AW1 and centrifuged at 6000 x *g* for 1 min. The column was then washed with 500 µl of Buffer AW2 and centrifuged at full speed for 3 min. Finally, the DNAs were eluted with 200 µl of TE buffer. The spin column was allowed to incubate at room temperature for 5 min before centrifuged at 6000 x *g* for 1 min. The integrity of genomic DNAs was then checked on 1% (w/v) denaturing agarose gel whereas purity and concentration were determined by using a NanoDrop ND-1000 UV-VIS spectrophotometer. Good quality DNAs should have A260/ A280 ratio of 1.7-1.9 and the A260/ A230 ratio of >2.0.

**Table 3.1:** Characteristics of 63 multiple myeloma patients

| Parameter at diagnosis | No. of patients (%) |
|---|---|
| Gender | |
| Male | 34 (53.97) |
| Female | 29 (46.03) |
| Age (years) | |
| ≤55 | 27 (42.86) |
| >55 | 36 (57.14) |
| Ethnic | |
| Malay | 36 (57.14) |
| Chinese | 14 (22.22) |
| Indian | 13 (20.63) |
| Karyotype (G-band) | |
| Abnormal[a] | 2 (3.17) |
| Normal | 37 (58.73) |
| Unknown[b] | 24 (38.10) |

[a] Multiple chromosomal abnormalities were seen with karyotyping
[b] Insufficient/ short/ no chromosome spread were available for cytogenetic analysis

### 3.1.3 Oligonucleotide aCGH

The aCGH experiments were performed by using two colour labeling system (Genomic DNA ULS Labeling Kit, Agilent Technologies). Briefly, genomic DNAs were fragmented at 95ºC for 10 min. Following fragmentation, 1.5 µg of control and patient DNAs were labeled with 1.5 µl of ULS- Cyanine 5 and ULS-Cyanine 3, respectively in separate tubes. Then, 2 µl of 10X labelling solution was added into each tube and top up with nuclease free water in a final volume of 20 µl. The mixture was incubated at 85ºC for 30 min in a PCR machine and then incubated on ice for 3 min. The labeled DNAs were purified to remove non-reacted Cy-ULS using Agilent KREApure column (Agilent Technologies). Briefly, KREApure column materials were resuspended by vortexing. Then, the KREApure column was pre-spin in a microcentrifuge at maximum speed for 1 min. The column was then washed with 300 µl of nuclease free water by centrifuging at maximum speed for 1 min. Finally, labeled DNAs was transferred to the column and centrifuged for another 1 min at maximum speed. The purified labeled DNAs were collected in the collection tube. Then, 1.5 µl of purified labeled DNAs were quantitated in NanoDrop ND-1000 UV-VIS spectrophotometer to measure the absorbance at 260 nm (DNA), 550 nm (Cy3), and 650 nm (Cy5). Degree of labeling was then calculated using formula below.

$$\text{Degree of labeling} = \frac{340 \times \text{pmol per µl dye} \times 100\%}{\text{ng per µl genomic DNA} \times 1000}$$

$$\text{Yield (ng/ µl)} = \text{DNA concentration (ng/ µl)} \times \text{sample volume (µl)}$$

As a general guideline, an optimal Cy5 degree of labeling lies between 0.75% and 2.5% and an optimal Cy3 degree of labeling lies between 1.75% and 3.5%. The DNA concentration after labeling should be approximately 1.5 µg because no amplification was performed during the labeling process. After checking the yield and degree of labeling, the labeled DNAs can be used for hybridisation or stored in -20ºC in the dark until ready for hybridisation.

Hybridisation master mix was prepared by adding 50 µl of Cot-1 DNA (1.0 mg/ mL) (Invitrogen), 5.2 µl of blocking agent, 260 µl of hybridisation buffer and 37.8 µl of nuclease free water. Patients and control labeled DNAs (approximately 37 µl in total) were combined and mixed in the hybridisation master mix. Then, the mixture was incubated in a thermal cycler at 95ºC for 3 min and then 37ºC for 30 min. After that, 130 µl of CGH-block was added to the tube. Then, 490 µl of the mixture was hybridised onto Human Genome CGH Microarray Kit 244k for 40 h at 65ºC at 20 rpm. After 40 h of incubation, the array was washed with wash buffer 1 (Agilent) for 5 min, followed by wash buffer 2 (Agilent) (prewarm at 37ºC overnight) for 1 min, acetonitrile for 10 s and finally stabilisation and drying solution for 30 s. The array was then scanned with Agilent array scanner G2505C. Agilent Feature Extraction Software Version 10.7.3.1 was used to extract data from raw microarray image files for further analysis.

### 3.1.4 aCGH data analysis

Agilent DNA Analytics software (v4.0) was used to visualize, detect and analyse aberration patterns from aCGH microarray profiles. Before the data was analysed, the data quality for each array were determined according to the Quality control (QC) metrics as listed in Table 3.2. All microarray data were analysed according to the human reference genome assembly hg18. Data were analysed by using ADM2 algorithm and then filtered by a minimum of 3 probes and minimum average absolute $\log_2$ ratio of 0.3, with maximum aberration of a total of 100 probes. Bin size 10 and threshold 6.0 were setted for the analysis. For probe penetrance analysis, the filter option was set to 30% with a minimum of 3 probes. Common aberrations were identified by using t-test and at p cut off of 0.05, overlap threshold of 0.9. Aberration segments were individually viewed with Ensembl genome browser 54.

**Table 3.2:** Quality control metrics for aCGH

| Metric Name | Excellent | Good | Evaluate |
|---|---|---|---|
| Is Good Grid | >1 | NA | <1 |
| Green/ red percentage feature non-uniformity outlier | <1 | 1-5 | >5 |
| Derivative log ratio spread | <0.20 | 0.20-0.30 | >0.30 |
| Green reproducibility | 0-0.05 | 0.05-0.2 | <0 or >0.2 |
| Green background noise | <5 | 5-15 | >15 |
| Green signal to noise | >100 | 20-100 | <20 |
| Green signal intensity | >150 | 50-150 | <50 |
| Red reproducibility | 0-0.05 | 0.05-0.2 | <0 or >0.2 |
| Red background noise | <5 | 5-15 | >15 |
| Red signal to noise | >100 | 20-100 | <20 |
| Red signal intensity | >150 | 50-150 | <50 |

### 3.1.5 qPCR verification for copy number aberration

Two copy number gain regions found by aCGH analysis were selected for verification by using TaqMan Copy Number Assay (Applied Biosystems). They were chromosomal gains at 1q42.3 and 7q22.3, where *LYST* and *NAMPT* genes are localised, respectively. Copy number for chromosomal 1q42.3 was assessed with specific TaqMan Copy Number Assay (Hs05736121_cn; Applied Biosystems). Probe and primers for chromosomal 7q22.3 were custom designed as following: FAM dye labeled probe CATGATGTTACTACTTTGAAATAACC, forward primer CCTAAAGAAGATATTATCCTTGTCCTCCGTAT and reverse primer CATAGTATGCACATATTAGACTCTTCGTTGA. The VIC® dye-labeled TaqMan® Copy Number Reference Assay targeted telomerase reverse transcriptase gene (*TERT*) located at chromosomal 5p15.33 (Applied Biosystems) was used as internal control.

Ten samples showing copy number gains by greater than $\log_2$ ratio of 0.3 (>1.7 folds) at chromosomal segments 1q42.3 and 7q22.3 as analysed by aCGH were selected for qPCR verification. Samples used to verify gains at chromosomal segment 1q42.3 were M04, M05, M16, M17, M20, M24, M27, M30, M80 and M84. On the other hand, Samples used to verify gains at chromosomal segment 7q22.3 were M07, M11, M16, M17, M28, M45, M74, M81, M100 and M103. Three MM samples without amplification at these regions were selected as negative controls (M38, M56 and M102 for chromosomal 1q42.3; M47, M49 and M56 for chromosomal 7q22.3). A15 was from the normal blood control. No template controls were also included in each plate to allow detection of contamination. Briefly, each sample of 20 ng (5 ng/ µl) genomic DNAs was prepared in triplicate containing 10 µl of 2X TaqMan Universal Genotyping Master Mix, 1 µl of FAM® dye-labeled TaqMan® Copy Number Assay, 1µl of VIC® dye-labeled TaqMan® Copy Number Reference Assay and 4 µl of nuclease free water. All qPCR

reactions were run on an ABI 7500 Fast Real-time PCR System (Applied Biosystems) in 96-well format and thermal cycling conditions were 95°C, 10 min followed by 40 cycles of 95°C for 15 s and 60°C for 1 min. The *TERT* reference gene is always present in two copies in a diploid genome and therefore it was selected as internal control in this study. *TERT* reference gene was used to normalise sample input and minimise the variation caused by PCR efficiencies in sample and normal control.

The real-time PCR results were then analysed using CopyCaller software v2.0 (Applied Biosystems) to determine the copy number of the samples. To remove poor quality data, filtering threshold was set to exclude samples with VIC crossing threshold (Ct) greater than 32. This means that sample with Ct greater than 32 in internal control (*TERT*), which was VIC-labeled will be excluded from the analysis. The relative quantity of the samples and the copy number were then calculated following formulas below. Copy number <1.5 or >2.5 will be called as having copy number change.

Relative quantification = $2^{-\Delta\Delta Ct}$

$\Delta Ct_{sample} = Ct_{sample} - Ct_{internal\ control}$

$\Delta Ct_{reference} = Ct_{reference} - Ct_{internal\ control}$

$\Delta\Delta Ct = \Delta Ct_{sample} - \Delta Ct_{reference}$

Ct = crossing threshold

Copy number = relative quantification x copy number for the normal control

= relative quantification x 2

## 3.2 RNA INTERFERENCE (RNAi)

The *NAMPT*-mediated silencing effects on cell proliferation and apoptosis were studied using RNAi approach. The RPMI-8226 myeloma cell line was used as hosts for RNAi study because it is an easy-to-transfect myeloma cell line compared to others.

### 3.2.1 Cell culture

The RPMI-8226 cells were purchased from American Type Culture Collection (ATCC, USA). Cells were cultured and maintained in RPMI1640 (ATCC) containing 10-15% fetal bovine serum (Lonza) in an incubator at *37*°C with humidified 5% $CO_2$. The cells were passaged every 3-4 days. Cells were cryopreserved in CELLBANKER cryopreservation medium (amsbio) and stored in liquid nitrogen according to manufacturer's protocol.

### 3.2.2 siRNA transfection

siRNA duplexes purchased from OriGene (OriGene Cat. No.: SR306835) were used to silence *NAMPT* gene in RPMI-8226 myeloma cells. The three unique siRNAs were labeled as NAMPT-a, NAMPT-b and NAMPT-c. The siRNA sequences and their corresponding binding sites were listed in Table 3.3. A total of 100 nM of siRNAs were used for transfection. Alternatively, 100 nM of each siRNA were pooled for transfection, the pooled siRNAs were designated as NAMPT-abc. Delivery of siRNAs into RPMI-8226 cells was conducted by Amaxa nucleofection method (Amaxa nucleofection kit V). Briefly, cells were resuspended in 100 µl of nucleofector V solution mixed with 100 nM of siRNAs or 300 nM of pooled siRNAs at a density of 5.0 X $10^6$ cells/ mL. Scrambled negative control siRNAs (OriGene) was used as negative control whereas 2 µl of pmaxGFP was used as indicator for successful transfection. The mixture was transferred to a cuvette and nucleofected using G-016 pulsing parameter with an Amaza

nucleofector apparatus. The cells were immediately transferred to pre-warm culture medium in 12 well plates. Success of transfection was determined by expression of green fluorescence signals under fluorescence microscope at 24 h post-transfection. Cells were collected at 24 h, 48 h and 72 h post transfection for downstream analysis. Two replicates was performed for each transfection and the transfection was carried out in two independent experiments.

**Table 3.3:** siRNA sequences and their corresponding nucleotide binding sites

| **siRNA** | **Sequences** | **Nucleotide binding sites and reference sequence accession** |
|---|---|---|
| NAMPT-a | AGAAUCUUAAGUUGGCUAAAUUCAA | 2938-2962 (NM_005746.2) |
| NAMPT-b | GACAUACCCUAUAGAAUUACUAACC | 2354-2378 (NM_005746.2) |
| NAMPT-c | AACAUGUAGUGAGAACAAUAAGCAT | 3604-3628 (NM_005746.2) |

### 3.2.3 Total RNA extraction

Total RNAs were extracted from the siRNA and scrambled negative control transfected cells by using Qiagen RNeasy mini kit following manufacturer's protocol. Generally, 600 µl of Buffer RLT was used to lyse the cells. The cell lysate was then transferred to a spin-column and centrifuged at full speed for 2 min. The flow-through was discarded and 1 volume of 70% (v/v) ethanol was added into the spin column and centrifuged for 15 s at ≥8000 x *g*. This was followed by adding 350 µl of Buffer RW1 and centrifuged for 15 s at ≥8000 x *g*. On-*column DNA digestion* was then performed with the RNase-free *DNase* set (Qiagen DNase I) by adding solution containing 10 µl of DNase I stock solution and 70 µl of RDD buffer. The spin column was incubated for 30 min at room temperature. After incubation, 350 µl of Buffer RW1 was added to the column and then centrifuged for 15 s at ≥8000 x *g*. Then, the column was washed with 500 µl of Buffer RPE and centrifuged for 15 s at ≥8000 x *g*. The column was washed with another 500 µl of Buffer RPE and centrifuged for 2 min at ≥8000 x *g*. Finally, 30 µl of RNase free water was added to the column and centrifuged for 1 min at ≥8000 x *g* to elute the RNA. The purity (A260 nm/ A280 nm) and concentrations of all the RNAs were determined by using a NanoDrop ND-1000 UV-VIS spectrophotometer. For mRNA and miRNA microarray studies, the RNA integrity number (RIN) was checked with Agilent's 2100 Bioanalyser by using RNA Nano Chip. Only samples with RIN >8.0 were selected for microarray study.

### 3.2.4 Quantitative real-time PCR (RT-QPCR)

Five hundred nanogram of RNAs were reverse transcribed to cDNA in a final volume of 20 µl reaction containing 10 µl of 2X Reverse Transcriptase Buffer Mix and 1 µl of 20X Enzyme Mix (Applied Biosystems high capacity RNA-to-cDNA kit). For RT-qPCR, each sample of 20 µl reactions was prepared in triplicate containing 10 µl of 10X TaqMan Gene Expression Master Mix, 1 µl of FAM dye-labeled TaqMan Gene Expression Assay and 50 ng of cDNA (up to 4 µl) (Applied Biosystems TaqMan gene expression assay). Pre-designed FAM dye-labeled TaqMan gene expression assay for *NAMPT* was used in this study (Table 3.4). The *GAPDH* was used as endogenous control to normalise sample input and minimize the variation between the sample and reference. The RT-qPCR for *NAMPT* and *GAPDH* of the same samples and non-template controls were run on the same plate. All RT-qPCR reactions were run on an ABI 7500 Fast Real-time PCR System (Applied Biosystems) in 96-well format and thermal cycling conditions were 95°C for 20 s, followed by 40 cycles of 95°C for 3 s and 60°C for 30 s. All samples were normalised to internal control and the fold change of expression levels in sample and control were calculated through relative quantification. Fold difference and percentage of gene knockdown were determined using formula below:

Relative quantification = $2^{-\Delta\Delta Ct}$

$\Delta Ct_{sample} = Ct_{sample} - Ct_{internal\ control}$

$\Delta Ct_{reference} = Ct_{reference} - Ct_{internal\ control}$

$\Delta\Delta Ct = \Delta Ct_{sample} - \Delta Ct_{reference}$

Ct = crossing threshold

Percentage of gene knockdown = $(1-2^{-\Delta\Delta Ct})$ X 100 %

**Table 3.4:** TaqMan gene expression assays for RT-qPCR

| No | Gene/ miRNA | Probe/ primer |
|---|---|---|
| 1 | NAMPT | Life Technologies (Cat. No.: Hs00237184_m1) |
| 2 | CCNA2 | Life Technologies (Cat. No.: Hs00996788_m1) |
| 3 | RASGRF2 | Life Technologies (Cat. No.: Hs00394798_m1) |
| 4 | RAD54L | Life Technologies (Cat. No.: Hs00936473_m1) |
| 5 | HKDC1 | Life Technologies (Cat. No.: Hs00228405_m1) |
| 6 | GAPDH | Life Technologies (Cat. No.: Hs02758991_g1) |

### 3.2.5 3-(4,5-Dimethyl-2-thiazolyl)-2,5-diphenyl-2H-tetrazolium (MTT) assay for cell proliferation

Treated and scrambled negative control treated cells were seeded onto 96-well plates at a density of 2.0 X $10^4$ cells/ mL in triplicate (100 µl/ well). Cell proliferation was evaluated at 24 h, 48 h and 72 h post-transfection. Briefly, after 24 h, 48 h and 72 h post transfection, 10 µl of MTT reagent (TREVIGEN) at a concentration of 5 g/ L was added to each well, and the cells were incubated for 4 h at *37*°C. Following incubation, 100 µl of Detergent Reagent was added to each well and the cells were incubated for another 2 h at 37°C. After the insoluble crystals were completely dissolved, the plate was read at absorbance of 570 nm using an Odyssey® SA Imaging System (Li-Cor, Lincoln, USA).

### 3.2.6 Annexin-V-staining for detection of apoptosis

Annexin-V staining was performed with Annexin-V-fluorescein isothiocyanate (FITC) apoptosis detection kit (BioVision, USA). In this assay, Annexin-V-FITC (1:100) and propidium iodide (PI, 0.5 µg/ mL) were used. Generally, approximately 3.0-5.0 X $10^5$ treated and scrambled negative control treated cells were collected by centrifugation. Cell pellet was washed with PBS and then resuspended in 500 µl of binding buffer. Five microliter of Annexin-V-FITC (1:100) and 2 µl of propidium iodide (PI, 0.5 µg/ mL) were added to the cell suspension and incubated for 10 min in the dark. Then, the cells were analysed by FACS Calibur instrument (Becton Dickinson BD). The data were

analysed using the Cell Quest software (Becton Dickinson BD). For each analysis, 10000 events were recorded. Two independent experiments were performed for each apoptosis assay.

### 3.2.7 Enzyme-linked immunosorbent assay (ELISA)

Approximately 3.0-5.0 X $10^5$ treated and scrambled negative control treated cells were collected and lysed for 30 min in the ice at 24 h, 48 h and 72 h post-transfection. Briefly, albumin (BSA) standards were prepared by diluting the BSA (2 mg/ mL) to concentrations of 25, 125, 250, 500, 750, 1000, 1500 and 2000 µg/ mL (BCA protein assay kit, Thermo Scientific). Then, 25 µl of the BSA standards, samples and blank controls were loaded into the microplate in duplicate. This was followed by adding 200 µl of BCA working reagents to each well. The solution was mixed on plate shaker for 30 s. Finally, the plate was cooled at room temperature and measured at absorbance of 562 nm on a plate reader (TECAN Sunrise). Standard curve was plotted based on the absorbance values of BSA standards vs its concentration in µg/ mL. The total protein concentration of the samples were then determined from the standard curve graph. Then, all the samples were diluted to 500 µg/ ml.

The ELISA assay was performed according to manufacturer's instructions (NAMPT Intracellular ELISA kit, BioVision). Generally, standard curve was generated using 2-fold serial dilutions of the control sample (16 ng/ mL – 0.062 ng/ mL). Then, 100 µl of the standards, samples and blank controls were loaded into a microplate in duplicate and incubated overnight at 4°C. Following overnight incubation, the plate was washed with 300 µl X 3 of 1X wash buffer 1. Then, 100 µl of detection antibody was added into each well and the plate was incubated for 1 h at 37°C. After incubation, the plate was washed with 300 µl X 3 of 1X wash buffer 1. Then, 100 µl of Detector was added to each well and further incubated at 37°C for 1 h. Then, the plate was washed

with 300 µl X 5 of 1X wash buffer 1. This is followed by adding 100 µl of TMB substrate solution. After 10 min, stop solution was added to each well and the plate was read at absorbance of 450 nm in an ELISA plate reader (TECAN Sunrise). The standard curve graph was plotted based on the absorbance values of serial diluted standards vs its concentration in ng/ mL. NAMPT protein concentrations of the samples were then determined based on the standard curve graph. Relative protein quantification was calculated according to formula below:

$$\text{Relative protein quantification} = \frac{\text{NAMPT protein concentration}_{\text{siRNA treated cells}}}{\text{NAMPT protein concentration}_{\text{control treated cells}}}$$

## 3.3 GENE EXPRESSION STUDY OF MM

Gene expression profiling was conducted for a total of 30 samples (19 clinical specimens, 8 myeloma cell lines and 3 normal controls) using Agilent one colour Low Input Quick Amp Labeling kit and Agilent SurePrint G3 Human GE 8x60K V2 Microarray kit. Approximately 60000 probes across the whole genome were analysed in a single experiment. The mRNA microarray data generated in this study are available in the NCBI Gene Expression Omnibus (GEO) as series accession identifier GSE72213.

### 3.3.1 Specimens

Approximately 0.1-2.0 ml of fresh bone marrow and whole blood were collected from MM patients and healthy donors. A total of 19 MM patients (MM1-MM19) and 3 normal controls (NB1, NB2 and NB3) were recruited in this study. All the patients are between ages 28-74 at the time of diagnosis. The mean and median age of the patients is 57 and 61 years old, respectively. Among 19 patients, 17 of them were newly diagnosed MM while the remaining 2 were relapsed cases. Bone marrow was aspirated from the

newly diagnosed patients before treatment. Patients' characteristics were summarised in Table 3.5. This study had been approved by the Medical Research & Ethics Committee (MREC), Ministry of Health, Malaysia (NMRR-09-731-4537). Written informed consent was obtained from all patients for being included in the study.

### 3.3.2 Cell lines

The RPMI-8226, U-266, MM.1S and IM-9 MM cells were purchased from American Type Culture Collection (ATCC, USA). Myeloma cell lines KMS-28-BM, KMS-20, KMS-12-BM and KMS-21-BM were obtained from Japanese Collection of Research Bioresources (JCRB) cell bank. Cell culture conditions and methods were as described in section 3.2.1.

### 3.3.3 mRNA microarray sample preparation

Total RNAs were extracted from bone marrow/ blood/ cells using RNeasy Mini Kit (Qiagen). For bone marrow and whole blood, 1 volume of sample was mixed with 5 volume of erythrocyte lysis (EL) buffer (Qiagen) and incubated for 15 min on ice to lyse the red blood cells. Then, the solution was centrifuge at 400 x *g* for 10 min at 4°C. Two volume of Buffer EL was then added to the cell pellet and centrifuge at 400 x *g* for 10 min at 4°C to collect the leukocytes. Then, the cell pellet was lysed in 600 µl of Buffer RLT. This was then followed by procedure as described in section 3.2.3.

Total RNAs concentration and RNA integrity number (RIN) were then determined by using a NanoDrop ND-1000 UV-VIS spectrophotometer and Bioanalyser. Samples with RIN >8.0 were used for microarray study. One hundred nanograms of total RNAs were used for each array. Labeling of total RNAs was carried out using one colour Agilent's Low Input Quick Amp Labeling kit. Samples were

prepared according to the Agilent's manufacturer's protocol. Briefly, 100 ng of total RNAs were mixed with 2 µl of diluted Spike-Mix, 0.8 µl of T7 promoter primer in a final volume of 5.3 µl and incubated in waterbath at 65°C for 10 min. This was followed by incubation with 2 µl of 5X First Strand Buffer, 1 µl of 0.1 M Dithiothreitol (DTT), 0.5 µl of 10 mM dNTP mix and 1.2 µl of AffinityScript RNase Block Mix at 40°C for 2 h. Immediately following cDNA synthesis, the mixture was added with 3.2 µl of 5X Transcription Buffer, 0.6 µl of 0.1 M DTT, 1 µl of NTP mix, 0.21 µl of T7 RNA polymerase Blend and 0.24 µl of Cyanine 3-CTP and then incubated at 40°C for 2 h.

Labeled RNAs was then purified with RNeasy mini spin columns (Qiagen RNeasy mini kit) to wash off unincorporated dyes. Briefly, 84 µl of nuclease free water, 350 µl of Buffer RLT and 250 µl of absolute ethanol were added to the samples. Then, 700 µl of the mixture was transferred to the spin column and centrifuged at 4°C for 30 s at 13000 rpm. The flow-through was discarded. This was followed by adding 500 µl of Buffer RPE and centrifuged at 4°C for 30 s at 13000 rpm. Then, another 500 µl of Buffer RPE was added and the column was centrifuged at 4°C for 1 min at 13000 rpm. Finally, the cRNA was eluted with 30 µl of nuclease free water and centrifuged at 4°C for 30 s at 13000 rpm to collect the flow through. The quantity and specific activity of cRNAs were then determined on Nanodrop ND-1000 UV–VIS spectrophotometer and calculated based on the formula below. Recommended cRNAs yield and specific activity were 0.825 µg and >=6, respectively.

$$\text{Yield} = \frac{(\text{Concentration of cRNA}) \times 30\ \mu\text{L (elution volume)}}{1000} = \mu\text{g of cRNA}$$

$$\text{Specific activity} = \frac{\text{Concentration of Cy3}}{\text{Concentration of cRNA}} \times 1000 = \text{pmol Cy3 per } \mu\text{g cRNA}$$

Six hundred nanograms of labeled cRNAs were then combined with 5 µl of 10X Blocking Agent and 1 µl of 25X Fragmentation Buffer in a final volume of 25 µl and incubated at 60°C for 30 min in the dark. The mixture was then added with 25 µl of 2X Hi-RPM Hybridisation Buffer. Forty microliter of the mixture was applied to SurePrint G3 Human GE 8x60K V2 Microarray Kit (Agilent Technologies, USA) and the array was hybridised at 65°C for 17 h with 10 rpm. Following hybridisation, the array was washed with Wash Buffer 1 and then prewarm Wash Buffer 2 for 1 min. The array was then scanned with Agilent DNA Microarray Scanner (G2505C) and Agilent Feature Extraction Software Version 10.7.3.1 was used to extract data from raw microarray image files in preparation for analysis. Sample preparation procedure was illustrated in Figure 3.1.

### 3.3.4 mRNA microarray data analysis

After feature extraction, the quality of the gene expression data was evaluated according to the QC metrics as shown in Table 3.6. Then, the microarray data were imported to GeneSpring software version 13.0 for further analysis. All the data were thresholded to 1 and normalised to 75$^{th}$ percentile. Baseline transformation was performed to median of all samples. The entities were then filtered where at least 1 sample out of 30 samples has 'present' and 'marginal' flags.

Significant differentially expressed genes between normal controls and MM samples were then identified by unpaired t-test. The Benjamin Hochberg false discovery rate multiple testing correction was applied. Entities were filtered at corrected p-value cut-off 0.01 and fold change ≥2.0. Hierarchical clustering analysis was performed to assess correlations among samples for each identified gene set with Euclidean distance metric and average linkage statistical methods. All the significance level of differentially expressed genes reported in this thesis is refers to the corrected $p<0.01$.

Pathway analysis was performed by using GeneSpring software version 13.0 to search for pathways that are statistically associated with the significantly differentially expressed genes (fold change ≥2.0 and $p<0.01$) in MM.

**Table 3.5:** Characteristics of 19 multiple myeloma patients

| Parameter at diagnosis | No. of patients (%) |
|---|---|
| Gender | |
| Male | 10 (52.63) |
| Female | 9 (47.37) |
| Age (years) | |
| ≤55 | 7 (36.84) |
| >55 | 12 (63.16) |
| Ethnic | |
| Malay | 11 (57.89) |
| Chinese | 3 (15.79) |
| Indian | - |
| Others | 5 (26.32) |
| Disease status | |
| New | 17 (89.47) |
| Relapse | 2 (10.53) |
| Karyotype (G-band) | |
| Abnormal[a] | 1 (5.26) |
| Normal | 13 (68.42) |
| Unknown[b] | 5 (26.32) |

[a] Hypodiploidy were seen with karyotyping
[b] Insufficient/ short/ no chromosome spread were available for cytogenetic analysis

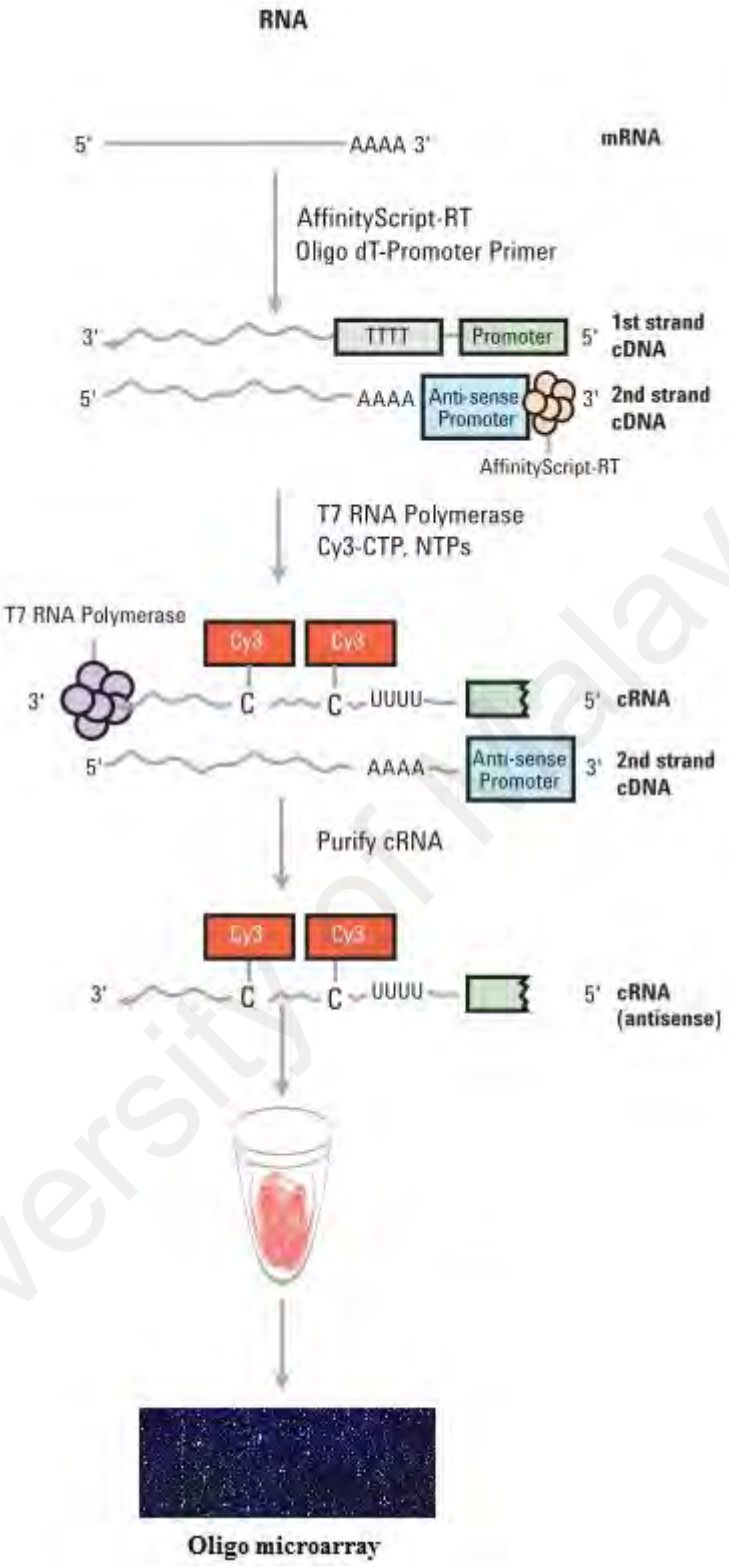


**Figure 3.1:** Schematic of amplified cRNAs procedure. 100 ng of total RNAs were used for labeling. The labeled cRNAs (600 ng) were hybridised onto SurePrint G3 Human GE 8x60K V2 Microarray Kit (Agilent Technologies, USA, obtained and modified from Agilent one colour microarray based gene expression analysis protocol).

**Table 3.6:** Quality control metrics for mRNA expression array

| Metric Name | Good | Evaluate |
|---|---|---|
| Is good grid | >1 | <1 |
| Percentage of feature that are non-uniformity outlier | <1 | >1 |
| Average of negative control net signal | <120 | >120 |
| Average of negative control background subtracted signal | -12 to 5 | <-12 or >5 |
| Standard deviation of negative control background subtracted signal | <10 | >10 |
| Residual of background detrending fit | <15 | >15 |
| The median percentage coefficient of variations for replicate non-control probes using the processed signal | 0-8 | <0 or >8 |
| The median percentage coefficient of variations for replicate spike-in controls using the processed signal | 0-8 | <0 or >8 |
| Absolute of slope of fit for signal vs concentration of E1a (spike in controls) | 0.9-1.2 | <0.9 or >1.2 |
| Detection limit | 0.01-2 | <0.01 or >2 |

### 3.3.5 Verification of microarray data by RT-qPCR

Four differentially expressed genes from microarray analysis were selected for further verification by using TaqMan RT-qPCR. They were *CCNA2*, *RASGRF2*, *RAD54L* and *HKDC1*. RT-qPCR was performed for 23-25 MM samples and 2 normal bloods NB1 and NB2 as controls. Information of these probes was listed in Table 3.4. The RT-qPCR was performed as described in section 3.2.4, in which *GAPDH* was used as the internal control gene. The fold differences/ relative quantification for the gene expression were calculated according to the formula stated under section 3.2.4.

## 3.4 MICRORNA (MIRNA) EXPRESSION STUDY OF MM

MicroRNA (miRNA) expression profiling was performed for the same cohort of samples used in gene expression study (19 clinical specimens, 8 myeloma cell lines and 3 normal controls) using one colour Agilent miRNA Complete Labeling and Hybridisation Kit and Agilent SurePrint Human miRNA Microarray, release 19.0, 8 X 60K microarray chip. This chip contained approximately 60K control probes and replicate probes of 2006 miRNAs. Characteristics of 19 MM patients were shown in Table 3.5. Expression levels of approximately 2006 miRNAs were evaluated for each sample. The miRNA microarray data generated in this study are available in the NCBI Gene Expression Omnibus (GEO) as series accession identifier GSE73048.

### 3.4.1 miRNA microarray sample preparation

Total RNAs were extracted from the bone marrow/ blood/ cells following the protocol as described in sections 3.3.3 (first paragraph) followed by 3.2.3. All labeling and hybridisation reaction were performed with Agilent miRNA Complete Labeling and Hybidisation Kit (Agilent Technologies) according to manufacturer's standard processing recommendations. Briefly, 100 ng of total RNAs from each sample was used for each array. The total RNAs were dephosphorylated with 0.5 µl of calf intestinal alkaline phosphatase, 0.4 µl of 10X calf intestinal phosphatase buffer and 1.1 µl of the diluted labeling Spike-in solution. The mixture was incubated at 37°C for 30 min. The mixture was then denatured by adding 2.8 µl of DMSO and incubated at 100°C for 5-10 min. The mixture was then ligated by adding 1.0 µl of 10X T4 RNA Ligase Buffer, 0.5 µl of T4 RNA Ligase and 3.0 µl of Cyanine3-pCp immediately after incubation. The mixture was then incubated at 16°C for 2 h.

Labeled RNAs were purified with MicroBioSpin 6 Column (Bio-Rad) to wash off unincorporated dyes. Briefly, the tip and cap of the MicroBioSpin Gel Column were removed to allow the buffer to drip into the collection tube. Then, the column was centrifuged at 1000 x *g* for 2 min. The flow-through was discarded. Then 38.7 µl of nuclease free water was added to each labeled sample and transferred into the gel bed. The tube was then centrifuged for 4 min at 1000 x *g* to elute the purified sample. Then, the purified labeled RNAs were dried in a vacuum concentrator at low heat about 30-45 min. Labeled miRNAs were resuspended with 17 µl of nuclease free water and mix with 1 µl of diluted Hybridisation Spike-In, 4.5 µl of GE Blocking Agent and 22.5 µl of Hi-RPM Hybridisation Buffer. Forty microliter of the mixture was hybridised onto a SurePrint Human miRNA Microarray, release 19.0, 8 X 60K microarray chip (Agilent Technologies) and incubated for 20 h at 55°C with 10 rpm. Following hybridisation, the array was washed in Wash Buffer 1 and then prewarm Wash Buffer 2, each for 1 min. The array was then scanned with Agilent array scanner G2505C. Image was analysed with Agilent Feature Extraction Software Version 10.7.3.1.

### 3.4.2 miRNA microarray data analysis

Before the miRNA data was imported into GeneSpring software for further statistical analysis, the quality of each array was evaluated based on the QC metrics listed in Table 3.7. After QC check, the data were then imported into GeneSpring software version 13.0 for analysis. The miRNA data were filtered at threshold 1. Normalisation was performed at 75$^{th}$ percentile. The entities were then filtered where at least 1 sample out of 30 samples have 'present' flag.

Significant differentially expressed miRNAs were identified by unpaired unequal variance t-test. The Benjamin Hochberg false discovery rate multiple testing correction was applied. Entities were filtered at corrected p-value cut-off 0.05 and fold

change ≥2.0. All the significance level of differentially expressed miRNA reported in this thesis is refers to the corrected $p<0.05$. Hierarchical clustering analysis was performed to assess correlations among samples for each identified gene set with Euclidean distance metric and average linkage statistical methods. Identification of differentially expressed target genes regulated by the differentially expressed miRNAs were predicted by TargetScan database which is integrated in GeneSpring Software. Integrative analysis of differentially expressed miRNA and mRNA expression profiles was performed at p-value cut off 0.05.

**Table 3.7:** Quality control metrics for miRNA expression array

| Metric Name | Excellent | Good | Evaluate |
|---|---|---|---|
| Is Good Grid | >1 | NA | <1 |
| Additive error (feature background noise) | <5 | 5-12 | >12 |
| Percentage of feature that are called population outlier | <8 | 8-15 | >15 |
| The median percentage coefficient of variations of background subtracted signals for replicate non-control probes | 0-10 | 10-15 | <0 or >15 |
| Labeling spike-in signal | | >2.50 | <2.50 |
| Hybridisation spike-in signal | | >2.50 | <2.50 |
| 75 percentile total gene signals (overall intensity of non-control probes) | 0.1 | | |

### 3.4.3 Verification of miRNA microarray results by RT-qPCR

Two differentially expressed miRNAs from microarray results were selected for further verification by RT-qPCR (miR-150-5p and miR-4430) using 20-22 MM samples and 2 normal bloods NB1 and NB2 as controls. Briefly, first strand cDNA synthesis was carried out using miScript Reverse Transcription Kit (Qiagen) in a final volume of 20 µl containing 4 µl of 5X miScript HiSpec Buffer, 2 µl of 10X miScript Nucleic Mix, 2 µl of miScript Reverse Transcriptase Mix and 500 ng of RNA template. All cDNA synthesis reaction was performed at 37°C for 1 h and stop at 95°C for 10 min in a thermal cycler.

Quantification of miRNA expression level was performed by using miScript SYBR Green PCR Kit (Qiagen). Commercially available validated primers were used (Table 3.8). RNU6 was used as the internal control miRNA. Each sample of 25 µl reactions containing 12.5 µl of 2X QuantiTect SYBR Green PCR master mix, 2.5 µl of primer and 2 µl of cDNA (50 ng) was prepared in duplicate. All RT-qPCR reactions were run on a Rotor-Gene Q 2-Plex (Qiagen, Hilden, Germany). Thermal cycling conditions were 95°C for 15 min, followed by 40 cycles of 94°C for 15 s, 55°C for 30 s and 70°C for 30 s. All samples were normalised to RNU6 and fold change of miRNA expression levels in MM relative to the normal controls were calculated through relative quantification ($2^{-\Delta\Delta Ct}$) (refer to formula in section 3.2.4).

**Table 3.8:** miRNA primers for RT-qPCR

| No | miRNA | Sequences |
|---|---|---|
| 1 | miR-150-5p | GeneCopoeia, Inc. (Cat. No.: HmiRQP0210) |
| 2 | miR-4430 | GeneCopoeia, Inc. (Cat. No.: HmiRQP2054) |
| 3 | RNU6 | GeneCopoeia, Inc. (Cat. No.: HmiRQP9001) |

## 3.5 STATISTICAL ANALYSIS

Statistical analysis for RNAi experiments, RT-qPCR, MTT, apoptosis and ELISA assays was performed using student t-test and statistical significance was defined as $p<0.05$, $p<0.01$ or $p<0.001$ whenever appropriate. Data were expressed as mean± SD for two or three independent experiments.

# CHAPTER 4: RESULTS

## 4.1 COPY NUMBER VARIATION STUDY OF MM

To identify copy number variations (CNVs) in MM, array comparative genomic hybridisation (aCGH) was performed for a total of 63 newly diagnosed MM patients using Agilent two colour labeling system and Agilent Human Genome CGH Microarray Kit 244k. The copy number variations in MM were determined by comparing the aCGH profiles of MM against normal controls using Agilent DNA Analytics software (v4.0). Two chromosomal gain regions detected by aCGH were selected for verification by using TaqMan Copy Number Assay. They were chromosomal regions 1q42.3 and 7q22.3, in which *LYST* and *NAMPT* genes are localised, respectively.

### 4.1.1 Genomic DNA extraction and purification

Genomic DNAs were isolated from 63 archival fixed bone marrow cells of MM patients and whole blood obtained from 60 healthy volunteers. Normal blood were divided into 6 groups, in which each group was pooled from 10 gender and ethnicity matched healthy individuals: male Malays (N1), female Malays (N2), male Chinese (N3), female Chinese (N4), male Indians (N5) and female Indians (N6). The integrity of the genomic DNAs was checked on 1% (w/v) agarose gel. As measured by NanoDrop ND-1000 UV-VIS spectrophotometer, all the samples were relatively pure, in which the A260/ A280 ratio were within the range of 1.7-1.9. In addition, the ratio of A260/ A230 of the samples were >2.0, which indicating the absence of organic compounds such as guanidinium isothiocyanate, alcohol and phenol as well as cellular contaminants such as

carbohydrates. Figure 4.1 showed the gel picture of genomic DNAs extracted from 63 MM and 6 pooled normal controls.

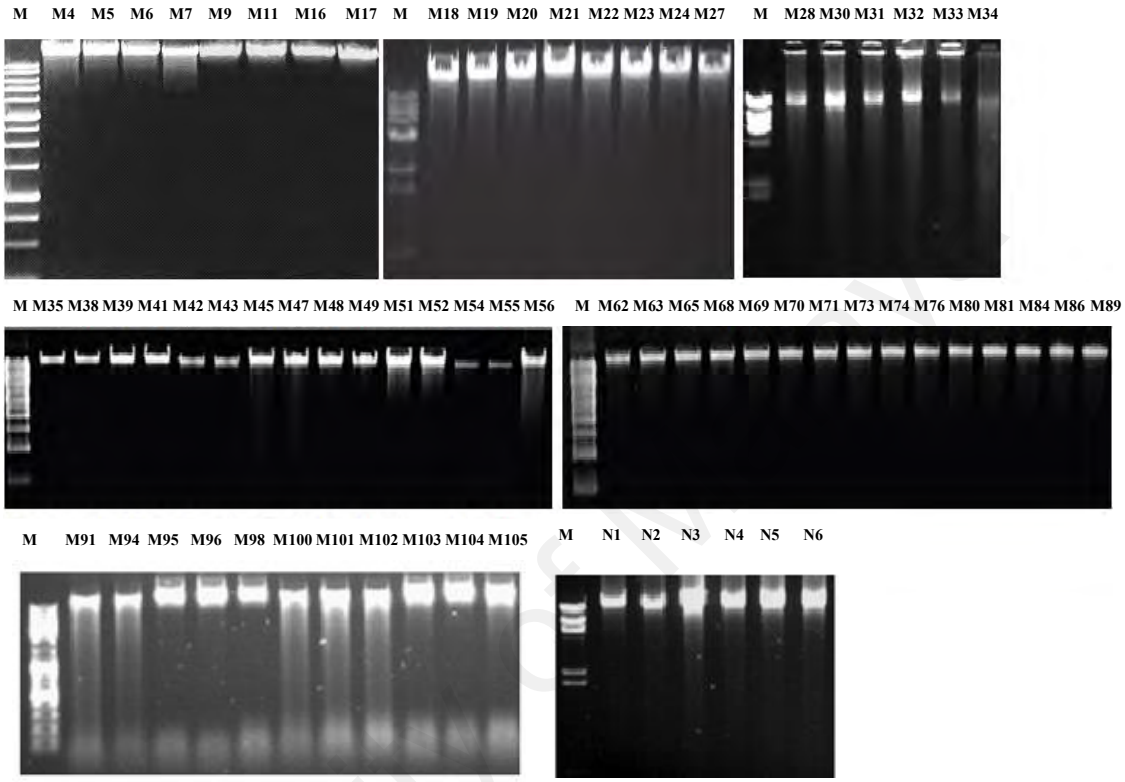


**Figure 4.1:** A representative of agarose gel electrophoresis of genomic DNAs extracted from 63 MM and 6 pooled normal controls (N1-N6). Clear bands of genomic DNAs were observed in all MM and controls with purity (A260/ A280) within the range of 1.7-1.9. M: 1 kb DNA marker N1: male Malays N2: female Malays N3: male Chinese N4: female Chinese N5: male Indians N6: female Indians.

### 4.1.2 Copy number variations (CNVs) were found in 100% of MM patients

A total of 63 aCGH profiles were generated in this study. The quality of each array was checked according to the QC metrics shown in Table 3.2. All the arrays that passed the QC metrics as shown in Table 3.2 were imported to Agilent DNA Analytics software (v4.0) for CNV analysis. Chromosome is always present in two copies in normal human genome. Therefore, the loss or gain of chromosome number is referred as having CNVs and this abnormality may play a critical role in generating disease phenotype. The study findings showed that CNVs were present in 63/63 (100%) of MM cases based on the individual aCGH profile.

Common CNVs is defined as small regions of genomic variations at the same loci across multiple samples. In this study, common CNVs were determined by analysing the aCGH profiles across 63 MM. Common CNVs with >30% of penetrance (percentage of patients carrying the CNVs) was identified. Figure 4.2 shows the copy number of chromosomes numbered 1-22, X and Y, and the percentage of penetrance in 63 MM samples analysed. When all 63 aCGH profiles were combined for analysis, the aCGH findings showed that copy number gains was more frequent than copy number losses in MM. In addition, the long arm of the chromosome (q-arm) is more frequently altered than the short arm (p-arm). Common copy number gains were identified at regions 1q, 2q, 3p, 3q, 4q, 5q, 6q, 7q, 8q, 9q, 10q, 11q, 13q, 14q, 15q, 21q and Xq while common chromosomal losses were identified at regions 14q. Interestingly, 27 and 5 genes are localised within the regions of copy number gains and losses, respectively. Genes residing in these CNV regions are shown in Figure 4.2. Details of the chromosomal regions, molecular regions and genes residing within the CNV regions are shown in Table 4.1. Based on the information on the molecular regions shown in Table 4.1, the aberration fragment sizes were estimated in the range of 1.50 kb-0.23 Mb. Besides that, two probes with different molecular regions were detected at chromosomal

regions where *LYST*, *PICALM* and *SAMSN1* are localised (Table 4.1). In these cases, the percentage of penetrance is calculated by taking the average percentage of penetrance of the two probes.

### 4.1.3 CNVs at chromosomal 1q42.3 and 7q22.3 were confirmed by qPCR

Due to limitation in samples, only 2 CNVs were selected for verification by TaqMan Copy Number Assay. They were at chromosomal regions 1q42.3 and 7q22.3. Gains of chromosomal 1q42.3 and 7q22.3 were identified in 47% (average of 2 identified probes, refer to Table 4.1) and 92% of samples studied (n=63) by aCGH analysis. The *LYST* and *NAMPT* were localised within 1q42.3 and 7q22.3, respectively. Chromosomal gain at 7q22.3 was selected for verification because high percentage of MM patients carrying this CNV (92%) and the gene residing in this aberration region, *NAMPT*, is an important enzyme involved in the pathogenesis of various human cancers including MM (the role of *NAMPT* is discussed in Chapter 1). On the other hand, gain at chromosomal region 1q42.3 was selected for verification because the gene residing in this aberration region, *LYST*, is a novel gene that has never been reported in association with human malignancies. The role of *LYST* is thought to maintain the lysosomal size, granule size and autophagy mechanism in human cells (Cullinane *et al*., 2013). Its relationship in myeloma development is unclear and it may be gene that worthy of future investigation.

Ten samples which showed copy number gains by greater than $\log_2$ ratio of 0.3 (>1.7 folds) at chromosomal segments 1q42.3 or 7q22.3 in aCGH were selected for qPCR verification (Chapter 3, section 3.1.5). The qPCR results were analysed with CopyCaller software v2.0. In CopyCaller software v2.0, samples with copy number of <1.50 or >2.50 copies will be called as having copy number change. The qPCR results

revealed that 9 out of 10 samples showed copy number gain at chromosomal 1q42.3 except for M24, which was detected as 2.31 copies (Figure 4.3A). Similarly, significant copy number gain at chromosomal 7q22.3 was also identified in 9 out of 10 samples except for M07, which was detected as 2.42 copies (Figure 4.3B). Although M24 and M07 were not called as having significant gains at 1q42.3 and 7q22.3, respectively by CopyCaller software v2.0, their copy numbers were very close to 2.50 (M24 = 2.31 and M07 = 2.42). In addition, 6 samples without copy number alteration at these regions in aCGH were used as negative controls in qPCR. They were M38, M56 and M102 for chromosomal 1q42.3 and M49, M47 and M56 for chromosomal 7q22.3. The qPCR results showed that there were 2 copies of chromosomal 1q42.3 in M38, M56 and M102 and 2 copies of chromosomal 7q22.3 in M49, M47 and M56 (Figure 4.3A & B). This scenario indicated that these samples are without copy number change at the chromosomal regions analysed and further confirmed the reliability of CNVs identified in aCGH profiles.

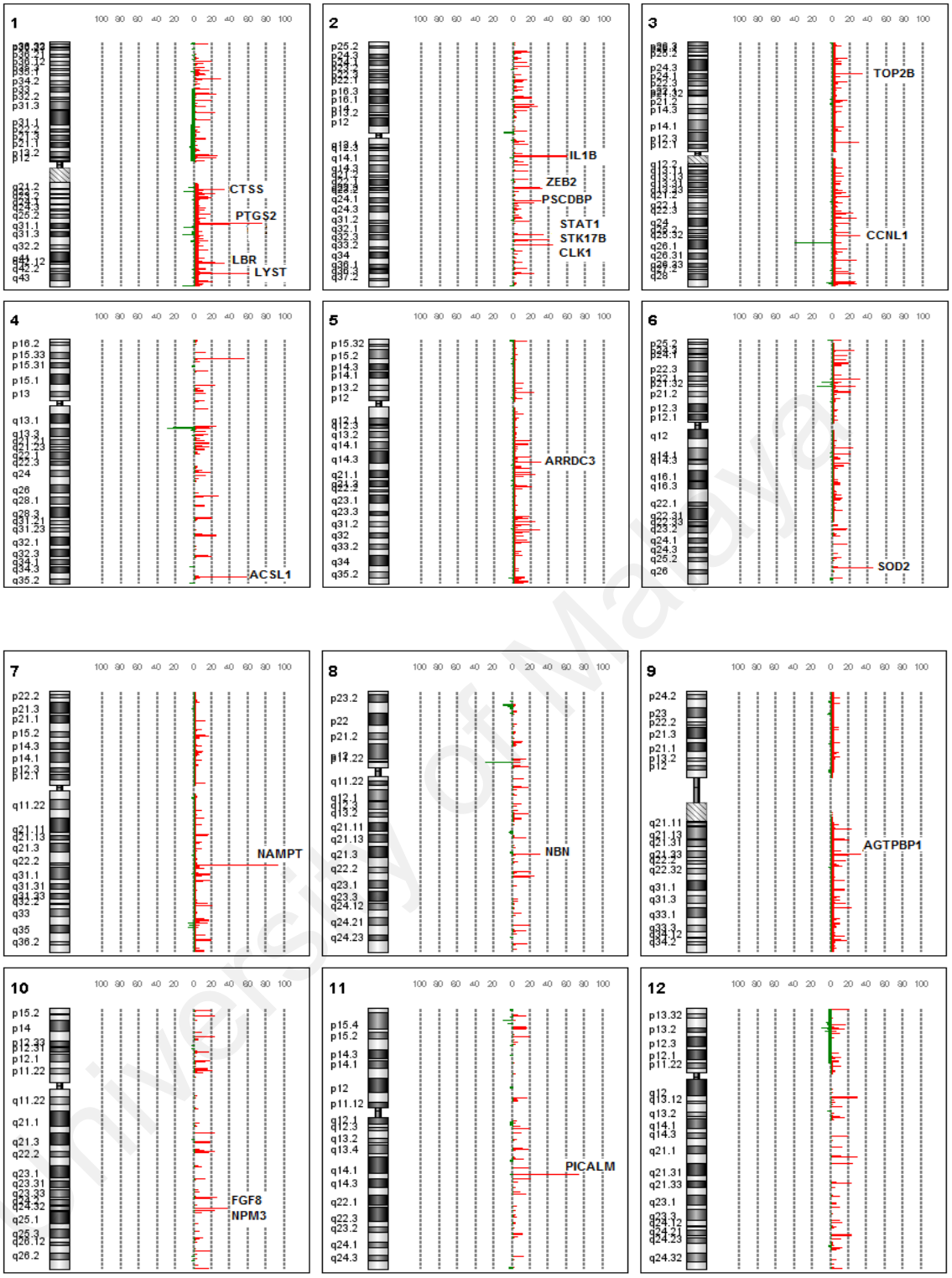


**Figure 4.2:** Copy number in chromosomes numbered 1-22, X and Y and percentage of penetrance in 63 MM samples analysed. Copy number gains and losses were indicated in red and green, respectively. Percentage of penetrance (0-100) is indicated on the top of each chromosome. Genes localised within the CNV regions by >30% of penetrance are indicated.

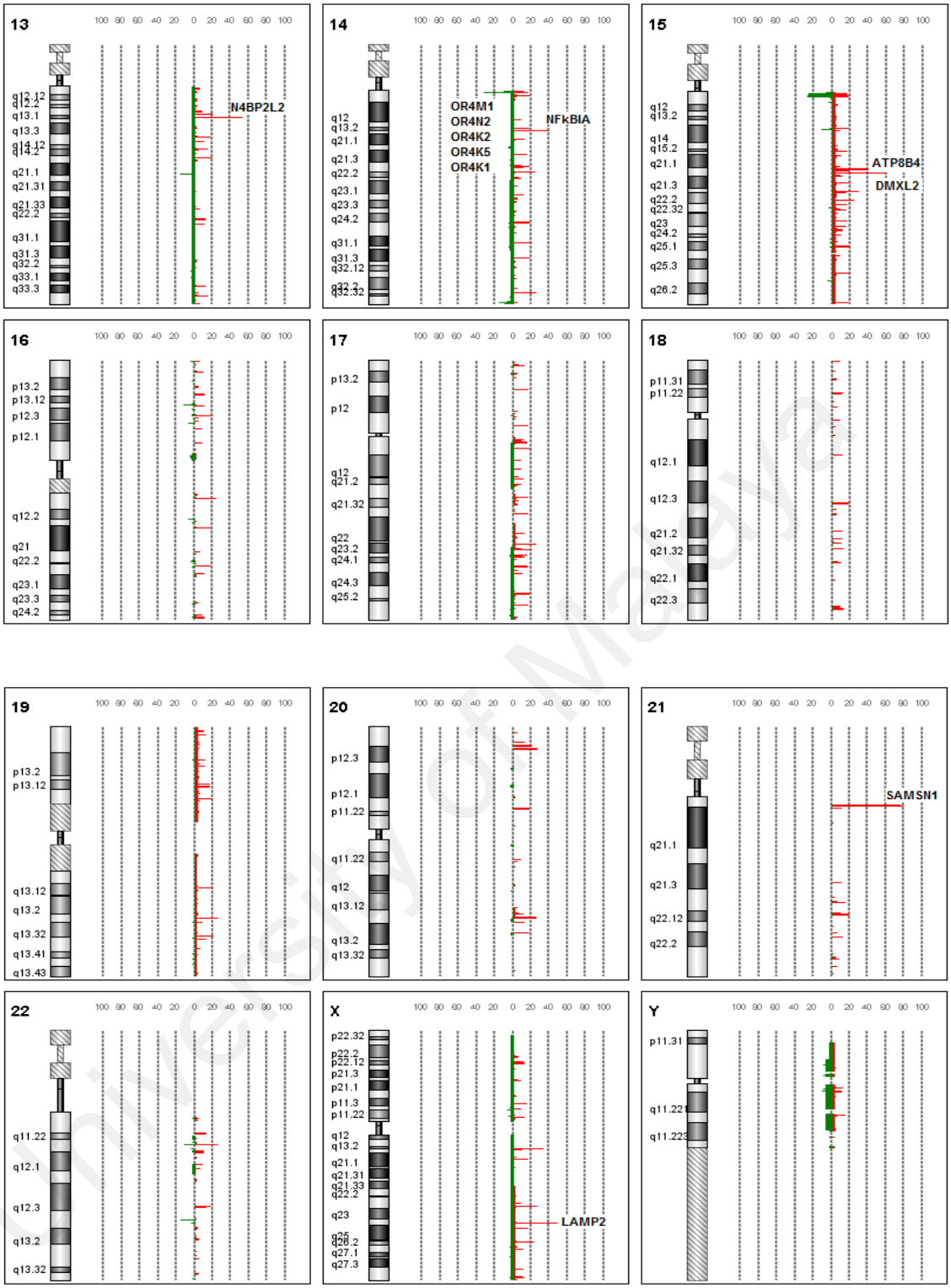


**Figure 4.2,** continued

**Table 4.1:** Common CNVs and their molecular regions and genes residing within the CNV regions (>30% penetrance and at $p<0.05$)

| Chromosome region | Molecular region | Aberrations | Penetrance | Gene |
|---|---|---|---|---|
| 1q21.2 | 148971976-149005023 | Gain | 33.3 | *CTSS* |
| 1q31.1 | 184907807-184911998 | Gain | 38.1 | *PTGS2* |
| 1q42.12 | 223656252-223669792 | Gain | 33.3 | *LBR* |
| 1q42.3 | 233892433-233926797 | Gain | 33.3 | *LYST* |
| 1q42.3 | 233926797-234063688 | Gain | 60.3 | *LYST* |
| 2q13 | 113303764-113310939 | Gain | 58.7 | *IL1B* |
| 2q22.3 | 144973952-144987741 | Gain | 31.7 | *ZEB2* |
| 2q24.1 | 157979874-158003860 | Gain | 30.2 | *PSCDBP* |
| 2q32.2 | 191549646-191572786 | Gain | 33.3 | *STAT1* |
| 2q32.3 | 196729308-196742885 | Gain | 39.7 | *STK17B* |
| 2q33.1 | 201430495-201434570 | Gain | 42.9 | *CLK1* |
| 3p24.2 | 25625572-25659041 | Gain | 33.3 | *TOP2B* |
| 3q25.31 | 158349618-158359603 | Gain | 30.2 | *CCNL1* |
| 4q35.1 | 185914232-185983415 | Gain | 57.1 | *ACSL1* |
| 5q14.3 | 90700575-90713014 | Gain | 30.2 | *ARRDC3* |
| 6q25.3 | 160023082-160033676 | Gain | 44.4 | *SOD2* |
| 7q22.3 | 105685720-105700507 | Gain | 92.1 | *NAMPT* |
| 8q21.3 | 91015377-91052791 | Gain | 30.2 | *NBN* |
| 9q21.33 | 87423777-87474448 | Gain | 33.3 | *AGTPBP1* |
| 10q24.32 | 103536061-103549109 | Gain | 36.5 | *FGF8, NPM3* |
| 11q14.21 | 85400842-85420427 | Gain | 73.0 | *PICALM* |
| 11q14.21 | 85420427-85452836 | Gain | 71.4 | *PICALM* |
| 13q13.1 | 31999429-32009312 | Gain | 52.4 | *N4BP2L2* |

**Table 4.1,** continued

| Chromosome region | Molecular region | Aberrations | Penetrance | Gene |
|---|---|---|---|---|
| 14q13.2 | 34940549-34942054 | Gain | 39.7 | *NFκBIA* |
| 15q21.2 | 47955679-48186620 | Gain | 39.7 | *ATP8B4* |
| 15q21.2 | 49537775-49626995 | Gain | 58.7 | *DMXL2* |
| 21q11.2 | 14794626-14815532 | Gain | 77.8 | *SAMSN1* |
| 21q11.2 | 14815532-14840578 | Gain | 76.2 | *SAMSN1* |
| Xq24 | 119454654-119467091 | Gain | 49.2 | *LAMP2* |
| 14q11.2 | 19297526-19473980 | Loss | 31.7 | *OR4M1, OR4N2, OR4K2, OR4K5, OR4K1* |

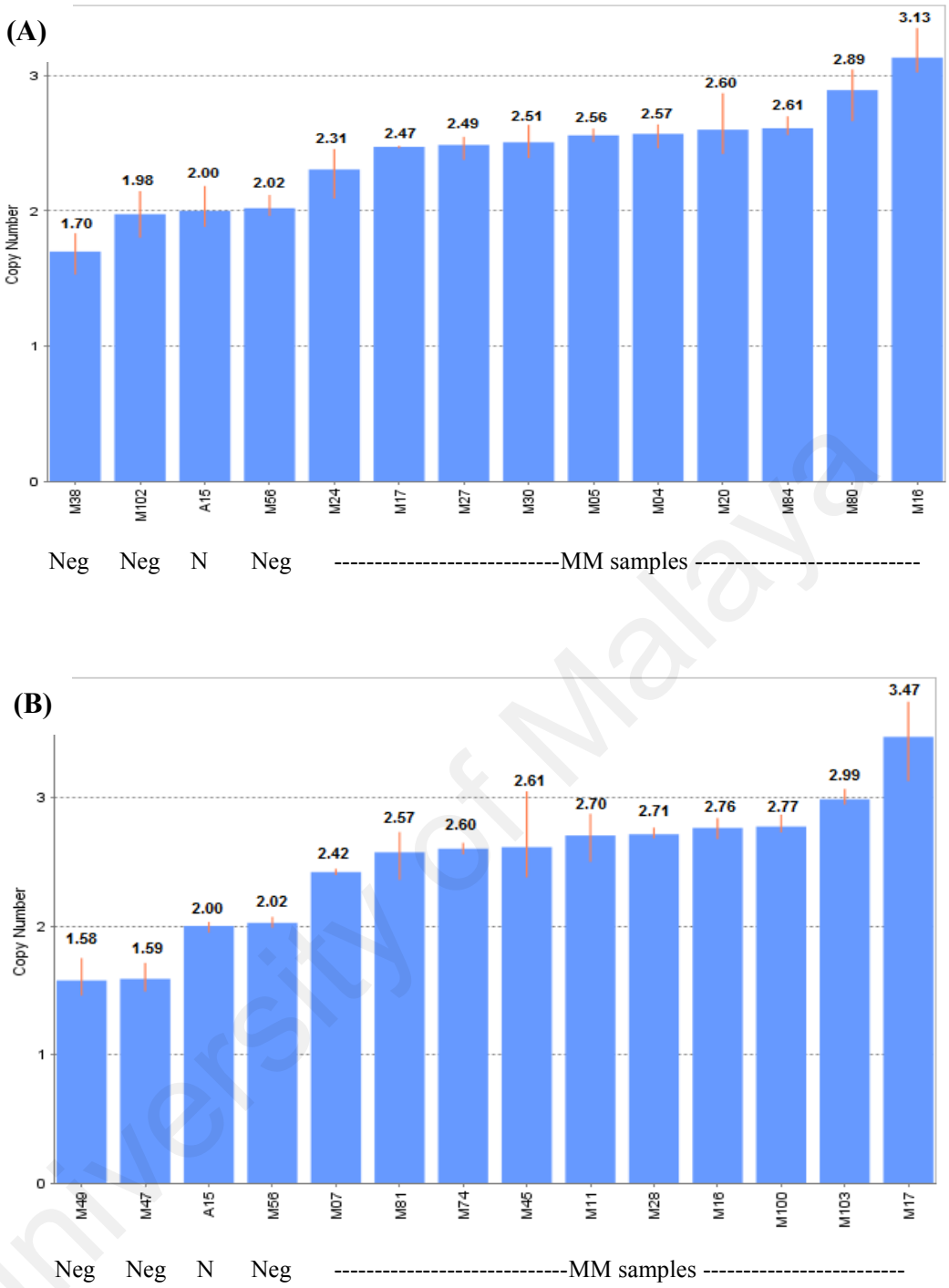


**Figure 4.3:** Copy number profiles of chromosomal regions 1q42.3 and 7q22.3 in MM samples. (A) Copy number profile for *LYST* gene, localised at chromosome 1q42.3 for 10 selected samples. Two copies of target were detected in negative controls (M38, M102 and M56). (B) Copy number profile for *NAMPT* gene, localised at chromosome 7q22.3 for 10 selected samples. Two copies of target were detected in negative controls (M47, M49 and M56). Two copies of target were detected in peripheral blood from normal individual (A15). Negative controls are MM samples without copy number alteration as analysed by aCGH. Each sample bar represented the mean calculated copy number for three sample replicates with an error bar shows the standard deviation. Neg: negative controls; N: normal control; MM: multiple myeloma.

## 4.2 *NAMPT* RNA INTERFERENCE (RNAi)

The aCGH findings revealed gain of chromosomal 7q22.3 in 92% of MM cases (n=63). This is the most common copy number gain region detected in aCGH study. Interestingly, *NAMPT* is a potential gene residing in this aberration region. The *NAMPT* is an important enzyme involved in $NAD^+$ salvage pathway and its expression level is elevated in various human cancers including MM (as discussed in Chapter 1). Elevated expression of *NAMPT* in MM highlighted its important roles in the transformation and progression of myeloma disease. In this study, the function of *NAMPT* gene in myeloma cell growth and survival was evaluated by RNA interference (RNAi) approach. In RNAi experiments, RPMI-8226 myeloma cell line was selected as host cells because it is easy-to-transfect compared to other MM cell lines. The *NAMPT*-mediated silencing effects on cell proliferation and apoptosis in RPMI-8226 were determined by using MTT and Annexin-V-FITC/ propidium iodide (PI) assays, respectively. The gene silencing effects on NAMPT protein expression was evaluated by ELISA assay.

### 4.2.1 Silencing of *NAMPT* gene with siRNA duplexes

The *NAMPT* mRNA expression was successfully knockdown by introducing siRNA duplexes into RPMI-8226 myeloma cells. Figure 4.4 shows the uptake of pmaxGFP by RPMI-8226 cells at 24 h post-transfection. The suceed of siRNAs delivery in RPMI-8226 myeloma cells was determined by counting the cells, which were transfected with pmaxGFP vectors using haemocytometer. The results revealed that more than 80% of the cells expressed the green fluorescent signals indicating that the transfection was successfully procured. To check whether the siRNAs transfection has successfully silenced the *NAMPT*, the expression of *NAMPT* in cells transfected with siRNA was compared with cells transfected with scrambled negative control using RT-qPCR

approach. The RT-qPCR results showed that the efficiency of the *NAMPT* gene silencing was approximately 50% at 24 h post-transfection when either NAMPT-a, NAMPT-b, or NAMPT-c was used for transfection [Figure 4.5 (A)]. The percentage of gene knockdown was decreased dramatically at 48 h post-transfection. On the other hand, when siRNA duplexes were combined (NAMPT-abc) and used to silence the *NAMPT*, the gene knockdown efficiency was significantly increased by >70% at 24 h post-transfection (20% higher compared to single siRNAs). The stability of the gene knockdown effect was maintained at >70% at 48 h post-transfection when the pooled siRNAs were used [Figure 4.5 (B)]. Given that siRNA pooling not only could increase gene silencing efficiency but also can reduce off-target effects and increase target specificity (Hannus *et al*., 2014). Therefore, in the present study, the siRNA study of *NAMPT* was performed by using pooled siRNAs (NAMPT-abc). The Ct values of *NAMPT* and internal control gene, *GAPDH*, calculated fold change ($2^{-\Delta\Delta Ct}$) and percentage of gene knockdown for siRNAs and scrambled negative control treated cells were measured in 2 independent experiments at 24 h and 48 h post-transfection by RT-qPCR (Table 4.2).

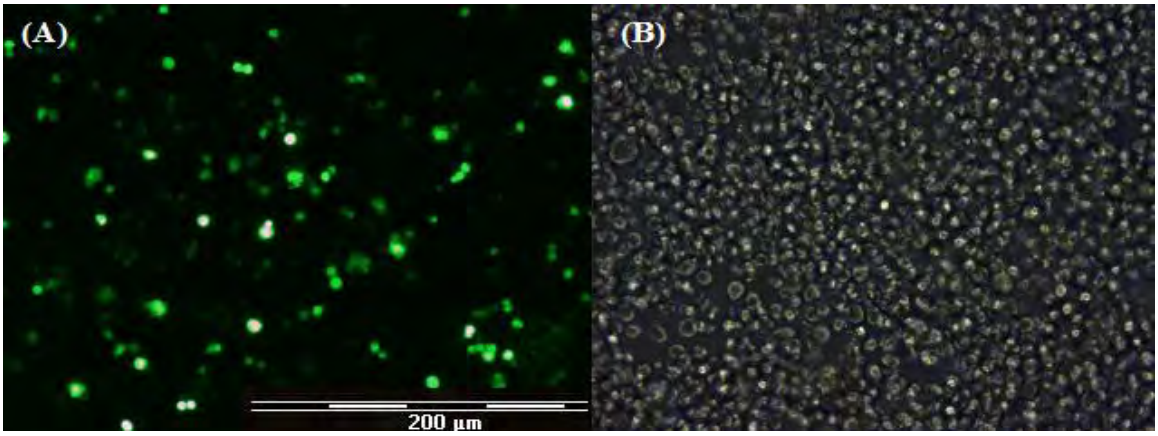


**Figure 4.4:** Estimated transfection efficacy by the up-take of green fluorescent protein by RPMI-8226 cells. (A) RPMI-8226 cells were nucleofected with pmaxGFP; the expression of green fluorescent protein was monitored at 24 h post-transfection. (B) Image of the same cells under regular microscope with the same magnification for (A).

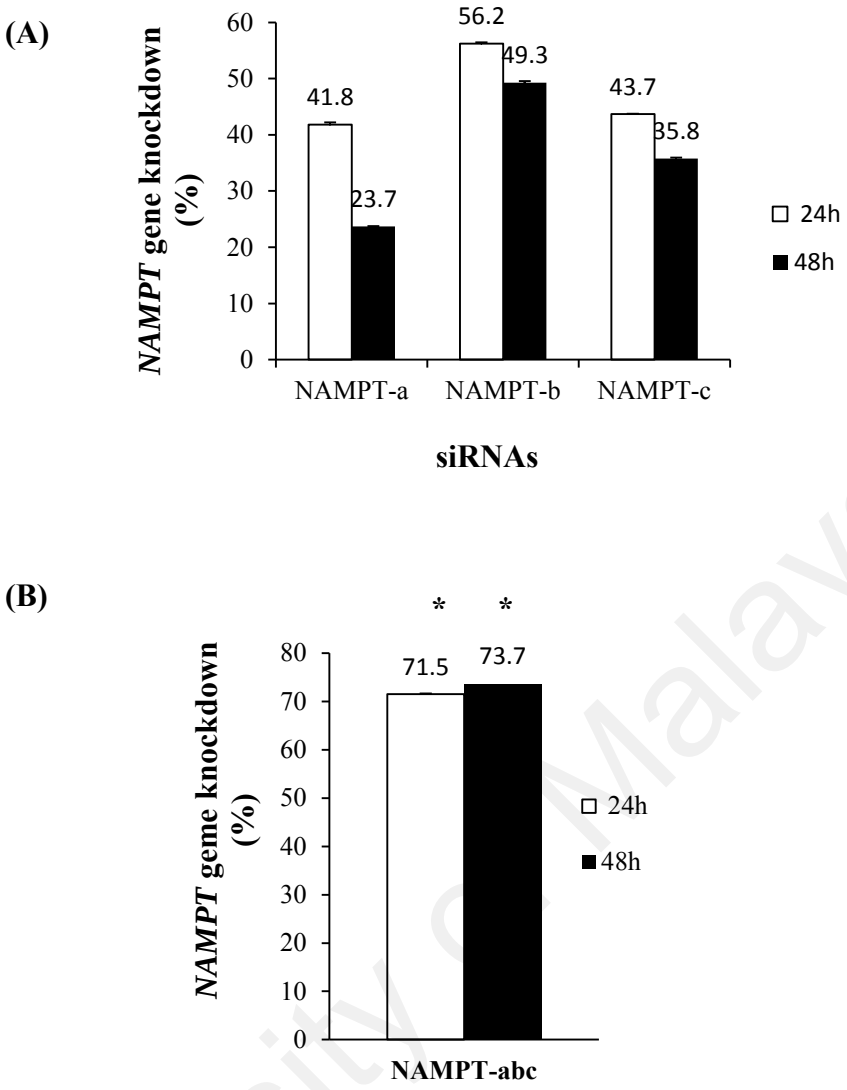


**Figure 4.5:** Effects of transfection with siRNAs on *NAMPT* gene knockdown in RPMI-8226 cells at 24 h and 48 h post-transfection as determined by RT-qPCR. RPMI-8226 cells were transfected with (A) 100 nM of single siRNA duplexes (either NAMPT-a, NAMPT-b, or NAMPT-c). (B) 300 nM of pooled siRNAs, NAMPT-abc (100 nM for each NAMPT-a, NAMPT-b, and NAMPT-c). The *NAMPT* gene expression levels in cells treated with siRNA and scrambled negative control were normalised against internal control *GAPDH* gene and relative quantification was calculated by $2^{-\Delta\Delta Ct}$. *NAMPT* expression was significantly knockdown by NAMPT-abc by >70%. Error bar shows the standard deviation between replicates. * $p<0.05$ compared with the control

**Table 4.2:** The Ct values of *NAMPT* and *GAPDH*, calculated fold change ($2^{-\Delta\Delta Ct}$) and percentage of gene knockdown for cells transfected with siRNAs and scrambled negative control at 24 h and 48 h post-transfection (for 2 independent experiments)

| siRNA | Ct mean 1 (*NAMPT*) | Ct mean 2 (*NAMPT*) | Ct *NAMPT* SD | Ct mean 1 (*GAPDH*) | Ct mean 2 (*GAPDH*) | Ct *GAPDH* SD | ΔCt mean | ΔΔCt | Fold change ($2^{-\Delta\Delta Ct}$) | Gene knockdown (%) |
|---|---|---|---|---|---|---|---|---|---|---|
| NAMPT-a (24h) | 22.20 | 21.93 | 0.06 | 18.39 | 17.90 | 0.06 | 3.92 | 0.78 | 0.58 | 41.8 |
| NAMPT-b (24h) | 22.53 | 22.39 | 0.07 | 18.30 | 17.97 | 0.06 | 4.33 | 1.19 | 0.44 | 56.2 |
| NAMPT-c (24h) | 21.96 | 21.98 | 0.04 | 18.02 | 17.99 | 0.04 | 3.97 | 0.83 | 0.56 | 43.7 |
| NAMPT-abc (24h) | 22.91 | 23.03 | 0.03 | 17.96 | 18.09 | 0.03 | 4.95 | 1.81 | 0.29 | 71.5 |
| NAMPT-a (48h) | 22.14 | 22.19 | 0.07 | 18.60 | 18.67 | 0.07 | 3.53 | 0.39 | 0.76 | 23.7 |
| NAMPT-b (48h) | 23.12 | 22.80 | 0.05 | 18.92 | 18.76 | 0.03 | 4.12 | 0.98 | 0.51 | 49.3 |
| NAMPT-c (48h) | 22.55 | 22.41 | 0.07 | 18.79 | 18.64 | 0.04 | 3.78 | 0.64 | 0.64 | 35.8 |
| NAMPT-abc (48h) | 23.41 | 23.40 | 0.06 | 18.31 | 18.37 | 0.07 | 5.07 | 1.93 | 0.26 | 73.7 |
| Scrambled negative control | 21.80 | 22.22 | 0.09 | 18.86 | 18.89 | 0.02 | 3.14 | | | |

### 4.2.2 *NAMPT*-mediated gene silencing inhibited proliferation of RPMI-8226 cells

The number of viable MM cells transfected with siRNAs and scrambled negative control were measured using MTT assay at 24 h, 48 h and 72 h post-transfection. Cell growth was significant decreased in cells transfected with NAMPT-abc up to 72 h post-transfection when compared to the cells transfected with scrambled negative control siRNA ($p<0.05$) (Figure 4.6). This result suggested that silencing of *NAMPT* gene further inhibited the cell growth in RPMI-8226 cells. The absorbance at 570 nm for NAMPT-abc and scrambled negative control treated cells as determined with MTT assay at 24 h, 48 h and 72 h post-transfection were shown in Table 4.3.

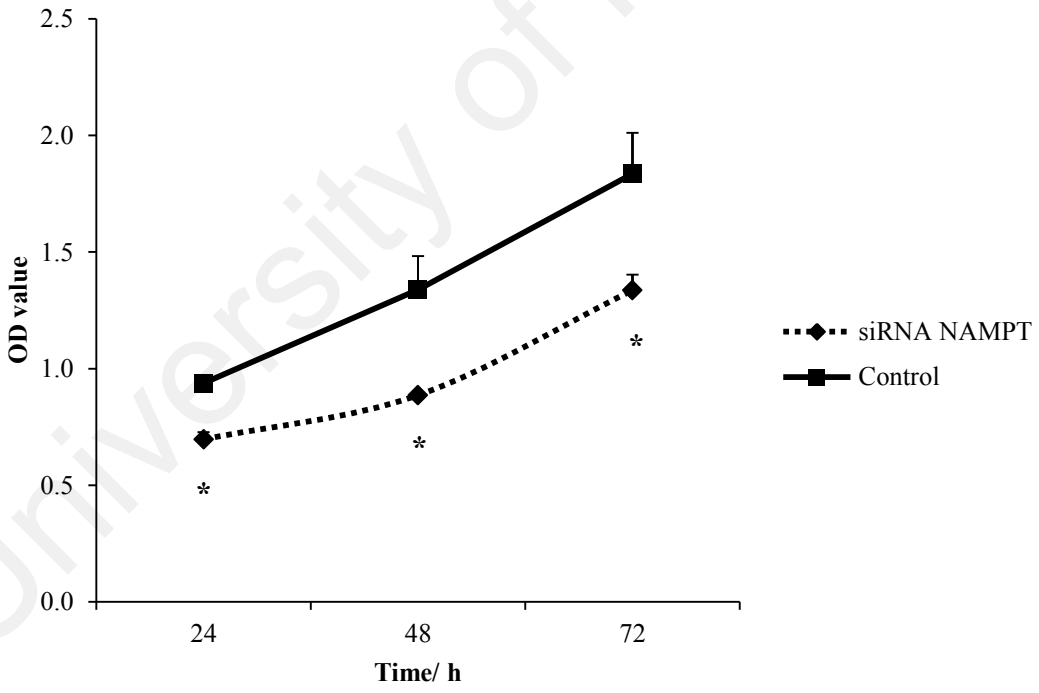


**Figure 4.6:** MTT assay was applied for determining cell proliferation of RPMI-8226 cells following transfection with 300 nM of NAMPT-abc siRNA or scrambled negative control siRNAs. Cells were treated with MTT reagent and absorbance was measured at 570 nm at 24 h, 48 h and 72 h post-transfection. Error bar shows the standard deviation between replicates. *$p<0.05$ compared to the control

**Table 4.3:** Optical density (OD) at 570 nm for RPMI-8226 cells transfected with NAMPT-abc and scrambled negative control as determined with MTT assay at 24 h, 48 h and 72 h post-transfection (for 2 independent transfections)

| siRNA | 24 h | | | | | | 48 h | | | | | | 72 h | | | | | |
|---|---|---|---|---|---|---|---|---|---|---|---|---|---|---|---|---|---|---|
| | Experiment 1 | | Experiment 2 | | OD Mean | SD | Experiment 1 | | Experiment 2 | | Mean | SD | Experiment 1 | | Experiment 2 | | OD Mean | SD |
| | OD 1 | OD 2 | OD 1 | OD 2 | | | OD 1 | OD 2 | OD 1 | OD 2 | | | OD 1 | OD 2 | OD 1 | OD 2 | | |
| **NAMPT -abc** | 0.67 | 0.74 | 0.68 | 0.70 | 0.70 | 0.03 | 0.90 | 0.87 | 0.89 | 0.88 | 0.89 | 0.01 | 1.40 | 1.35 | 1.24 | 1.35 | 1.34 | 0.07 |
| **Control siRNA** | 0.93 | 0.96 | 0.91 | 0.95 | 0.94 | 0.02 | 1.46 | 1.47 | 1.22 | 1.21 | 1.34 | 0.14 | 1.82 | 1.95 | 1.59 | 1.98 | 1.84 | 0.18 |

### 4.2.3 Silencing of *NAMPT* induced apoptosis in RPMI-8226 cells

To investigate the biological effect of *NAMPT*-mediated gene silencing on the apoptosis in RPMI-8226 cells, the apoptotic events of the cells tranfected with NAMPT-abc was determined using Annexin V-FITC/ PI staining at 48 h post-transfection. The flow cytometry analysis showed that the cells transfected with NAMPT-abc significantly increased the numbers of early (7.89% vs 15.57%; $p<0.05$) and late apoptotic cells (21.54% vs 39.50%; $p<0.05$) compared to the cells transfected with scrambled negative control. As shown in Figure 4.7, R4 and R3 region represents the percentage of early and late apoptotic cells, respectively. This result suggests that *NAMPT*-mediated gene silencing could increase apoptotic cell death in RPMI-8226 myeloma cells.

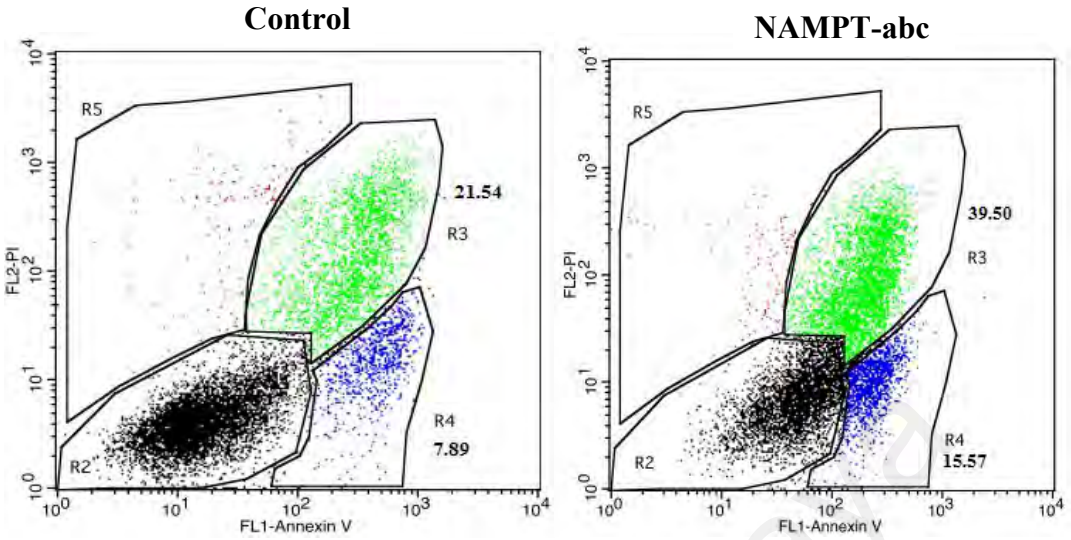


**Figure 4.7:** Analysis of apoptosis in RPMI-8226 cells transfected with scrambled negative control and NAMPT-abc as analysed by flow cytometry at 48 h post-transfection. RPMI-8226 cells were labeled with Annexin-V-FITC and 0.5 µg/ mL of PI. Scatter graphs show significant increased in the numbers of early apoptotic cells (7.89% vs 15.57%; $p<0.05$) and late apoptotic cells (21.54% vs 39.50%; $p<0.05$) compared to the scrambled negative control treated cells. R2 = viable cells; R3 = late apoptotic cells; R4 = early apoptotic cells and R5 = death cells.

### 4.2.4 Decreased protein expression level after the silencing of *NAMPT* gene

ELISA assay was performed to measure the NAMPT protein expression level in RPMI-8226 cells transfected with siRNAs and scrambled negative control. To determine the NAMPT protein concentration in the samples, the standard curve graph was first generated by using 2-fold serial dilutions of the control sample of known concentration (16 ng/ mL – 0.062 ng/ mL) (refer to Chapter 3, section 3.2.7). The standards, samples and controls were then loaded into the ELISA plate in duplicate. After overnight incubation, the plate was washed and read at absorbance of 450 nm in an ELISA plate reader. Table 4.4 shows the absorbance values at 450 nm of the serial diluted standards. The standard curve graph was then plotted based on the absorbance values (450 nm) of serial diluted standards vs its concentration in ng/ mL (Figure 4.8). The protein concentration of siRNAs and scrambled negative control treated cells were determined by the equation $y = 0.1967x$ generated from the standard curve graph, where y is the absorbance at 450 nm and x is the protein concentration (ng/ ml) (Figure 4.8). The absorbance values at 450 nm and NAMPT protein concentrations in NAMPT-abc, NAMPT-b and scrambled negative control treated cells as measured by ELISA assay at 24 h, 48 h and 72 h post transfection were shown in Table 4.5. Figure 4.9 shows the relative NAMPT protein concentration in NAMPT-abc and NAMPT-b treated cells at 24 h, 48 h and 72 h post transfection compared to the scramble negative control treated cells ($p<0.01$).

The ELISA results showed that the *NAMPT* gene knockdown using NAMPT-abc resulted in a dramatic reduction of the NAMPT protein levels as early as 24 h post-transfection ($p<0.01$) (Figure 4.9). Moreover, the ELISA assay exhibited that NAMPT protein expression levels were also reduced in the cells transfected with NAMPT-b although this siRNAs can only knockdown the gene by approximately 50% at 24 h and 48 h post-transfection (Figures 3.5 & 3.9).

**Table 4.4:** Optical density (OD) at 450 nm for 2-fold serial diluted standards as determined with ELISA assay

| Concentration (ng/ ml) | OD 1 | OD 2 | mean | mean – blank |
|---|---|---|---|---|
| Blank | 0.085 | 0.091 | 0.088 | 0.000 |
| 0.0625 | 0.126 | 0.129 | 0.128 | 0.040 |
| 0.1250 | 0.167 | 0.151 | 0.159 | 0.071 |
| 0.2500 | 0.189 | 0.192 | 0.191 | 0.103 |
| 0.5000 | 0.260 | 0.245 | 0.253 | 0.165 |
| 1.0000 | 0.370 | 0.387 | 0.379 | 0.291 |
| 2.0000 | 0.582 | 0.598 | 0.590 | 0.502 |
| 4.0000 | 0.950 | 0.970 | 0.960 | 0.872 |
| 8.0000 | 1.671 | 1.784 | 1.728 | 1.640 |
| 16.0000 | 3.150 | 3.167 | 3.159 | 3.071 |

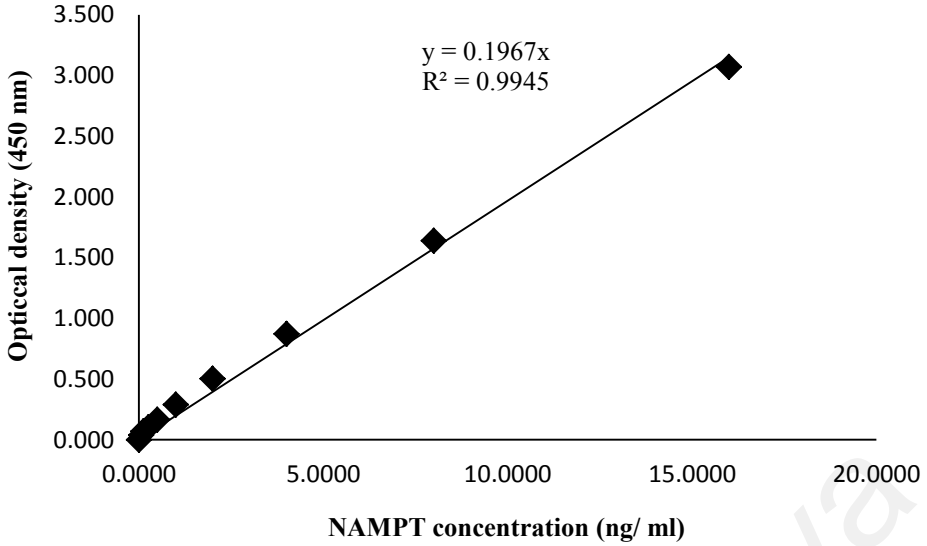


**Figure 4.8:** ELISA standard curve generated from the absorbance at 450 nm of serial diluted standards against concentrations in ng/ ml. The formula line was generated according to the standard curve and individual samples can be quantified with this graph.

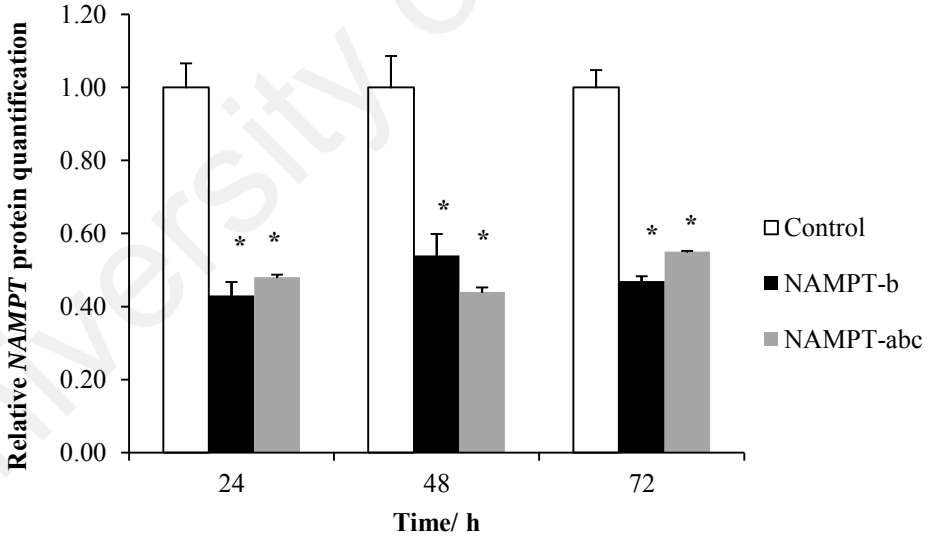


**Figure 4.9:** Relative NAMPT protein concentration in RPMI-8226 cells transfected with NAMPT-b, NAMPT-abc and scrambled negative control siRNAs. Protein expression levels were significantly reduced in RPMI-8226 cells transfected with NAMPT-b and NAMPT-abc compared to the control at 24 h, 48 h and 72 h post-transfection. Error bar shows standard deviation between replicates. * $p<0.01$ compared with the control

**Table 4.5:** Optical density (OD) at 450 nm and NAMPT protein concentrations for RPMI-8226 cells transfected with NAMPT-b, NAMPT-abc and scrambled negative control as measured with ELISA assay at 24 h, 48 h and 72 h post transfection

| siRNA | Time /h | OD 1 | OD 2 | Mean OD | NAMPT concentration (ng/ ml) | SD | CV (%) |
|---|---|---|---|---|---|---|---|
| **NAMPT-b** | 24 | 0.85 | 0.91 | 0.88 | 4.02 | 0.04 | 4.27 |
| | 48 | 1.11 | 1.03 | 1.07 | 5.00 | 0.06 | 5.48 |
| | 72 | 0.97 | 0.95 | 0.96 | 4.42 | 0.01 | 1.40 |
| **NAMPT-abc** | 24 | 0.96 | 0.97 | 0.97 | 4.46 | 0.01 | 0.73 |
| | 48 | 0.88 | 0.89 | 0.89 | 4.05 | 0.01 | 1.36 |
| | 72 | 1.09 | 1.10 | 1.10 | 5.12 | 0.00 | 0.19 |
| **Scramble negative control** | 24 | 1.97 | 1.88 | 1.93 | 9.34 | 0.07 | 3.42 |
| | 48 | 1.96 | 1.84 | 1.90 | 9.19 | 0.09 | 4.51 |
| | 72 | 1.96 | 1.89 | 1.92 | 9.33 | 0.05 | 2.46 |

## 4.3 GENE EXPRESSION STUDY OF MM

Although it is best to use the same sample sets in aCGH for gene expression study so that the correlation between the DNA copy number and gene expression can be studied, unfortunately, the sample sets used in aCGH were not suitable for gene expression microarray. Genomic DNAs are stable in archival bone marrow cells but their RNAs are most likely degraded and not suitable to be used for gene expression study. Therefore, new set of samples consisting of 19 fresh MM specimens and 3 normal controls, and 8 MM cell lines were recruited for gene expression study. The aim of this study was to identify differentially expressed genes underlying the molecular pathogenesis of MM by using Agilent microarray platform. The gene expression study was carried out by using Agilent one colour labeling system and Agilent SurePrint G3 Human GE 8x60K V2 Microarray. By using this array, approximately 60000 probes across the whole genome can be analysed simultaneously in a single experiment. All the gene expression data were analysed by using GeneSpring software version 13.0 to identify differentially expressed genes in MM compared to the normal controls. Four differentially expressed genes (*CCNA2*, *RAD54L*, *RASGRF2* and *HKDC1*) were verified by RT-qPCR using TaqMan gene expression assay.

### 4.3.1 TOTAL RNA isolation

Total RNAs were successfully isolated from 19 fresh MM bone marrow (MM1-MM19), 8 MM cell lines (IM-9, U-266, RPMI-8226, KMS-20, KMS-12-BM, KMS-28-BM, KMS-21-BM and MM.1S) and 3 normal controls (NB1, NB2 and NB3). Agilent's 2100 Bioanalyser results showed that the RNA integrity number was >8.0 in all samples (10 indicating maximum RNA integrity). Gel-like images for all the total RNA samples as generated by Bioanalyser were shown in Figure 4.10 and the RNA integrity number (RIN) for each sample was listed in Table 4.6. All the RNA samples were relatively pure, in which the ratio of A260 nm/ A280 nm was within the range of 1.80-2.10 as measured by NanoDrop ND-1000 UV-VIS spectrophotometer.

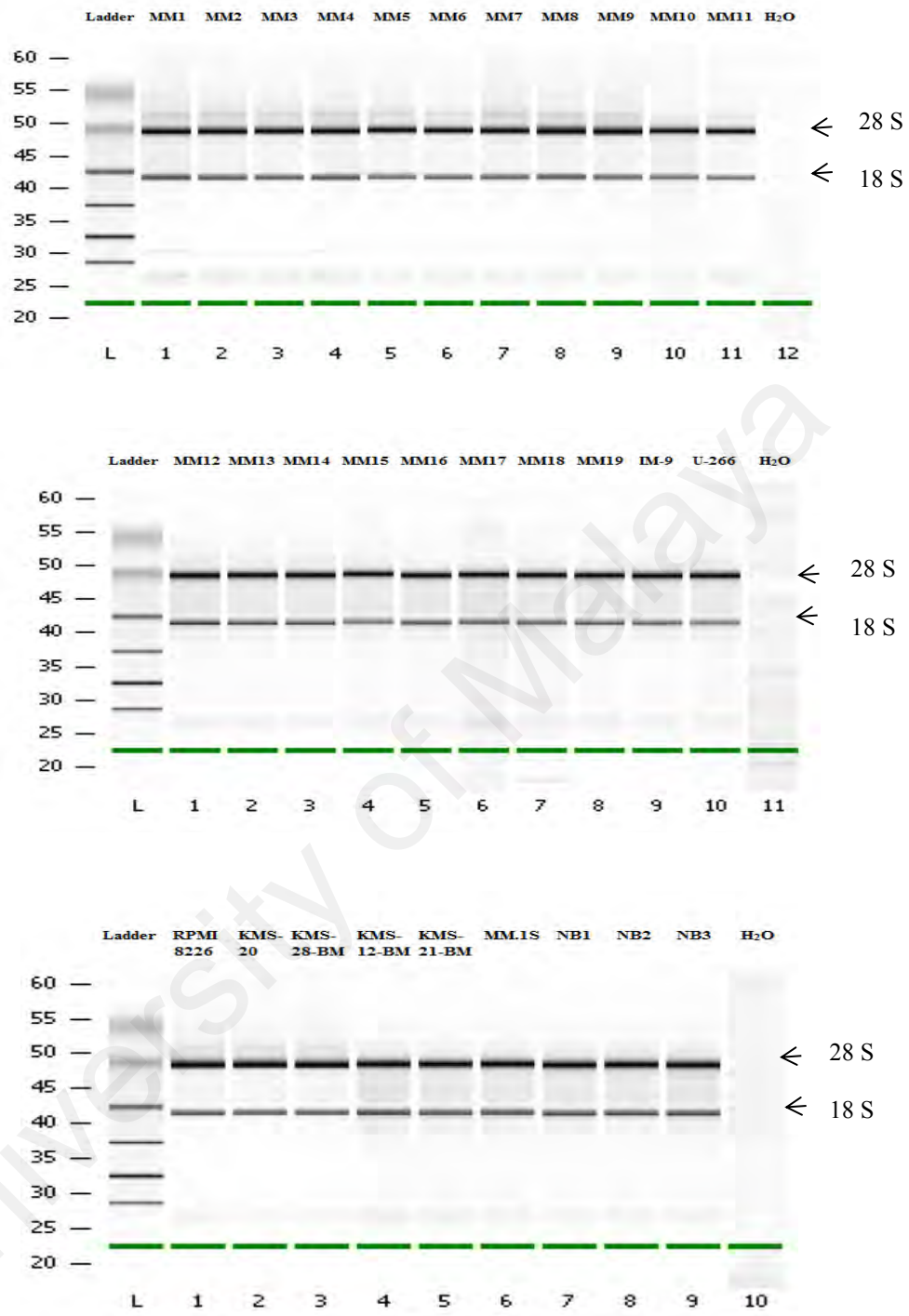


**Figure 4.10:** Gel-like images of total RNAs isolated from 19 MM clinical specimens (MM1-MM19), 8 myeloma cell lines (IM-9, U-266, RPMI-8226, KMS-20, KMS-28-BM, KMS-12-BM, KMS-21-BM and MM.1S) and 3 normal controls (NB1, NB2 and NB3) as generated by Bioanalyser. The 18-S and 28-S ribosomal RNA bands are clearly visible on the gel images.

**Table 4.6:** RNA integrity number (RIN) for each sample as determined by Bioanalyser

| Sample | RNA integrity number (RIN) |
|---|---|
| MM1 | 9.40 |
| MM2 | 9.20 |
| MM3 | 9.60 |
| MM4 | 9.70 |
| MM5 | 9.10 |
| MM6 | 9.30 |
| MM7 | 8.80 |
| MM8 | 8.70 |
| MM9 | 8.90 |
| MM10 | 9.30 |
| MM11 | 9.70 |
| MM12 | 9.70 |
| MM13 | 8.70 |
| MM14 | 8.80 |
| MM15 | 8.70 |
| MM16 | 8.90 |
| MM17 | 9.20 |
| MM18 | 9.10 |
| MM19 | 9.70 |
| IM-9 | 9.70 |
| U-266 | 9.60 |
| RPMI-8226 | 9.90 |
| KMS-20 | 10.00 |
| KMS-28-BM | 10.00 |
| KMS-12-BM | 10.00 |
| KMS-21-BM | 9.90 |
| MM.1S | 10.00 |
| NB1 | 8.70 |
| NB2 | 9.10 |
| NB3 | 9.50 |

### 4.3.2 Comparison of gene expression profiles between MM and normal controls

Before the microarray data were imported to GeneSpring software for analysis, the quality of each array was evaluated according to the QC metrics shown in Table 3.6. As shown in Table 3.6, the average negative control signal was in the range of 80-120, which is higher than the recommended signal (<40). However, this signal value is consistent across all the arrays indicating that it might be specific to the sample type/ conditions used in this study. The higher average negative control signal or background signal could be caused by continuous use of the washing tanks, slide holder and magnetic bead, and thus it can be different from one laboratory to another. In this study, the same set of accessories was used in all experiments to minimise variation in background signals, which might be generated by the traces of fluorescent residue from previous experiments.

To identify molecular targets potentially involved in the transformation and development of MM, gene expression profiles of a total of 27 MM samples (19 clinical specimens and 8 MM cell lines) were compared against 3 normal controls. Out of 50739 probes retained in the analysis after normalisation and filtered probe sets by 'present' and 'marginal' flags, 377 probes (348 mRNAs) were significantly differential expressed by ≥2.0 fold change at corrected p-value cut off 0.01 in the MM group compared to the normal control group. Out of 377 probes, 189 (172 mRNAs) and 188 (176 mRNAs) of them were significantly up-regulated and down-regulated in MM relative to the normal control, respectively. The volcano plot showed the normalised expression of probe sets in MM relative to the normal controls (Figure 4.11). Significant differentially expressed probes, which were ≥2.0 fold change ($\log_2 2 = 1$) and at corrected p-value cut off 0.01 ($-\log_{10} 0.01 = 2$) were indicated in red. The details of up-regulated and down-regulated probes were shown in Appendixes A & B, respectively. Negative in fold change indicated down-regulation.

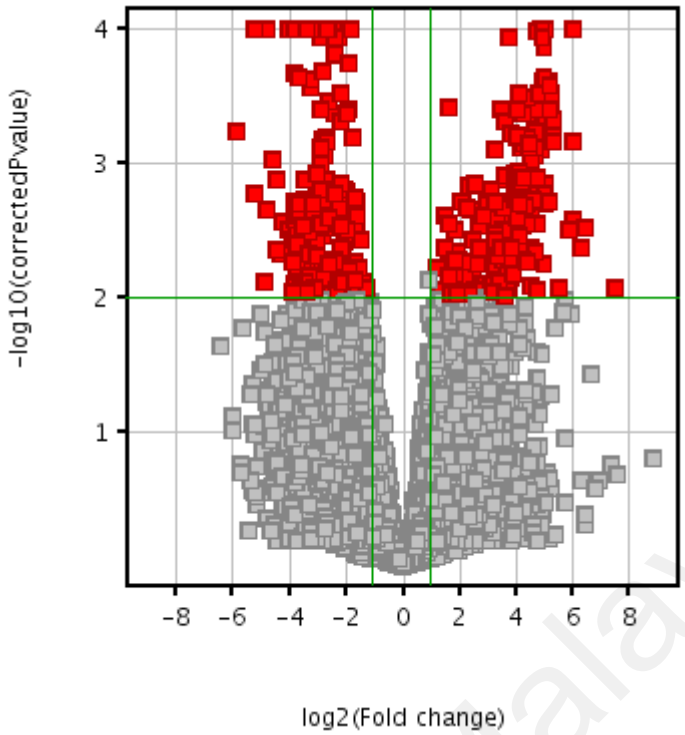


**Figure 4.11:** Volcano plot showing the normalised expression of probe sets in MM relative to the normal controls. A total of 377 significant differentially expressed probes were identified and they were indicated in red (fold change ≥2.0 and $p<0.01$).

### 4.3.3 Unsupervised hierarchical clustering

Unsupervised hierarchical clustering was applied to classify samples based on the degree of similarities in gene expression. Genes with similar expression patterns are grouped together and are connected by a series of branches or dendrogram. Degree of similarity between genes was measured by Euclidean distance metric and the similarity between clusters was measured by Average linkage statistical method. In this study, unsupervised hierarchical clustering was performed for the 377 differentially expressed probes in MM compared to the normal group (≥2.0 fold change; $p<0.01$) The unsupervised hierarchical clustering algorithm classified the 30 samples into two distinct clusters: a MM cell cluster and a normal cell cluster (Figure 4.12). This scenario depicting that gene expression changes is involved in the transition of normal cells to myeloma cells. The hierarchical clustering analysis showed that most of the MM cell lines were classified in sub-clusters separately from the clinical specimens (Figure 4.12).

### 4.3.4 Pathways associated with significant differentially expressed genes in MM

Several pathways which were statistically associated with significant differentially expressed genes in MM vs normal controls (fold change ≥2.0 and $P<0.01$) were identified and listed in Table 4.7.

**Table 4.7:** Pathways associated with differentially expressed genes in MM vs normal controls

| Pathway | Gene (fold change in MM vs normal control) |
|---|---|
| MAPK signaling pathway | *RASGRF2* (-5.52), *RPS6KA5* (-4.45), *IκBKB* (-3.07) |
| TP53 network | *BOK* (-6.35) |
| Notch signaling pathway | *FHL1* (-4.17) |
| Wnt signaling pathway | *FZD5* (3.08) |

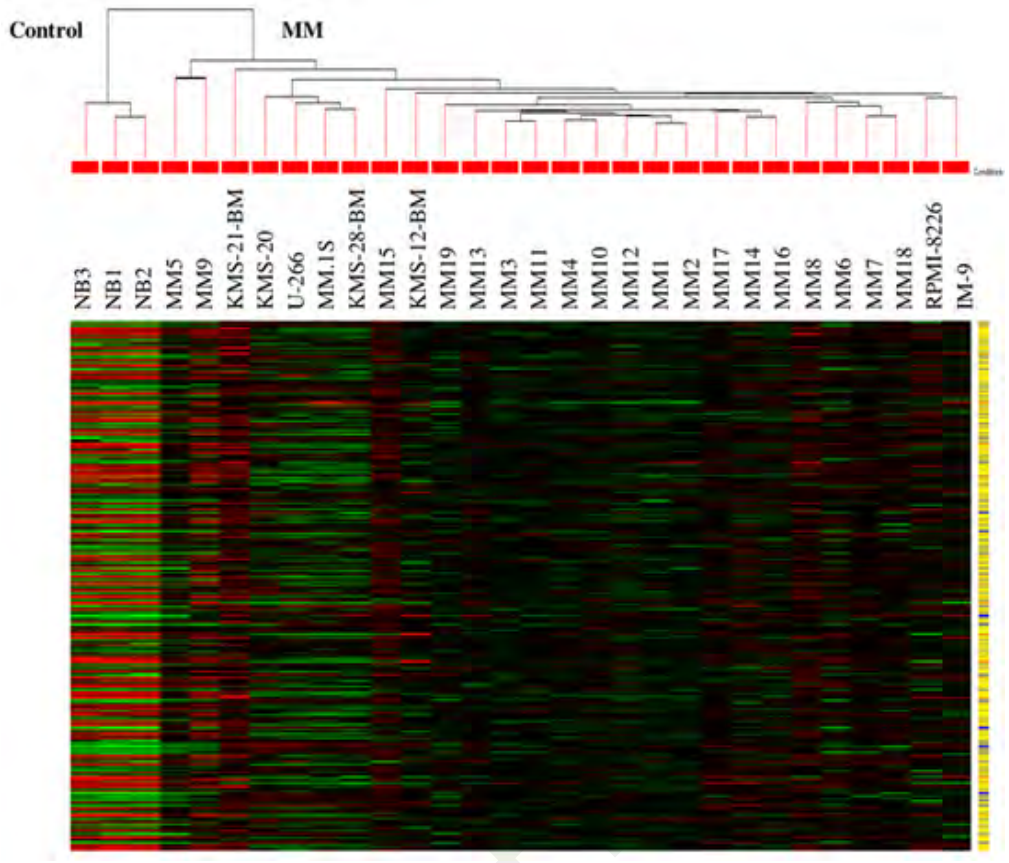


**Figure 4.12:** Unsupervised hierarchical clustering analysis of 30 mRNA expression profiles consisting of 27 MM and 3 normal controls. Two distinct clusters were classified, which discriminated the normal controls from the MM (≥2.0 fold change; $p<0.01$). Each column represents the gene expression levels from a single sample and each row represents the expression of a gene across all samples.

### 4.3.5 Verification of microarray data by RT-qPCR

To verify the reliability of microarray data, four genes namely *CCNA2*, *RAD54L*, *RASGRF2* and *HKDC1* were selected for verification by TaqMan RT-qPCR. The *GAPDH* was used as internal control gene in this assay. Information of pre-designed TaqMan probes/ primers were listed in Table 3.4. The *CCNA2*, *RAD54L*, *RASGRF2* and *HKDC1* were selected for verification by RT-qPCR because they were differentially expressed genes in MM compared to the normal controls (≥2.0 fold change; $p<0.01$) and they play critical functions in oncogenesis (refer to Chapter 4). Besides that, *CCNA2*, *RAD54L*, *RASGRF2* and *HKDC1* have been predicted as potential miRNA-targets in the integrative analysis of differentially expressed miRNA and mRNA expressional profiles (Table 4.11). Verification of *CCNA2*, *RAD54L*, *RASGRF2* and *HKDC1* were performed by using the same cohort of samples used for gene/ miRNA expression microarrays. Two normal controls (NB1 and NB2) and 23-25 MM were used for verification depending on the availability of the samples.

The microarray analysis showed that *CCNA2* and *RAD54L* were significantly up-regulated while *RASGRF2* and *HKDC1* were down-regulated in MM group compared to the normal control group (≥2.0 fold change and at $p<0.01$). The RT-qPCR results confirmed that the expression patterns of *CCNA2*, *RAD54L*, *RASGRF2* and *HKDC1* were consistent with the microarray analysis. In RT-qPCR, the relative expression/ fold change of gene between sample and control was calculated based on $2^{-\Delta\Delta Ct}$. Relative expression ($2^{-\Delta\Delta Ct}$) greater than 1 is up-regulated while lower than 1 is down-regulated in MM compared to the control. In this study, relative expression below 2.0 fold change is considered as no difference between MM and controls. Therefore, relative expression between 0.0-0.5 is considered as decrease expression by ≥2.0 folds while 0.5-1.0 is considered as no difference in expression. The RT-qPCR results indicated that all four genes, *CCNA2*, *RAD54L*, *RASGRF2* and *HKDC1* were

significantly differentially expressed at ≥2.0 fold change ($p<0.001$). The summary of mean relative expression and significance level in RT-qPCR in comparison with microarray analysis is illustrated in Table 4.8. These findings demonstrated a strong correlation between the microarray and RT-qPCR platforms. Importantly, in this validation method, the fold changes cannot directly compared between microarray and RT-qPCR assays due to differences in platforms and calculation methods, but the general trend of up-regulation and down-regulation can be compared.

Table 4.9 shows the relative expression of *CCNA2* and *RAD54L* in each MM relative to the normal controls after normalisation with endogenous control gene, *GAPDH*. The *CCNA2* and *RAD54L* were up-regulated in all samples studied (25/25 for *CCNA2* and 24/24 for *RAD54L*) (≥2.0; $p<0.001$). On the other hand, Table 4.10 shows the relative expression of *RASGRF2* and *HKDC1* in each MM compared to the normal controls after normalisation with internal control gene, *GAPDH*. The expression of *RASGRF2* and *HKDC1* were down-regulated in 23/23 myeloma samples analysed (≥2.0; $p<0.001$).

**Table 4.8:** Fold change and significance level of *CCNA2*, *RAD54L*, *RASGRF2* and *HKDC1* in RT-qPCR and microarray analysis. Negative in fold change indicated down-regulation. The $2^{-\Delta\Delta Ct}$ between 0.0-0.5 indicated down-regulation. The expression patterns of all the genes detected by RT-qPCR were consistent with the microarray analysis

| Gene | Microarray | | RT-qPCR | |
|---|---|---|---|---|
| | **Fold change (myeloma/ normal)** | **Significance level** | **Fold change ($2^{-\Delta\Delta Ct}$) (myeloma/ normal)** | **Significance level** |
| *CCNA2* | 19.7 | p<0.01 | 10.5 | P<0.001 |
| *RAD54L* | 17.0 | p<0.001 | 8.8 | P<0.001 |
| *RASGRF2* | -5.5 | p<0.01 | 0.020 | P<0.001 |
| *HKDC1* | -9.5 | p<0.01 | 0.043 | P<0.001 |

**Table 4.9:** Relative expression of *CCNA2* and *RAD54L* in myeloma samples vs normal controls as calculated by $2^{-\Delta\Delta Ct}$. Standard deviation (SD) was calculated based on replicate samples

| Samples | *CCNA2* | | *RAD54L* | |
|---|---|---|---|---|
| | **Relative expression** | **SD** | **Relative expression** | **SD** |
| MM1 | 9.0 | 0.04 | 4.5 | 0.00 |
| MM2 | 7.7 | 0.08 | - | - |
| MM3 | 4.2 | 0.10 | 2.8 | 0.06 |
| MM4 | 6.1 | 0.07 | 7.5 | 0.05 |
| MM6 | 4.8 | 0.12 | 2.7 | 0.06 |
| MM7 | 4.6 | 0.11 | 2.8 | 0.03 |
| MM8 | 8.4 | 0.05 | 11.4 | 0.04 |
| MM10 | 9.1 | 0.07 | 10.0 | 0.09 |
| MM11 | 3.5 | 0.06 | 6.7 | 0.04 |
| MM12 | 8.5 | 0.07 | 4.6 | 0.09 |
| MM13 | 9.6 | 0.04 | 8.6 | 0.05 |
| MM14 | 3.8 | 0.03 | 5.4 | 0.07 |
| MM15 | 3.4 | 0.00 | 4.5 | 0.03 |
| MM16 | 6.1 | 0.01 | 5.3 | 0.04 |
| MM17 | 3.1 | 0.01 | 2.4 | 0.03 |
| MM18 | 4.9 | 0.04 | 4.3 | 0.04 |
| MM19 | 5.9 | 0.00 | 4.6 | 0.03 |
| KMS-12-BM | 22.9 | 0.04 | 21.6 | 0.04 |
| KMS-20 | 23.6 | 0.08 | 10.1 | 0.02 |
| KMS-21-BM | 3.1 | 0.08 | 3.3 | 0.04 |
| MM.1S | 33.8 | 0.07 | 16.2 | 0.07 |
| U-266 | 31.5 | 0.03 | 13.8 | 0.06 |
| KMS-28-BM | 32.7 | 0.05 | 38.9 | 0.03 |
| IM-9 | 5.4 | 0.02 | 7.8 | 0.02 |
| RPMI-8226 | 5.7 | 0.05 | 12.5 | 0.02 |

**Table 4.10:** Relative expression of *RASGRF2* and *HKDC1* in myeloma samples vs normal controls as calculated by $2^{-\Delta\Delta Ct}$. Standard deviation (SD) was calculated based on replicate samples

| Samples | *RASGRF2* | | *HKDC1* | |
|---|---|---|---|---|
| | **Relative expression** | **SD** | **Relative expression** | **SD** |
| MM1 | 0.028 | 0.03 | 0.036 | 0.03 |
| MM3 | 0.011 | 0.02 | 0.016 | 0.09 |
| MM4 | 0.020 | 0.24 | 0.002 | 0.59 |
| MM6 | 0.092 | 0.17 | 0.082 | 0.15 |
| MM8 | 0.049 | 0.06 | 0.021 | 0.13 |
| MM10 | 0.030 | 0.11 | 0.104 | 0.05 |
| MM11 | 0.012 | 0.06 | 0.052 | 0.34 |
| MM12 | 0.006 | 0.08 | 0.003 | 0.14 |
| MM13 | 0.018 | 0.03 | 0.023 | 0.04 |
| MM14 | 0.003 | 0.39 | 0.006 | 0.19 |
| MM15 | 0.027 | 0.19 | 0.030 | 0.14 |
| MM16 | 0.008 | 0.06 | 0.011 | 0.05 |
| MM17 | 0.010 | 0.12 | 0.017 | 0.25 |
| MM18 | 0.083 | 0.04 | 0.061 | 0.16 |
| MM19 | 0.044 | 0.04 | 0.045 | 0.01 |
| KMS-12-BM | 0.000 | 0.84 | 0.004 | 1.19 |
| KMS-20 | 0.002 | 0.25 | 0.004 | 0.37 |
| KMS-21-BM | 0.015 | 0.17 | 0.022 | 0.02 |
| MM.1S | 0.000 | 0.16 | 0.006 | 0.15 |
| U-266 | 0.003 | 0.08 | 0.064 | 0.08 |
| KMS-28-BM | 0.001 | 0.13 | 0.382 | 0.02 |
| IM-9 | 0.000 | 0.36 | 0.016 | 0.33 |
| RPMI-8226 | 0.001 | 0.04 | 0.007 | 0.42 |

## 4.4 MICRORNA (MIRNA) EXPRESSION STUDY OF MM

MicroRNA (miRNA) expression study was performed by Agilent microarray platform. The purpose of this study was to identify potential miRNAs and miRNA-targets involved in the initiation and progression of MM. The study subjects were from the same cohort of samples used in gene expression study (19 MM specimens, 8 cell lines and 3 normal controls). One colour labelling system and Agilent SurePrint Human miRNA Microarray, release 19.0, 8 X 60K microarray chip were used in this study. This chip allowed the evaluation of approximately 2006 miRNAs expression levels simultaneously in a single experiment. Differentially expressed miRNAs were determined by comparing the miRNA expression profiles of MM relative to the normal controls using GeneSpring software version 13.0. Using the same software, miRNA-target prediction was performed by integrating the sample-matched differentially expressed mRNAs and miRNAs profiles to determine potential miRNA-targets in the oncogenesis of MM. Finally, two miRNAs namely miR-150-5p and miR-4430 were verified by SYBR Green RT-qPCR approach.

### 4.4.1 Total RNA isolation

Total RNAs from the same set of samples used in gene expression study were utilised for miRNA expression study. They were 19 MM (MM1-MM19), 8 myeloma cell lines (IM-9, U-266, RPMI-8226, KMS-20, KMS-28-BM, KMS-21-BM, KMS-12-BM and MM.1S) and 3 normal controls (NB1, NB2 and NB3). The gel-like images of total RNAs generated by Bioanalyser were shown in Figure 4.10 and the RIN for each sample was shown in Table 4.6.

### 4.4.2 Comparison of miRNA expression profiles between MM and normal controls

Before the microarray data were imported to GeneSpring software for analysis, the quality of each array was evaluated according to the QC metrics shown in Table 3.7. All the arrays passed the QC metrics as shown in Table 3.7 were subjected for further analysis. After normalisation and filtered probe sets by 'present' flags, fold change and significance level, 1781 out of 2027 miRNAs retained in the analysis were differentially expressed by ≥2.0 fold change in MM compared to the normal controls at corrected p-value cut off 0.05. Out of 1781 miRNAs, 1773 and 8 miRNAs were over-expressed and under-expressed, respectively in MM. Top 100 differentially over-expressed probes and the 8 under-expressed probes were listed in Appendixes C & D. The volcano plot showed the normalised expression of probes in MM relative to the normal controls (Figure 4.13). Significant differentially expressed probes, which were ≥2.0 fold change ($\log_2 2 = 1$) and at corrected p-value cut off 0.05 ($-\log_{10} 0.05 = 1.3$) were indicated in red (Figure 4.13).

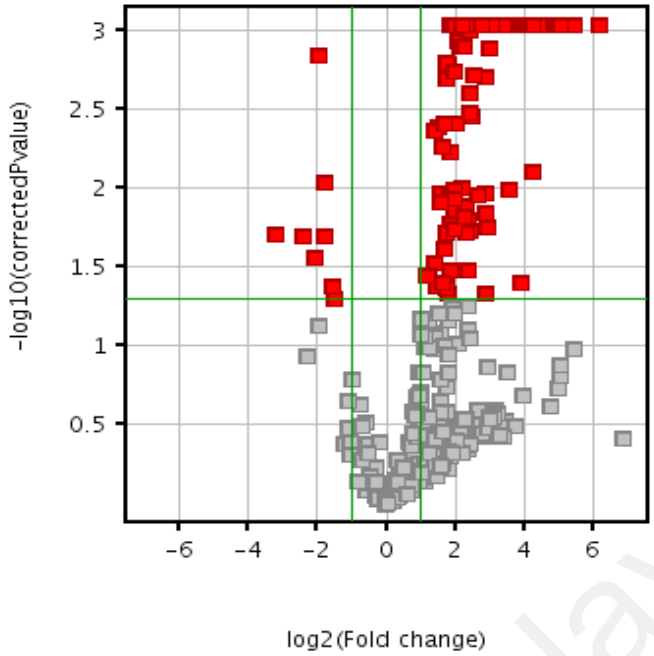


**Figure 4.13:** Volcano plot showing the normalised miRNA expression in MM relative to the normal controls. A total of 1781 significant differentially expressed miRNA were identified and they were indicated in red (≥2.0 fold change; $p<0.05$).

### 4.4.3 Unsupervised hierarchical clustering

Unsupervised hierarchical clustering was applied to classify samples based on the degree of similarities in miRNA expression. The miRNAs with similar expression patterns are grouped together and are connected by a series of branches or dendrogram. Degree of similarity between miRNAs was measured by Euclidean distance metric and the similarity between clusters was measured by Average linkage method. In this study, unsupervised hierarchical clustering algorithm was performed for the 17 differentially expressed probes in MM compared to the normal group (≥2.0 fold change and at p-value cut off 0.05). Unfortunately, normal controls were not separated from the MM in the hierarchical clustering analysis (Figure 4.14). Unlike hierarchical clustering analysis in gene expression microarray, the normal samples can be clustered clearly from the MM samples (Figure 4.12). This scenario is discussed further in section 4.3.

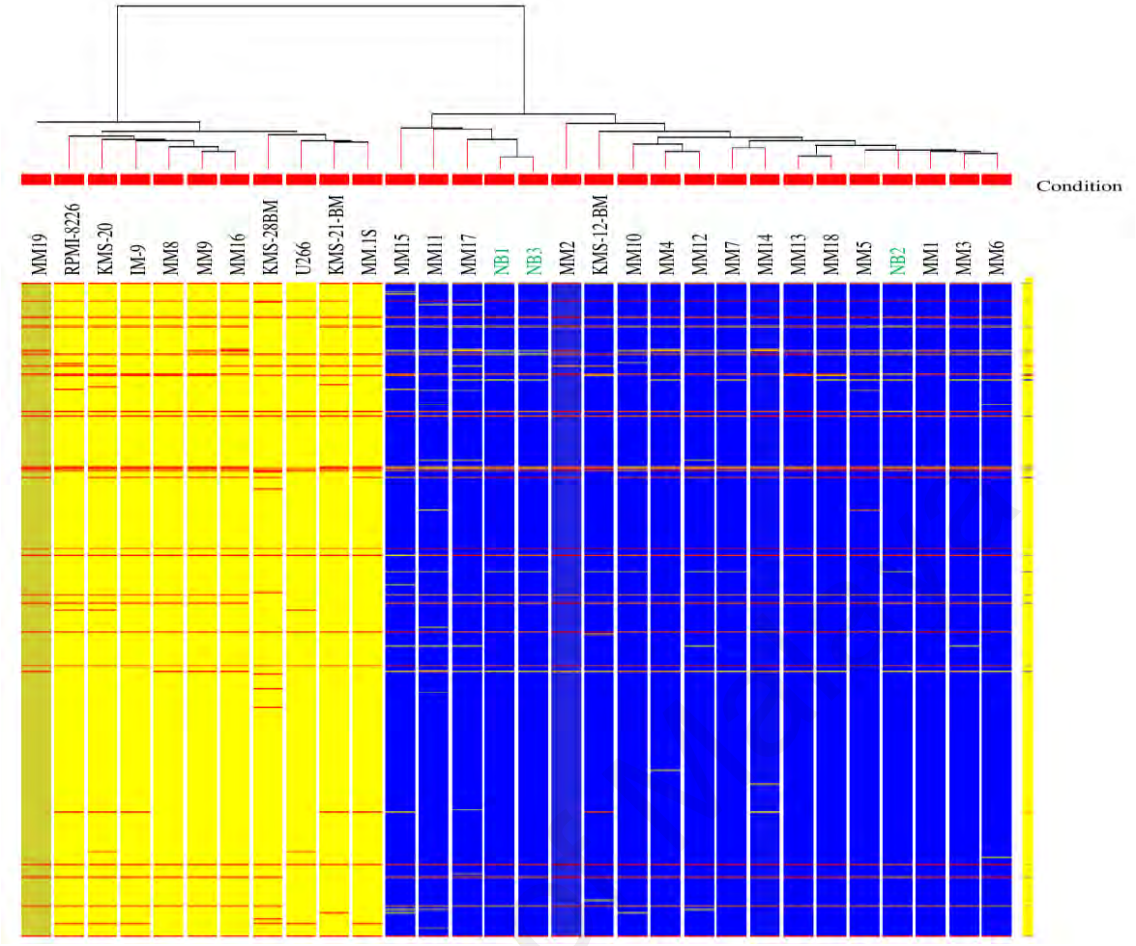


**Figure 4.14:** Unsupervised hierarchical clustering analysis of 30 miRNA expression profiles consisting of 27 MM and 3 normal controls. The clustering analysis had classified the 30 samples into 2 clusters (yellow and blue) based on the similarities in miRNAs expression. Most of the MM cell lines were grouped together (except for KMS-12-BM) in the yellow cluster. Four MM were grouped under yellow cluster whereas the remaining 15 MM were grouped under blue cluster. Unfortunately, the normal samples (NB1, NB2 and NB3) were not clustered separately from the MM (≥2.0 fold change; $p<0.05$). Each column represents the miRNA expression levels from a single sample and each row represents the expression of a miRNA across all samples.

### 4.4.4 miRNA-mRNA integrative analysis

The miRNA-target prediction was performed by integrating the 377 differentially expressed mRNAs and 1781 differentially expressed miRNAs to identify potential miRNA-targets underlying the molecular pathogenesis of MM. Targeted genes for differentially expressed miRNAs were predicted using TargetScan, which was integrated in the GeneSpring software. The integrative analysis revealed 11 differentially expressed target genes (≥2.0 fold change and at p-value cut off 0.05). They were identified as procollagen C-endopeptidase enhancer 2 (*PCOLCE2*), abnormal spindle-like, microcephaly associated (*ASPM*), cytoskeleton associated protein 2-like (*CKAP2L*), cyclin A2 (*CCNA2*), SH2-domain binding protein 1 (*SHCBP1*), DNA repair and recombination protein RAD54-like (*RAD54L*), NDC80 kinetochore complex component (*NUF2*), catenin (cadherin-associated protein), alpha-like 1 (*CTNNAL1*), hexokinase domain containing 1(*HKDC1*), cysteinyl leukotriene receptor 2 (*CYSLTR2*) and Ras protein-specific guanine nucleotide-releasing factor 2 (*RASGRF2*). Eight out of 11 genes were significantly up-regulated in this study (*PCOLCE2, ASPM, CKAP2L*, *CCNA2, SHCBP1, RAD54L, NUF2 and CTNNAL1*). Three of the genes were identified as significant down-regulated genes in this study (*HKDC1, CYSLTR2 and RASGRF2*). The details of the dysregulated miRNAs and their differentially expressed mRNA targets were listed in Appendix E. Interestingly, when compared the top 100 up- and down-regulated miRNAs with the 11 targeted genes, 15 anti-correlated miRNAs and 5 potential target genes were identified (Table 4.11). These 15 anti-correlated miRNAs and 5 potential target genes will be discussed in the discussion chapter of this thesis.

**Table 4.11:** Differentially expressed miRNAs and their potential targeted genes which were dysregulated at opposite expression (negative in fold change indicated down-regulation in MM).

| Gene (fold change) | miRNA (fold change) | miRNA accession no |
|---|---|---|
| RAD54L (17.00) | miR-150-5p (-3.52) | MIMAT0000451 |
| CCNA2 (19.69) | miR-150-5p (-3.52) | MIMAT0000451 |
| | miR-374a-5p (-2.96) | MIMAT0000727 |
| CYSLTR2 (-7.35) | miR-125b-5p (21.91) | MIMAT0000423 |
| | miR-4698 (9.84) | MIMAT0019793 |
| | miR-1290 (17.32) | MIMAT0005880 |
| | miR-1183 (8.20) | MIMAT0005828 |
| | miR-9-5p (8.07) | MIMAT0000441 |
| | miR-4433-3p (7.90) | MIMAT0018949 |
| | miR-33a-5p (7.90) | MIMAT0000091 |
| | miR-4734 (7.89) | MIMAT0019859 |
| HKDC1 (-9.53) | miR-1290 (17.32) | MIMAT0005880 |
| | miR-4698 (9.84) | MIMAT0019793 |
| | miR-4430 (9.34) | MIMAT0018945 |
| | miR-328 (8.22) | MIMAT0000752 |
| | miR-4763-5P (7.97) | MIMAT0019912 |
| RASGRF2 (-5.52) | miR-125b-5p (8.22) | MIMAT0000423 |
| | miR-9-5p (8.07) | MIMAT0000441 |
| | mir-211-5p (7.91) | MIMAT0000268 |
| | miR-370 (7.90) | MIMAT0000722 |

### 4.4.5 Verification of miRNA expression by RT-qPCR

Due to the limitation in samples, only two differentially expressed miRNAs (miR-150-5p and miR-4430) were selected for further verification by SYBR Green RT-qPCR approach. The miR-150-5p and miR-4430 were selected for verification because both of them were differentially expressed in MM indicating that they are important in the pathogenesis of MM. More importantly, miR-150-5p was identified as a potential negative regulator for *CCNA2* and *RAD54L* while miR-4430 was identified as a possible negative regulator for *HKDC1* (as analysed by integrative analysis of patient-matched mRNA and miRNA expressional profiles) (Table 4.11). The reliability of *CCNA2*, *RAD54L*, *RASGRF2* and *HKDC1* expression have been confirmed by RT-qPCR (Table 4.9 and 4.10), this prompt us to confirm the expression of their negative regulators, miR-150-5p and miR-4430 by using RT-qPCR. Besides that, miR-150-5p is a critical miRNAs involved in B cell differentiation, which highlighted its important roles in myelomagenesis. On the other hand, miR-4430 was selected for verification because of its novelty and its possible role in regulating an important hexokinase *HKDC1*, which involved in catalysing the phosphorylation of glucose suggesting its importance role in supplying energy for the rapidly proliferating cancer cells. Verification of miR-150-5p and miR-4430 were performed by using the same cohort of samples used for gene/ miRNA expression microarrays. Two normal controls (NB1 and NB2) and 20-22 MM were used for verification depending on the availability of the samples. The RNU6 was used as internal control for the RT-qPCR. The information of the validated primers used for RT-qPCR was listed in Table 3.8.

According to the microarray analysis, miR-150-5p was under-expressed while miR-4430 was over-expressed in MM compared to the normal controls ($\geq$2.0 fold change; $p<0.05$). In RT-qPCR, the relative expression/ fold change of gene between sample and control was calculated based on $2^{-\Delta\Delta Ct}$. Relative expression ($2^{-\Delta\Delta Ct}$) greater

than 1 is up-regulated while lower than 1 is down-regulated in MM compared to the control. In this study, relative expression below 2.0 fold change is considered as no difference between MM and controls. Therefore, relative expression between 0.0-0.5 is considered as decrease expression by ≥2.0 while 0.5-1.0 is considered as no difference in expression. Our RT-qPCR results found that miR-150-5p was significantly down-regulated whereas miR-4430 was up-regulated in myeloma group compared to the normal control group (≥2.0; $p<0.001$). The RT-qPCR results were concordant with the microarray data. The summary of mean relative expression and significance level of miR-150-5p and miR-4430 in RT-qPCR in comparison with microarray analysis is illustrated in Table 4.12. Importantly, in this validation method, the fold changes cannot directly compared between microarray and RT-qPCR assays due to the differences in platforms and calculation methods, but the general trend of up-regulation and down-regulation can be compared.

Table 4.13 shows the relative expression of miR-150-5p in 22 MM samples analysed after normalisation with the RNU6. The miR-150-5p expression was down-regulated in 21/22 myeloma samples by ≥2.0 fold change except for MM3 ($p<0.001$),. In contrast, miR-4430 was up-regulated in 11/20 myeloma samples by ≥2.0 folds except MM3, MM4, MM11, MM12, MM15, MM17, MM18, KMS-20 and MM.1S ($p<0.001$). Table 4.14 illustrates the relative expression of miR-4430 in 20 myeloma samples.

**Table 4.12:** Fold change and significance level of miR-150-5p and miR-4430 in myelomas vs normal controls in RT-qPCR in comparison with microarray data. Negative in fold change indicates down-regulation in microarray while $2^{-\Delta\Delta Ct}$ between 0.0-0.5 in RT-qPCR indicated down-regulation. The expression patterns of all the miRNAs detected by RT-qPCR were consistent with microarray findings

| **miRNA** | **Microarray** | | **RT-qPCR** | |
|---|---|---|---|---|
| | **Fold change (myeloma/ normal)** | **Significance level** | **Fold change ($2^{-\Delta\Delta Ct}$) (myeloma/ normal)** | **Significance level** |
| miR-150-5p | -3.5 | P<0.05 | 0.094 | P<0.001 |
| miR-4430 | 9.3 | P<0.05 | 6.3 | P<0.001 |

**Table 4.13:** Relative expression of miR-150-5p in myeloma samples vs normal controls as calculated by $2^{-\Delta\Delta Ct}$. Standard deviation (SD) was calculated based on replicate sample

| Samples | miR-150-5p | |
|---|---|---|
| | Relative expression | SD |
| MM1 | 0.316 | 0.22 |
| MM3 | 0.646 | 0.61 |
| MM4 | 0.032 | 0.24 |
| MM8 | 0.018 | 0.05 |
| MM10 | 0.104 | 0.14 |
| MM11 | 0.099 | 0.26 |
| MM12 | 0.013 | 0.20 |
| MM13 | 0.083 | 0.21 |
| MM14 | 0.023 | 0.17 |
| MM15 | 0.047 | 0.11 |
| MM16 | 0.033 | 0.67 |
| MM17 | 0.017 | 0.13 |
| MM18 | 0.210 | 0.43 |
| MM19 | 0.297 | 0.56 |
| KMS-12-BM | 0.035 | 0.25 |
| KMS-20 | 0.070 | 0.38 |
| KMS-21-BM | 0.010 | 0.30 |
| MM.1S | 0.001 | 0.32 |
| U-266 | 0.000 | 0.45 |
| KMS-28-BM | 0.000 | 0.13 |
| IM-9 | 0.000 | 0.57 |
| RPMI-8226 | 0.003 | 0.48 |

**Table 4.14:** Relative expression of miR-4430 in myeloma samples vs normal controls as calculated by $2^{-\Delta\Delta Ct}$. Standard deviation (SD) was calculated based on replicate samples

| Samples | miR-4430 | |
|---|---|---|
| | Relative expression | SD |
| MM3 | 1.3 | 0.00 |
| MM4 | 0.3 | 0.22 |
| MM8 | 3.8 | 0.10 |
| MM10 | 2.5 | 0.16 |
| MM11 | 1.7 | 0.06 |
| MM12 | 1.0 | 0.07 |
| MM13 | 3.2 | 0.13 |
| MM14 | 4.3 | 0.21 |
| MM15 | 0.9 | 0.13 |
| MM16 | 3.3 | 0.04 |
| MM17 | 1.5 | 0.20 |
| MM18 | 0.9 | 0.15 |
| KMS-12-BM | 47.8 | 0.12 |
| KMS-20 | 1.9 | 0.21 |
| KMS-21-BM | 6.7 | 0.36 |
| MM.1S | 0.8 | 0.21 |
| U-266 | 8.8 | 0.45 |
| KMS-28-BM | 7.2 | 0.04 |
| IM-9 | 14.4 | 0.53 |
| RPMI-8226 | 14.1 | 0.21 |

# CHAPTER 5: DISCUSSION

## 5.1 WHOLE GENOME SCREENING OF CHROMOSOMAL ABERRATION IN MM

In this study, several CNVs and genes localised within the CNV regions were revealed. Two CNV regions 1q42.3 and 7q22.3, where *LYST* and *NAMPT* genes are localised were verified by qPCR using 10 samples for each CNV. The qPCR results showed 90% of concordance between aCGH and real-time PCR platforms (Figure 4.3). Since the qPCR and aCGH are two different platforms, slightly different in calculated copy number is considered normal. This might explain why M24 and M07 showed copy number gains at 1q42.3 and 7q22.3, respectively in aCGH analysis but not in the qPCR (Figure 4.3).

In this aCGH study, copy number variations were identified in 100% of MM patients suggests the importance of genomic imbalances in the pathogenesis of MM. This percentage is consistent with the findings reported by Smetana *et al*. (2014) and Largo *et al*. (2007). Importantly, only 2 out of 63 patients showed clonal genomic abnormalities at diagnosis by conventional G-banded karyotype analysis (Table 3.1). This scenario showed that aCGH is more sensitive than conventional G-banded karyotype in the analysis of chromosomal copy number change. The conventional G-banded karyotype relies heavily on sufficient good quality metaphase spreads, which can be difficult to obtain. In addition, the likelihood of obtaining abnormal metaphase spreads decreases due to low proliferative index of myeloma cells (Kryukov *et al*., 2013; Riegel, 2014). Unlike conventional G-banded karyotype technique, aCGH has high sensitivity in the identification of relatively small amplification and deletion in the chromosome and more importantly this technique does not rely on metaphase spreads for analysis.

The aCGH findings revealed common copy number gains in 1q, 2q, 3p, 3q, 4q, 5q, 6q, 7q, 8q, 9q, 10q, 11q, 13q, 14q, 15q, 21q and Xq, and copy number loss in 14q. According to Smetana *et al*. (2014) and Kjeldsen (2016), they found copy number gains in odd-numbered chromosomes 3, 5, 7, 9, 11, 15, 19 and 21 as well as gain in 1q21 by aCGH approach. The *CKS1B* and acidic leucine-rich nuclear phosphoprotein 32 family member E (*ANP32E*) genes have been identified as important genes in 1q21, a region which is associated with poor prognosis in MM. Common copy number gain in 1q21 was identified in this study too and cathepsin S (*CTSS*) was identified in this region. The *CTSS* is function in immune system and it has been described in association with MM pathogenesis (Favis *et al*., 2011). Besides that, loss of 14q, a chromosome which is involved in IgH rearrangements was detected in this study. The loss of 14q was also reported as common CNVs by Smetana *et al*. (2014) and Kjeldsen (2016). However, copy number gains were detected in even-numbered chromosomes 2, 4, 6, 8, 10 and 14 in this study although these genomic alterations are not frequently found in MM. This observation could be because samples without plasma cells enrichment were used for aCGH in this study. Another possible reason might be because more than half of the samples used in previous studied are cytogenetically abnormal compared to only 2 in this study (Smetana *et al*. 2014 and Kjeldsen 2016).

No consistent gene was found when we compared the genes residing in the CNVs regions with differentially expressed genes identified in this study. This is most likely due to different cohort of samples used for the aCGH and gene expression assays. Apart from different samples in these two assays, the sample size in gene expression study (n=27) might be too small if compared to the aCGH (n=63). Some of the important genes might be missed as a consequence of small sample size. More importantly, not all DNA copy number aberrations effect on the gene expression level, other molecular mechanisms might regulate the gene expression, for example miRNA

expression, methylation, histone modification and gene networks (Huang *et al*., 2006). To further analyse if any of the CNVs is associated with altered gene expression, candidate genes identified in the present study were compared to the Oncomine gene expression database (www.oncomine.org). Four genes localised within the copy number gain regions were significantly over-expressed at mRNA levels in two published datasets on MM patients vs normal controls ($p<0.05$) (Zhan *et al*., 2002; Agnelli *et al*., 2009). They are nicotinamide phosphoribosyltransferase (*NAMPT*), lysosomal associated membrane protein 2 (*LAMP2*), superoxide dismutase 2 (*SOD2*) and NEDD4 binding protein 2-like 2 (*N4BP2L2*). The functions of these 4 genes and other important genes localised in the CNVs regions identified in this study are discussed below.

Ninety two percent of MM patients in this study showed copy number gain at chromosomal region 7q22.3, where *NAMPT* gene is localised. The *NAMPT* also known as pre-B colony enhancing factor (*PBEF*) or visfatin can function as a growth factor, cytokine and nicotinamide phosphoribosyltransferase (Samal *et al*., 1994; Martin *et al*., 2001; Ognjanovic *et al*., 2001). The expression of *NAMPT* is elevated in prostate, brain, colon and rectum cancers as well as MM (Hufton *et al*., 1999; Van Beijnum *et al*., 2002; Wang *et al*., 2011; Cea *et al*., 2012). The $NAD^+$ level is increases to provide sufficient energy for the survival of rapidly proliferating cancer cells through activation of nicotinamide adenine dinucleotide (NAD) salvage pathway and over-expression of *NAMPT*. It has been shown that apoptosis and autophagy cell death were increased when *NAMPT* was suppressed in MM (de la Puente *et al*., 2014; Prideaux *et al*., 2014). It can also reduce osteoclastogenesis, a bone resorption event in MM (de la Puente *et al*., 2014). The small molecule compound inhibitor of *NAMPT* known as FK866/ APO866 can be used to trigger cytotoxicity in myeloma cells *in vitro* and *in vivo* (Wang *et al*., 2011). The discovery of FK866/ APO866 has opened up the prospect of trailing novel targeted therapies for patients with MM. The *NAMPT*-mediated gene silencing effects

on cell proliferation and apoptosis of RPMI-8226 myeloma cell is discussed in more detail in section 4.5.

Copy number gain at chromosomal segment Xq24, in whch *LAMP2* gene is localised is identified in 49% of MM patients in this study. The *LAMP2* gene is one of the major components involved in ubiquitin proteasome system and autophagic lysosomal pathway (Dominguez-B *et al*., 2015). The *LAMP2* gene plays a pivotal role in maintaining the lysosome fusion and autophagosome maturation in cells (Bagshaw *et al*., 2005; Huynh *et al*., 2007; Fehrenbacher *et al*., 2008; Chen *et al*., 2014). Dysregulation of *LAMP2* is detected in acute myeloid leukemia (AML) (Xu *et al*., 2008). Lysosomes in AML are usually larger than normal cells. Thus, lysosomal mass and biogenesis are increased in AML to generate more amino acids and nucleotides for cell proliferation. It has been shown that the leukemic cell death is increased upon knockdown of *LAMP2* gene (Sukhai *et al*., 2013). This suggested that the decreased expression of *LAMP2* causes changes in lysosomal membrane integrity, structure and size of leukemic cells. Recently, Damaghi *et al*. and team (2015) reported that up-regulation of *LAMP2* was associated with prolong breast cancer cell survival *in vitro*, *in vivo* and in patient samples under acidic environment. Acidic environments are favoured in many tumour cells and it promoted tumour cell growth over normal cell. It is thought that under acidic environment, *LAMP2* is translocated from lysosomes to the plasma membrane of the tumour cells to protect the membrane from non-enzymatic or enzymatic acid hydrolysis and thereby preventing tumour cell death (Damaghi *et al*., 2015). Moreover, *LAMP2* also facilitates lysosomal enzymes secretion, which is required by the tumour cells to promote angiogenesis, cell growth and invasion (Damaghi *et al*., 2015). Although the role of *LAMP2* has not been studied in MM, it is possible that the over-expression of *LAMP2* promotes myeloma cell survival through

the similar mechanisms as observed in breast cancer cells. Further study of the role of *LAMP2* in MM is needed to determine its actual role in myeloma pathogenesis.

Gain of chromosomal 6q25.3 was found in 44% of MM cases in the present study and the *SOD2* gene is residing in this region. The SOD2 protein binds to the superoxide by products of oxidative phosphorylation and converts them to hydrogen peroxide and diatomic oxygen. The role of *SOD2* under oxidative stress highlighted its important aspect in the pathogenesis of cancerous cells. The expression level of *SOD2* gene is increased in aggressive tumour (Minig *et al*., 2009). Mutation or methylation of the promoter region of *SOD2* gene is shown to down-regulate manganese superoxide dismutase (*MnSOD*), a putative tumour suppressor in cancer cells (Pani *et al*., 2004; Minig *et al*., 2009). Mutation in *SOD2* gene has been found in carcinoma of the breast (Pani *et al*., 2004; Minig *et al*., 2009). Interestingly, Song and his team (2013) had found that silencing of *SOD2* gene increased the sensitivity of bortezomib treatment in KMS20 myeloma cells while *SOD* inhibitor (2-methoxyestradiol) rendered KMS20 sensitivity to apoptosis. This finding suggested the possibility of implementing *SO2* inhibitor in MM treatment.

On the other hand, the function of *N4BP2L2* gene is not well understood except that this gene has been proposed as a novel transcriptional modulator in association with growth factor independent 1 transcriptional repressor (*GFI1*) and neutrophil elastase (*ELA2*) (Salipante *et al*., 2009). The understanding of the role of *N4BP2L2* in myelomagenesis is very limited although it was over-expressed in MM in this study. Nevertheless, more than half of the MM patient studied (52%) carried copy number gain at chromosomal region 13q13.1, where *N4BP2L2* is localised. The percentage of penetrance is quite high and this gene is worth further experimental investigation in the future.

Apart from *NAMPT*, *LAMP2*, *SOD2* and *N4BP2L2*, the SAM domain, SH3 domain and nuclear localisation signals 1 (*SAMSN1*) and phosphatidylinositol binding clathrin assembly protein (*PICALM*) are two potential genes localised in CNV regions 21q11.2 and 11q14.21, respectively. These copy number gain regions were identified in >70% of MM cases studied. Copy number aberrations at chromosomal regions where *SAMSN1* and *PICALM* are localised had been reported by Dickens *et al.* (2010) in Oncomine database. Previous findings showed that *SAMSN1* is highly expressed in MM, acute myeloid leukaemia, and lymphoma (Claudio *et al*., 2001; Zhu *et al*., 2004). Its up-regulation is mediated by B cell activators interleukin-4 (*IL-4*), *CD40L*, and anti–immunoglobulin (Ig)M. The induction of *SAMSN1* by *IL-4* involves multiple signaling cascades such as activation of signal transducer and activator of transcription 6 (Stat6), phosphoinositide 3-kinase (PI 3-kinase), protein kinase C (PKC), and NF-κB pathways (Zhu *et al*., 2004). Although *SAMSN1* is highly expressed in cancers, silencing of *SAMSN1* in lymphoma cell line did not have any effect on the cell proliferation (Zhu *et al*., 2004). Therefore, it is suggested that *SAMSN1* is most likely participated in B cell activation and differentiation instead of proliferation. On the contrary, Noll *et al*. (2014) reported that *SAMSN1* was a tumour suppressor gene, which is frequently down-regulated in MM. Their studied showed that *SAMSN1* restoration resulted in the suppression of myeloma disease development *in vivo*. In this study, although gain of chromosomal region 21q11.2 where *SAMSN1* is localised was detected but the gene expression at mRNA level is unknown. Based on the controversy in above mentioned findings, it is important to find out whether *SAMSN1* acts as an oncogene or tumour suppressor in MM development and malignancy.

Gain of chromosome 11q14-q25 is another frequent event in MM (Gutiérrez *et al*., 2001 & 2004). The *PICALM* was found in 11q14-q25 in this study. By using microarray technology, Largo and co-workers (2006) had reported the over-expression of the *PICALM* transcript and the amplification of its corresponding genomic region in MM cell lines. The over-expression of *PICALM* was confirmed in MM cell lines but not in the patient sample. The *PICALM* gene is functions in endocytosis, transcriptional regulation, iron homeostasis and cell proliferation. In addition, structural chromosomal abnormality involving genetic locus of *PICALM* has been reported in leukaemia and lymphomas (Dreyling *et al*., 1996; Caudell *et al*., 2008; Huh *et al*., 2010). Example include translocation involving *PICALM* and Acute lymphoblastic leukaemia 1-fused 10 (*AF10*) (10p12) or Mixed-Lineage Leukemia (*MLL*) (11q23), which resulted in fusion genes *PICALM-AF10* or *PICALM-MLL*. It is suggested that *PICALM* rearrangements confer growth advantage by impairing endocytosis, with consequent up-regulation of its surface expression (Di Fiore and Gill, 1999; Di Fiore and De Camilli, 2001; Di Fiore, 2009; Hupalowska and Miaczynska, 2012). Nevertheless, *PICALM* fusion protein has never been described in MM. Modulation of *PICALM* expression has been shown to affect the intracellular iron level (Scotland *et al*., 2012). Therefore, it is worthy to investigate whether *PICALM* over-expression promotes cell proliferation by boosting iron uptake in myeloma patients. It is important to investigate whether iron chelation can be a potential therapy for myeloma patients with high expression of *PICALM* and iron levels.

Chromosomal segments containing genes such as lysosomal trafficking regulator (*LYST*), CDC2-like kinase 1 (*CLK1*), acyl-CoA synthetase long-chain family member 1 (*ACSL1*) and nuclear factor of kappa light polypeptide *gene* enhancer in B-cells inhibitor, alpha (*NFκB1A*) were amplified in more than 40% of myeloma patients in this study. Very limited information about these genes was obtained and they represent

novel genes that have never been described in the pathogenesis of MM. More studies need to be carried out to determine the function of these genes in MM.

## 5.2 IDENTIFICATION OF DIFFERENTIALLY EXPRESSED GENES IN MM

In gene expression microarray, 348 differentially expressed mRNAs have been identified in MM compared to the normal group using microarray (Appendices A & B). The differentially expressed genes identified in this study were compared with previously reported microarray findings of MM by Jones *et al*. (1989), Chng and Fonseca (2009), Broyl *et al*. (2010), Chung *et al*. (2013), Kassambara *et al*. (2013), Nara *et al*. (2013) and Kai *et al*. (2014). Interestingly, many of the previously reported genes are consistently differentially expressed in this study. They are *CCNA2*, *BIRC5*, *CENPA*, *CENPF*, *CCNB1*, *CCNB2*, *CDC25C*, *KIF14*, *DEPDC1*, *CDK1*, *RAD51AP1*, *CHEK1*, *PLK1*, *NUF2*, *AURKB*, *CDC20*, *BUB1*, *BUB1B*, *NEK2*, *TTK*, *TK1*, *CKAP2L*, *KIF11*, *KIF20A*, *SKA1*, *TPX2*, *ASPM*, *TOP2A*, *E2F1*, *E2F7*, *E2F8*, *CDCA8*, *EXO1*, *PCNA*, *ZWINT*, *KIF2C*, *KIF15*, *UBE2T*, *UBE2S*, *IRF2*, *CD1C*, *EZH2*, *IκBKB* and *HIST2H3A* (Jones *et al*., 1989; Chng and Fonseca, 2009; Broyl *et al*., 2010; Chung *et al*., 2013; Kassambara *et al*., 2013; Nara *et al*., 2013; Kai *et al*., 2014). The functions of these genes are listed in Table 5.1. As shown in Table 5.1, majority of the genes are involved in cell cycle and cell cycle checkpoints, DNA repair, mitotic/ spindle checkpoints, cell proliferation, mismatch repair pathway and kinetochore and microtubule attachment.

Other important genes such as RAD54-like (*S. cerevisiae*) (*RAD54L*), hexokinase domain containing 1 (*HKDC1*), Ras protein-specific guanine nucleotide-releasing factor 2 (*RASGRF2*), cysteinyl leukotriene receptor 2 (*CYSLTR2*), diaphanous-related formin 3 (*DIAPH3*), denticleless E3 ubiquitin protein ligase homolog (*DTL*), SHC SH2-domain binding protein 1 (*SHCBP1*), spindle and kinetochore associated

complex subunit 3 (*SKA3*), apoptosis-inducing, TAF9-like domain 1 (*APITD1*) and anillin, actin binding protein (*ANLN*) are novel candidate genes, which might play pivotal roles underlying the molecular pathogenesis of MM (Krona *et al*., 2004; Chng *et al*., 2006; Ueki *et al*., 2008; Ruiz *et al*., 2009; Agarwal *et al*., 2011; Wolf *et al*., 2011; Asano *et al*., 2013; Bengtsson *et al*., 2013; Chuang *et al*., 2013; Jiao *et al*., 2013; Morley *et al*., 2015). The functions of these novel differentially expressed genes are depicted in Table 5.1. The roles of *RAD54L*, *HKDC1* and *CYSLTR2* in oncogenesis are discussed in more details at the end of this section and in section 5.4.

Apart from that, the differentially expressed mRNAs identified in this study were compared with the frequently altered genetic events in MM as discussed in Chapter 2. For instance, translocations involving the IgH locus [t(11;14), t(4;14), t(14;16) and t(14;20)], aberrations in chromosome 1, 13 and 17p13.1. Our results revealed that none of the differentially expressed genes identified in this study is associated with genes involved in the frequently translocated regions in MM such as *CCND1* [t(11;14)(q13;q32)], *FGFR3*/ *MMSET* [t(4;14) (p16;q32)], *c-MAF* [t(14;16)(q32;q23)] and *MAF-B* [t(14;20)(q32;q11)]. This might be because the sample size is too small and many important genes could be missed out during the analysis.

Thirty out of 348 (8.6%) differentially expressed genes are residing in chromosome 1, in which 14 of them are localised at chromosome 1p whereas the remaining 16 at chromosome 1q. Twenty four out of 30 of them were up-regulated in MM, they are solute carrier 6 (neurotransmitter transporter, glycine) 9 (*SLC6A9*), Rh blood group, CcEe antigens (*RHCE*), histone cluster 2, H3a (*HIST2H3A*), DTL, origin recognition complex, subunit 1 (*ORC1*), KIF14, ASPM, kinesin family member 2C (*KIF2C*), aurora kinase A and ninein interacting protein (*AUNIP*), NIMA-related kinase 2 (*NEK2*), transmembrane protein 56 (*TMEM56*), exonuclease 1 (*EXO1*), centromere protein F (*CENPF*), *RAD54L*, NDC80 kinetochore complex component (*NUF2*),

aldehyde dehydrogenase 4A1 (*ALDH4A1*), cell division cycle associated 8 (*CDCA8*), DEP domain containing 1 (*DEPDC1*), ubiquitin-conjugating enzyme E2T (*UBE2T*), cell division cycle 20 (*CDC20*), potassium channel tetramerization domain containing 3 (*KCTD3*), organic solute carrier partner 1 (*OSCP1*), apoptosis-inducing, TAF9-like domain 1 (*APITD1*) and small nucleolar RNA, C/D box 75 (*SNORD75*). In contrast, six genes were down-regulated in MM compared to the normal controls, they are Fc receptor-like 3 (*FCRL3*), CD1c molecule (*CD1C*), carbonic anhydrase VI (*CA6*), RAB GTPase activating protein 1-like (*RABGAP1L*), kinesin family member 28 (*KIF28*) and Heat shock 70 kDa protein 6 (*HSP76*). Previous findings indicated that the short arm of chromosome 1 (1p) is commonly involved in deletions while the long arm in gains (1q) (Marzin *et al*., 2006). We found that 11/24 of the up-regulated genes are localised at chromosomal region 1q (*HIST2H3A, DTL, KIF14, ASPM, NEK2, EXO1, CENPF, NUF2, UBE2T, KCTD3* and *SNORD75*) while only 1/6 of the down-regulated genes is localised at 1p (*CA6*). One of the up-regulated genes, *HIST2H3A* is residing at 1q21, a commonly gain chromosomal region which is associated with poor prognosis in MM (Rajan and Rajkumar, 2015). The *HIST2H3A* plays a central role in transcription regulation, DNA repair, DNA replication and chromosomal stability. Up-regulation of *HIST2H3A* in this study further highlighted its critical function in MM development and progression. The high numbers of differentially expressed genes are localised in chromosome 1 (n=30/348) demonstrated that chromosome 1 plays a critical role in the genetic events that lead to malignant transformation in MM. This also explains why chromosome 1 is frequently deleted/ amplified in MM patients.

Apart from chromosome 1, loss of chromosome 13 is an adverse prognostic factor in MM and other cancers. Interestingly, we found that *CYSLTR2*, *DIAPH3* and *SKA3* are differentially expressed in MM and they are localised at chromosome 13. The *CYSLTR2* was down-regulated while *DIAPH3* and *SKA3* were up-regulated in MM.

Loss of chromosomal region at 13q14.2 has been reported in MM, in which it is associated with deletion of a tumour suppressor gene, *RB1* (Chng *et al*., 2006).. Excitingly, we found that *CYSLTR2* is localised in 13q14.2 as well. Although the actual molecular mechanism of *CYSLTR2* in MM is still unknown but it has been shown to play an essential role in proliferation and migration of colon cancer cells via CysLT signaling (Bengtsson *et al*., 2013). This observation highlighted the possible role of *CYSLTR2* as a putative tumour suppressor gene in MM. Despite of *RB1*, *CYSLTR2* might be another potential gene in 13q14.2, in which its losses might contribute to the oncogenesis of MM. Further study is needed to determine the roles of *CYSLTR2* in myelomagenesis.

Another significant finding revealed the up-regulation of aurora kinase B (*AURKB*) gene, which is localised at chromosome 17p13.1, a commonly deleted region in MM. The TP53 is residing in this chromosomal region and it is typically deleted in fewer than 20% of patients later in the disease course (Drach *et al*., 1998). The mitotic kinase *AURKB* gene functions in regulating the attachment of mitotic spindle to the centromere during cell division (Chng *et al*., 2008). Normal expression of *AURKB* is essentially important in maintaining proper cell division processes while abnormal expression of *AURKB* gene causes high centrosome amplification in MM (Chng *et al*., 2008). Aurora kinase inhibitors are important therapeutic targets in haematological malignancies, and many of them are currently under clinical development. Aurora kinase inhibitors such as ENMD-2076, MLN8237, AT9283 and Danusertib are currently used in different stages of clinical trial in MM (Farag, 2011).

**Table 5.1:** Differentially expressed genes and their functions and fold difference in expression levels in MM relative to the normal controls

| Function | Genes (Fold change) |
|---|---|
| Cell cycle and cell cycle checkpoint | *CCNA2* (19.69), *BIRC5* (29.55), *CENPA* (36.61), *CENPF* (13.42), *CCNB1* (15.42), *CCNB2* (30.48), *CDC25C* (17.74), *KIF14* (26.97), *DEPDC1* (12.29), *CDK1* (30.34) |
| DNA repair | *RAD54L* (17.00), *RAD51AP1* (24.70), *CHEK1* (11.13) |
| Mitotic/ spindle checkpoints | *PLK1* (15.79), *NUF2* (16.94), *AURKB* (19.06), *CDC20* (11.06), *BUB1* (18.11), *BUB1B* (22.85), *CENPA* (36.61), *NEK2* (21.93), *TTK* (38.82), *TK1* (21.85), *CKAP2L* (39.65), *KIF11* (13.69), *KIF20A* (32.46), *SKA1* (38.56), *TPX2* (21.29), *DTL* (32.18) |
| Cell proliferation | *ASPM* (25.85), *TOP2A* (22.59), *TTK* (38.82), *E2F1* (13.75), *E2F7* (29.85), *E2F8* (30.65), *CDCA8* (12.62), *SHCBP1* (18.12) |
| Mismatch repair pathway | *EXO1* (21.62), *PCNA* (5.95) |
| Kinetochore and microtubule attachment | *ZWINT* (14.78), *AURKB* (19.06), *BIRC5* (29.55), *CENPA* (36.61), *TTK* (38.82), *KIF2C* (25.48), *SKA3* (20.14), *APITD1* (5.42) |
| Centrosome | *KIF11* (13.69), *KIF15* (18.40), *AURKB* (19.06) |
| Ubiquitin proteasome | *UBE2T* (11.58), *UBE2S* (6.14) |
| Fanconi anaemia pathway | *UBE2T* (11.58) |
| Cytokine | *IRF2* (-14.55) |
| Metabolism | *HKDC1* (-9.53) |
| Major histocompatibility complex (MHC) | *CD1C* (-5.94) |
| Cytoskeleton | *DIAPH3* (29.97), *ANLN* (40.16) |
| Polycomb | *EZH2* (5.49) |
| NFκB pathway | *IκBKB* (-3.07) |
| RAS related pathway | *RASGRF2* (-5.52) |
| CysLT signaling | *CYSLTR2* (-7.35) |
| Histone | *HIST2H3A* (38.56) |

### 5.2.1 Identification of pathways in MM

Mitogen activated protein kinase (MAPK) signaling pathway is a crucial pathway that contributes to the pathogenesis of MM via activating myeloma cell proliferation and protecting MM cell death (Steinbrunn *et al*., 2012). It is commonly caused by activating mutations of either *K-RAS*, *N-RAS* or *BRAF* genes (Kim *et al*., 2016). In this study, we found 3 significantly down-regulated genes in MM, which are related to MAPK signaling pathway. They were *RASGRF2* (-5.52), ribosomal protein S6 kinase A5 (*RPS6KA5*) (-4.45) and inhibitor of nuclear factor kappa B kinase subunit beta (*IκBKB*) (-3.07). Differential expression of *RASGRF2* and *RPS6KA5* genes has never been reported in MM. *RPS6KA5* or *MSK1* is required for the mitogen or stress-induced phosphorylation of the transcription factors *CREB1* and *ATF1* and for the regulation of the transcription factors *RELA*, *STAT3* and *ETV1*, and that contributes to gene activation by histone phosphorylation and functions in the regulation of inflammatory genes (Wiggin *et al*., 2002). The roles of RAS related gene, *RASGRF2* in oncogenesis is discussed in section 5.4. Apart from that, *IκBKB* not only involved in MAPK pathway but also an important component in NFκB pathway, in which it is discussed in more detail in section 5.5.

Besides MAPK signaling pathway, this study revealed down-regulation of a component of TP53 network in MM. It was identified as Bcl-2 related ovarian killer (*BOK*) gene. *BOK* gene was significantly down-regulated by 6.35 folds in MM in this study. The role of *BOK* has been implicated in ovarian cancer but it has never been reported in myelomagenesis (Einsele-Scholz *et al*., 2016). We suggest that *BOK* induces apoptosis and therefore its down-regulation in MM might suppress apoptotic event and led to the uncontrolled proliferation of myeloma cells.

The roles of Notch signaling pathway in regulating cell differentiation, apoptosis, proliferation and haematopoiesis highlighted its important functions in oncogenesis in various cancers including MM (Colombo *et al*., 2015). For the first time, our study had identified down-regulation (-4.17) of four and a half LIM domains 1 (*FHL1*) gene in MM, a component of Notch signaling pathway. Abnormality in *FHL1* is most likely associated with carcinogenesis. Reduced expression of *FHL1* has been shown to induce lung cancer cell growth through G1 and G2/ M cell cycle arrest (Niu *et al*., 2012). The function of *FHL1* gene has never been studied in MM cells and remains an interesting gene that worth for further investigation.

Alteration of Wnt pathway is also an important factor that promotes initiation and progression of MM. Wnt proteins regulate cell proliferation, mortility and morphology and required in the lymphopoiesis and early stages of B and T cell development (Kim *et al*., 2011). Interestingly, we found up-regulation of one of the ten Frizzled receptors in the human genome, frizzled class receptor 5 (*FZD5*) in the present study (3.08). *FZD5* is thought to be a receptor for Wnt5A ligand. It has been implicated in MM and contributes to the impairment of osteoblast function in MM (Garcia-Gomez *et al*., 2014).

## 5.3 IDENTIFICATION OF DIFFERENTIALLY EXPRESSED MICRORNA IN MM

The miRNA expression study revealed a total of 1781 differentially expressed miRNAs in MM compared to the control group. Unfortunately, the unsupervised hierarchical clustering analysis did not clearly discriminate the MM samples from the normal controls (Figure 4.18). According to Wang and Xi (2013), miRNA expression arrays are more difficult to analyse compared to gene expression arrays. This is because good quality microarray analysis required constant expression of genes on the array. Majority of the miRNA expression are not constant on the array, they are normally weakly or not expressed. This circumstance was also observed in our study as only 2027 out of approximately 60K probes on the arrays can be detected after the data were normalised and filtered as described in section 3.4.2. Apart from that, another reason why the normal controls were not grouped together might be the natural high variability of miRNA expression among the normal controls (Daniel *et al*., 2015). For instance, the age and ethnicities of the controls used in this study. Besides that, sample size used in this study might be too small to significantly separate the normal from the disease group since majority of the miRNAs are weakly or not expressed on the array. More biological replicates are needed to minimise the variability of the samples and increase the power of statistical test in clustering analysis.

Previous studies showed that miRNA biogenesis in B cell malignancies are associated with a global increase in miRNA expression whereas T cell malignancies with decrease in overall miRNA expression (Lawrie *et al*., 2008 &2009; Zhang *et al*., 2009; Zhou *et al*., 2010). The findings of this study are consistent with their results. The vast majority of differentially expressed miRNAs identified in this study were up-regulated in MM compared to the normal controls (1773 up-regulated miRNAs compared to 8 down-regulated miRNAs). The differentially expressed miRNAs identified in the present study were compared with global miRNA expression in MM

reported by Pichiorri *et al*. (2008), Lionetti *et al*. (2009), Gutiérrez *et al*. (2010), Zhou *et al*. (2010), Chi *et al*. (2011) and Yusnita *et al*. (2012). The miRNAs such as miR-125b, miR-20a, miR-21 and miR-194 were consistently up-regulated in this study compared to their findings. In contrast, Chi *et al*. (2011) had found that miR-361 was up-regulated in MM compared to the normal but it was down-regulated in this study. Besides that, Gutiérrez *et al*. (2010) had found that miR-196b and miR-214 were down-regulated in MM subtypes carrying t(4;14) and t(14;16) translocations compared to the normal controls but these two miRNAs were up-regulated in the MM group in this study. These miRNAs were expressed in different patterns compared to other studies due to many factors. The main factor could be the nature of the samples. The expression of the miRNA in tumour cells is varied depending on the potential influences of the different biological and cellular contexts (Nam *et al*., 2014). For instance, their expression could be affected by methylation status, transcription factors and miRNA processing (post-transcriptional) mechanism, which were unknown in this study (Gulyaeva *et al*., 2016; Siomi and Siomi, 2010). Another reason could be the molecular characteristics of the samples. For example in the studied reported by Gutiérrez *et al*. (2010), they classified their samples based on cytogenetic subtypes, therefore the miRNA expression profiles were more specific to certain MM subtypes.

The aberrant miRNAs identified in this study play important functions in survival, proliferation, migration, invasion and drug resistance of myeloma cells. Their function, target or clinical relevance in MM oncogenesis is listed in Table 4.2. The roles of important aberrant miRNAs such as miR21, miR-20a, miR-215, miR-194 and miR-196b are discussed below in more detail.

The up-regulation of miR-21 is facilitated by activation of IL6-JAK-STAT pathway and STAT3- a major mediator of growth, proliferation and survival of myeloma cells conferred by bone marrow microenvironment. Aberration of miR-21 is

thought to contribute to the early development of MM (Chi *et al*., 2011). Apart from that, miR-20a is belongs to miR-17-92 cluster. The over-expression of miR-20a in MM was shown to inhibit apoptotic genes, *BIM* and *SOCS-1*, a negative regulator of IL-6/STAT3 pathway (Pichiorri *et al*., 2008).

The miR-194, miR-215, miR-214 and miR-196b were previously reported as tumour suppressors in MM development and progression, they activated p53 by directly repressing mouse double minute 2 homolog (*MDM2*) (Zhang *et al*., 2015). The miR-194, miR-215, miR-214 inhibit myeloma cell proliferaton via p53-mediated apoptosis, cell cycle arrest and senescence (Zhang *et al*., 2015). Apart from that, miR-196b is down-regulated in MM and its down-regulation is associated with *CCND2* over-expression (Misiewicz-Krzeminska *et al*., 2016). The miR-196b was reported as a negative regulator of Fas cell surface death receptor (*FAS*) and *c-Myc* in leukaemia (Bhatia *et al*., 2010; Li *et al*., 2012). It is suggested that miR-196b is one of the key miR in modulating cell proliferation and apoptosis in cancerous cells.

**Table 5.2:** Aberrant miRNAs and their function, target and clinical relevance in multiple myeloma oncogenesis

| miRNA | Fold Change | Chromosome | Function/target/clinical relevance |
|---|---|---|---|
| miR-125b | 21.9 | 7 | Association with B cell maturation (Malumbres *et al*., 2009). High expression resulted in down-regulation of interferon regulatory factor 4 (*IRF4*) and B-lymphocyte-induced maturation protein 1 *(Blimp1*) (Gururajan *et al*., 2010). Reduction of cell death in dexamethasone induced MM (Murray *et al*., 2013). *p53* regulator (Murray *et al*., 2013). Inhibits *TNFAIP3* and elevates NF-κB activity (Kim *et al*., 2012) |
| miR-148a | 19.2 | 7 | Up-regulation in plasma cells of MM and association with shorter progression free survival (Huang *et al*., 2012). |
| miR-196b | 12.5 | 7 | Down-regulation increased *CCND2* expression and induced cell cycle at G1 to S phase (Saki *et al*., 2014; Misiewicz-Krzeminska *et al*., 2016). |
| miR-21 | 10.9 | 17 | Induction by IL-6/STAT3 pathway upon adherence of bone marrow cells and bone marrow stromal cells (Löffler *et al*., 2007). Over-expression inhibited apoptosis and increased drug resistance (Wang *et al*., 2011). Association with early pathogenesis of MM (Chi *et al*., 2011). |
| miR-20a | 9.2 | 13 | Up-regulation by *c-MYC* over-expression (Pichiorri *et al*., 2008). Aberration was associated with down-regulation of pro-apoptotic genes, *BIM* and *SOC-1* (Anderson and Carrasco, 2011). Up-regulation in plasma cells of MM and correlation with shorter progression free survival (Chen *et al*., 2011; Gao *et al*., 2012). Association with *CCND2* over-expression and promotion of cell cycle at G1 to S phase (Saki *et al*., 2014). |

**Table 4.2,** continued

| miRNA | Fold Change | Chromosome | Function/target/clinical relevance |
|---|---|---|---|
| miR-194-5p miR-215 | 8.4 | 1 | Inhibition in cell migration and invasion by targeting *IGF1* and insulin-like growth factor 1 receptor (*IGF1R*). Direct transcriptional target of *p53*. Down-regulation was associated with promoter hypermethylation, which would impair the *p53*/ Mouse Double Minute 2 Homolog (*MDM2*) loop and promotion of MM development (Pichiorri *et al*., 2010). |
| miR-330-3p | 7.9 | 19 | Over-expression in aggressive MM and association with shorter overall survival rate (Lionetti *et al*., 2013). |
| miR-214 | 7.9 | 1 | Down-regulation was caused by DNA methylation and resulted in inhibition of myeloma cell proliferation (Gutiérrez *et al*., 2010). Target Proteasome (prosome, macropain) 26S subunit, non-ATPase 10 (*PSMD10*) and anti- silencing function 1B (*ASF1B*) (Saki *et al*., 2014). |
| miR-150-5p | -3.5 | 19 | Control B cell differentiation by targeting *c-Myb* (Xiao *et al*., 2007; Fernando *et al*., 2012). Promote cell growth, invasion and metastasis via interaction with Mucin 4 (Grammatikakis *et al*., 2013). Potential target of survivin (Undi *et al*., 2013). Target tumour associated macrophages (*TAMs*) to induce *VEGF* production and tumour growth via angiogenesis (Liu *et al*., 2013). Potential therapeutic target in MM (Palagani (Palagani *et al*., 2014). |
| miR-361-3p | -4.3 | X | Association with t(11;14) translocation. Target *PPP2R4*, the activation of *IL-6* signaling and resulted in increased cell growth and survival (Lionetti *et al*., 2009). |

## 5.4 MIRNA-TARGET PREDICTION IN MM

Although putative identification of miRNA targets using seed sequence complementary matching can be obtained via databases such as TargetScan, PITA, PicTar and TarBase, the false positive rate for the prediction is relatively high. In the present study, an integrated analysis of matched miRNA and mRNA expression data was performed to identify the miRNA-targets, which at the same time were significantly differentially expressed in MM. The miRNA-target prediction analysis revealed that *CCNA2*, *CYSLTR2*, *RASGRF2* and *HKDC1* were regulated by more than one miRNAs (except for *RAD54L*) (Table 4.3). We found that only a few out of 15 putative miRNAs identified in this study are concomitant with cancers. They were identified as miR-150, miR-125b, miR-33a, miR-9 and miR-211. Interestingly, miR-150 and miR-125b are closely related to B cell differentiation and MM is the malignancies of B cells; this therefore highlighted their crucial roles in myelomagenesis (Marques *et al*., 2015). Previous reports showed that *c-Myb*, Mucin 4, tumour associated macrophages (*TAMs*) and survivin/ *BIRC5* are potential targets of miR-150 (Xiao *et al*., 2007; Fernando *et al*., 2012; Grammatikakis *et al*., 2013; Liu *et al*., 2013; Undi *et al*., 2013; Marques *et al*., 2015). Interestingly, there is no report yet describing the interaction between miR-150 and *RAD54L* or *CCNA2*. Our findings exhibited the possible roles of miR-150 in regulating two important cell cycle associated genes, *RAD54L* and *CCNA2*. The *RAD54L* is function in DNA double strand break repair and chromatin remodeling in G1/ S-transition via homologous recombination (Mjelle *et al*., 2015). Failure in DNA repair will eventually result in gene mutations, deletions and oncogenic translocations that can lead to oncogenesis (Agarwal *et al*., 2011; Mjelle *et al*., 2015). Elevated expression of *RAD54L* has been identified in colon and breast cancers, lymphoma and meningiomas (Leone *et al*., 2003). The *RAD54L* is a putative oncogene localised in the frequently gain chromosomal region 1p32-35.3 (Tong *et al*., 2015). We revealed for the

first time that over-expression of *RAD54L* is associated with down-regulation of miR-150. Another putative target of miR-150 identified in this study is the *CCNA2* gene. The *CCNA2* has been long recognised as a pivotal gene involved in controling cell cycle at the G1/ S and G2/ M transitions (Gao *et al*., 2014). It is also one of the genes in 20 genes signature used for outcome prediction and prognostic assessment in MM (García-Escudero *et al*., 2010).

Aberrant expression of miR-125b is implicated in cancers of the colon, prostate and lymphomas (Jacinto *et al*., 2007; Mahapatra *et al*., 2012). The *IRF4*, *Blimp1* and *p53* are found to be its possible targets (Gururajan *et al*., 2010; Murray *et al*., 2013). Recently, it is suggested that miR-125b mimics significantly induce anti-multiple myeloma activity and prolonged survival of myeloma cells *in vitro* and *in vivo* by targeting *IRF4* (Morelli *et al*., 2015). The integrative analysis of matched miRNA and mRNA expression data revealed new potential targets of miR-125b, namely *RASGRF2* and *CYSLTR2*. Low expression of *RASGRF2* has been described in lymphomas, lung cancer, cancer cell lines and primary tumour but not in MM (Chen *et al*., 2006). The *RASGRF2* is a tumour suppressor gene participating in H-ras signaling pathway (Gu and Chen, 2012). It plays pivotal roles in regulating conversion of active or inactive forms of RAS protein (Chen *et al*., 2006). RAS protein is an important component in signal transduction pathway as it activates intracellular pathways that affect directly in biological processes related to cell proliferation, survival and motility (Ruiz *et al*., 2009). Ultimately, disruption of normal biological processes through anomaly in *RASGRF2* could facilitate cancerous cell growth and disease progression. Besides *RASGRF2*, *CYSLTR2* is another significant target of miR-125b identified in this study. The importance of *CTSLTR2* in myelomagenesis has been discussed in section 4.2. Herein, this thesis reported for the first time that over-expression of miR-125b might down-

regulate *RASGRF2* and *CYSLTR2* and therefore turn-off the tumour suppressive function of *RASGRF2* and *CYSLTR2* in MM.

Besides *RAD54L*, *CCNA2*, *RASGRF2* and *CYSLTR2*, *HKDC1* was another new miRNA target found under integrative analysis of miRNA-target in this study. The *HKDC1* is associated with Alzheimer disease. Research on the role of *HKDC1* in cancer is very limited. It was found to be up-regulated in liver cancer (Wei *et al*., 2014). It functions as hexokinase, which involved in catalysing the phosphorylation of glucose suggesting its importance in supplying energy for the rapidly proliferating cancer cells. The role of hexokinase in cancers was further confirmed by Wolf *et al*. (2011) who postulated that hexokinase facilitates cell growth by glucose phosphorylation and mitochondrial translocation mediated by AKT signaling in glioblastoma multiforme. Apart from that, *HKDC1* was found to be a potential novel therapeutic target for lung cancer (Li and Huang, 2014). Biological function of *HKDC1* in MM is not well understood, more study need to be carried out to investigate whether it is also a promising molecular target in MM therapy.

Other miRNAs such as miR-33a, miR-9 and miR-211 have been described in relation with cancers. The miR-33a exhibits tumour suppressive properties in various human cancers including colorectal, breast, lung, pancreatic and melanoma (Ibrahim *et al*., 2011; Blandino *et al*., 2012; Rice *et al*., 2013; Liang *et al*., 2015; Zhou *et al*., 2015). Its over-expression is closely related with epigenetic regulators such as Pim-1 Proto-Oncogene, Serine/Threonine Kinase (*Pim-1*), high mobility AT-hook 2 (*HMGA2*), *c-Myc* and hypoxia-inducible factor-1a (*HIF-1a*) (Ibrahim *et al*., 2011; Rice *et al*., 2013; Blandino *et al*., 2012; Zhou *et al*., 2015). In contrast to above findings, its over-expression is believed to down-regulate *twist* family bHLH transcription factor (*TWIST*) and led to chemoresistant and decrease cisplatin-induced apoptosis cells in

osteosarcoma, which suggested its oncogenic role in osteosarcoma tumourigenesis (Zhou *et al*., 2014). In contrary, miR-33a was up-regulated in myeloma cases in this study suggests that it might act as onco-miR in myelomagenesis. This study postulates that *CYSLTR2* is a possible target regulated by miR-33a.

There are three independent miR-9 genes in human, namely miR-9-1 on chromosome 1; miR-9-2 on chromosome 5 and miR-9-3 on chromosome 15, with identical mature miR-9 sequence. Similar with miR-33a, miR-9 can serve as tumour suppressor or onco-miR although it is more frequently down-regulated in cancers (Wang *et al*., 2013). miR-9 has been identified as a tumour suppressor miR in ovarian cancer, neuroblastoma, gastric carcinoma and nasopharygeal carcinoma (Luo *et al*., 2009; Zhang *et al*., 2012; Wang *et al*., 2013; Lu *et al*., 2014). Induction of miR-9 represses *NFκB1* gene, which in turn inhibits cell proliferation in ovarian cancer (Wang *et al*., 2013). The miR-9 also lowers matrix metalloproteinase 14 (*MMP-14*) to prevent tumour cell growth, metastasis and angiogenesis in neuroblastoma cells (Zhang *et al*., 2012). miR-9 is down-regulated in gastric carcinoma and shown to target RAB34, member RAS oncogene family (*RAB34*) (Luo *et al*., 2009). Plasma miR-9 is identified as a potential biomarker in metastasis prediction in nasopharygeal carcinoma (Lu *et al*., 2014). In contrast to the above, miR-9 acts as an onco-miR in which its expression is shown to target SOCS5 to enhance tumour cell metastasis and invasion in prostate carcinoma (Seashols-Williams *et al*., 2016). In this study, we found that miR-9 was over-expressed in MM and it might be a negative regulator for *RASGRF2* and *CYSLTR2* genes.

To date, miR-211 is found to play a tumour suppressive role in ovarian cancer (Xia *et al*., 2015). Induction of miR-211 expression causes down-regulation of *Cyclin D1* and *CDK6* in ovarian cancer, which subsequently decreases tumour cell proliferation through inactivation of cell cycle genes (Xia *et al*., 2015). In contrast, recent findings showed that miR-211 is located in the intron 6 of melastatin and silencing of miR-211 suppresses the metastatic potential in melanoma (Moussay *et al*., 2011).

In this study, we found that miR-33a, miR-9 and miR-211 were up-regulated in MM. The miRNA-mRNA enrichment analysis indicated that *CYSLTR2* or/and *RASGRF2* are two predicted negative correlated target genes for miR-33a, miR-9 and miR-211 (Table 4.3). These miRNA-target sets have never been desribed previously. Based on the importance of these miRNAs and mRNAs in oncogenesis, we believe that they represent new important information that are worth for further investigation. Other miRNAs identified in the miRNA-target integrative analysis such as miR-4698, miR-4430, miR-1290 and etc. are novel miRNAs that have never been reported in association with human tumourigenesis. Their functions in MM development are remains to be investigated.

Importantly, it is apparent that loss or gain of function of specific miRNAs contributes to cellular transformation and tumourigenesis in MM. From the miRNA-target prediction analysis described in the literature and present findings, it is obvious that whether the miRNAs have oncogenic or tumour suppressive activity (or both) is depending on the cellular context and cell type that they are expressed in (Gounaris-Shannon and Chevassut, 2013). Therefore, understanding the miRNA regulator networks is critical to delineate the complex mechanisms underlying the malignant transformation and progression of MM.

## 5.5 IDENTIFICATION OF CNV/ GENE/ MICRORNA IN NFκB PATHWAY IN MM

The NFκB is a transcriptional factor that regulates a variety of genes that are crucial to immune system, cell proliferation, inflammation, and tumor development (Ma *et al*., 2011). The NFκB activation is one of the most important key factors in the survival and proliferation of myeloma cells (Demchenko and Kuehl, 2010). Interestingly, based on the genomics (CNVs), gene and miRNA microarray results in the present study, several CNV/ gene/ miRNA involved in NFκB pathway were identified. The aCGH findings revealed copy number gain in 14q32.2, a region where *NFκBIA* is localised (Table 4.1). In gene expression profiling of MM, *IκBKB* was found to be down-regulated in MM (Table 5.1). Other than that, miR-21 and miR-125b were up-regulated in MM in this study (Table 4.2). The *NFκBIA*, *IκBKB*, miR-21 and miR-125b are components directly or indirectly involved in NFκB pathway.

The *NFκBIA* encodes for *IκBα*, an NFκB inhibitor to interact with REL proto-oncogene, NFκB Subunit (*REL*) dimers to inhibit activity of NFκB/ REL complexes by trapping REL dimers in the cytoplasm through masking of their nuclear localization signals to suppress NFκB activity (Scherer *et al*., 1995). On the other hand, *IκBKB* phosphorylates and degrades the inhibitor in the inhibitor/ NFκB complex, causing dissociation of the inhibitor and activation of NFκB (Schmid and Birbach, 2008). Although we found gain in 14q32.2, where *NFκBIA* is localised and down-regulation of *IκBKB* in this study, which is contradict with their roles in NFκB pathway, it is suggests that other molecular events such as methylation, microRNA and transcription factors might affect the gene expression.

In MM, over-expression of miR-21 is induced by IL-6/STAT3 pathway upon adherence of bone marrow cells and bone marrow stromal cells (Löffler *et al*., 2007). Over-expression of miR-21 lowers the expression of *PTEN*, a known inhibitor of AKT phosphorylation that promotes NFκB activation and tumourigenesis in MM (Ma *et al*., 2011; Leone *et al*., 2013). Besides that, miR-125b over-expression inhibits *TNFAIP3* and elevated NF-κB activity suggesting that *TNFAIP3* is a negative target of miR-125b (Kim *et al*., 2012). Both miR-21 and miR-125b were up-regulated in this study. This study finding further supported the important role of NFκB signaling pathway in MM development and malignancy.

## 5.6 *NAMPT*-MEDIATED GENE SILENCING IN RPMI-8226 MYELOMA CELLS

Multiple myeloma is a highly heterogeneous disease which consists of molecular subtypes with varying clinicopathological features and disease outcomes (Prideaux *et al*., 2014). This disease remains incurable although the advent of treatment paradigms has improved the overall survival rate in the patients. Drug resistance is the major problem in MM therapy, which highlighted the importance of identifying new molecular targeted agents to combat this disease (de la Puente *et al*., 2014). From the aCGH findings, we found gain at chromosomal region 7q22.3, where the *NAMPT* gene is localised in 92% of myeloma patients analysed. Interestingly, *NAMPT* is the only gene residing within the copy number change region and it plays an important role in NAD+ salvage pathway as discussed in Chapter 2, section 2.4. Based on the previous findings, the expression level of *NAMPT* transcript is higher in cancerous cells compared to the normal cells (Hufton *et al*., 1999; Van Beijnum *et al*., 2002; Wang *et al*., 2011; Cea *et al*., 2012). In this study, the role of *NAMPT* gene in myeloma cell growth and apoptosis is investigated using siRNA approach.

Nucleofection method was performed to deliver the siRNAs into RPMI-8226 myeloma cells. Nucleofection is a fast and effective method designed specifically for hard-to-transfect cells such as MM. In this study, the gene knockdown efficiency and the stability of the gene silencing effects were increased when three different siRNA duplexes were combined for transfection. Our result showed that pooled siRNAs could improve gene knockdown efficiency besides its ability in reducing off-target effects (Hannus *et al*., 2014). *NAMPT*-mediated gene silencing results suggest that knockdown of *NAMPT* gene reduces cell growth and increases apoptosis demonstrating that *NAMPT* gene may be a potential molecular target in myeloma therapy. More importantly, the reduction of NAMPT protein levels in cells treated with NAMPT-b and NAMPT-abc ($P<0.01$) suggests that the gene silencing has successfully suppressed the *NAMPT* translation in RPMI-8226. However, the gene silencing effects on cell growth and apoptosis need to be confirmed in other MM cell lines.

Recent studied showed that FK866/ APO866, a small molecule inhibitor of *NAMPT* is able to inhibit *NAMPT* and induce MM cell death through autophagy mechanism in MM cell lines and xenograft models. The NAD+ intracellular shortage, triggered by FK866 treatment, could cause autophagic cell death via two possible molecular mechanisms. The first mechanism is induced by inhibiting mammalian target of rapamycin (mTOR) signaling, a critical negative regulator of autophagy, along with a decrease in phosphoinositide 3-kinase and protein kinase B/AKT (Cea *et al*., 2013). The second mechanism is induced by transcriptional activation of several autophagy-related genes through the inhibition of mitogen-activated protein kinase signaling pathway and nuclear localisation of transcription factor EB (Cea *et al*., 2013). However, these studies showed that the treatment of MM with FK866/ APO866 did not induce apoptotic cell death (Cea *et al*., 2012 & 2013). Although these studies showed that MM cell death is induced by autophagy rather than apoptosis, it is possible that the pharmacological

restriction of NAD+ in MM cells triggers apoptotic signaling, which is then limits by concomitant onset of autophagy and the aborted apoptosis could then switch autophagy into MM cell death program. This explains why apoptosis cell death is observed in the current study.

Several promising *NAMPT* inhibitors such as FK866/ APO866, GMX1778, GMX1778 and GMX1777 have been identified (Hjarnaa *et al*., 1999; Hovstadius *et al*., 2002; Ravaud *et al*., 2005; Olesen *et al*., 2008 & 2010; von Heideman *et al*., 2010). The effectiveness of these small molecule inhibitors in MM therapy is vastly dependent on the successful binding of the inhibitors to the *NAMPT*. Drug resistance might be a major concern if the patient carries mutation at the binding domain of *NAMPT* gene, which blocks the binding of small molecule inhibitors to *NAMPT* gene (Wang *et al*., 2014). Therefore, new *NAMPT* inhibitors are urgently needed to serve as alternative treatment option for patients who exhibit *NAMPT* gene over-expression and mutations.

## 5.7 RESEARCH LIMITATIONS

Although the research has reached its aims, there are some unavoidable limitations in this study. Firstly, different set of samples are used for the copy number variation study and gene/ miRNA expression studies. In addition, due to budget and time constraints the sample size used in the gene expression/ miRNA expression studies may have been too small. These might explain why the potential genes residing within the copy number change regions identified by aCGH are not found to be differentially expressed in the gene expression analysis. Secondly, plasma cells enrichment was not performed for all the samples used in this study. For aCGH study, the archival samples were fixed in methanol and glacial acetic acid. The component and morphology of the cell surface are disrupted by fixative and no longer suitable for plasma cell separation by surface markers. For mRNA and miRNA microarrays, although fresh bone marrow aspirates were collected from the patients but the sample volumes are too little for cell separation (0.1-1.0 ml). To obtain sufficient amount of cells for downstream application, bigger sample volume is needed for cell sorting either by magnetic beads or flow cytometry techniques as cell loss undoubtedly occurred during the washing processes. Thirdly, normal peripheral bloods were used as controls in this study although they are not the perfect control to compare against bone marrow specimens. However, it is the only alternative to use due to the difficulties in recruiting normal bone marrow from healthy volunteer. Lastly, the molecular characteristic of the samples were determined by conventional cytogenetics analysis only, no further classification are done by FISH technique due to limitation in sample volume and research fund.

## 5.8 FUTURE DIRECTION

Future research is aims to recruit more MM specimens to confirm the current gene/ miRNA microarray findings. In addition, although thousands of aberrant miRNAs have been identified in association with MM cell growth and survival, majority of them are meaningless if their real targets are not identified. Future research is aiming to confirm the biological relevance of the miRNA-target identified in the present study by using luciferase reporter assay. Once the relationship of the miRNA and its target has been verified, the function of the genes and miRNAs on myeloma pathogenesis can be determined by gene silencing/ over-expression and miRNA mimic/ inhibitor in cell lines and animal models. Apart from that, future exploration also aims to identify new *NAMPT* inhibitors in MM such as miRNAs that regulating *NAMPT* gene expression. We believe besides small molecule inhibitors, miRNAs are other important therapeutic targets for MM disease in future.

Although high-throughput sequencing or next generation sequencing is already available when the time this project was proposed, the cost of the application is too high at that time. The good news is that the cost for next generation sequencing is gradually decreases in the past two years. Therefore, future research can apply this technology on MM to allow a more precise characterisation of the molecular structure underlying the disease and discovery of novel molecular alterations involved in the disease development and progression.

# CHAPTER 6: CONCLUSION

To date, MM is still an incurable disease. Very limited information is known about the actual genetic and molecular mechanisms underlying its pathogenesis. In the present study, microarray technique was used to identify potential molecular targets underlying the pathogenesis of MM. Information on the genomic and epigenetic events such as CNVs, genes/ miRNAs expression, and potential miRNA-target in MM development and malignancy were successfully procured.

In summary, common copy number gains were detected at regions 1q, 2q, 3p, 3q, 4q, 5q, 6q, 7q, 8q, 9q, 10q, 11q, 13q, 14q, 15q, 21q and Xq while common copy number loss was identified at regions 14q. Gain of 7q22.3 was the most common CNV (92%) and *NAMPT* was identified in this region. Besides that, the *CTSS*, *LYST*, *CLK1*, *ACSL1* and *NFκBIA* are genes localised within the CNVs and they represent novel information that have never been previously described in MM. Interestingly, *CTSS* is localised in 1q21.2, a frequently gain region which is associated with poor prognosis in MM.

Besides common CNVs, *HIST2H3A*, *CYSLTR2* and *AURKB* were identified as the 3 most significant differentially expressed genes, which are localised in the frequently altered chromosomal regions described in literature, namely 1q21, 13q14.2 and 17p13.1, respectively. In miRNA expression study, miR-150 and miR-125b were identified as two significant differentially expressed miRNAs associated with B cell development. In addition, the miRNA-target integrative analysis of the matched mRNA and miRNA profiles revealed inverse correlation between 5 putative target genes and 15 miRNAs. All 5 target genes, namely *RAD54L*, *CCNA2*, *CYSLTR2*, *RASGRF2* and *HKDC1* play critical functions in oncogenesis. Lastly, the present study confirmed that *NAMPT* plays pivotal roles in survival and proliferation of RPMI-8226 myeloma cells

by using RNAi approach. In conclusion, the outcomes of this research has expanded our knowledge on the genomic and epigenetic mechanisms underlying the molecular pathogenesis of MM and also opens up clues and avenues for future investigation of myelomagenesis.

Figure 6.1 illustrates the summary of significant findings obtained in this study. The diagram shows the possible functions and interactions of the most significant CNVs, genes and miRNAs identified in this study in contributing to the molecular pathogenesis of MM.

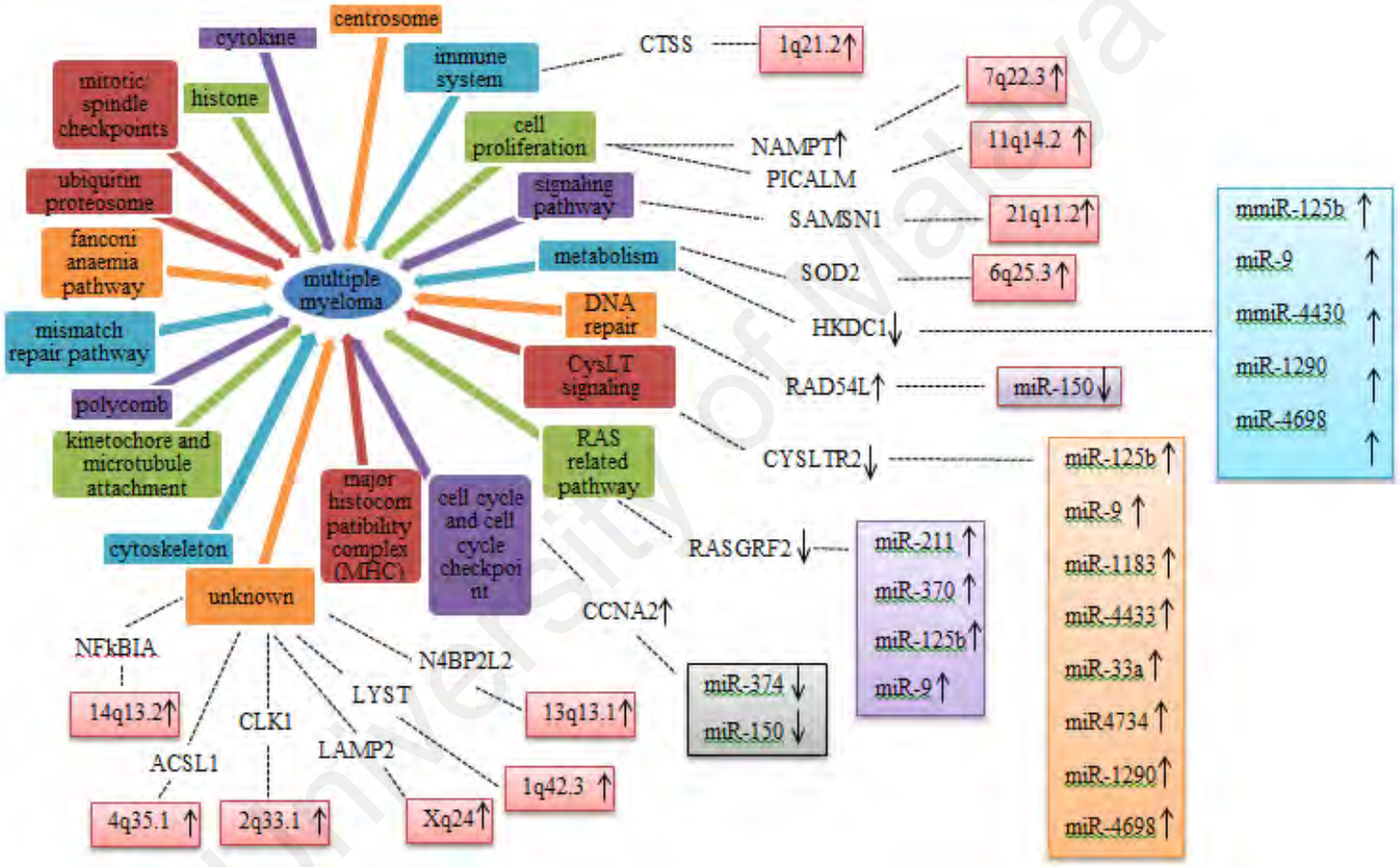


**Figure 6.1:** Function and interaction of significant CNVs, genes and miRNAs underlying the molecular pathogenesis of MM.

## REFERENCES


Abdi, J., Chen, G., & Chang, H. (2013). Drug resistance in multiple myeloma: latest findings and new concepts on molecular mechanisms. *Oncotarget*, *4*(12), 2186-2207.

Agarwal, S., van Cappellen, W. A., Guénolé, A., Eppink, B., Linsen, S. E., Meijering, E., … Essers, J. (2011). ATP-dependent and independent functions of Rad54 in genome maintenance. *The Journal of Cell Biology*, *192*(5), 735-750.

Agnelli, L., Bicciato, S., Mattioli, M., Fabris, S., Intini, D., Verdelli, D., … Neri, A. (2005). Molecular classification of multiple myeloma: a distinct transcriptional profile characterizes patients expressing CCND1 and negative for 14q32 translocations. *Journal of Clinical Oncology*, *23*(29), 7296-7306.

Agnelli, L., Mosca, L., Fabris, S., Lionetti, M., Andronache, A., Kwee, I., … Neri, A. (2009). A SNP microarray and FISH-based procedure to detect allelic imbalances in multiple myeloma: an integrated genomics approach reveals a wide gene dosage effect. *Genes Chromosomes Cancer*, *48*(7), 603-614.

Alexander, L., & Benninghoff, D. (1965). Familial multiple myeloma. *Journal of the National Medical Association*, *57*(6), 471-475.

Alexandra, L. T., Cristian, C., Jun, Q., Joseph, J. W., Kimal, R., Nancy, L. K., … Steven, T. R. (2015). Identification of potential glucocorticoid receptor therapeutic targets in multiple myeloma. *Nuclear Receptor Signaling*, *13*, e006.

Amodio, N., Bellizzi, D., Leotta, M., Raimondi, L., Biamonte, L., D'Aquila, P., … Tassone, P. (2013). miR-29b induces SOCS-1 expression by promoter demethylation and negatively regulates migration of multiple myeloma and endothelial cells. *Cell Cycle*, *12*(23), 3650-3662.

Amodio, N., Di Martino, M. T., Foresta, U., Leone, E., Lionetti, M., Leotta, M., … Tassone, P. (2012). miR-29b sensitizes multiple myeloma cells to bortezomib-induced apoptosis through the activation of a feedback loop with the transcription factor Sp1. *Cell Death & Disease*, *3*, e436.

Amodio, N., Stamato, M. A., Gullà, A. M., Morelli, E., Romeo, E., Raimondi, L., … Tassone, P. (2016). Therapeutic targeting of miR-29b/HDAC4 epigenetic loop in multiple myeloma. *Molecular Cancer Therapeutics*, *15*(6), 1364-1375.

An, G., Xu, Y., Shi, L., Zhong, S., Deng, S., Xie, Z., … Qiu, L. (2014). Chromosome 1q21 gains confer inferior outcomes in multiple myeloma treated with bortezomib but copy number variation and percentage of plasma cells involved have no additional prognostic value. *Haematologica*, *99*(2), 353-359.

Anderson, K. C., & Carrasco, R. D. (2011). Pathogenesis of myeloma. *Annual Review of Pathology*, *6*, 249-274.

Aqeilan, R. I., Calin, G. A., & Croce, C. M. (2010). miR-15a and miR-16-1 in cancer: discovery, function and future perspectives. *Cell Death & Differentiation*, *17*, 215-220.

Asano, E., Hasegawa, H., Hyodo, T., Ito, S., Maeda, M., Takahashi, M., … Senga, T. The Aurora-B-mediated phosphorylation of SHCBP1 regulates cytokinetic furrow ingression. *Journal of Cell Science*, *126*(Pt 15), 3263-3270.

Attaelmannan, M., & Levinson, S. S. (2000). Understanding and identifying monoclonal gammopathies. *Clinical Chemistry*, *46*(8 Pt 2), 1230-1238.

Attal, M., Harousseau, J. L., Leyvraz, S., Doyen, C., Hulin, C., Benboubker, L., … Inter-Groupe Francophone du Myélome (IFM). (2006). Maintenance therapy with thalidomide improves survival in patients with multiple myeloma. *Blood*, *108*(10), 3289-3294.

Avet-Loiseau, H., Attal, M., Moreau, P., Charbonnel, C., Garban, F., Hulin, C., … Mathiot, C. (2009). Genetic abnormalities and survival in multiple myeloma: the experience of the Intergroupe Francophone du Myélome. *Blood*, *109*(8), 3489-3495.

Avet-Loiseau, H., Facon, T., Daviet, A., Godon, C., Rapp, M. J., Harousseau, J. L., … Bataille, R. (1999). 14q32 translocations and monosomy 13 observed in monoclonal gammopathy of undetermined significance delineate a multistep process for the oncogenesis of multiple myeloma. Intergroupe Francophone du Myelome. *Cancer Research*, *59*(18), 4546-4550.

Avet-Loiseau, H., Gerson, F., Magrangeas, F., Minvielle, S., Harousseau, J. L., Bataille, R., & Intergroupe Francophone du Myélome. (2001). Rearrangement of the c-myc oncogene are present in 15% of primary human multiple myeloma tumors. *Blood*, *98*(10), 3082-3086.

Avet-Loiseau, H., Li, C., Magrangeas, F., Gouraud, W., Charbonnel, C., Harousseau, J-L., … Minvielle, S. (2009). Prognostic Significance of Copy-Number Alterations in Multiple Myeloma. *Journal of clinical oncology*, *27*(27), 4585-4590.

Avet-Loiseau, H., Malard, F., Campion, L., Magrangeas, F., Sebban, C., Lioure, B., … Intergroupe Francophone du Myélome. (2011). Translocation t(14;16) and multiple myeloma: is it really an independent prognostic factor? *Blood*, *117*(6), 2009-2011.

Bagshaw, R. D., Mahuran, D. J., & Callahan, J. W. (2005). A proteomic analysis of lysosomal integral membrane proteins reveals the diverse composition of the organelle. *Molecular & Cellular Proteomics*, *4*(2), 133-143.

Bagshaw, R. D., Mahuran, D. J., & Callahan, J. W. (2005). Lysosomal membrane proteomics and biogenesis of lysosomes. *Molecular Neurobiology*, *32*(1), 27-41.

Balcárková, J., Urbánková, H., Scudla, V., Holzerová, M., Bacovský, J., Indrák, K., & Jarosová, M. (2009). Gain of chromosome arm 1q in patients in relapse and progression of multiple myeloma. *Cancer Genetic Cytogenetic*, *192*(2), 68-72.

Barlogie, B., Jagannath, S., Vesole, D. H., Naucke, S., Cheson, B., Mattox, S., … Tricot, G. (1997). Superiority of tandem autologous transplantation over standard therapy for previously untreated multiple myeloma. *Blood*, *89*(3), 789-793.

Bartel, D. P. (2009). MicroRNAs: target recognition and regulatory functions. *Cell*, *136*(2), 215–233.

Becker, N. (2011). Epidemiology of multiple myeloma. *Recent Results Cancer Research*, *183*, 25-35.

Bengtsson, A. M., Jönsson, G., Magnusson, C., Salim, T., Axelsson, C., & Sjölander, A. (2013). The cysteinyl leukotriene 2 receptor contributes to all-trans retinoic acid-induced differentiation of colon cancer cells. *BMC Cancer*, *13*, 336.

Bergsagel, P. L., Kuehl, W. M., Zhan, F., Sawyer, J., Barlogie, B., & Shaughnessy, J. Jr. (2005). Cyclin D dysregulation: an early and unifying pathogenic event in multiple Myeloma. *Blood*, *106*(1), 296–303.

Bergsagel, P. L., Mateos, M. V., Gutierrez, N. C., Rajkumar, S. V., & San Miguel, J. F. (2013). Improving overall survival and overcoming adverse prognosis in the treatment of cytogenetically high-risk multiple myeloma. *Blood*, *121*(6), 884-892.

Blandino, G., Valerio, M., Cioce, M., Mori, F., Casadei, L., Pulito, C., … Strano, S. (2012). Metformin elicits anticancer effects through the sequential modulation of DICER and c-MYC. *Nature Communications*, *3*, 865.

Bortnick, A., & Allman, D. (2013). What is and what should always have been: long-lived plasma cells induced by T cell-independent antigens. *Journal of Immunology*, *190*(12), 5913-5918.

Brito, J. L., Walker, B., Jenner, M., Dickens, N. J., Brown, N. J., Ross, F. M., … Morgan, G. J. (2009). MMSET deregulation affects cell cycle progression and adhesion regulons in t(4;14) myeloma plasma cells. *Haematologica*, *94*(1), 78-86.

Bronevetsky, Y., & Ansel, K. M. (2013). Regulation of miRNA biogenesis and turnover in the immune system. *Immunological Reviews*, *253*(1), 304-316.

Brown, L. M., Gridley, G., Pottern, L. M., Baris, D., Swanso, C. A., Silverman, D. T., … Fraumeni, J. F. Jr. (2001). Diet and nutrition as risk factors for multiple myeloma among blacks and whites in the United States. *Cancer Causes Control*, *12*(2), 117-125.

Broyl, A., Hose, D., Lokhorst, H., de Knegt, Y., Peeters, J., Jauch, A., … Sonneveld, P. (2010). Gene expression profiling for molecular classification of multiple myeloma in newly diagnosed patients. *Blood*, *116*(14), 2543-2553.

Carrasco, D. R., Tonon, G., Huang, Y., Zhang, Y., Sinha, R., Feng, B., … Depinho, R. A. (2006). High-resolution genomic profiles define distinct clinico-pathogenetic subgroups of multiple myeloma patients. *Cancer Cell*, *9*(4), 313-325.

Caudell, D., & Aplan, P.D. (2008). The role of CALM-AF10 gene fusion in acute leukemia. *Leukemia*, *22*(4), 678-685.

Cea, M., Cagnetta, A., Fulciniti, M., Tai, Y-T., Hideshima, T., Chauhan, D., … Anderson, K. C. (2012). Targeting $NAD^+$ salvage pathway induces autophagy in multiple myeloma cells via mTORC1 and extracellular signal-regulated kinase (ERK1/2) inhibition. *Blood*, *120*(17), 3519-3529.

Cea, M., Cagnetta, A., Patrone, F., Nencioni, A., Gobbi, M., & Anderson, K. C. (2013). Intracellular NAD+ depletion induces autophagic death in multiple myeloma cells. *Autophagy*, *9*(3), 410-412.

Chang, H., Qi, X. Y., & Stewart, A. K. (2005). t(11;14) does not predict long-term survival in myeloma. *Leukemia*, *19*(6), 1078-1079.

Chang, X., Zhu, Y., Shi, C., & Stewart, A. K. (2014). Mechanism of immunomodulatory drugs' action in the treatment of multiple myeloma. *Acta Biochimica et Biophysica Sinica* (Shanghai), *46*(3), 240-253.

Chen, H., Suzuki, M., Nakamura, Y., Ohira, M., Ando, S., Iida, T., … Kimura, H. (2006). Aberrant methylation of RASGRF2 and RASSF1A in human non-small cell lung cancer. *Oncology Reports*, *15*(5), 1281-1285.

Chen, L., Li, C., Zhang, R., Gao, X., Qu, X., Zhao, M., … Li, J. (2011). miR-17-92 cluster microRNAs confers tumorigenicity in multiple myeloma. *Cancer Letters*, *309*(1), 62-70.

Chi, J., Ballabio, E., Chen, X. H., Kušec, R., Taylor, S., Hay, D., … Lawrie, C. H. (2011). MicroRNA expression in multiple myeloma is associated with genetic subtype, isotype and survival. *Biology Direct*, *6*, 23.

Chiarugi, A., Dölle, C., Felici, R., & Ziegler, M. (2012). The NAD metabolome—a key determinant of cancer cell biology. *Nature Review of Cancer*, *12*(11), 741-752.

Child, J. A., Morgan, G. J., Davies, F. E., Owen, R. G., Bell, S. E., Hawkins, K., … Medical Research Council Adult Leukaemia Working Party. (2003). High-dose chemotherapy with hematopoietic stem-cell rescue for multiple myeloma. *New England Journal of Medicine*, *348*(19), 1875-1883.

Chng, W. J., & Fonseca, R. (2009). Centrosomes and myeloma; Aneuploidy and proliferation. *Environmental and Molecular Mutagenesis*, *50*(8), 697-707.

Chng, W. J., Braggio, E., Mulligan, G., Bryant, B., Remstein, E., Valdez, R., … Fonseca, R. (2008). The centrosome index is a powerful prognostic marker in myeloma and identifies a cohort of patients that might benefit from aurora kinase inhibition. *Blood*, *111*(3), 1603-1609.

Chng, W. J., Glebov, O., Bergsagel, P. L., & Kuehl, W. M. (2007). Genetic events in the pathogenesis of multiple myeloma. *Best Practice Research Clinical Haematology*, *20*(4), 571-596.

Chng, W. J., Gonzalez-Paz, N., Price-Troska, T., Jacobus, S., Rajkumar, S. V., Oken, M. M., … Fonseca, R. (2008). Clinical and biological significance of RAS mutations in multiple myeloma. *Leukemia*, *22*(12), 2280-2284.

Chng, W. J., Price-Troska, T., Gonzalez-Paz, N., Van Wier, S., Jacobus, S., Blood, E., … Fonseca, R. (2007). Clinical significance of TP53 mutation in myeloma. *Leukemia*, *21*(3), 582-584.

Chng, W. J., Santana-Dávila, R., Van Wier, S. A., Ahmann, G. J., Jalal, S. M., Bergsagel, P. L., … Fonseca, R. (2006). Prognostic factors for hyperdiploid-myeloma: effects of chromosome 13 deletions and IgH translocations. *Leukemia*, *20*(5), 807-813.

Chng, W. J., Van Wier, S. A., Ahmann, G. J., Winkler, J. M., Jalal, S. M., Bergsagel, P. L., … Fonseca, R. (2005). A validated FISH trisomy index demonstrates the hyperdiploid and nonhyperdiploid dichotomy in MGUS. *Blood*, *106*(6), 2156-2161.

Chng, W., Shanmugam, V., Chesi, M., Bergsagel, P. L., Carpten, J., & Fonseca, R. (2007). Identification of common and genetic subtype specific molecular programs associated with progression from monoclonal gammopathy of undetermined significance (MGUS) to myeloma (MM). *Clinical Cancer Research*, *13*(22), B60.

Chng, W-J., Baker, A., Henry, T., Price-Troska, T., Van Wier, S., Chung, T-H., … Fonseca, R. (2006). Combined High Resolution Array Comparative Genomic Hybridization and Gene Expression Profiling Reveal Rb1 Haploinsufficiency as a Possibile Tumorigenic Mechanism in Myeloma. *Blood (ASH Annual Meeting Abstracts)*, *108*, 113.

Christoffersen, N. R., Shalgi, R., Frankel, L. B., Leucci, E., Lees, M., Klausen, … Lund, A. H. (2010). p53-independent upregulation of miR-34a during oncogene-induced senescence represses MYC. *Cell Death & Differentiation*, *17*(2), 236-245.

Chuang, H. Y., & Ou, Y. H. (2013). Overexpression of anillin in colorectal cancer promotes the cell proliferation, cell mobility and cell invasion. *Cancer Research, 74*, 4068.

Chung, T-H., Mulligan, G., Fonseca, R., & Chng, W. J. (2013). A Novel Measure of Chromosome Instability Can Account for Prognostic Difference in Multiple Myeloma. *PLoS One*, *8*(6), e66361.

Claudio, J. O., Zhu, Y. X., Benn, S. J., Shukla, A.H., McGlade, C. J., Falcioni, N., & Stewart, A. K. (2001). HACS1 encodes a novel SH3-SAM adaptor protein differentially expressed in normal and malignant hematopoietic cells. *Oncogene*, *20*(38), 5373-5377.

Colla, S., Tagliaferri, S., Morandi, F., Lunghi, P., Donofrio, G., Martorana, D., … Giuliani, N. (2007). The new tumor-suppressor gene inhibitor of growth family member 4 (ING4) regulates the production of proangiogenic molecules by myeloma cells and suppresses hypoxia-inducible factor-1 alpha (HIF-1alpha) activity: involvement in myeloma-induced angiogenesis. *Blood*, *110*(13), 4464-4475.

Colombo, M., Galletti, S., Garevelli, S., Platonova, N., Paoli, A., Basile, A., … Chiaramonte, R. (2015). Notch signaling deregulation in multiple myeloma: A rational molecular target. *Oncotarget*, *6*(29), 26826-26840.

Corre, J., Munshi, N., & Avet-Loiseau, H. (2015). Genetics of multiple myeloma: another heterogeneity level? *Blood*, *125*(12), 1870-1876.

Cosco, D., Cilurzo, F., Maiuolo, J., Federico, C., Di Martino, M. T., Cristiano, M. C., … Paolino, D. (2015). Delivery of miR-34a by chitosan/ PLGA nanoplexes for the anticancer treatment of multiple myeloma. *Scientific Reports*, *5*, 17579.

Cullinane, A. R., Schäffer A. A., & Huizing, M. (2013). The BEACH is hot: a LYST of emerging roles for BEACH-domain containing proteins in human disease. *Traffic*, *14*(7), 749-766.

Daniels, S. I., Sillé, F. C. M., Goldbaum, A., Yee, B., Key, E., Zhang, L, … Thomas, R. (2014). Improving power to detect changes in blood miRNA expression by accounting for sources of variability in experimental designs. *Cancer Epidemiol Biomarkers Prevention*, *23*(12), 2658-2666.

Davison, T. S., Johnson, C. D., & Andruss, B. F. (2006). Analyzing micro-RNA expression using microarrays. *Methods in Enzymology*, *411*, 14-34.

De Bruyne, E., Bos, T. J., Schuit, F., Van Valckenborgh, E., Menu, E., Thorrez, L., … Vanderkerken, K. (2010). IGF-1 suppresses Bim expression in multiple Myeloma via epigenetic and posttranslational mechanisms. *Blood*, *115*(12), 2430-2440.

De la Puente, P., Muz, B., Azab, F., Luderer, M., & Azab, A. K. (2014). Molecularly Targeted Therapies in Multiple Myeloma. *Leukemia Research and Treatment*, *2014*, 976567.

De Mel, S., Lim, S. H., Tung, M. L., & Chng, W-J. (2014). Implications of Heterogeneity in Multiple Myeloma. *BioMed Research International*, *2014*, 232546.

De Raeve, H. R., & Vanderkerken, K. (2005). The role of the bone marrow microenvironment in multiple myeloma. *Histology and Histopathology*, *20*, 1227-1250.

De Vos, J., Thykjaer, T., Tarte, K., Ensslen, M., Raynaud, P., Requirand, G., … Klein, B. (2002). Comparison of gene expression profiling between malignant and normal plasma cells with oligonucleotide arrays. *Oncogene*, *21*(44), 6848-6857.

Decaux, O., Lodé, L., Magrangeas, F., Charbonnel, C., Gouraud, W., Jézéquel, P., … Intergroupe Francophone du Myélome. (2008). Prediction of survival in multiple myeloma based on gene expression profiles reveals cell cycle and chromosomal instability signatures in high-risk patients and hyperdiploid signatures in low-risk patients: a study of the Intergroupe Francophone du Myélome. *Journal of Clinical Oncology*, *26*(29), 4798-4805.

Demchenko, Y. N., & Kuehl, W. M. (2010). A critical role for the NFkB pathway in multiple myeloma. *Oncotarget*, *1*(1), 59-68.

DeVita, V. T. Jr, Hellman, S., & Rosenberg, S. A. (1997). *Cancer: Principles and Practice of Oncology* (5th ed). Philadelphia: Lippincott-Raven Publishers.

Di Fiore, P. P. (2009). Endocytosis, signaling and cancer, much more than meets the eye. *Molecular Oncology*, *3*(4), 273–279.

Di Fiore, P. P., & De Camilli, P. (2001). Endocytosis and signaling. An inseparable partnership. *Cell*, *106*(1), 1-4.

Di Fiore, P. P., & Gill, G. N. (1999). Endocytosis and mitogenic signaling. *Current Opinion in Cell Biology*, *11*(4), 483-488.

Di Martino, M. T., Campani, V., Misso, G., Gallo Cantafio, M. E., Gullà, A., Foresta, U., … Caraglia, M. (2014). In vivo activity of miR-34a mimics delivered by stable nucleic acid lipid particles (SNALPs) against multiple myeloma. *PLoS One*, *9*(2), e90005.

Di Martino, M. T., Gullà, A., Gallo Cantafio, M. E., Altomare, E., Amodio, N., Leone, E., … Tassone, P. (2014). In vitro and in vivo activity of a novel locked nucleic acid (LNA)-inhibitor-miR-221 against multiple myeloma cells. *PLoS One*, *9*(2), e89659.

Di Martino, M. T., Gulla, A., Gallo Cantofio, M. E. G., Lionetti, M., Leone, E., Amodio, N., … Tassone, P. (2013). In vitro and in vivo anti-tumor activity of miR-221/222 inhibitors in multiple myeloma. *Oncotarget*, *4*(2), 242-255.

Di Martino, M. T., Leone, E., Amodio, N., Foresta, U., Lionetti, M., Pitari, M. R., … Tassone, P. (2012). Synthetic miR-34a mimics as a novel therapeutic agent for multiple myeloma: in vitro and in vivo evidence. *Clinical Cancer Research*, *18*(22), 6260-6270.

Dib, A., Gabrea, A., Glebov, O. K., Bergsagel, P. L., & Kuehl, W. M. (2008). Characterization of MYC translocations in multiple myeloma cell lines. *Journal of the National Cancer Institute Monographs*, *2008*(39), 25-31.

Dickens, N. J., Walker, B. A., Leone, P. E., Johnson, D. C., Brito, J. L., Zeisig, A., … Morgan, G. J. (2010). Homozygous deletion mapping in myeloma samples identifies genes and an expression signature relevant to pathogenesis and outcome. *Clinical Cancer Research*, *16*(6), 1856-1864.

Dimopoulos, K., Gimsing, P., & Grønbæk, K. (2013). Aberrant microRNA expression in multiple myeloma. *European Journal of Haematology*, *91*(2), 95-105.

Dimopoulos, K., Gimsing, P., & Grønbæk, K. (2014). The role of epigenetics in the biology of multiple myeloma. *Blood Cancer Journal*, *2*(4), e207.

Drach, J., Ackermann, J., Fritz, E., Krömer, E., Schuster, R., Gisslinger, H., … Huber, H. (1998). Presence of a p53 gene deletion in patients with multiple myeloma predicts for short survival after conventional-dose chemotherapy. *Blood*, *92*(3), 802-809.

Dreyling, M. H., Martinez-Climent, J. A., Zheng, M., Mao, J., Rowley, J. D., & Bohlander, S. K. (1996). The t(10;11)(p13;q14) in the U937 cell line results in the fusion of the AF10 gene and CALM, encoding a new member of the AP-3 clathrin assembly protein family. *Proc National Academic of Science USA*, *93*(10), 4804-4809.

Dvir-Ginzberg, M., Gagarina, V., Lee, E. J., & Hall, D. J. (2008). Regulation of cartilage-specific gene expression in human chondrocytes by SirT1 and nicotinamide phosphoribosyltransferase. *Journal of Biological Chemistry*, *283*(52), 36300-36310.

Eby, C. S. (2007). Bleeding and Thrombosis Risks in Plasma Cell Dyscrasias. *American Society of Hematology Education Book*, *2007*(1), 158-164.

Ehrlich, L. A., & and Roodman, G. D. (2005). The role of immune cells and inflammatory cytokines in Paget's disease and multiple Myeloma. *Immunological Reviews*, *208*, 252-266.

Einsele-Scholz, S., Malmsheimers, S., Bertram, K., Stehle, D., Johanning, J., Manz, M., … Essmann, F. (2016). Bok is a genuine multi-BH-domain protein that triggers apoptosis in the absence of Bax and Bak. *Journal of Cell Science*, *129*(11), 2213-2223.

Elnenaei, M. O., Hamoudi, R. A., Swansbury, J., Gruszka-Westwood, A. M., Brito-Babapulle, V., Matutes, E., & Catovsky, D. (2003). Delineation of the minimal region of loss at 13q14 in multiple myeloma. *Genes Chromosomes Cancer*, *36*(1), 99-106.

Ezzeldin, M., Borrego-Diaz, E., Taha, M., Esfandyari, T., Wise, A. L., Peng, W., … Farassati, F. (2014). RalA signaling pathway as a therapeutic target in hepatocellular carcinoma (HCC). Molecular Oncology, *8*(5), 1043-1053.

Facon, T., vet-Loiseau, H., Guillerm, G., Moreau, P., Geneviève, F., Zandecki, M., … Mary, J. Y. (2001). Chromosome 13 abnormalities identified by FISH analysis and serum beta2-microglobulin produce a powerful myeloma staging system for patients receiving high-dose therapy. *Blood*, *97*(6), 1566-1571.

Favis, R., Sun, Y., van de Velde, H., Broderick, E., Levey, L., Meyers, M., … Ricci, D. S. (2011). Genetic variation associated with bortezomib-induced peripheral neuropathy. *Pharmacogenetics & Genomics*, *21*(3), 121-129.

Fehrenbacher, N., Bastholm, L., Kirkegaard-Sørensen, T., Rafn, B., Bøttzauw, T., Nielsen, C., … Jäättelä, M. (2008). Sensitization to the lysosomal cell death pathway by oncogene-induced down-regulation of lysosome-associated membrane proteins 1 and 2. *Cancer Research*, *68*(16), 6623-6633.

Feige, J. N., Lagouge, M., Canto, C., Strehle, A., Houten, S. M., Milne, J. C., … Auwerx, J. (2008). Specific SIRT1 activation mimics low energy levels and protects against diet-induced metabolic disorders by enhancing fat oxidation. *Cell metabolism*, *8*(5), 347-358.

Fenton, J. A., Pratt, G., Rothwell, D. G., Rawstron, A. C., & Morgan, G. J. (2004). Translocation t(11;14) in multiple myeloma: Analysis of translocation breakpoints on der(11) and der(14) chromosomes suggests complex molecular mechanisms of recombination. *Genes Chromosomes Cancer*, *39*(2), 151-155.

Ferlay, J., Soerjomataram, I., Ervik, M., Dikshit, R., Eser, S., Mathers, C., … Bray, F. (2013). GLOBOCAN 2012 v1.0, Cancer Incidence and Mortality Worldwide: IARC CancerBase No. 11 [Internet]. Retrieved from http://globocan.iarc.fr.

Fernando, T. R. Rodriguez-Malave, N. I., & Rao, D. S. (2012). MicroRNAs in B cell development and malignancy. *Journal of Hematology & Oncology*, *5*, 7.

Firkin, F. (2009). Screening for multiple myeloma. *Australian Prescriber*, *32*, 92-94.

Fonseca, R., Bailey, R. J., Ahmann, G. J., Rajkumar, S. V., Hoyer, J. D., Lust, J. A., … Dewald, G. W. (2002). Genomic abnormalities in monoclonal gammopathy of undetermined significance. *Blood*, *100*(4), 1417-1424.

Fonseca, R., Debes-Marun, C. S., Picken, E. B., Dewald, G. W., Bryant, S. C., Winkler, J. M., … Greipp, P. R. (2003). The recurrent IgH translocations are highly associated with nonhyperdiploid variant multiple myeloma. *Blood*, *102*(7), 2562-2567.

Fonseca, R., Oken, M. M., Harrington, D., Bailey, R. J., Van Wier, S. A., Henderson, K. J., … Dewald, G. W. (2001). Deletions of chromosome 13 in multiple myeloma identified by interphase FISH usually denote large deletions of the q arm or monosomy. *Leukemia*, *15*(6), 981-986.

Fritschi, L., Ambrosini, G. L., Kliewer, E. V., Johnson, K. C., & Canadian Cancer Registries Epidemiologic Research Group. Dietary fish intake and risk of leukaemia, multiple myeloma, and non-Hodgkin lymphoma. *Cancer Epidemiology Biomarkers Prevention*, *13*(4), 532-537.

Fulco, M., Cen, Y., Zhao, P., Hoffman, E. P., McBurney, M. W., Sauve, A. A., & Sartorelli, V. (2008). Glucose restriction inhibits skeletal myoblast differentiation by activating SIRT1 through AMPK-mediated regulation of Nampt. *Developmental Cell*, *14*(5), 661-673.

Gabrea, A., Martelli, M. L., Qi, Y., Roschke, A., Barlogie, B., Shaughnessy, J. D. Jr., … Kuehl, W. M. (2008). Secondary genomic rearrangements involving immunoglobulin or MYC loci show similar prevalences in hyperdiploid and nonhyperdiploid myeloma tumors. *Genes Chromosomes & Cancer*, *47*(7), 573-590.

Gao, T., Han, Y., Yu, L., Ao, S., Li, Z., & Ji, J. (2014). CCNA2 is a prognostic biomarker for ER+ breast cancer and tamoxifen resistance. *PLoS ONE*, *9*(3), e91771.

Gao, X., Zhang, R., Qu, X., Zhao, M., Zhang, S., Wu, H., … Chen, L. (2012). MiR-15a, miR-16-1 and miR-17-92 cluster expression are linked to poor prognosis in multiple myeloma. *Leukemia Research*, *36*(12), 1505-1509.

García-Escudero, R., Martínez-Cruz, A. B., Santos, M., Lorz, C., Segrelles, C., Garaulet, G., Saiz-Ladera, C., … Paramio, J. M. (2010). Gene expression profiling of mouse p53-deficient epidermal carcinoma defines molecular determinants of human cancer malignancy. *Molecular Cancer*, *9*, 193.

Garcia-Gomez, A., Las Rivas, J., Ocio, E. M., Diaz-Rodriguez, E., Montero, J. C., Martin, M., … Garayao, M. (2014). Transcriptomic profile induced in bone marrow mesenchymal stromal cells after interaction with multiple myeloma cells: implications in myeloma progression and myeloma bone disease. *Oncotarget*, *5*(18), 8284-8305.

Gazitt, Y. (1999). TRAIL is a potent inducer of apoptosis in myeloma cells derived from multiple myeloma patients and is not cytotoxic to hematopoietic stem cells. *Leukemia*, *13*(11), 1817–1824.

Gertz, M. A., & Greipp, P. R. (2003). *Hematologic malignancies: multiple myeloma and related plasma cell disorders*. Berlin, Germany: Springer-Verlag Berlin Heidelberg.

Geschickter, C., & Copeland, M. (1928). Multiple myeloma. *Archives Surgery*, *16*(4), 807-863.

Ghobrial, M. (2012). Myeloma as a model for the process of metastasis: implications for therapy. *Blood*, *120*(1), 20-30.

Giuliani, N., Storti, P., Bolzoni, M., Palma, B. D., & Bonomini, S. (2011). Angiogenesis and multiple myeloma. *Cancer Microenvironment*, *4*(3), 325-337.

Gozzetti, A., Frasconi, A., & Crupi, R. (2014). Molecular cytogenetics of multiple myeloma. *Austin Journal of Cancer and Clinical Research*, *1*(4), 1020.

Grammatikakis, I., Gorospe, M., & Abdelmohsen, K. (2013). Modulation of Cancer Traits by Tumor Suppressor microRNAs. *International Journal of Molecular Sciences*, *14*(1), 1822-1842.

Greipp, P. R., San Miguel, J., Durie, B. G., Crowley, J. J., Barlogie, B., Bladé, J., … Westin, J. (2005). International staging system for multiple myeloma. *Journal of Clinical Oncology*, *23*(15), 3412-3420.

Gullà, A., Di Martino, M. T., Gallo Cantafio, M. E., Amodio, N., Botta, C., Pitari, M. R., … Tassone, P. (2016). A 13 mer LNA-i-miR-221 inhibitor restores drug sensitivity in melphalan-refractory multiple myeloma cells. *Clinical Cancer Research*, *22*(5), 1222- 1233.

Gulyaeva, L. F., & Kushlinskiy, N. E. (2016). Regulatory mechanisms of microRNA expression. *Journal of Translational Medicine*, *14*, 143.

Gururajan, M., Haga, C. L., Das, S., Leu, C. M., Hodson, D., Josson, S., … Cooper, M. D. (2010). MicroRNA 125b inhibition of B cell differentiation in germinal centers. *International Immunology*, *22*(7), 583-592.

Gutiérrez, N. C., García, J. L., Hernández, J. M., Lumbreras, E., Castellanos, M., Rasillo, A., … San Miguel, J. F. (2004). Prognostic and biologic significance of chromosomal imbalances assessed by comparative genomic hybridization in multiple myeloma. *Blood*, *104*(9), 2661-2666.

Gutiérrez, N. C., Hernández, J. M., García, J. L., Cañizo, M. C., González, M., Hernández, J., … San Miguel, J. F. (2001). Differences in genetic changes between multiple myeloma and plasma cell leukemia demonstrated by comparative genomic hybridization. *Leukemia*, *15*(5), 840-845.

Gutiérrez, N. C., Sarasquete, M. E., Misiewicz-Krzeminska, I., Delgado, M., De Las Rivas, J., Ticona, F. V., … San Miguel, J. F. (2010). Deregulation of microRNA expression in the different genetic subtypes of multiple myeloma and correlation with gene expression profiling. *Leukemia*, *24*(3), 629-637.

Hannus, M., Beitzinger, M., Engelmann, J. C., Weickert, M-T., Spang, R., Hannus, S., & Meister, G. (2014). siPools: highly complex but accurately defined siRNA pools eliminate off-target effects. *Nucleic Acids Research*, *42*(12), 8049-8061.

Hao, M., Zhang, L., An, G., Sui, W., Yu, Z., Zou, D., … Qiu, L. (2011). Suppressing miRNA-15a/-16 expression by interleukin-6 enhances drug-resistance in myeloma cells. *Journal of Hematology Oncology*, *4*, 37.

Hastings, P. J., Lupski, J. R., Rosenberg, S. M., & and Ira. G. (2009). Mechanisms of change in gene copy number. *Nature Reviews Genetics*, *10*(8), 551-564.

Hermansen, N. E., Borup, R., Andersen, M. K., Vangsted, A. J., Clausen, N. T., Kristensen, D. L., … Gimsing, P. (2016). Gene expression risk signatures maintain prognostic power in multiple myeloma despite microarray probe set translation. *International Journal of laboratory Hematology*, *38*(3), 298-307.

Hermeking, H. (2010). The miR-34 family in cancer and apoptosis. *Cell Death & Differentiation*, *17*(2), 193-199.

Hideshima, T., Mitsiades, C., Tonon, g., Richardson, P. G., & and Anderson, K. C. (2007). Understanding multiple Myeloma pathogenesis in the bone marrow to identify new therapeutic targets. *Nature Reviews Cancer*, *7*(8), 585-598.

Hideshima, T., Nakamura, N., Chauhan, D., & Anderson, K. C. (2001). Biologic sequelae of interleukin-6 induced PI3-K/Akt signaling in multiple Myeloma. *Oncogene*, *20*(42), 5991-6000.

Hjarnaa, P. J., Jonsson, E., Latini, S., Dhar, S., Larsson, R., Bramm, E., … Binderup, L. (1999). CHS 828, a novel pyridyl cyanoguanidine with potent antitumor activity in vitro and in vivo. *Cancer Research*, *59*(22), 5751-5757.

Hovstadius, P., Larsson, R., Jonsson, E., Skov, T., Kissmeyer, A. M., Krasilnikoff, K., … Ahlgren, J. (2002) A Phase I study of CHS 828 in patients with solid tumor malignancy. *Clinical Cancer Research*, *8*(9), 2843-2850.

Huang, J. J., Yu, J., Li, J. Y., Liu, Y. T., & Zhong, R. Q. (2012). Circulating microRNA expression is associated with genetic subtype and survival of multiple myeloma. *Medical Oncology*, *29*(4), 2402-2408.

Huang, J., Sheng, H-H., Shen, T., Hu, Y-J., Xiao, H-S., Zhang, Q., & Zhang, Q-H. (2006). Correlation between genomic DNA copy number alterations and transcriptional expression in hepatitis B virus-associated hepatocellular carcinoma. *FEBS Letters*, *580*(15), 3571-3581.

Hufton, S. E., Moerkerk, P. T., Brandwijk, R., de Bruïne, A. P., Arends, J. W., & Hoogenboom, H. R. (1999). A profile of differentially expressed genes in primary colorectal cancer using suppression substractive hybridization. *Federation of European Biochemical Societies Letter*, *463*(1-2), 77-82.

Huh, J. Y., Chung, S., Oh, D., Kang, M. S., Eom, H. S., Cho, E. H., … Kong, S. Y. (2010). Clathrin assembly lymphoid myeloid leukemia-AF10-positive acute leukemias: a report of 2 cases with a review of the literature. *Korean Journal of Laboratory Medicine*, *30*(2), 117-121.

Hupalowska, A., & Miaczynska, M. (2012). The new faces of endocytosis in signaling. *Traffic 13*(1), 9-18.

Hussein, M. A. (2007). Multiple Myeloma: Most Common End-Organ Damage and Management. *Journal of the National Comprehensive Cancer Network*, *5*, 170-178.

Huynh, K. K., Eskelinen, E. L., Scott, C. C., Malevanets, A., Saftig, P., & Grinstein, S. (2007). LAMP proteins are required for fusion of lysosomes with phagosomes. *European Molecular Biology Organisation Journal*, *26*(2), 313-324.

Ibrahim, A. F., Weirauch, U., Thomas, M., Grünweller, A., Hartmann, R. K., & Aigner, A. (2011). MicroRNA replacement therapy for miR-145 and miR-33a is efficacious in a model of colon carcinoma. *Cancer Research*, *71*(15), 5214-5224.

Inoue, K., Mallakin, A., & Frazier, D. P. (2007). Dmp1 and tumor suppression. *Oncogene*, *26*(30), 4329-4335.

International Myeloma Working Group. (2003). Criteria for the classification of monoclonal gammopathies, multiple myeloma and related disorders: a report of the International Myeloma Working Group. *British Journal of Haematology*, *121*(5), 749-757.

Ise, M., & Takagi, T. (2007). Bone lesion in multiple myeloma. *Nihon Rinsho*, *65*(12), 2224-2228.

Jacinto, F. V., Ballestar, E., Ropero, S., & Esteller, M. (2007). Discovery of epigenetically silenced genes by methylated DNA immunoprecipitation in colon cancer cells. *Cancer Research*, *67*(24), 11481-11486.

Jain, M., Ascensao, J., & Schechter, G. (2009). Familial myeloma and monoclonal gammopathy: a report of eight African American families. *American Journal of Hematology*, *84*(1), 34-38.

Jenner, E. (2014). Serum free light chains in clinical laboratory diagnostics. *Clinica Chimica Acta*, *427*, 15-20.

Jiao, X., Hooper, S. D., Djureinovic, T., Larsson, C., Wärnberg, F., Tellgren-Roth, C., … Sjöblom, T. (2013). Gene rearrangements in hormone receptor negative breast cancers revealed by mate pair sequencing. *BMC Genomics*, *14*, 165.

Johnson, D. C., Weinhold, N., Mitchell, J., Chen, B., Stephens, O. W., Försti, A., … Morgan, G. J. (2016). Genetic factors influencing the risk of multiple myeloma bone disease. *Leukemia*, *30*(4), 883-888.

Jones, R. A., Master, P. S., Child, J. A., Roberts, B. E., & Scott, C. S. (1989). Diagnostic differentiation of chronic B-cell malignancies using monoclonal antibody L161 (CD1c). *British Journal of Haematology*, *71*(1), 43-46.

Kai, X., Chellappa, V., Donado, C., Reyon, D., Sekigami, Y., Ataca, D., … Pillai, S. (2014). IκB kinase β (IKBKB) mutations in lymphomas that constitutively activate canonical nuclear factor κB (NFκB) signaling. *The Journal of Biological Chemistry*, *289*(39), 26960-26972.

Kalff, A., & Spencer, A. (2012). The t(4;14) translocation and FGFR3 overexpression in multiple myeloma: prognostic implications and current clinical strategies. *Blood Cancer Journal*, *2*(9), e89.

Kassambara, A., Schoenhals, M., Moreaux, J., Veyrune, J. L., Rème, T., Goldschmidt, H., … Klein, B. (2013). Inhibition of DEPDC1A, a bad prognostic marker in multiple myeloma, delays growth and induces mature plasma cell markers in malignant plasma cells. *PLoS One*, *8*(4), e62752.

Katzmann, J. A., Dispenzieri, A., Kyle, R. A., Snyder, M. R., Plevak, M. F., Larson, D. R, … Rajkumar, S. V. (2006). Elimination of the need for urine studies in the screening algorithm for monoclonal gammopathies by using serum immunofixation and free light chain assays. *Mayo Clinic Proceeding*, *81*(12), 1575-1578.

Kim, M. Y., Woo, E. M., Chong, Y. T., Homenko, D. R., & Kraus, W. L. (2006). Acetylation of estrogen receptor alpha by p300 at lysines 266 and 268 enhances the deoxyribonucleic acid binding and transactivation activities of the receptor. *Molecular Endocrinology*, *20*(7), 1479-1493.

Kim, S. (2005). HuntING4 new tumor suppressors. *Cell Cycle*, *4*(4), 516-517.

Kim, S. J., Shin, H-T., Lee, H-O., Kim, N. K. D. Yun, J. W., Hwang, J. H., Park, W-Y. (2016). Recurrent mutations of MAPK pathway genes in multiple myeloma but not in amyloid light-chain amyloidosis. *Oncotarget*, *7*(42), 68350-68359.

Kim, S. W., Ramasamy, K., Bouamar, H., Lin A. P., Jiang, D., & Aguiar, R. C. (2012). MicroRNAs miR-125b and miR-125b constitutively activate the NF-kB pathway by targeting the tumor necrosis factor alpha-induced protein 3 (TNFAIP3, A20). *Proceeding of National Academy of Sciences USA*, *109*(20): 7865-7870.

Kim, Y., Reifenberger, G., Lu, D., Endo, T., Carson, D. A., Gast, S-M., Meschenmoser, K., … Schmidt-Wolf, I. G. H. (2011). Influencing the Wnt signaling pathway in multiple myeloma. *Anticancer Research*, *31*, 725-730.

Kjeldsen, E. (2016). Identification of prognostically relevant chromosomal abnormalities in routine diagnostics of multiple myeloma using genomic profiling. *Cancer Genomics Proteomics*, *13*(2), 91-127.

Ko, H. L., & Ren, E. C. (2012), Functional Aspects of PARP1 in DNA Repair and Transcription. *Biomolecules*, *2*(4), 524-548.

Koura, D. T., & Langston, A. A. (2013). Inherited predisposition to multiple myeloma. *Therapeutic Advances in Hematology*, *4*(4), 291-297.

Kristinsson, S. Y., Bjorkholm, M., Goldin, L., Blimark, C., Mellqvist, U., Wahlin, A., … Landgren, O. (2009). Patterns of hematologic malignancies and solid tumors among 37,838 first-degree relatives of 13,896 patients with multiple myeloma in Sweden. *International Journal of Cancer*, *125*, 2147–2150.

Kristinsson, S. Y., Goldin, L. R., Bjorkholm, M., Koshiol, J., Turesson, I., & Landgren, O. (2009). Genetic and immune-related factors in the pathogenesis of lymphoproliferative and plasma cell malignancies. *Haematologica*, *94*(11), 1581-1589.

Krol, J., Loedige, I., & Filipowicz, W. (2010). The widespread regulation of microRNA biogenesis, function and decay. *Nature Reviews Genetics*, *11*(9), 597-610.

Krona, C., Ejeskär, K., Carén, H., Abel, F., Sjöberg, R. M., & Martinsson, T. (2004). A novel 1p36.2 located gene, APITD1, with tumour-suppressive properties and a putative p53-binding domain, shows low expression in neuroblastoma tumours. *British Journal of Cancer*, *91*(6), 1119-1130.

Kryukov, F., Dementyeva, E., Kubiczkova, L., Jarkovsky, J., Brozova, L., Petrik, J., … Hajek, R. (2013). Cell cycle genes co-expression in multiple myeloma and plasma cell leukemia. *Genomics*, *102*(4), 243-249.

Kuiper, R., Broyl, A., de Knegt, Y., van Vliet, M. H., van Beers, E. H., van der Holt, B., … Sonneveld, P. (2012). A gene expression signature for high-risk multiple myeloma. *Leukemia*, *26*(11), 2406-2413.

Kuiper, R., van Duin, M., van Vliet, M. H., Broijl, A., van der Holt, B., el Jarari, L., … Sonneveld, P. (2015). Prediction of high and low risk multiple myeloma based on gene expression and the International Staging System. *Blood*, *126*(17), 1996-2004.

Kumar, S. K., Mikhael, J. R., Buadi, F. K., Dingli, D., Dispenzieri, A., Fonseca, R., … Bergsagel, P. L. (2009). Management of newly diagnosed symptomatic multiple myeloma: Updated Mayo Stratification of Myeloma and Risk-Adapted Therapy (mSMART) Consensus Guidelines. *Mayo Clinic Proceeding*, *84*(12), 1095-1110.

Kumar, S., & Rajkumar, S. V. (2008). Many facets of bortezomib resistance/ susceptibility. *Blood*, *112*(6), 2177-2178.

Kyle, R. A., & Rajkumar, S. V. (2009). Criteria for diagnosis, staging, risk stratification and response assessment of multiple myeloma. *Leukemia*, *23*(1), 3-9.

Kyle, R. A., Buadi, F. I., & Vinc Ent Rajkumar, S. (2011). Management of Monoclonal Gammopathy of Undetermined Significance (MGUS) and Smoldering Multiple Myeloma (SMM). *Oncology (Williston Park)*, *25*(7), 578-586.

Landgren O, Gridley G, Turesson I, Caporaso, N. E., Goldin, L. R., Baris, D., … Linet, M. S. (2006). Risk of monoclonal gammopathy of undetermined significance (MGUS) and subsequent multiple myeloma among African American and white veterans in the United States. *Blood*, *107*(3), 904-906.

Landgren, O. (2013). Monoclonal gammopathy of undetermined significance and smoldering multiple myeloma: biological insights and early treatment strategies. *Hematology American Society of Hematology Education Program*, *2013*, 478-487.

Landgren, O., Kyle, R. A., Pfeiffer, R. M., Katzmann, J. A., Caporaso, N. E., Hayes, R. B., … Rajkumar, S.V. (2009). Monoclonal gammopathy of undetermined significance (MGUS) consistently precedes multiple myeloma: a prospective study. *Blood*, *113*(22), 5412-5417.

Lankat-Buttgereit, B., & Goke, R. (2009). The tumour suppressor Pdcd4: recent advances in the elucidation of function and regulation. *Biology of the Cell*, *101*(6), 309-317.

Largo, C., Alvarez, S., Saez, B., Blesa, D., Martin-Subero, J., Gonzalez-Garcia, I., … Cigudosa, J. (2006). Identification of overexpressed genes in frequently gained/amplified chromosome regions in multiple myeloma. *Haematologica*, *91*(2), 184-191.

Largo, C., Saéz, B., Alvarez, S., Suela, J., Ferreira, B., Blesa, D., … Cigudosa, J. C. (2007). Multiple myeloma primary cells show a highly rearranged unbalanced genome with amplifications and homozygous deletions irrespective of the presence of immunoglobulin-related chromosome translocations. *Haematologica*, *92*(6), 795-802.

Lawrie, C. H., Chi, J., Taylor, S., Tramonti, D., Ballabio, E., Palazzo, S., … Hatton, C. S. (2009). Expression of microRNAs in diffuse large B cell lymphoma is associated with immunophenotype, survival and transformation from follicular lymphoma. *Journal of Cellular and Molecular Medicine*, *13*(7), 1248-1260.

Lawrie, C. H., Cooper, C. D., Ballabio, E., Chi, J., Tramonti, D., & Hatton, C. S. (2009). Aberrant expression of microRNA biosynthetic pathway components is a common feature of haematological malignancy. *British Journal of Haematology*, *145*(4), 545-548.

Lawrie, C. H., Saunders, N. J., Soneji, S., Palazzo, S., Dunlop, H. M., Cooper, C. D., … Hatton, C. S. (2008). MicroRNA expression in lymphocyte development and malignancy. *Leukemia*, *22*(7), 1440-1446.

Leone, E., Morelli, E., Di Martino, M. T., Amodio, N., Foresta, U., Gullà, A., … Tassone, P. (2013). Targeting miR-21 inhibits in vitro and in vivo multiple myeloma cell growth. *Clinical Cancer Research*, *19*(8), 2096-2106.

Leone, P. E., Mendiola, M., Alonso, J., Paz-y-Miño, C., & Pestaña, A. (2003). Implications of a RAD54L polymorphism (2290C/T) in human meningiomas as a risk factor and/or a genetic marker. *BMC Cancer*, *3*, 6.

Leotta, M., Biamonte, L., Raimondi, L., Ronchetti, D., Di Martino, M. T., Botta, C., … Amodio, N. (2014). A p53-dependent tumor suppressor network is induced by selective miR-125a-5p inhibition in multiple myeloma cells. *Journal of Cellular Physiology*, *229*(12), 2106-2116.

Li, G. H., & Huang, J. F. (2014). Inferring therapeutic targets from heterogeneous data: HKDC1 is a novel potential therapeutic target for cancer. *Bioinformatics*, *30*(6), 748-752.

Li, Y., Wang, X., Zheng, H., Wang, C., Minvielle, S., Magrangeas, F., … Li, C. (2013). Classify hyperdiploidy status of multiple myeloma patients using gene expression profiles. *PLoS One*, *8*(3), e58809.

Li, Y., Zhang, B., Li, W., Wang, L., Yan, Z., Li, H., … Li, Z. (2016). MiR-15a/16 regulates the growth of myeloma cells, angiogenesis and antitumor immunity by inhibiting Bcl-2, VEGF-A and IL-17 expression in multiple myeloma. *Leukemia Research*, *49*, 73-79.

Li, Z., & Rana, T. M. (2012). Molecular mechanisms of RNA-triggered gene silencing machineries. *Accounts of Chemical Research*, *45*(7), 1122-1131.

Li, Z., Huang, H., Chen, P., He, M., Li, Y., Arnovitz, S., … Chen, J. (2012). miR-196b directly targets both HOXA9/MEIS1 oncogenes and FAS tumour suppressor in MLL-rearranged leukaemia. *Nature Communications*, *3*, 688.

Liang, C., Yu, X. J., Guo, X. Z., Sun, M. H, Wang, Z., Song, Y., … Li, Y. Y. (2015). MicroRNA-33a-mediated downregulation of Pim-3 kinase expression renders human pancreatic cancer cells sensitivity to gemcitabine. *Oncotarget*, *6*(16), 14440-14455.

Lim, K. H., Baines, A. T., Fiordalisi, J. J., Shipitsin, M., Feig, L. A., Cox, A. D., … Counter, C. M. (2005). Activation of RalA is critical for Ras-induced tumorigenesis of human cells. *Cancer Cell*, *7*(6), 533-545.

Lionetti, M., Biasiolo, M., Agnelli, L., Todoerti, K., Mosca, L., Fabris, S., … Neri, A. (2009). Identification of microRNA expression patterns and definition of a microRNA/mRNA regulatory network in distinct molecular groups of multiple myeloma. *Blood*, *114*(25), e20-26.

Lionetti, M., Musto, P., Di Martino, M. T., Fabris, S., Agnelli, L., Todoerti K, … Neri, A. (2013). Biological and clinical relevance of miRNA expression signatures in primary plasma cell leukemia. *Clinical Cancer Research*, *19*(12), 3130-3142.

Liu, Y., Zhao, L., Li, D., Yin, Y., Zhang, C. Y., Li, J., & Zhang, Y. (2013). Microvesicle-delivery miR-150 promotes tumorigenesis by up-regulating VEGF, and the neutralization of miR-150 attenuate tumor development. *Protein Cell*, *4*(12), 932-941.

Lodé, L., Eveillard, M., Trichet, V., Soussi, T., Wuillème, S., Richebourg, S., … Avet-Loiseau, H. (2010). Mutations in TP53 are exclusively associated with del(17p) in multiple myeloma. *Haematologica*, *95*(11), 1973-1976.

Löffler, D., Brocke-Heidrich, K., Pfeifer, G., Stocsits, C., Hackermüller, J., Kretzschmar, A. K., … Horn, F. (2007). Interleukin-6 dependent survival of multiple myeloma cells involves the Stat3-mediated induction of microRNA-21 through a highly conserved enhancer. *Blood*, *110*(4), 1330-1333.

Lu, J., Xu, X., Liu, X., Peng, Y., Zhang, B., Wang, L., … Li, X. (2014). Predictive value of miR-9 as a potential biomarker for nasopharyngeal carcinoma metastasis. *British Journal of Cancer*, *110*, 392-398.

Luo, H., Zhang, H., Zhang, Z., Zhang, X., Ning, B., Guo, J., … Wu, X. (2009). Down-regulated miR-9 and miR-433 in human gastric carcinoma. *Journal of Experimental Clinical Cancer Research*, *28*, 82.

Lynch, H., Watson, P., Tarantolo, S., Wiernik, P., Quinn-Laquer, B., Isgur, … Weisenburger, D. (2005). Phenotypic heterogeneity in multiple myeloma families. *Journal of Clinical Oncology*, *23*(4), 685–693.

Ma, X., Becker Buscaglia, L. E., Barker, J. R., & Li, Y. (2011). MicroRNAs in NF-kappaB signaling. *Journal of Molecular Cell Biology*, *3*(3): 159-166.

Mahapatra, S., Klee, E. W., Young, C. Y., Sun, Z., Jimenez, R. E., Klee, G. G., … Donkena, K. V. (2012). Global methylation profiling for risk prediction of prostate cancer. *Clinical Cancer Research*, *18*(10), 2882-2895.

Male, H., Patel, V., Jacob, M. A., Borrego-Diaz, E., Wang, K., Young, D. A., … Farassati, F. (2012). Inhibition of RalA signaling pathway in treatment of non-small cell lung cancer. *Lung Cancer*, *77*(2), 252-259.

Malumbres, R., Sarosiek, K. A., Cubedo, E., Ruiz, J. W., Jiang, X., Gascoyne, R. D., … Lossos, I. S. (2009). Differentiation stage-specific expression of microRNAs in B lymphocytes and diffuse large B-cell lymphomas. *Blood*, *113*(16), 3754-3764.

Mandema, E., & Wildervanck, L. (1954). Kahler's disease (multiple myeloma) in two sisters. *Journal Genetics Human*, *3*(3), 170-175.

Manier, S., Sacco, A., Leleu, X., Ghobrial, I. M., & Roccaro, A. M. (2012). Bone marrow microenvironment in multiple myeloma progression. *Journal of Biomedical & Biotechnology*, *2012*, 157496.

Martin, P.R., Shea, R.J., & Mulks, M. (2001). Identification of a plasmid-encoded gene from Haemophilus ducreyi which confers NAD independence. *Journal of Bacteriology*, *183*(4), 1168-1174.

Marzin, Y., Jamet, D., Douet-Guilbert, N., Morel, F., Le Bris, M. J., Morice, P., … De Braekeleer, M. (2006). Chromosome 1 abnormalities in multiple myeloma. *Anticancer Research*, *26*(2A), 953-959.

Meyerding, H. (1925). Multiple myeloma. *Radiology 5*, 132.

Mi, S., Lu, J., Sun, M., Li, Z., Zhang, H., Neilly, M. B., … Chen, J. (2007). MicroRNA expression signatures accurately discriminate acute lymphoblastic leukemia from acute myeloid leukemia. *Proceedings of the National Academy of Sciences of the United States of America*, *104*(50), 19971-19976.

Michan, S., & Sinclair, D. (2007). Sirtuins in mammals: insights into their biological function. *Biochemical Journal*, *404*(1), 1-13.

Minig, V., Kattan, Z., van Beeumen, J., Brunner, E., & Becuwe, P. (2009). Identification of ddb2 protein as a transcriptional regulator of constitutive sod2 gene expression in human breast cancer cells. *Journal of Biological Chemistry*, *284*(21), 14165-14176.

Mirabella, F., Wu, P., Wardell, C. P., Kaiser, M. F., Walker, B. A., Johnson, D. C., & Morgan, G. J. (2013). MMSET is the key molecular target in t(4;14) myeloma. *Blood Cancer Journal*, *3*, e114.

Mjelle, R., Hegre, S. A., Aas, P. A., Slupphaug, G., Drabløs, F, Saetrom, P., & Krokan, H. E. (2015). Cell cycle regulation of human DNA repair and chromatin remodeling genes. *DNA Repair (Amst)*, *30*, 53-67.

Moreau, P., Facon, T., & Leleu, X. (2002). Recurrent 14q32 translocations determine the prognosis of multiple myeloma, especially in patients receiving intensive chemotherapy. *Blood*, *100*(5), 1579-1583.

Morelli, E., Leone, E., Cantafio, M. E., Di Martino, M. T., Amodio, N., Biamonte, L., … Tassone, P. (2015). Selective targeting of IRF4 by synthetic microRNA-125b-5p mimics induces anti-multiple myeloma activity in vitro and in vivo. *Leukemia*, *29*(11), 2173-2183.

Morley, S., You, S., Pollan, S., Choi, J., Zhou, B., Hager, M. H., … Freeman, M. R. (2015). Regulation of microtubule dynamics by DIAPH3 influences amoeboid tumor cell mechanics and sensitivity to taxanes. *Scientific reports*, *5*, 12136.

Moussay, E., Wang, K., Cho, J-H., van Moer, K., Pierson, S., Paggetti, J., … Galas, D. J. (2011). MicroRNA as biomarkers and regulators in B-cell chronic lymphocytic leukemia. *Proceeding National Academic of Science USA*, *108*(16), 6573-6578.

Munshi, N. C., & Avet-Loiseau, H. (2011). Genomics in Multiple Myeloma. *Clinical Cancer Research*, *17*, 1234.

Murray, M. Y., Rushworth, S. A, Zaitseva, L., Bowles, K. M., & Macewan, D. J. (2013). Attenuation of dexamethasone-induced cell death in multiple myeloma is mediated by miR-125b expression. *Cell Cycle*, *12*(13), 2144-2153.

Nam, J. W., Rissland, O. S., Koppstein, D., Abreu-Goodger, C., Jan, C. H., Agarwal, V., … Bartel, D. P. (2014). Global analyses of the effect of different cellular contexts on microRNA targeting. *Molecular Cell*, *53*(6), 1031-1043.

Nara, M., Teshima, K., Watanabe, A., Ito, M., Iwamoto, K., Kitabayashi, A., … Tagawa, H. (2013). Bortezomib reduces the tumorigenicity of multiple myeloma via downregulation of upregulated targets in clonogenic side population cells. *PLoS One*, *8*(3), e56954.

Niu, C., Liang, C., Gua, J., Cheng, L., Zhang, H., Qin, X., … Ye, Q. (2012). Downregulation and growth inhibitory role of FHL1 in lung cancer. *International Journal of Cancer*, *130*(11), 2549-2556.

Nutt, S. L., Hodgkin, P. D., Tarlinton, D. M., & Corcoran, L. M. (2015). The generation of antibody-secreting plasma cells. *Nature Reviews Immunology*, *15*(3), 160-171.

O'Sullivan, G. J., Carty, F. L., & Cronin, C. G. (2015). Imaging of bone metastasis: an update. *World Journal of Radiology*, *7*(8), 202-211.

Ognjanovic, S., Bao, S., Yamamoto, S. Y., Garibay-Tupas, J., Samal, B., & Bryant-Greenwood, G. D. (2001). Genomic organization of the gene coding for human pre-B-cell colony enhancing factor and expression in human fetal membranes. *Journal of Molecular Endocrinology*, *26*(2), 107-117.

Olesen, U. H., Christensen, M. K., Bjorkling, F., Jaattela, M., Jensen, P. B., Sehested, M., & Nielsen, S. J. (2008). Anticancer agent CHS-828 inhibits cellular synthesis of NAD. *Biochemical and Biophysical Research Community*, *367*(4), 799-804.

Olesen, U. H., Petersen, J. G., Garten, A., Kiess, W., Yoshino, J., Imai, S-I., … Sehested, M. (2010). Target enzyme mutations are the molecular basis for resistance towards pharmacological inhibition of nicotinamide phosphoribosyltransferase. *BMC Cancer*, *10*, 677.

Omar, Z. A., & Ibrahim Tamin, N. S. (2011). *National cancer registry report: Malaysia cancer statistics-data and figure.* Malaysia: National Cancer Registry, Ministry of Health.

Palagani, A., Op de Beeck, K., Naulaerts, S., Diddens, J., Sekhar Chirumamilla, C., Van Camp, G., … Berghe, W. V. (2014). Ectopic microRNA-150-5p transcription sensitizes glucocorticoid therapy response in MM1S multiple myeloma cells but fails to overcome hormone therapy resistance in MM1R cells. *PLoS ONE*, *9*(12), e113842.

Palumbo, A., Avet-Loiseau, H, Oliva, S., Lokhorst, H. M., Goldschmidt, H., Rosinol, L., … Moreau, P. (2015). Revised international staging system for multiple myeloma: A report from international myeloma working group. *Journal of Clinical Oncology*, *33*(26), 2863-2869.

Pani, G., Colavitti, R., Bedogni, B., Fusco, S., Ferraro, D., Borrello, S., & Galeotti, T. (2004). Mitochondrial superoxide dismutase: a promising target for new anticancer therapies. *Current Medicinal Chemistry*, *11*(10), 1299-1308.

Pichiorri, F., Suh, S. S., Ladetto, M., Kuehl, M., Palumbo, T., Drandi, D., … Croce, C. M. (2008). MicroRNAs regulate critical genes associated with multiple myeloma pathogenesis. *Proceeding of the National Academic of Science U S A*, *105*(35), 12885-12890.

Pichiorri, F., Suh, S. S., Rocci, A., De Luca, L., Taccioli, C., Santhanam, R., … Croce, C. M. (2010). Downregulation of p53-inducible microRNAs 192, 194, and 215 impairs the p53/MDM2 autoregulatory loop in multiple myeloma development. *Cancer Cell*, *18*(4), 367-381.

Pitari, M. R., Rossi, M., Amodio, N., Botta, C., Morelli, E., Federico, C., … Tassone, P. (2015). Inhibition of miR-21 restores RANKL/ OPG ratio in multiple myeloma-derived bone marrow stromal cells and impairs the resorbing activity of mature osteoclasts. *Oncotarget*, *6*(29), 27343-27358.

Podar, K., & Anderson, K. C. (2005). The pathophysiologic role of VEGF in hematologic malignancies: therapeutic implications. *Blood*, *105*(4), 1383-1395.

Potter, H., & Heller, R. (2010). Transfection by Electroporation. *Current protocols in molecular biology*. doi:10.1002/0471142727.mb0903s62.

Prideaux, S. M., O'Brien, E. C., & Chevassut, T. J. (2014). The genetic architecture of multiple myeloma. *Advances in Hematology*, *2014*, 864058.

Prideaux, S. M., O'Brien, E. C., & Chevassut, T. J. (2014). The RAG Model: A New Paradigm for Genetic Risk Stratification in Multiple Myeloma. *Bone Marrow Research*, *2014*, 526568.

Raimondi, L., Amodio, N., Di Martino, M. T., Altomare, E., Leotta, M., Caracciolo, D., … Tassone, P. (2014). Targeting of multiple myeloma-related angiogenesis by miR-199a-5p mimics: in vitro and in vivo anti-tumor activity. Oncotarget, *5*(10), 3039-3054.

Raimondi, L., de Luca, A., Morellim E., Giavaresi, G., Tagliaferri, P., Tassone, P., & Amodio, N. (2016). MicroRNAs: novel crossroads between myeloma cells and the bone marrow microenvironment. *BioMedical Research International*, *2016*, 6504593.

Rajan, A. M., & Rajkumar, S. V. (2015). Interpretation of cytogenetic results in multiple myeloma for clinical practice. *Blood Cancer Journal*, *5*, e365.

Rajkumar, S. V. (2012). Multiple myeloma: 2012 update on diagnosis, risk-stratification, and management. *American Journal of Hematology*, *87*(1), 78-88.

Rajkumar, S. V., Dimopoulos, M. A., Palumbo, A., Blade, J., Merlini, G., Mateos, M. V., … Miguel, J. F. (2014). International myeloma working group updated criteria for the diagnosis of multiple myeloma. *The Lancet Oncology*, *15*(12), e538-548.

Rajkumar, S. V., Richardson, P. G., Hideshima, T., & Anderson, K. C. (2004). Proteasome inhibition as a novel therapeutic target in human cancer. *Journal of Clinical Oncology*, *23*(3), 630-639.

Rasmussen, T., Hudlebusch, H. R., Knudsen, L. M., & Johnsen, H. E. (2002). FGFR3 dysregulation in multiple myeloma: frequency and prognostic relevance. *British Journal of Haematology*, *117*(3), 626-628.

Ravaud, A., Cerny, T., Terret, C., Wanders, J., Bui, B. N., Hess, D., … Twelves, C. (2005). Phase I study and pharmacokinetic of CHS-828, a guanidino-containing compound, administered orally as a single dose every 3 weeks in solid tumours: an ECSG/EORTC study. *European Journal of Cancer*, *41*(5), 702-707.

Renshaw, C., Ketley, N., Møller, H., & Davies, E. A. (2010). Trends in the incidence and survival of multiple myeloma in South East England 1985-2004. *BMC Cancer*, *10*, 74.

Revollo, J. R., Grimm, A. A., & Imai, S. (2004). The NAD biosynthesis pathway mediated by nicotinamide phosphoribosyltransferase regulates Sir2 activity in mammalian cells. *Journal of Biological Chemistry*, *279*(49), 50754-50763.

Revollo, J. R., Körner, A., Mills, K. F., Satoh, A., Wang, T., Garten, A., … Imai, S-i. (2007). Nampt/PBEF/Visfatin regulates insulin secretion in beta cells as a systemic NAD biosynthetic enzyme. *Cell Metabolism*, *6*(5), 363-375.

Rice, S. J., Lai, S., Wood, L. W. Helsley, K. R., Runkle, E. A., Winslow, M. M., & Mu, D. (2013). MicroRNA-33a Mediates the Regulation of High Mobility Group AT-Hook 2 Gene (*HMGA2*) by Thyroid Transcription Factor 1 (TTF-1/NKX2–1). *The Journal of Biological Chemistry*, *288*(23), 16348-16360.

Riegel, M. (2014). Human molecular cytogenetics: From cells to nucleotides. *Genetic and Molecular Biology*, *37*(1 Suppl), 194-209.

Rio-Machin, A., Ferreira, B. I. Henry, T., Gómez-López, G., Agirre, X., Alvarez, S., … Cigudosa, J. C. (2013). Downregulation of specific miRNAs in hyperdiploid multiple myeloma mimics the oncogenic effect of IgH translocations occurring in the non-hyperdiploid subtype. *Leukemia*, *27*(4), 925-931.

Rongvaux, A., Andris, F., Van Gool, F., & Leo, O. (2013). Reconstructing eukaryotic NAD metabolism. *Bioessays*, *25*(7), 683-690.

Rongvaux, A., Galli, M., Denanglaire, S., Van Gool, F., Drèze, P. L., Szpirer, C., … Leo, O. (2008). Nicotinamide phosphoribosyl transferase/pre-B cell colony-enhancing factor/visfatin is required for lymphocyte development and cellular resistance to genotoxic stress. *Journal of Immunology*, *181*(7), 4685-4695.

Roodman, G. D. (2002). Role of the Bone Marrow Microenvironment in Multiple Myeloma. *Journal of bone and mineral research*, *17*(11), 1921-1925.

Ruiz, S., Santos, E., & Bustelo. X. R. (2009). The Use of Knockout Mice Reveals a Synergistic Role of the Vav1 and Rasgrf2 Gene Deficiencies in Lymphomagenesis and Metastasis. *PLoS ONE*, *4*(12), e8229.

Sahar, S., & Sassone-Corsi, P. (2009). Metabolism and cancer: the circadian clock connection. *Nature Reviews Cancer*, *9*, 886-896.

Saki, N., Abroun, S, Hajizamani, S., Rahim, F., & Shahjahani, M. (2014). Association of Chromosomal Translocation and miRNA expression with the pathogenesis of multiple myeloma. *Cell Journal*, *16*(2), 99-110.

Samal, B., Sun, Y., Stearns, G., Xie, C., Suggs, S., & McNiece I. (1994). Cloning and characterization of the cDNA encoding a novel human pre-B-cell colony enhancing factor. *Molecular Cell Biology*, *14*(2), 1431-1437.

Samy, E. F., Ross, J., Bolton, E., Morris, E. J., & Oliver, S. E. (2015). Variation in incidence and survival by ethnicity for patients with myeloma in England (2002-2008). *Leukaemia Lymphoma*, *11*, 1-8.

Scherer, D. C., Brockman, J. A., Chen, Z., Maniatis, T., & Ballard, D. W. (1995). Signal-induced degradation of I kappa B alpha requires site-specific ubiquitination. *Proceeding of the National Academic of Sciences USA*, *92*(24): 11259-11263.

Schiewer, M. J., Goodwin, J. F., Han, S., Brenner, J. C., Augello, M. A., Dean, J. L., … Knudsen, K. (2012), Dual roles of PARP-1 promote cancer growth and progression. *Cancer Discovery*, *2*(12), 1134-1149.

Schmid, J. A., & Birbach, A. IkappaB kinase beta (IKKbeta/IKK2/IKBKB)-a key molecule in signaling to the transcription factor NF-kappa B. *Cytokine Growth Factor Reviews*, *19*(2): 157-165.

Scotland, P. B., Heath, J. L., Conway, A. E., Porter, N. B., Armstrong, M. B., Walker, J. A., … Wechsler, D. S. (2012). The PICALM Protein Plays a Key Role in Iron Homeostasis and Cell Proliferation. *PLoS ONE*, *7*(8), e44252.

Seashols-Williams, S. J., Budd, W., Clark, G. C., Wu, Q., Daniel, R., Dragoescu, E., & Zehner, Z. E. (2016). miR-9 acts as an oncomiR in prostate cancer through multiple pathways that drive tumour progression and metastasis. *Plos One*, *11*(7), e0159601.

Segges, P., & and Braggio, E. (2011). Genetic Markers Used for Risk Stratification in Multiple Myeloma. *Genetics Research International*, *2011*, 798089.

Serpico, D., Molino, L., & Di Cosimo, S. (2014). microRNAs in breast cancer development and treatment. *Cancer Treatment Reviews*, *40*(5), 595-604.

Shackelford, R. E., Mayhall, K., Maxwell, N. M., Kandil, E., & Coppola, D. (2013). Nicotinamide Phosphoribosyltransferase in Malignancy: a review. *Genes & Cancer*, *4*(11-12), 447-456.

Shapiro-Shelef, M., & Calame, K. (2005). Regulation of plasma-cell development. *Nature Reviews Immunology*, *5*(3), 230-242.

Shaughnessy, J. D. Jr., Zhan, F., Burington, B. E., Huang, Y., Colla, S., Hanamura, I., … & Barlogie, B. (2007). A validated gene expression model of high-risk multiple myeloma is defined by deregulated expression of genes mapping to chromosome 1. *Blood*, *109*(6), 2276-2284.

Shin, H. J., Kim, K., Lee, J. J., Song, M. K., Lee, E. Y., Park, S. H., … Chung, J. S. (2015). The t(11;14)(q13;q32) translocation as a poor prognostic parameter for autologous stem cell transplantation in myeloma patients with extramedullary plasmacytoma. *Clinical Lymphoma, Myeloma & Leukemia*, *15*(4), 227-235.

Sibley, K., Fenton, J. A., Dring, A. M., Ashcroft, A. J., Rawstron, A. C., & Morgan, G. J. (2002). A molecular study of the t(4;14) in multiple myeloma. *British Journal of Haematology, 118*(2), 514-520.

*Siomi, H., & Siomi, M. C. (2010). Posttranscriptional Regulation of MicroRNA Biogenesis in Animals.* Molecular Cell*,* 38 *(3), 323-332.*

Smadja, N. V., Bastard, C., Brigaudeau, C., Leroux, D., & Frunchart, C. (2001). Hypodiploidy is a major prognostic factor in multiple myeloma. *Blood*, *98*(7), 2229-2238.

Smadja, N. V., Leroux, D., Soulier, J., Dumont, S., Arnould, C., Taviaux, S., … Bastard, C. (2003). Further cytogenetic characterization of multiple myeloma confirms that 14q32 translocations are a very rare event in hyperdiploid cases. *Genes Chromosome Cancer*, *38*(3), 234-239.

Smetana, J., Frohlich, J., Zaoralova, R., Vallova, V., Greslikova, H., Kupska, R., … Kuglik, P. (2014). Genome-Wide Screening of Cytogenetic Abnormalities in Multiple Myeloma Patients Using Array-CGH Technique: A Czech Multicenter Experience. *BioMed Research International*, *2014*, 209670.

Sonneveld, P. (2006). Gain of 1q21 in multiple myeloma: from bad to worse? *Blood*, *108*(5), 1426-1427.

Steinbrunn, T., Stuhmer, T., Sayehli, C., Chatterjee, M., Einsele, H., & Bargou, R. C. (2012). Combined targeting of MEK/ MAPK and PI3K/ Akt signalling in multiple myeloma. *British Journal of Haematology*, *159*(4), 430-440.

Su, N., Qian, M., & Deng, M. (2013). Integrative Approaches for microRNA Target Prediction: Combining Sequence Information and the Paired mRNA and miRNA Expression Profiles. *Current Bioinformatics*, *8*(1), 37-45.

Sukhai, M. A., Prabha, S., Hurren, R., Rutledge, A. C., Lee, A. Y., Sriskanthadevan, S., … Schimmer, A. D. (2013). Lysosomal disruption preferentially targets acute myeloid leukemia cells and progenitors. *Journal of Clinical Investigation*, *123*(1), 315-328.

Sun, C. Y., She, X. M., Qin, Y., Chu, Z. B., Chen, L., Ai, L. S., … Hu, Y. (2013). miR-15a and miR-16 affect the angiogenesis of multiple myeloma by targeting VEGF. *Carcinogenesis*, *34*(2), 426-435.

Tanuma, N., Shima, H., Nakamura, K., & Kikuchi, K. (2001). Protein tyrosine phosphatase epsilonC selectively inhibits interleukin-6- and interleukin- 10-induced JAK-STAT signaling. *Blood*, *98*(10), 3030-3034.

Teoh, P. J., & Chng, W. J. (2014). p53 Abnormalities and Potential Therapeutic Targeting in Multiple Myeloma. *BioMedical Research International*, *2014*, 717919.

Thomson, D. W., Bracken, C. P., & Goodall, G. J. (2011). Experimental strategies for microRNA target identification. *Nucleic Acids Research*, *39*(16), 6845-6853.

Tomas, P., Miroslava, V., Jiri, M., Jana, B., Jaroslav, B., Marie, J., & Vlastimil, S. (2015). Translocation t(8;14) in multiple myeloma defines patients with very poor prognosis – single centre experience. *Clinical Lymphoma, Myeloma and leukemia*, *15*, e122.

Tong, Y., Merino, D., Nimmervoll, B., Gupta, K., Wang, Y. D., Finkelstein, D., … Gilbertson, R. J. (2015). Cross-Species Genomics Identifies TAF12, NFYC, and RAD54L as Choroid Plexus Carcinoma Oncogenes. *Cancer Cell*, *27*(5), 712-727.

Tosi, P. (2013). Diagnosis and treatment of bone disease in multiple myeloma: spotlight on spinal involvement. *Scientifica*, *2013*, 104546.

Tuchman, S. A., Shapiro, G. R., Ershler, W. B., Badros, A., Cohen, H. J., Dispenzieri, A., … Yates, J. W. (2014). Multiple myeloma in the very old: An IASIA conference report. *Journal of the National Cancer Institute*, *106*(5).

Ueki, T., Nishidate, T., Park, J. H., Lin, M. L., Shimo, A., Hirata, K., … & Katagiri, T. (2008). Involvement of elevated expression of multiple cell-cycle regulator, DTL/RAMP (denticleless/RA-regulated nuclear matrix associated protein), in the growth of breast cancer cells. *Oncogene*, *27*(43), 5672-5683.

Undi, R. B., Kandi, R., & Gutti, R. K. (2013). MicroRNAs as Haematopoiesis Regulators. *Advances in Hematology*, *2013*, 695754.

Välk, K., Vooder, T., Kolde, R., Reintam, M. A., Petzold, C., Vilo, J., & Metspalu, A. (2010). Gene expression profiles of non-small cell lung cancer: survival prediction and new biomarkers. *Oncology*, *79*(3-4), 283-292.

Van Beijnum, J. R., Moerkerk, P. T., Gerbers, A. J., De Bruïne, A. P., Arends, J. W., Hoogenboom, H. R., & Hufton, S. E. (2002). Target validation for genomics using peptide-specific phage antibodies: a study of five gene products overexpressed in colorectal cancer. *International Journal of Cancer*, *101*(2), 118-127.

van der Veer, E., Ho, C., O'Neil, C., Barbosa, N., Scott, R., Cregan, S. P., & Pickering, J. G. (2007). Extension of human cell lifespan by nicotinamide phosphoribosyltransferase. *Journal of Biological Chemistry*, *282*(15), 10841-10845.

van der Veer, E., Nong, Z., O'Neil, C., Urquhart, B., Freeman, D., & Pickering, J. G. (2005). Pre-B-cell colony-enhancing factor regulates NAD+-dependent protein deacetylase activity and promotes vascular smooth muscle cell maturation. *Circulation Research*, *97*(1), 25-34.

Van Laar, R., Flinchum, R., Brown, N., Ramsey, J., Riccitelli, S., Heuck, C., … Shaughnessy, J. D. Jr. (2014). Translating a gene expression signature for multiple myeloma prognosis into a robust high-throughput assay for clinical use. *BMC Medical Genomics*, *7*, 25.

Van Wier, S., Braggio, E., Baker, A., Ahmann, G., Levy, J., Carpten, J. D., & Fonseca, R. (2013). Hypodiploid multiple myeloma is characterized by more aggressive molecular markers than non-hyperdiploid multiple myeloma. *Haematologica*, *98*(10), 1586-1592.

Velasco, R., & Bruna, J. (2012). Neurologic complications in multiple myeloma and plasmacytoma. *European Association of Neurooncology Magazine*, *2*(2), 71-77.

Venkateshaiah, S. U., Khan, S., Ling, W., Bam, R., Li, X., van Rhee, F., Usmani, S., … Yaccoby, S. (2013). NAMPT/PBEF1 enzymatic activity is indispensable for myeloma cell growth and osteoclast activity. *Experimental Hematology*, *41*(6), 547-557.

von Heideman, A., Berglund, A., Larsson, R., & Nygren, P. (2010). Safety and efficacy of NAD depleting cancer drugs: results of a phase I clinical trial of CHS 828 and overview of published data. *Cancer Chemotherapy and Pharmacology*, *65*(6), 1165-1172.

Walker, B. A., Leone , P. E., Chiecchio, L., Dickens, N. J., Jenner, M. W., Boyd, K. D., … Morgan, G. J. (2010). A compendium of myeloma-associated chromosomal copy number abnormalities and their prognostic value. *Blood*, *116*(15), e56-65.

Walker, B. A., Wardell, C. P., Johnson, D. C., Kaiser, M. F., Begum, D. B., Dahir, N. B., … Morgan, G. J. (2013). Characterization of IGH locus breakpoints in multiple myeloma indicates a subset of translocations appear to occur in pregerminal center B cells. *Blood 121*(17), 3413-3419.

Wang, B., & Xi, Y. (2013). Challenges for microRNA microarray data analysis. *Microarray (Basel)*, *2*(2), 34-50.

Wang, J., Zhang, K. Y., Liu, S. M., & Sen, S. (2014). Tumor-Associated circulating micrornas as biomarkers of cancer. *Molecules*, *19*(2), 1912-1938.

Wang, L. Q., Kwong, Y. L., Kho, C. S. B., Wong, K. F., Wong, K. Y., Ferracin, M., … Chim, C. S. (2013). Epigenetic inactivation of *miR-9* family microRNAs in chronic lymphocytic leukemia - implications on constitutive activation of NFκB pathway. *Molecular Cancer*, *12*, 173.

Wang, N., Bartlow, P., Ouyang, Q., & Xie, X-Q. (2014). Recent advances in antimultiple myeloma drug development. *Pharmaceutical Patent Analyst*, *3*(3), 261-277.

Wang, W., Elkins, K., Oh, A., Ho, Y-C., Wu, J., Li, H., … Belmont, L. D. (2014). Structural Basis for Resistance to Diverse Classes of NAMPT Inhibitors. *PLoS ONE*, *9*(10), e109366.

Wang, X., Li, C., Ju, S., Wang, Y., Wang, H., & Zhong, R. (2011). Myeloma cell adhesion to bone marrow stromal cells confers drug resistance by microRNA-21 up-regulation. *Leukemia & Lymphoma*, *52*(10), 1991-1998.

Waxman, A. J., Mink, P. J., Devesa, S. S., Anderson, W. F., Weiss, B. M., Kristinsson, S. Y., … Landgren, O. (2010). Racial disparities in incidence and outcome in multiple myeloma: a population-based study. *Blood*, *116*(25), 5501-5506.

Wei, L., Lian, B., Zhang, Y., Li, W., Gu, J., He, X., & Xie, L. (2014). Application of microRNA and mRNA expression profiling on prognostic biomarker discovery for hepatocellular carcinoma. *BMC Genomics*, *15*(Suppl 1), S13.

Weiss, B. M., Abadie, J., Verma, P., Howard, R. S., & Kuehl, W. M. (2009). A monoclonal gammopathy precedes multiple myeloma in most patients. *Blood*, *113*(22), 5418-5422.

Wiggin, G. R., Soloaga, A., Foster, J. M., Murray-Tait, V., Cohen, P., & Arthur, J. S. C. (2002). MSK1 and MSK2 are required for the mitogen and stress induced phosphorylation of CREB and ATF1 in fibroblasts. *Molecular Cell Biology*, *22*(8), 2871-2881.

Wildes, T. M., Rosko, A., & Tuchman, S. A. (2014). Multiple myeloma in the older adult: better prospects, more challenges. *Journal of Clinical Oncology*, *32*(24), 2531-2540.

Wolf, A., Agnihotri, S., Micallef, J., Mukherjee, J., Sabha, N., Cairns, R., … Guha, A. (2011). Hexokinase 2 is a key mediator of aerobic glycolysis and promotes tumor growth in human glioblastoma multiforme. *Journal of Experimental Medicine*, *208*(2), 313-326.

Wu, S., Yu, W., Qu, X., Wang, R., Xu, J., Zhang, Q., … & Chen, L. (2014). Argonaute 2 promotes myeloma angiogenesis via microRNA dysregulation. *Journal of Hematology & Oncology*, *7*, 40.

Xi, Y., & Chen, Y. (2015). Oncogenic and therapeutic targeting of PTEN loss in bone malignancies. *Journal of Cellular Biochemistry*, *116*(9), 1837-1847.

Xia, B., Yang, S., Liu, T., & Lou, G. (2015). miR-211 suppresses epithelial ovarian cancer proliferation and cell-cycle progression by targeting Cyclin D1 and CDK6. *Molecular Cancer*, *14*, 57.

Xiao, C., Calado, D. P., Galler, G., Thai, T. H., Patterson, H. C., Wang, J., … Rajewsky, K. (2007). MiR-150 controls B cell differentiation by targeting the transcription factor c-Myb. *Cell*, *131*(1), 146-159.

Xie, Z., & Chng, W. J. (2014). MMSET: role and therapeutic opportunities in multiple myeloma. *Biomedical Research International*, *2014*, 636514.

Xu, Y., Fang, F., Dhar, S. K., Bosch, A., St. Clair, W. H., Kasarskis, E. J., & St. Clair, D. K. (2008). Mutations in the sod2 promoter reveal a molecular basis for an activating protein 2-dependent dysregulation of manganese superoxide dismutase expression in cancer cells. *Molecular Cancer Research*, *6*(12), 1881-1893.

Yan, S., Guo, Q., Fu, F., Wang, Z., Yin, Z., Wei, Y., & Yang, J. (2015). The role of miR-29b in cancer: regulation, function, and signaling. *Journal of OncoTargets & Therapy*, *8*, 539-548.

Yusnita, Y., Norsiah, Zakiah, I., Chang, K. M., Purushotaman, V. S., Zubaidah, Z., & Jamal, R. (2012). MicroRNA (miRNA) expression profiling of peripheral blood samples in multiple myeloma patients using microarray. *Malaysian Journal of Pathology*, *34*(2), 133-143.

Zhan, F., Hardin, J., Kordsmeier, B., Bumm, K., Zheng, M., Tian, E., … Shaughnessy, J. Jr. (2002). Global gene expression profiling of multiple myeloma, monoclonal gammopathy of undetermined significance, and normal bone marrow plasma cells. *Blood*, *99*(5), 1745-1757.

Zhang, H., Luo, X. Q., Zhang, P., Huang, L. B., Zheng, Y. S., Wu, J., … Chen, Y. Q. (2009). MicroRNA patterns associated with clinical prognostic parameters and CNS relapse prediction in pediatric acute leukemia. *PLoS ONE*, *4*(11), e7826.

Zhang, H., Qi, M., Li, S., Qi, T., Mei, H., Huang, K., … Tong, Q. (2012). microRNA-9 targets matrix metalloproteinase 14 to inhibit invasion, metastasis, and angiogenesis of neuroblastoma cells. *Molecular Cancer Therapeutics*, *11*(7), 1454-1466.

Zhang, J., Jima, D. D., Jacobs, C., Fischer, R., Gottwein, E., Huang, G., … Dave, S. S. (2009). Patterns of microRNA expression characterize stages of human B-cell differentiation. *Blood*, *113*(19), 4586-4594.

Zhang, T., Berrocal, J. G., Frizzell, K. M., Gamble, M. J., DuMond, M. E., Krishnakumar, R., … Kraus, W.L. (2009). Enzymes in the NAD+ salvage pathway regulate SIRT1 activity at target gene promoters. *Journal of Biological Chemistry*, *284*(30), 20408-20417.

Zhang, Y., Liu, W., Xu, Y., Li, C., Wang, Y., Yang, H., Zhang, C., … & Li, X. (2015). Identification of Subtype Specific miRNA-mRNA Functional Regulatory Modules in Matched miRNA-mRNA Expression Data: Multiple Myeloma as a Case. *BioMedical Research International*, *2015*, 501262.

Zhang, Y-K., Wang, H., Leng, Y., Li, Z-L., Yang, Y-F., Xiao, F-J., … Wang, L-S. (2011). Overexpression of microRNA-29b induces apoptosis of multiple myeloma cells through down regulating Mcl-1. *Biochemical & Biophysical Research Communications*, *414*(1), 233–239.

Zhao, J. J., Chu, Z. B., Hu, Y., Lin, J., Wang, Z., Jiang, M., … Carrasco, R. D. (2015). Targeting the miR-221-222/PUMA/BAK/BAX pathway abrogates dexamethasone resistance in multiple myeloma. *Cancer Research*, *75*(20), 4384-4397.

Zhou, J., Xu, D., Xie, H., Tang, J., Liu, R., Li, J., … Cao, K. (2015). miR-33a functions as a tumor suppressor in melanoma by targeting HIF-1α. *Cancer Biology & Therapy*, *16*(6), 846-855.

Zhou, Y., Barlogie, B., & Shaughnessy, J. D. Jr. (2009). The molecular characterization and clinical management of multiple myeloma in the post-genome era. *Leukemia*, *23*(11), 1941-1956.

Zhou, Y., Chen, L., Barlogie, B., Stephens, O., Wu, X., Williams, D. R., … Shaughnessy, J. D. Jr. (2010). High-risk myeloma is associated with global elevation of miRNAs and overexpression of EIF2C2/AGO2. *Proceedings of the National Academy of Sciences USA*, *107*(17), 7904-7909.

Zhou, Y., Huang, Z., Wu, S., Zang, X., Liu, M., & Shi, J. (2014). miR-33a is up-regulated in chemoresistant osteosarcoma and promotes osteosarcoma cell resistance to cisplatin by down-regulating TWIST. *Journal of the Experimental & Clinical Cancer Research*, *33*, 12.

Zhou, Y., Uddin, S., Zimmerman, T., Kang, J-A., Ulaszek, J., & Wickrema, A. (2008), Growth Control of Multiple Myeloma Cells through Inhibition of Glycogen Synthase Kinase-3. *Leukemia & Lymphoma*, *49*(10), 1945-1953.

Zhu, Y. X., Benn, S., Li, Z. H., Wei, E., Masih-Khan, E., Trieu, Y., … Stewart, A. K, (2004). The SH3-SAM adaptor HACS1 is up-regulated in B cell activation signaling cascades. *Journal of Experimental Medicine*, *200*(6), 737-747.

Zojer, N., Konigsberg, R., Ackermann, J., Fritz, E., Dallinger, S., Krömer, E., … Drach, J. (2000). Deletion of 13q14 remains an independent adverse prognostic variable in multiple myeloma despite its frequent detection by interphase fluorescence in situ hybridization. *Blood*, *95*(6), 1925-1930.

Zweegman, S., Palumbo, A., Bringhen, S., & Sonneveld, P. (2014). Age and aging in blood disorders: multiple myeloma. *Haematologica*, *99*(7), 1133-1137.

## LIST OF PUBLICATIONS AND PAPERS PRESENTED

**Publications:**

Bong, I. P. N., Ng, C. C., Lam, K. Y., Puteri Baharuddin, & Zakaria Z. (2014). Identification of novel pathogenic copy number aberrations in multiple myeloma: the Malaysian context. *Molecular Cytogenetics*, *7*(1), 24. doi: 10.1186/1755-8166-7-24.

Bong, I. P. N., Ng, C. C., Fakiruddin, S.K., Lim, M. N., & Zakaria, Z. (2016). Small interfering RNA-mediated silencing of nicotinamide phosphoribosyltransferase (*NAMPT*) and lysosomal trafficking regulator (*LYST*) induce growth inhibition and apoptosis in human multiple myeloma cells: A preliminary study. *Bosnian Journal of Medical Sciences*, *16*(4), 268-275. doi: 10.17305/bjbms.2016.1568.

Bong, I. P. N., Ng, C. C., Puteri Baharuddin, & Zakaria, Z. (2017). microRNA expression patterns and target prediction in multiple myeloma development and malignancy. *Genes & Genomics*, *39*(5), 533-540. doi: 10.1007/s13258-017-0518-7.

**Presentations:**

**Poster presentations:**

Bong, I. P. N., Ng, C. C., Puteri Baharuddin, & Zakaria, Z. Effective Silencing of *NAMPT* and *LYST* with siRNA in Human Myeloma RPMI8226 Cells. Poster presented at 2014 International Congress of Pathology and Laboratory Medicine, August 26-28, 2014, Shangri-La Hotel, Kuala Lumpur, Malaysia.

Bong, I. P. N., Ng, C. C., Puteri Baharuddin, & Zakaria, Z. Identification of molecular targets in the pathogenesis of multiple myeloma. Poster presented at 40$^{th}$ Malaysian Society for Biochemistry and Molecular Biology, June 10-11, 2015, Putrajaya Marriott Hotel, Putrajaya, Malaysia.

**Oral presentation:**

Bong, I. P. N. Identification of molecular targets in the pathogenesis of multiple myeloma: array comparative genomic hybridisation (aCGH), gene expression and miRNA expression profiling and *in vitro* analysis of nicotinamide phosphoribosyltransferase (*NAMPT*) and miR-26a. Orally presented at Candidature Defence, July 25, 2015, Institute of Biological Sciences, University of Malaya, Malaysia.

**APPENDIX A:** Up-regulated probes by ≥2.0 fold change at p<0.01 in multiple myeloma relative to the normal controls

| No | Probe Name | Fold Change (Multiple Myeloma vs Normal) | Gene Symbol | Description |
|---|---|---|---|---|
| 1 | A_23_P57709 | 178.08125 | *PCOLCE2* | Homo sapiens procollagen C-endopeptidase enhancer 2 (PCOLCE2), mRNA [NM_013363] |
| 2 | A_19_P00322533 | 85.571266 | *CRNDE* | Homo sapiens colorectal neoplasia differentially expressed (non-protein coding) (CRNDE), transcript variant 3, long non-coding RNA [NR_110453] |
| 3 | A_32_P104063 | 76.81967 | *CRNDE* | Homo sapiens colorectal neoplasia differentially expressed (non-protein coding) (CRNDE), transcript variant 3, long non-coding RNA [NR_110453] |
| 4 | A_23_P133956 | 65.30242 | *KIFC1* | Homo sapiens kinesin family member C1 (KIFC1), mRNA [NM_002263] |
| 5 | A_33_P3402615 | 64.758354 | *SLC6A9* | Homo sapiens solute carrier family 6 (neurotransmitter transporter, glycine), member 9 (SLC6A9), transcript variant 2, mRNA [NM_201649] |
| 6 | A_23_P62634 | 64.36604 | *RHCE* | Homo sapiens Rh blood group, CcEe antigens (RHCE), transcript variant 1, mRNA [NM_020485] |
| 7 | A_23_P137035 | 59.21905 | *PIR* | Homo sapiens pirin (iron-binding nuclear protein) (PIR), transcript variant 1, mRNA [NM_003662] |

| No | Probe Name | Fold Change (Multiple Myeloma vs Normal) | Gene Symbol | Description |
|---|---|---|---|---|
| 8 | A_33_P3254946 | 45.523502 | *PLEKHH3* | Homo sapiens pleckstrin homology domain containing, family H (with MyTH4 domain) member 3 (PLEKHH3), transcript variant 1, mRNA [NM_024927] |
| 9 | A_23_P356684 | 40.164352 | *ANLN* | Homo sapiens anillin, actin binding protein (ANLN), transcript variant 1, mRNA [NM_018685] |
| 10 | A_23_P388812 | 39.653458 | *CKAP2L* | Homo sapiens cytoskeleton associated protein 2-like (CKAP2L), mRNA [NM_152515] |
| 11 | A_23_P259586 | 38.816673 | *TTK* | Homo sapiens TTK protein kinase (TTK), transcript variant 1, mRNA [NM_003318] |
| 12 | A_33_P3257678 | 38.562836 | *HIST2H3A* | Homo sapiens histone cluster 2, H3a (HIST2H3A), mRNA [NM_001005464] |
| 13 | A_24_P322354 | 38.558018 | *SKA1* | Homo sapiens spindle and kinetochore associated complex subunit 1 (SKA1), transcript variant 1, mRNA [NM_001039535] |
| 14 | A_23_P133123 | 38.068417 | *MND1* | Homo sapiens meiotic nuclear divisions 1 homolog (S. cerevisiae) (MND1), transcript variant 1, mRNA [NM_032117] |
| 15 | A_24_P413884 | 36.612972 | *CENPA* | Homo sapiens centromere protein A (CENPA), transcript variant 1, mRNA [NM_001809] |
| 16 | A_23_P104651 | 35.9334 | *CDCA5* | Homo sapiens cell division cycle associated 5 (CDCA5), mRNA [NM_080668] |

| No | Probe Name | Fold Change (Multiple Myeloma vs Normal) | Gene Symbol | Description |
|---|---|---|---|---|
| 17 | A_23_P148475 | 35.86176 | *KIF4A* | Homo sapiens kinesin family member 4A (KIF4A), mRNA [NM_012310] |
| 18 | A_23_P51085 | 35.299755 | *SPC25* | Homo sapiens SPC25, NDC80 kinetochore complex component (SPC25), mRNA [NM_020675] |
| 19 | A_23_P256956 | 32.456154 | *KIF20A* | Homo sapiens kinesin family member 20A (KIF20A), mRNA [NM_005733] |
| 20 | A_24_P346855 | 32.36563 | *MKI67* | Homo sapiens marker of proliferation Ki-67 (MKI67), transcript variant 1, mRNA [NM_002417] |
| 21 | A_23_P10385 | 32.183777 | *DTL* | Homo sapiens denticleless E3 ubiquitin protein ligase homolog (Drosophila) (DTL), transcript variant 1, mRNA [NM_016448] |
| 22 | A_23_P217319 | 31.231327 | *FGF13* | Homo sapiens fibroblast growth factor 13 (FGF13), transcript variant 1, mRNA [NM_004114] |
| 23 | A_24_P238499 | 31.150667 | *TYMSOS* | Homo sapiens TYMS opposite strand (TYMSOS), mRNA [NM_001012716] |
| 24 | A_33_P3386262 | 31.10579 | *CDT1* | Homo sapiens chromatin licensing and DNA replication factor 1 (CDT1), mRNA [NM_030928] |
| 25 | A_19_P00802201 | 30.949633 | | |
| 26 | A_33_P3807062 | 30.809633 | *HJURP* | Homo sapiens Holliday junction recognition protein (HJURP), transcript variant 1, mRNA [NM_018410] |

| No | Probe Name | Fold Change (Multiple Myeloma vs Normal) | Gene Symbol | Description |
|---|---|---|---|---|
| 27 | A_23_P35871 | 30.651064 | *E2F8* | Homo sapiens E2F transcription factor 8 (E2F8), transcript variant 1, mRNA [NM_024680] |
| 28 | A_23_P65757 | 30.481562 | *CCNB2* | Homo sapiens cyclin B2 (CCNB2), mRNA [NM_004701] |
| 29 | A_23_P138507 | 30.335405 | *CDK1* | Homo sapiens cyclin-dependent kinase 1 (CDK1), transcript variant 1, mRNA [NM_001786] |
| 30 | A_32_P150891 | 29.97297 | *DIAPH3* | Homo sapiens diaphanous-related formin 3 (DIAPH3), transcript variant 1, mRNA [NM_001042517] |
| 31 | A_32_P210202 | 29.845247 | *E2F7* | Homo sapiens E2F transcription factor 7 (E2F7), mRNA [NM_203394] |
| 32 | A_23_P45799 | 29.742676 | *ORC1* | Homo sapiens origin recognition complex, subunit 1 (ORC1), transcript variant 1, mRNA [NM_004153] |
| 33 | A_23_P118815 | 29.546677 | *BIRC5* | Homo sapiens baculoviral IAP repeat containing 5 (BIRC5), transcript variant 3, mRNA [NM_001012271] |
| 34 | A_23_P50096 | 28.09995 | *TYMS* | Homo sapiens thymidylate synthetase (TYMS), mRNA [NM_001071] |
| 35 | A_23_P117852 | 27.940935 | *KIAA0101* | Homo sapiens KIAA0101 (KIAA0101), transcript variant 1, mRNA [NM_014736] |
| 36 | A_33_P3230548 | 26.966316 | *KIF14* | Homo sapiens kinesin family member 14 (KIF14), mRNA [NM_014875] |

| No | Probe Name | Fold Change (Multiple Myeloma vs Normal) | Gene Symbol | Description |
|---|---|---|---|---|
| 37 | A_24_P314571 | 26.915525 | *SPC24* | SPC24, NDC80 kinetochore complex component [Source:HGNC Symbol;Acc:26913] [ENST00000592540] |
| 38 | A_23_P94422 | 26.166994 | *MELK* | Homo sapiens maternal embryonic leucine zipper kinase (MELK), transcript variant 1, mRNA [NM_014791] |
| 39 | A_32_P62997 | 26.070894 | *PBK* | Homo sapiens PDZ binding kinase (PBK), transcript variant 1, mRNA [NM_018492] |
| 40 | A_23_P52017 | 26.046165 | *ASPM* | Homo sapiens asp (abnormal spindle) homolog, microcephaly associated (Drosophila) (ASPM), transcript variant 1, mRNA [NM_018136] |
| 41 | A_24_P397107 | 25.806473 | *CDC25A* | Homo sapiens cell division cycle 25A (CDC25A), transcript variant 1, mRNA [NM_001789] |
| 42 | A_33_P3288159 | 25.657679 | *ASPM* | Homo sapiens asp (abnormal spindle) homolog, microcephaly associated (Drosophila) (ASPM), transcript variant 1, mRNA [NM_018136] |
| 43 | A_23_P34788 | 25.479038 | *KIF2C* | Homo sapiens kinesin family member 2C (KIF2C), mRNA [NM_006845] |
| 44 | A_23_P88331 | 25.476065 | *DLGAP5* | Homo sapiens discs, large (Drosophila) homolog-associated protein 5 (DLGAP5), transcript variant 1, mRNA [NM_014750] |

| No | Probe Name | Fold Change (Multiple Myeloma vs Normal) | Gene Symbol | Description |
|---|---|---|---|---|
| 45 | A_24_P399888 | 25.174349 | *CENPM* | Homo sapiens centromere protein M (CENPM), transcript variant 2, mRNA [NM_001002876] |
| 46 | A_23_P99292 | 24.70008 | *RAD51AP1* | Homo sapiens RAD51 associated protein 1 (RAD51AP1), transcript variant 2, mRNA [NM_006479] |
| 47 | A_23_P160537 | 24.659613 | *AUNIP* | Homo sapiens aurora kinase A and ninein interacting protein (AUNIP), transcript variant 2, mRNA [NM_024037] |
| 48 | A_23_P385861 | 24.517101 | *CDCA2* | Homo sapiens cell division cycle associated 2 (CDCA2), mRNA [NM_152562] |
| 49 | A_24_P225616 | 24.41442 | *RRM2* | Homo sapiens ribonucleotide reductase M2 (RRM2), transcript variant 2, mRNA [NM_001034] |
| 50 | A_23_P35219 | 23.528912 | *NEK2* | Homo sapiens NIMA-related kinase 2 (NEK2), transcript variant 1, mRNA [NM_002497] |
| 51 | A_23_P163481 | 22.853998 | *BUB1B* | Homo sapiens BUB1 mitotic checkpoint serine/threonine kinase B (BUB1B), mRNA [NM_001211] |
| 52 | A_23_P314805 | 22.817875 | *TMEM56* | Homo sapiens transmembrane protein 56 (TMEM56), transcript variant 2, mRNA [NM_152487] |
| 53 | A_23_P118834 | 22.55871 | *TOP2A* | Homo sapiens topoisomerase (DNA) II alpha 170kDa (TOP2A), mRNA [NM_001067] |
| 54 | A_23_P107421 | 21.845085 | *TK1* | Homo sapiens thymidine kinase 1, soluble (TK1), mRNA [NM_003258] |

| No | Probe Name | Fold Change (Multiple Myeloma vs Normal) | Gene Symbol | Description |
|---|---|---|---|---|
| 55 | A_23_P23303 | 21.622639 | *EXO1* | Homo sapiens exonuclease 1 (EXO1), transcript variant 3, mRNA [NM_003686] |
| 56 | A_33_P3339361 | 21.58801 | *ARHGAP11A* | Homo sapiens Rho GTPase activating protein 11A (ARHGAP11A), transcript variant 2, mRNA [NM_199357] |
| 57 | A_23_P68610 | 21.292704 | *TPX2* | Homo sapiens TPX2, microtubule-associated (TPX2), mRNA [NM_012112] |
| 58 | A_23_P57588 | 20.76743 | *GTSE1* | Homo sapiens G-2 and S-phase expressed 1 (GTSE1), mRNA [NM_016426] |
| 59 | A_33_P3291831 | 20.490063 | *CEP55* | Homo sapiens centrosomal protein 55kDa (CEP55), transcript variant 1, mRNA [NM_018131] |
| 60 | A_24_P319613 | 20.323118 | *NEK2* | Homo sapiens NIMA-related kinase 2 (NEK2), transcript variant 1, mRNA [NM_002497] |
| 61 | A_23_P57379 | 20.170956 | *CDC45* | Homo sapiens cell division cycle 45 (CDC45), transcript variant 2, mRNA [NM_003504] |
| 62 | A_33_P3308105 | 20.1566 | *GGH* | Homo sapiens gamma-glutamyl hydrolase (conjugase, folylpolygammaglutamyl hydrolase) (GGH), mRNA [NM_003878] |
| 63 | A_33_P3216008 | 20.143261 | *SKA3* | Homo sapiens spindle and kinetochore associated complex subunit 3 (SKA3), transcript variant 1, mRNA [NM_145061 ] |
| 64 | A_23_P58321 | 19.687443 | *CCNA2* | Homo sapiens cyclin A2 (CCNA2), mRNA [NM_001237] |

| No | Probe Name | Fold Change (Multiple Myeloma vs Normal) | Gene Symbol | Description |
|---|---|---|---|---|
| 65 | A_23_P130182 | 19.064548 | *AURKB* | Homo sapiens aurora kinase B (AURKB), transcript variant 1, mRNA [NM_004217] |
| 66 | A_23_P70007 | 18.959665 | *HMMR* | Homo sapiens hyaluronan-mediated motility receptor (RHAMM) (HMMR), transcript variant 2, mRNA [NM_012484] |
| 67 | A_23_P151150 | 18.61518 | *FOXM1* | Homo sapiens forkhead box M1 (FOXM1), transcript variant 1, mRNA [NM_202002] |
| 68 | A_23_P80902 | 18.396692 | *KIF15* | Homo sapiens kinesin family member 15 (KIF15), mRNA [NM_020242] |
| 69 | A_23_P379614 | 18.39257 | *OIP5* | Homo sapiens Opa interacting protein 5 (OIP5), mRNA [NM_007280] |
| 70 | A_23_P323751 | 18.12145 | *FAM83D* | Homo sapiens family with sequence similarity 83, member D (FAM83D), mRNA [NM_030919] |
| 71 | A_32_P96719 | 18.118479 | *SHCBP1* | Homo sapiens SHC SH2-domain binding protein 1 (SHCBP1), mRNA [NM_024745] |
| 72 | A_23_P124417 | 18.111977 | *BUB1* | Homo sapiens BUB1 mitotic checkpoint serine/threonine kinase (BUB1), transcript variant 1, mRNA [NM_004336] |
| 73 | A_23_P208880 | 18.025799 | *UHRF1* | Homo sapiens ubiquitin-like with PHD and ring finger domains 1 (UHRF1), transcript variant 2, mRNA [NM_013282] |
| 74 | A_23_P70249 | 17.742025 | *CDC25C* | Homo sapiens cell division cycle 25C (CDC25C), transcript variant 1, mRNA [NM_001790] |

| No | Probe Name | Fold Change (Multiple Myeloma vs Normal) | Gene Symbol | Description |
|---|---|---|---|---|
| 75 | A_23_P401 | 17.344902 | *CENPF* | Homo sapiens centromere protein F, 350/400kDa (CENPF), mRNA [NM_016343] |
| 76 | A_23_P74115 | 17.0038 | *RAD54L* | Homo sapiens RAD54-like (S. cerevisiae) (RAD54L), transcript variant 1, mRNA [NM_003579] |
| 77 | A_23_P74349 | 16.938984 | *NUF2* | Homo sapiens NUF2, NDC80 kinetochore complex component (NUF2), transcript variant 1, mRNA [NM_145697] |
| 78 | A_23_P48669 | 16.818756 | *CDKN3* | Homo sapiens cyclin-dependent kinase inhibitor 3 (CDKN3), transcript variant 1, mRNA [NM_005192] |
| 79 | A_24_P323598 | 16.588112 | *ESCO2* | Homo sapiens establishment of sister chromatid cohesion N-acetyltransferase 2 (ESCO2), mRNA [NM_001017420] |
| 80 | A_33_P3247022 | 16.540804 | *CCNE2* | Homo sapiens cyclin E2 (CCNE2), mRNA [NM_057749] |
| 81 | A_23_P150935 | 16.49531 | *TROAP* | Homo sapiens trophinin associated protein (TROAP), transcript variant 1, mRNA [NM_005480] |
| 82 | A_33_P3350488 | 16.320126 | *NUSAP1* | Homo sapiens nucleolar and spindle associated protein 1 (NUSAP1), transcript variant 1, mRNA [NM_016359] |
| 83 | A_23_P50426 | 16.304495 | *KANK2* | Homo sapiens KN motif and ankyrin repeat domains 2 (KANK2), transcript variant 1, mRNA [NM_015493] |
| 84 | A_33_P3237359 | 15.818415 | *HMGB3* | Homo sapiens high mobility group box 3 (HMGB3), mRNA [NM_005342] |

| No | Probe Name | Fold Change (Multiple Myeloma vs Normal) | Gene Symbol | Description |
|---|---|---|---|---|
| 85 | A_33_P3326210 | 15.79934 | *ESCO2* | Homo sapiens establishment of sister chromatid cohesion N-acetyltransferase 2 (ESCO2), mRNA [NM_001017420] |
| 86 | A_23_P118174 | 15.789652 | *PLK1* | Homo sapiens polo-like kinase 1 (PLK1), mRNA [NM_005030] |
| 87 | A_33_P3397443 | 15.688941 | *PKMYT1* | Homo sapiens protein kinase, membrane associated tyrosine/threonine 1 (PKMYT1), transcript variant 2, mRNA [NM_182687] |
| 88 | A_33_P3319041 | 15.517986 | *HMGB3* | Homo sapiens high mobility group box 3 (HMGB3), mRNA [NM_005342] |
| 89 | A_23_P118246 | 15.5082445 | *GINS2* | Homo sapiens GINS complex subunit 2 (Psf2 homolog) (GINS2), mRNA [NM_016095] |
| 90 | A_23_P122197 | 15.420313 | *CCNB1* | Homo sapiens cyclin B1 (CCNB1), mRNA [NM_031966] |
| 91 | A_23_P214907 | 15.417895 | *MTHFD1L* | Homo sapiens methylenetetrahydrofolate dehydrogenase (NADP+ dependent) 1-like (MTHFD1L), transcript variant 2, mRNA [NM_015440] |
| 92 | A_24_P67681 | 15.351326 | | |
| 93 | A_32_P192970 | 15.19389 | *ALDH4A1* | Homo sapiens aldehyde dehydrogenase 4 family, member A1 (ALDH4A1), transcript variant P5CDhS, mRNA [NM_170726] |
| 94 | A_23_P155969 | 14.871344 | *PLK4* | Homo sapiens polo-like kinase 4 (PLK4), transcript variant 1, mRNA [NM_014264] |

| No | Probe Name | Fold Change (Multiple Myeloma vs Normal) | Gene Symbol | Description |
|---|---|---|---|---|
| 95 | A_23_P361419 | 14.858692 | *DEPDC1B* | Homo sapiens DEP domain containing 1B (DEPDC1B), transcript variant 1, mRNA [NM_018369] |
| 96 | A_23_P100127 | 14.852844 | *CASC5* | Homo sapiens cancer susceptibility candidate 5 (CASC5), transcript variant 1, mRNA [NM_170589] |
| 97 | A_23_P63789 | 14.780457 | *ZWINT* | Homo sapiens ZW10 interacting kinetochore protein (ZWINT), transcript variant 2, mRNA [NM_032997] |
| 98 | A_23_P420551 | 14.155386 | *CIT* | Homo sapiens citron rho-interacting serine/threonine kinase (CIT), transcript variant 2, mRNA [NM_007174] |
| 99 | A_23_P254733 | 13.856413 | *CENPU* | Homo sapiens centromere protein U (CENPU), transcript variant 1, mRNA [NM_024629] |
| 100 | A_23_P80032 | 13.748679 | *E2F1* | Homo sapiens E2F transcription factor 1 (E2F1), mRNA [NM_005225] |
| 101 | A_24_P227091 | 13.692478 | *KIF11* | Homo sapiens kinesin family member 11 (KIF11), mRNA [NM_004523] |
| 102 | A_23_P373119 | 13.404962 | *HMGB3P1* | Homo sapiens high mobility group box 3 pseudogene 1 (HMGB3P1), non-coding RNA [NR_002165] |
| 103 | A_33_P3307903 | 13.375899 | *CDKN3* | Homo sapiens cyclin-dependent kinase inhibitor 3 (CDKN3), transcript variant 1, mRNA [NM_005192] |

| No | Probe Name | Fold Change (Multiple Myeloma vs Normal) | Gene Symbol | Description |
|---|---|---|---|---|
| 104 | A_23_P206059 | 13.280887 | *PRC1* | Homo sapiens protein regulator of cytokinesis 1 (PRC1), transcript variant 1, mRNA [NM_003981] |
| 105 | A_21_P0004083 | 13.149219 | | |
| 106 | A_33_P3374210 | 13.051616 | *MKI67* | Homo sapiens marker of proliferation Ki-67 (MKI67), transcript variant 1, mRNA [NM_002417] |
| 107 | A_24_P218979 | 13.037722 | *CDCA3* | Homo sapiens cell division cycle associated 3 (CDCA3), mRNA [NM_031299] |
| 108 | A_23_P100344 | 12.885926 | *ORC6* | Homo sapiens origin recognition complex, subunit 6 (ORC6), transcript variant 1, mRNA [NM_014321] |
| 109 | A_23_P143190 | 12.827913 | *MYBL2* | Homo sapiens v-myb avian myeloblastosis viral oncogene homolog-like 2 (MYBL2), transcript variant 1, mRNA [NM_002466] |
| 110 | A_23_P375 | 12.619921 | *CDCA8* | Homo sapiens cell division cycle associated 8 (CDCA8), transcript variant 2, mRNA [NM_018101] |
| 111 | A_24_P335620 | 12.443381 | *SLC7A5* | Homo sapiens solute carrier family 7 (amino acid transporter light chain, L system), member 5 (SLC7A5), mRNA [NM_003486] |
| 112 | A_33_P3286372 | 12.330724 | *C2orf48* | chromosome 2 open reading frame 48 [Source:HGNC Symbol;Acc:26322] [ENST00000381786] |
| 113 | A_23_P200310 | 12.291142 | *DEPDC1* | Homo sapiens DEP domain containing 1 (DEPDC1), transcript variant 2, mRNA [NM_017779] |

| No | Probe Name | Fold Change (Multiple Myeloma vs Normal) | Gene Symbol | Description |
|---|---|---|---|---|
| 114 | A_33_P3286422 | 11.930416 | *FANCA* | Homo sapiens Fanconi anemia, complementation group A (FANCA), transcript variant 2, mRNA [NM_001018112] |
| 115 | A_23_P88740 | 11.858504 | *CENPN* | Homo sapiens centromere protein N (CENPN), transcript variant 3, mRNA [NM_018455] |
| 116 | A_23_P89509 | 11.830511 | *SPAG5* | Homo sapiens sperm associated antigen 5 (SPAG5), mRNA [NM_006461] |
| 117 | A_23_P345707 | 11.78066 | *TICRR* | Homo sapiens TOPBP1-interacting checkpoint and replication regulator (TICRR), mRNA [NM_152259] |
| 118 | A_24_P24685 | 11.587623 | | |
| 119 | A_24_P462899 | 11.584373 | *CENPW* | Homo sapiens centromere protein W (CENPW), transcript variant 2, mRNA [NM_001012507] |
| 120 | A_23_P115482 | 11.5795355 | *UBE2T* | Homo sapiens ubiquitin-conjugating enzyme E2T (putative) (UBE2T), mRNA [NM_014176] |
| 121 | A_23_P32707 | 11.3520155 | *ESPL1* | Homo sapiens extra spindle pole bodies homolog 1 (S. cerevisiae) (ESPL1), mRNA [NM_012291] |
| 122 | A_33_P3349536 | 11.134906 | *CHEK1* | Homo sapiens checkpoint kinase 1 (CHEK1), transcript variant 2, mRNA [NM_001114121] |
| 123 | A_23_P149200 | 11.059343 | *CDC20* | Homo sapiens cell division cycle 20 (CDC20), mRNA [NM_001255] |
| 124 | A_23_P71727 | 11.048157 | *CKS2* | Homo sapiens CDC28 protein kinase regulatory subunit 2 (CKS2), mRNA [NM_001827] |
| 125 | A_33_P3217819 | 10.918668 | *CCNE2* | Homo sapiens cyclin E2 (CCNE2), mRNA [NM_057749] |

| No | Probe Name | Fold Change (Multiple Myeloma vs Normal) | Gene Symbol | Description |
|---|---|---|---|---|
| 126 | A_23_P146830 | 10.828218 | *SLC25A10* | Homo sapiens solute carrier family 25 (mitochondrial carrier; dicarboxylate transporter), member 10 (SLC25A10), transcript variant 2, mRNA [NM_012140] |
| 127 | A_21_P0000197 | 10.418412 | *HIST1H2AG* | Homo sapiens histone cluster 1, H2ag (HIST1H2AG), mRNA [NM_021064] |
| 128 | A_33_P3323847 | 10.319724 | *RECQL4* | Homo sapiens RecQ protein-like 4 (RECQL4), mRNA [NM_004260] |
| 129 | A_23_P157795 | 10.123477 | *CTNNAL1* | Homo sapiens catenin (cadherin-associated protein), alpha-like 1 (CTNNAL1), transcript variant 1, mRNA [NM_003798] |
| 130 | A_24_P48248 | 9.896511 | *C17orf53* | Homo sapiens chromosome 17 open reading frame 53 (C17orf53), transcript variant 1, mRNA [NM_024032] |
| 131 | A_33_P3293353 | 9.586164 | *KCTD3* | Homo sapiens potassium channel tetramerization domain containing 3 (KCTD3), mRNA [NM_016121] |
| 132 | A_24_P96780 | 9.48718 | *CENPF* | Homo sapiens centromere protein F, 350/400kDa (CENPF), mRNA [NM_016343] |
| 133 | A_33_P3237874 | 9.383109 | *TROAP* | Homo sapiens trophinin associated protein (TROAP), transcript variant 2, mRNA [NM_001100620] |
| 134 | A_33_P3659876 | 9.365539 | *NCAPG2* | Homo sapiens non-SMC condensin II complex, subunit G2 (NCAPG2), transcript variant 2, mRNA [NM_001281932] |

| No | Probe Name | Fold Change (Multiple Myeloma vs Normal) | Gene Symbol | Description |
|---|---|---|---|---|
| 135 | A_24_P225970 | 9.313586 | *SGOL1* | Homo sapiens shugoshin-like 1 (S. pombe) (SGOL1), transcript variant A1, mRNA [NM_001012409] |
| 136 | A_23_P370989 | 9.313251 | *MCM4* | Homo sapiens minichromosome maintenance complex component 4 (MCM4), transcript variant 1, mRNA [NM_005914] |
| 137 | A_23_P7636 | 9.295173 | *PTTG1* | Homo sapiens pituitary tumor-transforming 1 (PTTG1), transcript variant 2, mRNA [NM_004219] |
| 138 | A_32_P103633 | 9.279168 | *MCM2* | Homo sapiens minichromosome maintenance complex component 2 (MCM2), transcript variant 1, mRNA [NM_004526] |
| 139 | A_32_P221799 | 9.271093 | *HIST1H2AM* | Homo sapiens histone cluster 1, H2am (HIST1H2AM), mRNA [NM_003514] |
| 140 | A_33_P3387831 | 9.232669 | *CENPM* | Homo sapiens centromere protein M (CENPM), transcript variant 1, mRNA [NM_024053] |
| 141 | A_33_P3867534 | 8.719691 | *MCM10* | Homo sapiens minichromosome maintenance complex component 10 (MCM10), transcript variant 1, mRNA [NM_182751] |
| 142 | A_33_P3254606 | 8.64984 | *WDR62* | Homo sapiens WD repeat domain 62 (WDR62), transcript variant 1, mRNA [NM_001083961] |
| 143 | A_24_P200000 | 8.468746 | *STEAP3* | Homo sapiens STEAP family member 3, metalloreductase (STEAP3), transcript variant 1, mRNA [NM_182915] |

| No | Probe Name | Fold Change (Multiple Myeloma vs Normal) | Gene Symbol | Description |
|---|---|---|---|---|
| 144 | A_23_P108437 | 8.458408 | *FZD5* | Homo sapiens frizzled class receptor 5 (FZD5), mRNA [NM_003468] |
| 145 | A_33_P3260605 | 8.4511385 | *CTNNAL1* | Homo sapiens catenin (cadherin-associated protein), alpha-like 1 (CTNNAL1), transcript variant 1, mRNA [NM_003798] |
| 146 | A_23_P122007 | 8.137289 | *C5orf30* | Homo sapiens chromosome 5 open reading frame 30 (C5orf30), mRNA [NM_033211] |
| 147 | A_23_P98431 | 7.6072454 | *HMBS* | Homo sapiens hydroxymethylbilane synthase (HMBS), transcript variant 1, mRNA [NM_000190] |
| 148 | A_23_P19712 | 6.7900863 | *GMNN* | Homo sapiens geminin, DNA replication inhibitor (GMNN), transcript variant 1, mRNA [NM_015895] |
| 149 | A_23_P212617 | 6.6481333 | *TFRC* | Homo sapiens transferrin receptor (TFRC), transcript variant 1, mRNA [NM_003234] |
| 150 | A_33_P3386344 | 6.3521433 | *FANCA* | Homo sapiens Fanconi anemia, complementation group A (FANCA), transcript variant 2, mRNA [NM_001018112] |
| 151 | A_33_P3217119 | 6.318004 | *OSCP1* | Homo sapiens organic solute carrier partner 1 (OSCP1), transcript variant 2, mRNA [NM_206837] |
| 152 | A_33_P3322307 | 6.249207 | *DDX11* | Homo sapiens DEAD/H (Asp-Glu-Ala-Asp/His) box helicase 11 (DDX11), transcript variant 5, mRNA [NM_001257145] |
| 153 | A_32_P171328 | 6.1425567 | *UBE2S* | Homo sapiens ubiquitin-conjugating enzyme E2S (UBE2S), mRNA [NM_014501] |

| No | Probe Name | Fold Change (Multiple Myeloma vs Normal) | Gene Symbol | Description |
|---|---|---|---|---|
| 154 | A_19_P00806947 | 6.0198646 | *PCNA* | Homo sapiens proliferating cell nuclear antigen (PCNA), transcript variant 1, mRNA [NM_002592] |
| 155 | A_23_P28886 | 5.8858314 | *PCNA* | Homo sapiens proliferating cell nuclear antigen (PCNA), transcript variant 1, mRNA [NM_002592] |
| 156 | A_23_P320862 | 5.720463 | *C9orf43* | Homo sapiens chromosome 9 open reading frame 43 (C9orf43), transcript variant 1, mRNA [NM_152786] |
| 157 | A_24_P223384 | 5.642763 | *HIST1H2AB* | Homo sapiens histone cluster 1, H2ab (HIST1H2AB), mRNA [NM_003513] |
| 158 | A_33_P3252196 | 5.489722 | *EZH2* | Homo sapiens enhancer of zeste homolog 2 (Drosophila) (EZH2), transcript variant 1, mRNA [NM_004456] |
| 159 | A_33_P3300395 | 5.4203014 | *APITD1* | Homo sapiens apoptosis-inducing, TAF9-like domain 1 (APITD1), transcript variant A, mRNA [NM_199294] |
| 160 | A_23_P124122 | 5.187816 | *PXMP2* | Homo sapiens peroxisomal membrane protein 2, 22kDa (PXMP2), mRNA [NM_018663] |
| 161 | A_23_P203947 | 5.1712966 | *DDX11* | Homo sapiens DEAD/H (Asp-Glu-Ala-Asp/His) box helicase 11 (DDX11), transcript variant 1, mRNA [NM_030653] |
| 162 | A_23_P107412 | 4.8170357 | *P4HB* | Homo sapiens prolyl 4-hydroxylase, beta polypeptide (P4HB), mRNA [NM_000918] |

| No | Probe Name | Fold Change (Multiple Myeloma vs Normal) | Gene Symbol | Description |
|---|---|---|---|---|
| 163 | A_33_P3288754 | 4.801691 | *C19orf48* | Homo sapiens chromosome 19 open reading frame 48 (C19orf48), transcript variant 3, mRNA [NM_001290149] |
| 164 | A_23_P215341 | 4.7863503 | *FKBP14* | Homo sapiens FK506 binding protein 14, 22 kDa (FKBP14), transcript variant 1, mRNA [NM_017946] |
| 165 | A_23_P41424 | 4.604358 | *SLC39A8* | Homo sapiens solute carrier family 39 (zinc transporter), member 8 (SLC39A8), transcript variant 1, mRNA [NM_022154] |
| 166 | A_23_P99930 | 4.425636 | *TIPIN* | Homo sapiens TIMELESS interacting protein (TIPIN), transcript variant 1, mRNA [NM_017858] |
| 167 | A_21_P0000530 | 4.4001327 | *LRRC75A-AS1* | Homo sapiens LRRC75A antisense RNA 1 (LRRC75A-AS1), transcript variant 27, long non-coding RNA [NR_045024] |
| 168 | A_24_P813147 | 4.2183547 | *TUBB8* | Homo sapiens tubulin, beta 8 class VIII (TUBB8), mRNA [NM_177987] |
| 169 | A_32_P101699 | 4.1761446 | *LOC729887* | PREDICTED: Homo sapiens uncharacterized LOC729887 (LOC729887), misc_RNA [XR_243500] |
| 170 | A_24_P188071 | 3.945975 | *TUBA1C* | Homo sapiens tubulin, alpha 1c (TUBA1C), mRNA [NM_032704] |
| 171 | A_23_P47565 | 3.83251 | *LDHA* | Homo sapiens lactate dehydrogenase A (LDHA), transcript variant 1, mRNA [NM_005566] |

| No | Probe Name | Fold Change (Multiple Myeloma vs Normal) | Gene Symbol | Description |
|---|---|---|---|---|
| 172 | A_23_P203949 | 3.7591608 | *DDX11* | Homo sapiens DEAD/H (Asp-Glu-Ala-Asp/His) box helicase 11 (DDX11), transcript variant 1, mRNA [NM_030653] |
| 173 | A_23_P100764 | 3.737359 | *SLC25A39* | Homo sapiens solute carrier family 25, member 39 (SLC25A39), transcript variant 2, mRNA [NM_016016] |
| 174 | A_33_P3410836 | 3.6720536 | *HIST1H4D* | Homo sapiens histone cluster 1, H4d (HIST1H4D), mRNA [NM_003539] |
| 175 | A_33_P3271975 | 3.5721247 | *LOC100132368* | Homo sapiens cDNA FLJ16817 fis, clone TLIVE2007192. [AK131565] |
| 176 | A_21_P0011874 | 3.544078 | *XLOC_014512* | BROAD Institute lincRNA (XLOC_014512), lincRNA [TCONS_l2_00014252] |
| 177 | A_21_P0000483 | 3.4737272 | *SNORD75* | Homo sapiens small nucleolar RNA, C/D box 75 (SNORD75), small nucleolar RNA [NR_003941] |
| 178 | A_21_P0009764 | 3.4655268 | | Q72GU7_THET2 (Q72GU7) Transporter, partial (6%) [THC2707376] |
| 179 | A_33_P3252043 | 3.4285958 | *P4HB* | Homo sapiens prolyl 4-hydroxylase, beta polypeptide (P4HB), mRNA [NM_000918] |
| 180 | A_24_P20873 | 3.1259587 | *HIST1H4I* | Homo sapiens histone cluster 1, H4i (HIST1H4I), mRNA [NM_003495] |
| 181 | A_23_P127579 | 3.0643048 | *PTS* | Homo sapiens 6-pyruvoyltetrahydropterin synthase (PTS), mRNA [NM_000317] |

| No | Probe Name | Fold Change (Multiple Myeloma vs Normal) | Gene Symbol | Description |
|---|---|---|---|---|
| 182 | A_23_P397019 | 3.045546 | *DNAJC25* | Homo sapiens DnaJ (Hsp40) homolog, subfamily C , member 25 (DNAJC25), transcript variant 1, mRNA [NM_001015882] |
| 183 | A_23_P60248 | 3.042878 | *TXN* | Homo sapiens thioredoxin (TXN), transcript variant 1, mRNA [NM_003329] |
| 184 | A_23_P9152 | 2.9570825 | *RCL1* | Homo sapiens RNA terminal phosphate cyclase-like 1 (RCL1), transcript variant 1, mRNA [NM_005772] |
| 185 | A_33_P3292854 | 2.7253678 | *CALR* | Homo sapiens calreticulin (CALR), mRNA [NM_004343] |
| 186 | A_33_P3317731 | 2.7147658 | | Homo sapiens cDNA FLJ27366 fis, clone UBA02727. [AK130876] |
| 187 | A_23_P334608 | 2.6828802 | *GUSB* | Homo sapiens glucuronidase, beta (GUSB), transcript variant 1, mRNA [NM_000181] |
| 188 | A_32_P90210 | 2.4490526 | *TAF9* | Homo sapiens TAF9 RNA polymerase II, TATA box binding protein (TBP)-associated factor, 32kDa (TAF9), transcript variant 4, mRNA [NM_001015892] |
| 189 | A_21_P0009367 | 2.2067888 | *XLOC_012586* | BROAD Institute lincRNA (XLOC_012586), lincRNA [TCONS_00025780] |

**APPENDIX B:** Down-regulated probes by ≥2.0 fold change at p<0.01 in multiple myeloma relative to the normal controls (negative in fold change indicates down-regulation)

| No | Probe Name | Fold Change (Multiple Myeloma vs Normal) | Gene Symbol | Description |
|---|---|---|---|---|
| 1 | A_23_P31376 | -57.677586 | *LRRN3* | Homo sapiens leucine rich repeat neuronal 3 (LRRN3), transcript variant 3, mRNA [NM_018334] |
| 2 | A_21_P0014504 | -36.999603 | | long intergenic non-protein coding RNA 402 [Source:HGNC Symbol;Acc:42732] [ENST00000419499] |
| 3 | A_23_P250302 | -36.961945 | *CCR3* | Homo sapiens chemokine (C-C motif) receptor 3 (CCR3), transcript variant 1, mRNA [NM_001837] |
| 4 | A_32_P164593 | -30.08926 | *ZMAT4* | Homo sapiens zinc finger, matrin-type 4 (ZMAT4), transcript variant 1, mRNA [NM_024645] |
| 5 | A_33_P3391796 | -28.37186 | *NOG* | Homo sapiens noggin (NOG), mRNA [NM_005450] |
| 6 | A_33_P3214516 | -27.840502 | | T cell receptor delta variable 2 [Source:HGNC Symbol;Acc:12263] [ENST00000390469] |
| 7 | A_21_P0000807 | -24.583532 | *LINC00861* | Homo sapiens long intergenic non-protein coding RNA 861 (LINC00861), transcript variant 2, long non-coding RNA [NR_038447] |
| 8 | A_21_P0014281 | -22.40508 | | BX096603 Soares_testis_NHT Homo sapiens cDNA clone IMAGp998H151782, mRNA sequence [BX096603] |
| 9 | A_32_P111306 | -21.77881 | *LINC00189* | Homo sapiens long intergenic non-protein coding RNA 189 (LINC00189), long non-coding RNA [NR_027072] |

| No | Probe Name | Fold Change (Multiple Myeloma vs Normal) | Gene Symbol | Description |
|---|---|---|---|---|
| 10 | A_23_P31996 | -19.971178 | *SLC46A2* | Homo sapiens solute carrier family 46, member 2 (SLC46A2), mRNA [NM_033051] |
| 11 | A_21_P0009364 | -19.157902 | *XLOC_012575* | BROAD Institute lincRNA (XLOC_012575), lincRNA [TCONS_00025765] |
| 12 | A_33_P3346972 | -16.15265 | | T cell receptor beta variable 6-6 [Source:HGNC Symbol;Acc:12231] [ENST00000390371] |
| 13 | A_21_P0000882 | -16.106894 | *RNF157-AS1* | Homo sapiens RNF157 antisense RNA 1 (RNF157-AS1), long non-coding RNA [NR_040017] |
| 14 | A_33_P3311971 | -15.272933 | | T cell receptor beta variable 6-5 [Source:HGNC Symbol;Acc:12230] [ENST00000390368] |
| 15 | A_23_P1602 | -15.040401 | *CDC42EP2* | Homo sapiens CDC42 effector protein (Rho GTPase binding) 2 (CDC42EP2), mRNA [NM_006779] |
| 16 | A_23_P210581 | -14.718163 | *KCNG1* | Homo sapiens potassium voltage-gated channel, subfamily G, member 1 (KCNG1), mRNA [NM_002237] |
| 17 | A_24_P340954 | -14.589577 | *ANKUB1* | Homo sapiens ankyrin repeat and ubiquitin domain containing 1 (ANKUB1), mRNA [NM_001144960] |
| 18 | A_23_P125082 | -14.5456915 | *IRF2* | Homo sapiens interferon regulatory factor 2 (IRF2), mRNA [NM_002199] |
| 19 | A_21_P0006825 | -14.542644 | *PRKCQ-AS1* | PRKCQ antisense RNA 1 [Source:HGNC Symbol;Acc:44689] [ENST00000608526] |

| No | Probe Name | Fold Change (Multiple Myeloma vs Normal) | Gene Symbol | Description |
|---|---|---|---|---|
| 20 | A_33_P3264416 | -14.535018 | | T cell receptor beta variable 18 [Source:HGNC Symbol;Acc:12193] [ENST00000566373] |
| 21 | A_21_P0014322 | -14.418633 | *LOC101928595* | PREDICTED: Homo sapiens uncharacterized LOC101928595 (LOC101928595), ncRNA [XR_243378] |
| 22 | A_23_P47904 | -14.3310585 | *CCDC65* | Homo sapiens coiled-coil domain containing 65 (CCDC65), transcript variant 1, mRNA [NM_033124] |
| 23 | A_33_P3378491 | -14.175201 | | T cell receptor beta variable 6-7 (non-functional) [Source:HGNC Symbol;Acc:12232] [ENST00000390373] |
| 24 | A_33_P3289121 | -14.090264 | *C2orf40* | Homo sapiens chromosome 2 open reading frame 40 (C2orf40), mRNA [NM_032411] |
| 25 | A_21_P0010236 | -13.956941 | *LOC101928126* | PREDICTED: Homo sapiens uncharacterized LOC101928126 (LOC101928126), ncRNA [XR_254026] |
| 26 | A_33_P3290853 | -13.679245 | | T cell receptor beta variable 11-2 [Source:HGNC Symbol;Acc:12181] [ENST00000471935] |
| 27 | A_21_P0008548 | -13.562015 | | chromosome 14 open reading frame 64 [Source:HGNC Symbol;Acc:20111] [ENST00000502187] |
| 28 | A_33_P3210258 | -13.446887 | | T cell receptor gamma variable 4 [Source:HGNC Symbol;Acc:12289] [ENST00000390345] |

| No | Probe Name | Fold Change (Multiple Myeloma vs Normal) | Gene Symbol | Description |
|---|---|---|---|---|
| 29 | A_33_P3343577 | -13.432579 | | T cell receptor beta variable 10-3 [Source:HGNC Symbol;Acc:12179] [ENST00000566578] |
| 30 | A_23_P38696 | -13.218175 | *DSC1* | Homo sapiens desmocollin 1 (DSC1), transcript variant Dsc1b, mRNA [NM_004948] |
| 31 | A_21_P0006645 | -13.208648 | *LOC101928150* | Homo sapiens uncharacterized LOC101928150 (LOC101928150), long non-coding RNA [NR_120634] |
| 32 | A_21_P0006826 | -12.972011 | *PRKCQ-AS1* | PRKCQ antisense RNA 1 [Source:HGNC Symbol;Acc:44689] [ENST00000609627] |
| 33 | A_23_P139654 | -12.805049 | *KLRC1* | Homo sapiens killer cell lectin-like receptor subfamily C, member 1 (KLRC1), transcript variant 2, mRNA [NM_007328] |
| 34 | A_19_P00808602 | -12.797196 | *LOC284837* | Homo sapiens uncharacterized LOC284837 (LOC284837), long non-coding RNA [NR_026961] |
| 35 | A_21_P0004878 | -12.679235 | *XLOC_005278* | BROAD Institute lincRNA (XLOC_005278), lincRNA [TCONS_00011803] |
| 36 | A_24_P115932 | -12.384757 | *PTGDR2* | Homo sapiens prostaglandin D2 receptor 2 (PTGDR2), mRNA [NM_004778] |
| 37 | A_33_P3336113 | -12.141015 | *TIGD3* | Homo sapiens tigger transposable element derived 3 (TIGD3), mRNA [NM_145719] |
| 38 | A_33_P3276845 | -11.906758 | | |

| No | Probe Name | Fold Change (Multiple Myeloma vs Normal) | Gene Symbol | Description |
|---|---|---|---|---|
| 39 | A_21_P0007040 | -11.880403 | *XLOC_009007* | BROAD Institute lincRNA (XLOC_009007), lincRNA [TCONS_00018657] |
| 40 | A_33_P3374162 | -11.852471 | | T cell receptor beta variable 27 [Source:HGNC Symbol;Acc:12208] [ENST00000390399] |
| 41 | A_24_P314786 | -11.805787 | *SLC4A10* | Homo sapiens solute carrier family 4, sodium bicarbonate transporter, member 10 (SLC4A10), transcript variant 2, mRNA [NM_022058] |
| 42 | A_23_P99653 | -11.800878 | | T cell receptor alpha variable 13-2 [Source:HGNC Symbol;Acc:12109] [ENST00000390439] |
| 43 | A_23_P112026 | -11.699629 | *IDO1* | Homo sapiens indoleamine 2,3-dioxygenase 1 (IDO1), mRNA [NM_002164] |
| 44 | A_24_P188800 | -11.689338 | *Mar-01* | Homo sapiens membrane-associated ring finger (C3HC4) 1, E3 ubiquitin protein ligase (MARCH1), transcript variant 2, mRNA [NM_017923] |
| 45 | A_24_P529627 | -11.535644 | | T cell receptor beta variable 6-1 [Source:HGNC Symbol;Acc:12226] [ENST00000390353] |
| 46 | A_24_P357468 | -11.46058 | | T cell receptor alpha variable 8-2 [Source:HGNC Symbol;Acc:12147] [ENST00000390434] |
| 47 | A_33_P3313338 | -11.3888235 | | T cell receptor alpha variable 17 [Source:HGNC Symbol;Acc:12113] [ENST00000390445] |

| No | Probe Name | Fold Change (Multiple Myeloma vs Normal) | Gene Symbol | Description |
|---|---|---|---|---|
| 48 | A_33_P3309621 | -11.203066 | *SIGLEC17P* | Homo sapiens sialic acid binding Ig-like lectin 17, pseudogene (SIGLEC17P), transcript variant 1, non-coding RNA [NR_047529] |
| 49 | A_33_P3843415 | -11.175032 | *WDR11-AS1* | Homo sapiens WDR11 antisense RNA 1 (WDR11-AS1), long non-coding RNA [NR_033850] |
| 50 | A_33_P3243439 | -11.061069 | *GPR162* | Homo sapiens G protein-coupled receptor 162 (GPR162), transcript variant A-2, mRNA [NM_019858] |
| 51 | A_33_P3397127 | -10.981832 | | T cell receptor beta variable 6-2 (gene/pseudogene) [Source:HGNC Symbol;Acc:12227] [ENST00000562386] |
| 52 | A_33_P3394471 | -10.800185 | | T cell receptor alpha variable 3 (gene/pseudogene) [Source:HGNC Symbol;Acc:12128] [ENST00000390425] |
| 53 | A_21_P0014811 | -10.675862 | | |
| 54 | A_21_P0008385 | -10.615363 | *XLOC_010924* | BROAD Institute lincRNA (XLOC_010924), lincRNA [TCONS_00022624] |
| 55 | A_33_P3326767 | -10.581039 | | PREDICTED: Homo sapiens uncharacterized LOC100996416 (LOC100996416), misc RNA [XR_159010] |
| 56 | A_21_P0008486 | -10.55861 | | chromosome 14 open reading frame 64 [Source:HGNC Symbol;Acc:20111] [ENST00000502187] |

| No | Probe Name | Fold Change (Multiple Myeloma vs Normal) | Gene Symbol | Description |
|---|---|---|---|---|
| 57 | A_32_P138396 | -10.534202 | *WDR86-AS1* | Homo sapiens cDNA FLJ38667 fis, clone HLUNG2006843. [AK095986] |
| 58 | A_21_P0006321 | -10.532041 | *XLOC_007858* | BROAD Institute lincRNA (XLOC_007858), lincRNA [TCONS_00016480] |
| 59 | A_21_P0008485 | -10.367762 | | chromosome 14 open reading frame 64 [Source:HGNC Symbol;Acc:20111] [ENST00000502187] |
| 60 | A_33_P3372910 | -10.366381 | *DDX58* | Homo sapiens DEAD (Asp-Glu-Ala-Asp) box polypeptide 58 (DDX58), mRNA [NM_014314] |
| 61 | A_23_P166993 | -10.121697 | *EPHB1* | Homo sapiens EPH receptor B1 (EPHB1), mRNA [NM_004441] |
| 62 | A_33_P3312209 | -10.029556 | | |
| 63 | A_33_P3250566 | -9.7718525 | | T cell receptor alpha variable 8-6 [Source:HGNC Symbol;Acc:12151] [ENST00000390443] |
| 64 | A_21_P0006828 | -9.694549 | *XLOC_008372* | BROAD Institute lincRNA (XLOC_008372), lincRNA [TCONS_00018111] |
| 65 | A_32_P47643 | -9.615738 | *FAM110C* | Homo sapiens family with sequence similarity 110, member C (FAM110C), mRNA [NM_001077710] |
| 66 | A_23_P202427 | -9.53164 | *HKDC1* | Homo sapiens hexokinase domain containing 1 (HKDC1), mRNA [NM_025130] |
| 67 | A_24_P178819 | -9.520547 | | T cell receptor alpha variable 12-2 [Source:HGNC Symbol;Acc:12106] [ENST00000390437] |

| No | Probe Name | Fold Change (Multiple Myeloma vs Normal) | Gene Symbol | Description |
|---|---|---|---|---|
| 68 | A_21_P0012213 | -9.516431 | | Homo sapiens chromosome 21 open reading frame 109 (C21orf109) mRNA, complete cds. [AF490769] |
| 69 | A_21_P0006823 | -9.368704 | *PRKCQ-AS1* | PRKCQ antisense RNA 1 [Source:HGNC Symbol;Acc:44689] [ENST00000414894] |
| 70 | A_21_P0002225 | -9.33152 | *XLOC_001496* | BROAD Institute lincRNA (XLOC_001496), lincRNA [TCONS_00003709] |
| 71 | A_33_P3301897 | -9.309808 | | T cell receptor beta variable 6-9 [Source:HGNC Symbol;Acc:12234] [ENST00000390379] |
| 72 | A_23_P159237 | -8.697575 | *GPR20* | Homo sapiens G protein-coupled receptor 20 (GPR20), mRNA [NM_005293] |
| 73 | A_33_P3213702 | -8.634369 | *KIF28P* | PREDICTED: Homo sapiens kinesin family member 28, pseudogene (KIF28P), mRNA [XM_001717074] |
| 74 | A_21_P0006827 | -8.555111 | *XLOC_008371* | BROAD Institute lincRNA (XLOC_008371), lincRNA [TCONS_00018110] |
| 75 | A_33_P3270489 | -8.542695 | *CCDC170* | Homo sapiens coiled-coil domain containing 170 (CCDC170), mRNA [NM_025059] |
| 76 | A_33_P3264569 | -8.342303 | | T cell receptor beta variable 10-2 [Source:HGNC Symbol;Acc:12178] [ENST00000426318] |
| 77 | A_24_P652502 | -8.2401 | | T cell receptor alpha variable 4 [Source:HGNC Symbol;Acc:12140] [ENST00000390426] |

| No | Probe Name | Fold Change (Multiple Myeloma vs Normal) | Gene Symbol | Description |
|---|---|---|---|---|
| 78 | A_33_P3238579 | -8.226816 | | T cell receptor beta variable 11-3 [Source:HGNC Symbol;Acc:12182] [ENST00000565202] |
| 79 | A_32_P208823 | -8.2262335 | *PLXDC1* | Homo sapiens plexin domain containing 1 (PLXDC1), mRNA [NM_020405] |
| 80 | A_23_P1331 | -8.225488 | *COL13A1* | Homo sapiens collagen, type XIII, alpha 1 (COL13A1), transcript variant 5, mRNA [NM_080801] |
| 81 | A_19_P00322645 | -8.209279 | *LOC283588* | Homo sapiens cDNA FLJ37957 fis, clone CTONG2009529. [AK095276] |
| 82 | A_24_P406601 | -8.159348 | *OLFM1* | Homo sapiens olfactomedin 1 (OLFM1), transcript variant 1, mRNA [NM_014279] |
| 83 | A_23_P130435 | -8.136248 | *LIM2* | Homo sapiens lens intrinsic membrane protein 2, 19kDa (LIM2), transcript variant 1, mRNA [NM_030657] |
| 84 | A_33_P3348270 | -7.9776893 | | T cell receptor beta variable 5-4 [Source:HGNC Symbol;Acc:12221] [ENST00000454561] |
| 85 | A_33_P3314850 | -7.784068 | | T cell receptor beta variable 6-4 [Source:HGNC Symbol;Acc:12229] [ENST00000390360] |
| 86 | A_23_P94186 | -7.7035236 | *LYPD2* | Homo sapiens LY6/PLAUR domain containing 2 (LYPD2), mRNA [NM_205545] |
| 87 | A_33_P3247890 | -7.698619 | | T cell receptor alpha variable 1-2 [Source:HGNC Symbol;Acc:12102] [ENST00000390423] |

| No | Probe Name | Fold Change (Multiple Myeloma vs Normal) | Gene Symbol | Description |
|---|---|---|---|---|
| 88 | A_33_P3407007 | -7.6611857 | *LINC00861* | Homo sapiens long intergenic non-protein coding RNA 861 (LINC00861), transcript variant 1, long non-coding RNA [NR_038446] |
| 89 | A_33_P3210499 | -7.6552224 | | T cell receptor beta variable 25-1 [Source:HGNC Symbol;Acc:12205] [ENST00000390398] |
| 90 | A_19_P00801823 | -7.5473595 | *XLOC_014512* | BROAD Institute lincRNA (XLOC_014512), lincRNA [TCONS_l2_00028399] |
| 91 | A_33_P3305203 | -7.5190463 | *LOC283588* | Homo sapiens cDNA FLJ37957 fis, clone CTONG2009529. [AK095276] |
| 92 | A_33_P3715843 | -7.447639 | *MGC40069* | Homo sapiens hypothetical protein MGC40069, mRNA (cDNA clone IMAGE:5216694). [BC032242] |
| 93 | A_23_P50517 | -7.4449463 | *ZNF541* | Homo sapiens zinc finger protein 541 (ZNF541), mRNA [NM_001277075] |
| 94 | A_24_P229151 | -7.400888 | | T cell receptor alpha variable 29/delta variable 5 (gene/pseudogene) [Source:HGNC Symbol;Acc:12127] [ENST00000390458] |
| 95 | A_24_P930111 | -7.3828797 | *SLC4A10* | Homo sapiens solute carrier family 4, sodium bicarbonate transporter, member 10 (SLC4A10), transcript variant 2, mRNA [NM_022058] |
| 96 | A_33_P3284533 | -7.3598037 | | T cell receptor alpha variable 14/delta variable 4 [Source:HGNC Symbol;Acc:12110] [ENST00000390440] |

| No | Probe Name | Fold Change (Multiple Myeloma vs Normal) | Gene Symbol | Description |
|---|---|---|---|---|
| 97 | A_23_P319466 | -7.3538184 | *CYSLTR2* | Homo sapiens cysteinyl leukotriene receptor 2 (CYSLTR2), mRNA [NM_020377] |
| 98 | A_33_P3393667 | -7.3499403 | | T cell receptor alpha variable 1-1 [Source:HGNC Symbol;Acc:12101] [ENST00000542354] |
| 99 | A_21_P0007055 | -7.329778 | *XLOC_008434* | BROAD Institute lincRNA (XLOC_008434), lincRNA [TCONS_00018704] |
| 100 | A_21_P0006980 | -7.297213 | *XLOC_008760* | BROAD Institute lincRNA (XLOC_008760), lincRNA [TCONS_00018462] |
| 101 | A_23_P157926 | -7.29252 | *LINGO2* | Homo sapiens leucine rich repeat and Ig domain containing 2 (LINGO2), transcript variant 1, mRNA [NM_152570] |
| 102 | A_33_P3436646 | -7.291939 | *LOC151657* | Homo sapiens cDNA FLJ33795 fis, clone CTONG1000097. [AK091114] |
| 103 | A_33_P3337485 | -7.2100725 | *CD248* | Homo sapiens CD248 molecule, endosialin (CD248), mRNA [NM_020404] |
| 104 | A_33_P3274514 | -7.209435 | | T cell receptor alpha variable 16 [Source:HGNC Symbol;Acc:12112] [ENST00000390444] |
| 105 | A_21_P0002476 | -7.20266 | *XLOC_002221* | BROAD Institute lincRNA (XLOC_002221), lincRNA [TCONS_00004347] |
| 106 | A_23_P98645 | -7.1448293 | *DCHS1* | Homo sapiens dachsous cadherin-related 1 (DCHS1), mRNA [NM_003737] |

| No | Probe Name | Fold Change (Multiple Myeloma vs Normal) | Gene Symbol | Description |
|---|---|---|---|---|
| 107 | A_23_P103803 | -7.118562 | *FCRL3* | Homo sapiens Fc receptor-like 3 (FCRL3), mRNA [NM_052939] |
| 108 | A_33_P3352758 | -6.9094877 | *NHSL2* | Homo sapiens NHS-like 2 (NHSL2), mRNA [NM_001013627] |
| 109 | A_21_P0013987 | -6.7819366 | *LOC100509780* | Homo sapiens cDNA FLJ25713 fis, clone TST05089. [AK098579] |
| 110 | A_33_P3416347 | -6.7759876 | | T cell receptor beta variable 23-1 (non-functional) [Source:HGNC Symbol;Acc:12201] [ENST00000390396] |
| 111 | A_21_P0008158 | -6.6888394 | *XLOC_010596* | BROAD Institute lincRNA (XLOC_010596), lincRNA [TCONS_00021993] |
| 112 | A_19_P00321597 | -6.669404 | *C14orf64* | Homo sapiens cDNA FLJ40624 fis, clone THYMU2013981. [AK097943] |
| 113 | A_33_P3404351 | -6.4862957 | | T cell receptor alpha variable 5 [Source:HGNC Symbol;Acc:12143] [ENST00000390427] |
| 114 | A_33_P3321085 | -6.4702005 | | T cell receptor alpha variable 2 [Source:HGNC Symbol;Acc:12116] [ENST00000390424] |
| 115 | A_24_P59053 | -6.435313 | | T cell receptor beta variable 3-1 [Source:HGNC Symbol;Acc:12212] [ENST00000390387] |
| 116 | A_21_P0007298 | -6.390403 | *XLOC_009327* | BROAD Institute lincRNA (XLOC_009327), lincRNA [TCONS_00019532] |
| 117 | A_21_P0009802 | -6.3839555 | *LOC102723540* | PREDICTED: Homo sapiens uncharacterized LOC102723540 (LOC102723540), ncRNA [XR_430234] |

| No | Probe Name | Fold Change (Multiple Myeloma vs Normal) | Gene Symbol | Description |
|---|---|---|---|---|
| 118 | A_33_P3276301 | -6.350825 | | T cell receptor beta variable 11-1 [Source:HGNC Symbol;Acc:12180] [ENST00000390367] |
| 119 | A_23_P253029 | -6.3503623 | *BOK* | Homo sapiens BCL2-related ovarian killer (BOK), mRNA [NM_032515] |
| 120 | A_21_P0009314 | -6.3393826 | *LOC102724792* | PREDICTED: Homo sapiens uncharacterized LOC102724792 (LOC102724792), ncRNA [XR_433367] |
| 121 | A_32_P738377 | -6.105303 | *LOC284837* | Homo sapiens uncharacterized LOC284837 (LOC284837), long non-coding RNA [NR_026961] |
| 122 | A_33_P3273474 | -5.938358 | *CD1C* | Homo sapiens CD1c molecule (CD1C), mRNA [NM_001765] |
| 123 | A_23_P404536 | -5.9345007 | *ENPP3* | Homo sapiens ectonucleotide pyrophosphatase/phosphodiesterase 3 (ENPP3), mRNA [NM_005021] |
| 124 | A_33_P3303507 | -5.746997 | | HSP76_HUMAN (P17066) Heat shock 70 kDa protein 6 (Heat shock 70 kDa protein B'), partial (7%) [THC2683968] |
| 125 | A_33_P3257428 | -5.599299 | | T cell receptor beta variable 7-7 [Source:HGNC Symbol;Acc:12241] [ENST00000390377] |
| 126 | A_23_P133386 | -5.5200458 | *RASGRF2* | Homo sapiens Ras protein-specific guanine nucleotide-releasing factor 2 (RASGRF2), mRNA [NM_006909] |
| 127 | A_33_P3356022 | -5.500632 | | T cell receptor alpha variable 35 [Source:HGNC Symbol;Acc:12134] [ENST00000390462] |

| No | Probe Name | Fold Change (Multiple Myeloma vs Normal) | Gene Symbol | Description |
|---|---|---|---|---|
| 128 | A_21_P0002200 | -5.497028 | *XLOC_001430* | BROAD Institute lincRNA (XLOC_001430), lincRNA [TCONS_00003640] |
| 129 | A_33_P3211968 | -5.439314 | *LOC100133207* | human full-length cDNA clone CS0DG006YJ19 of B cells (Ramos cell line) of Homo sapiens (human). [BX247990] |
| 130 | A_21_P0008650 | -5.436687 | | |
| 131 | A_21_P0013164 | -5.4348464 | *LPAL2* | Homo sapiens lipoprotein, Lp(a)-like 2, pseudogene (LPAL2), transcript variant 2, non-coding RNA [NR_028093] |
| 132 | A_33_P3362359 | -5.431764 | | T cell receptor beta variable 23/OR9-2 (non-functional) [Source:HGNC Symbol;Acc:12202] [ENST00000390389] |
| 133 | A_21_P0012663 | -5.4254293 | *XLOC_014512* | BROAD Institute lincRNA (XLOC_014512), lincRNA [TCONS_l2_00021110] |
| 134 | A_32_P133072 | -5.3276553 | *SPON1* | Homo sapiens spondin 1, extracellular matrix protein (SPON1), mRNA [NM_006108] |
| 135 | A_21_P0002691 | -5.27899 | *XLOC_002473* | BROAD Institute lincRNA (XLOC_002473), lincRNA [TCONS_00004565] |
| 136 | A_33_P3366662 | -5.250103 | | T cell receptor alpha variable 10 [Source:HGNC Symbol;Acc:12103] [ENST00000390432] |
| 137 | A_24_P376760 | -5.223123 | *CA6* | Homo sapiens carbonic anhydrase VI (CA6), transcript variant 1, mRNA [NM_001215] |

| No | Probe Name | Fold Change (Multiple Myeloma vs Normal) | Gene Symbol | Description |
|---|---|---|---|---|
| 138 | A_21_P0008354 | -5.168245 | *XLOC_010866* | BROAD Institute lincRNA (XLOC_010866), lincRNA [TCONS_00022548] |
| 139 | A_33_P3265920 | -5.0725937 | *PTPN4* | Homo sapiens protein tyrosine phosphatase, non-receptor type 4 (megakaryocyte) (PTPN4), mRNA [NM_002830] |
| 140 | A_21_P0012214 | -4.974954 | | |
| 141 | A_33_P3399864 | -4.9384723 | *ZNF792* | Homo sapiens zinc finger protein 792 (ZNF792), mRNA [NM_175872] |
| 142 | A_21_P0004714 | -4.886775 | *FLJ38122* | Homo sapiens uncharacterized LOC401289 (FLJ38122), long non-coding RNA [NR_104177] |
| 143 | A_24_P92558 | -4.870102 | *ZNF674* | Homo sapiens zinc finger protein 674 (ZNF674), transcript variant 1, mRNA [NM_001039891] |
| 144 | A_23_P428887 | -4.8139844 | *KLHL34* | Homo sapiens kelch-like family member 34 (KLHL34), mRNA [NM_153270] |
| 145 | A_24_P115651 | -4.7551417 | *ENKUR* | Homo sapiens enkurin, TRPC channel interacting protein (ENKUR), transcript variant 1, mRNA [NM_145010] |
| 146 | A_23_P67618 | -4.720383 | *ZNF792* | Homo sapiens zinc finger protein 792 (ZNF792), mRNA [NM_175872] |
| 147 | A_23_P250358 | -4.706445 | *HERC6* | Homo sapiens HECT and RLD domain containing E3 ubiquitin protein ligase family member 6 (HERC6), transcript variant 1, mRNA [NM_017912] |
| 148 | A_33_P3362296 | -4.694415 | *KCNG1* | potassium voltage-gated channel, subfamily G, member 1 [Source:HGNC Symbol;Acc:6248] [ENST00000396017] |

| No | Probe Name | Fold Change (Multiple Myeloma vs Normal) | Gene Symbol | Description |
|---|---|---|---|---|
| 149 | A_23_P80242 | -4.6825843 | *SEZ6L* | Homo sapiens seizure related 6 homolog (mouse)-like (SEZ6L), transcript variant 1, mRNA [NM_021115] |
| 150 | A_24_P273799 | -4.6028223 | *ZNF641* | Homo sapiens zinc finger protein 641 (ZNF641), transcript variant 1, mRNA [NM_152320] |
| 151 | A_33_P3412752 | -4.5966034 | *LOC100128607* | Homo sapiens cDNA FLJ45251 fis, clone BRHIP2009177. [AK127186] |
| 152 | A_33_P3275070 | -4.571823 | | Homo sapiens cDNA FLJ33983 fis, clone DFNES2004684. [AK091302] |
| 153 | A_21_P0005376 | -4.46484 | | PREDICTED: Homo sapiens uncharacterized LOC102723446 (LOC102723446), ncRNA [XR_426177] |
| 154 | A_24_P418152 | -4.461187 | *FLJ40194* | Homo sapiens uncharacterized FLJ40194 (FLJ40194), long non-coding RNA [NR_034161] |
| 155 | A_23_P37375 | -4.45359 | *RPS6KA5* | Homo sapiens ribosomal protein S6 kinase, 90kDa, polypeptide 5 (RPS6KA5), transcript variant 1, mRNA [NM_004755] |
| 156 | A_24_P28295 | -4.44316 | *RABGAP1L* | Homo sapiens RAB GTPase activating protein 1-like (RABGAP1L), transcript variant 4, mRNA [NM_001243765] |
| 157 | A_21_P0001575 | -4.173303 | *XLOC_000986* | BROAD Institute lincRNA (XLOC_000986), lincRNA [TCONS_00001648] |
| 158 | A_33_P3398392 | -4.1671906 | *FHL1* | four and a half LIM domains 1 [Source:HGNC Symbol;Acc:3702] [ENST00000370674] |

| No | Probe Name | Fold Change (Multiple Myeloma vs Normal) | Gene Symbol | Description |
|---|---|---|---|---|
| 159 | A_23_P116850 | -4.1360717 | *KRT2* | Homo sapiens keratin 2 (KRT2), mRNA [NM_000423] |
| 160 | A_21_P0014822 | -4.0920415 | | Homo sapiens cDNA clone IMAGE:4186600. [BC061902] |
| 161 | A_21_P0006622 | -4.081043 | *GATA3-AS1* | Homo sapiens GATA3 antisense RNA 1 (GATA3-AS1), transcript variant 1, long non-coding RNA [NR_104327] |
| 162 | A_33_P3253089 | -4.0715437 | *FAM19A1* | Homo sapiens family with sequence similarity 19 (chemokine (C-C motif)-like), member A1 (FAM19A1), transcript variant 1, mRNA [NM_213609] |
| 163 | A_32_P797019 | -3.9730058 | | aminopeptidase-like 1 [Source:HGNC Symbol;Acc:16244] [ENST00000532531] |
| 164 | A_24_P932594 | -3.8863883 | *ULK2* | Homo sapiens unc-51 like autophagy activating kinase 2 (ULK2), transcript variant 1, mRNA [NM_014683] |
| 165 | A_23_P120281 | -3.8577156 | *EDAR* | Homo sapiens ectodysplasin A receptor (EDAR), mRNA [NM_022336] |
| 166 | A_33_P3303945 | -3.7513373 | *OR52N4* | Homo sapiens olfactory receptor, family 52, subfamily N, member 4 (OR52N4), mRNA [NM_001005175] |
| 167 | A_33_P3209885 | -3.6618292 | *PLXDC1* | Homo sapiens plexin domain containing 1 (PLXDC1), mRNA [NM_020405] |
| 168 | A_23_P78742 | -3.5390449 | *FLT3LG* | Homo sapiens fms-related tyrosine kinase 3 ligand (FLT3LG), transcript variant 3, mRNA [NM_001459] |

| No | Probe Name | Fold Change (Multiple Myeloma vs Normal) | Gene Symbol | Description |
|---|---|---|---|---|
| 169 | A_32_P197825 | -3.5229225 | *PLGLB1* | Homo sapiens plasminogen-like B1 (PLGLB1), mRNA [NM_001032392] |
| 170 | A_33_P3252598 | -3.5168307 | *DEFB136* | Homo sapiens defensin, beta 136 (DEFB136), mRNA [NM_001033018] |
| 171 | A_33_P3220207 | -3.3920834 | *ARMC3* | Homo sapiens armadillo repeat containing 3 (ARMC3), transcript variant 3, mRNA [NM_001282746] |
| 172 | A_33_P3367037 | -3.376261 | | Q53GD0_HUMAN (Q53GD0) Hydroxysteroid (17-beta) dehydrogenase 2 variant (Fragment), partial (16%) [THC2724742] |
| 173 | A_33_P3252475 | -3.3379936 | *C14orf64* | Homo sapiens chromosome 14 open reading frame 64 (C14orf64), long non-coding RNA [NR_015430] |
| 174 | A_33_P3379581 | -3.3268943 | *UBR2* | Homo sapiens ubiquitin protein ligase E3 component n-recognin 2 (UBR2), transcript variant 2, mRNA [NM_001184801] |
| 175 | A_32_P95960 | -3.305552 | *CLEC2D* | Homo sapiens C-type lectin domain family 2, member D (CLEC2D), transcript variant 2, mRNA [NM_001004419] |
| 176 | A_33_P3373348 | -3.2767255 | *AFF3* | AF4/FMR2 family, member 3 [Source:HGNC Symbol;Acc:6473] [ENST00000483600] |
| 177 | A_21_P0009050 | -3.274661 | *XLOC_011980* | BROAD Institute lincRNA (XLOC_011980), lincRNA [TCONS_00024702] |

| No | Probe Name | Fold Change (Multiple Myeloma vs Normal) | Gene Symbol | Description |
|---|---|---|---|---|
| 178 | A_33_P3420204 | -3.2589555 | *CRTC1* | Homo sapiens CREB regulated transcription coactivator 1 (CRTC1), transcript variant 3, mRNA [NM_001098482] |
| 179 | A_23_P16006 | -3.215658 | *ZNF600* | Homo sapiens zinc finger protein 600 (ZNF600), mRNA [NM_198457] |
| 180 | A_21_P0005688 | -3.1457279 | *XLOC_006774* | BROAD Institute lincRNA (XLOC_006774), lincRNA [TCONS_00014675] |
| 181 | A_21_P0003351 | -3.0795827 | | |
| 182 | A_24_P132518 | -3.074406 | *IKBKB* | Homo sapiens inhibitor of kappa light polypeptide gene enhancer in B-cells, kinase beta (IKBKB), transcript variant 1, mRNA [NM_001556] |
| 183 | A_21_P0010097 | -3.0723813 | *ZNF831* | PREDICTED: Homo sapiens zinc finger protein 831 (ZNF831), transcript variant X5, mRNA [XM_006723698] |
| 184 | A_33_P3383988 | -2.9680889 | | T cell receptor alpha variable 9-2 [Source:HGNC Symbol;Acc:12154] [ENST00000390441] |
| 185 | A_33_P3354539 | -2.9321494 | *CHURC1* | Homo sapiens churchill domain containing 1 (CHURC1), transcript variant 1, mRNA [NM_145165] |
| 186 | A_21_P0012485 | -2.807684 | *XLOC_014512* | BROAD Institute lincRNA (XLOC_014512), lincRNA [TCONS_l2_00019714] |
| 187 | A_33_P3421365 | -2.7064092 | *ZNF169* | Homo sapiens zinc finger protein 169 (ZNF169), mRNA [NM_194320] |
| 188 | A_23_P21409 | -2.5074155 | *CEP63* | Homo sapiens centrosomal protein 63kDa (CEP63), transcript variant 4, mRNA [NM_001042384] |

**APPENDIX C:** Top 100 up-regulated miRNAs in multiple myeloma compared to the normal controls by ≥2.0 fold change at $p<0.05$

| No | systematic name | Fold Change (Multiple Myeloma vs Normal) | mirbase accession No |
|---|---|---|---|
| 1 | hsa-miR-193b-3p | 72.696 | MIMAT0002819 |
| 2 | hsa-miR-183-5p | 42.81074 | MIMAT0000261 |
| 3 | hsa-miR-96-5p | 33.432415 | MIMAT0000095 |
| 4 | hsa-miR-630 | 30.826603 | MIMAT0003299 |
| 5 | hsa-miR-551b-3p | 28.938314 | MIMAT0003233 |
| 6 | hsa-miR-125b-5p | 21.910614 | MIMAT0000423 |
| 7 | hsa-miR-148a-3p | 19.154634 | MIMAT0000243 |
| 8 | hsa-miR-99a-5p | 18.97416 | MIMAT0000097 |
| 9 | hsa-miR-5703 | 18.140188 | MIMAT0022496 |
| 10 | hsa-miR-9-3p | 17.780647 | MIMAT0000442 |
| 11 | hsa-miR-1290 | 17.324305 | MIMAT0005880 |
| 12 | hsa-miR-1228-3p | 16.917711 | MIMAT0005583 |
| 13 | hsa-miR-6073 | 16.259237 | MIMAT0023698 |
| 14 | hsa-miR-4651 | 15.470672 | MIMAT0019715 |
| 15 | hsa-miR-4449 | 14.707131 | MIMAT0018968 |
| 16 | hsa-miR-196b-5p | 12.451211 | MIMAT0001080 |
| 17 | hsa-miR-143-3p | 12.203119 | MIMAT0000435 |
| 18 | hsa-miR-4778-5p | 11.505524 | MIMAT0019936 |
| 19 | hsa-miR-3188 | 11.321307 | MIMAT0015070 |
| 20 | hsa-miR-1234-3p | 11.275728 | MIMAT0005589 |
| 21 | hsa-miR-4446-3p | 11.0353155 | MIMAT0018965 |
| 22 | hsa-miR-3648 | 10.888356 | MIMAT0018068 |
| 23 | hsa-miR-210 | 10.8686695 | MIMAT0000267 |
| 24 | hsa-miR-21-3p | 10.865276 | MIMAT0004494 |
| 25 | hsa-miR-718 | 10.6935005 | MIMAT0012735 |
| 26 | hsa-miR-4484 | 10.66886 | MIMAT0019018 |
| 27 | hsa-miR-765 | 10.617614 | MIMAT0003945 |
| 28 | hsa-miR-3682-3p | 10.019291 | MIMAT0018110 |
| 29 | hsa-miR-4698 | 9.836284 | MIMAT0019793 |
| 30 | hsa-miR-1246 | 9.541015 | MIMAT0005898 |
| 31 | hsa-miR-1233-1-5p | 9.489333 | MIMAT0022943 |
| 32 | hsa-miR-422a | 9.459081 | MIMAT0001339 |
| 33 | hsa-miR-4430 | 9.340585 | MIMAT0018945 |
| 34 | hsa-miR-550a-3p | 9.284138 | MIMAT0003257 |
| 35 | hsa-miR-1469 | 9.275376 | MIMAT0007347 |
| 36 | hsa-miR-4685-5p | 9.191523 | MIMAT0019771 |
| 37 | hsa-miR-497-5p | 9.180842 | MIMAT0002820 |
| 38 | hsa-miR-20a-3p | 9.175086 | MIMAT0004493 |
| 39 | hsa-miR-431-3p | 9.139491 | MIMAT0004757 |
| 40 | hsa-miR-193b-5p | 9.138991 | MIMAT0004767 |
| 41 | hsa-miR-598 | 8.991602 | MIMAT0003266 |

| No | systematic name | Fold Change (Multiple Myeloma vs Normal) | mirbase accession No |
|---|---|---|---|
| 42 | hsa-miR-6512-5p | 8.982444 | MIMAT0025480 |
| 43 | hsa-miR-196a-5p | 8.972707 | MIMAT0000226 |
| 44 | hsa-miR-132-3p | 8.964459 | MIMAT0000426 |
| 45 | hsa-miR-23a-5p | 8.565206 | MIMAT0004496 |
| 46 | hsa-miR-627 | 8.497789 | MIMAT0003296 |
| 47 | hsa-miR-940 | 8.402196 | MIMAT0004983 |
| 48 | hsa-miR-205-5p | 8.398831 | MIMAT0000266 |
| 49 | hsa-miR-194-5p | 8.380732 | MIMAT0000460 |
| 50 | hsa-miR-215 | 8.379484 | MIMAT0000272 |
| 51 | hsa-miR-100-5p | 8.295616 | MIMAT0000098 |
| 52 | hsa-miR-4538 | 8.249183 | MIMAT0019081 |
| 53 | hsa-miR-328 | 8.221823 | MIMAT0000752 |
| 54 | hsa-miR-4690-5p | 8.220384 | MIMAT0019779 |
| 55 | hsa-miR-340-5p | 8.207941 | MIMAT0004692 |
| 56 | hsa-miR-1183 | 8.20255 | MIMAT0005828 |
| 57 | hsa-miR-4701-5p | 8.157882 | MIMAT0019798 |
| 58 | hsa-miR-4522 | 8.153399 | MIMAT0019060 |
| 59 | hsa-miR-4436b-5p | 8.149684 | MIMAT0019940 |
| 60 | hsa-miR-550a-3-5p | 8.132994 | MIMAT0020925 |
| 61 | hsa-miR-4745-5p | 8.128381 | MIMAT0019878 |
| 62 | hsa-miR-885-5p | 8.117832 | MIMAT0004947 |
| 63 | hsa-miR-10b-3p | 8.104628 | MIMAT0004556 |
| 64 | hsa-miR-203a | 8.083766 | MIMAT0000264 |
| 65 | hsa-miR-129-1-3p | 8.07458 | MIMAT0004548 |
| 66 | hsa-miR-9-5p | 8.074543 | MIMAT0000441 |
| 67 | hsa-miR-4530 | 8.069372 | MIMAT0019069 |
| 68 | hsa-miR-516a-5p | 8.051895 | MIMAT0004770 |
| 69 | hsa-miR-542-3p | 8.021954 | MIMAT0003389 |
| 70 | hsa-miR-4649-3p | 8.006126 | MIMAT0019712 |
| 71 | hsa-miR-4792 | 8.002802 | MIMAT0019964 |
| 72 | hsa-miR-10b-5p | 7.994181 | MIMAT0000254 |
| 73 | hsa-miR-7-1-3p | 7.986075 | MIMAT0004553 |
| 74 | hsa-miR-4763-5p | 7.9657655 | MIMAT0019912 |
| 75 | hsa-miR-4767 | 7.959038 | MIMAT0019919 |
| 76 | hsa-miR-181d | 7.953306 | MIMAT0002821 |
| 77 | hsa-miR-424-3p | 7.9429507 | MIMAT0004749 |
| 78 | hsa-miR-30a-5p | 7.9296923 | MIMAT0000087 |
| 79 | hsa-miR-4743-5p | 7.9248753 | MIMAT0019874 |
| 80 | hsa-miR-200b-3p | 7.924423 | MIMAT0000318 |
| 81 | hsa-miR-3617-3p | 7.9185796 | MIMAT0022966 |
| 82 | hsa-miR-4697-3p | 7.918378 | MIMAT0019792 |
| 83 | hsa-miR-4695-3p | 7.9177628 | MIMAT0019789 |
| 84 | hsa-miR-34b-5p | 7.908678 | MIMAT0000685 |

| No | systematic name | Fold Change (Multiple Myeloma vs Normal) | mirbase accession No |
|---|---|---|---|
| 85 | hsa-miR-211-5p | 7.9085317 | MIMAT0000268 |
| 86 | hsa-miR-4728-3p | 7.90797 | MIMAT0019850 |
| 87 | hsa-miR-518e-5p | 7.9050035 | MIMAT0005450 |
| 88 | hsa-miR-650 | 7.900557 | MIMAT0003320 |
| 89 | hsa-miR-370 | 7.897305 | MIMAT0000722 |
| 90 | hsa-miR-4433-3p | 7.896072 | MIMAT0018949 |
| 91 | hsa-miR-6075 | 7.896021 | MIMAT0023700 |
| 92 | hsa-miR-33a-5p | 7.895879 | MIMAT0000091 |
| 93 | hsa-miR-664a-5p | 7.8958526 | MIMAT0005948 |
| 94 | hsa-miR-4695-5p | 7.8933973 | MIMAT0019788 |
| 95 | hsa-miR-2276 | 7.8887444 | MIMAT0011775 |
| 96 | hsa-miR-4734 | 7.8881354 | MIMAT0019859 |
| 97 | hsa-miR-6069 | 7.8876023 | MIMAT0023694 |
| 98 | hsa-miR-214-3p | 7.8817987 | MIMAT0000271 |
| 99 | hsa-miR-4417 | 7.881361 | MIMAT0018929 |
| 100 | hsa-miR-330-3p | 7.861473 | MIMAT0000751 |

**APPENDIX D:** Down-regulated miRNAs in multiple myeloma compared to the normal controls by ≥2.0 fold change at $p<0.05$ (negative in fold change indicates down-regulation)

| No | systematic name | Fold Change (Multiple Myeloma vs Normal) | mirbase accession No |
|---|---|---|---|
| 1 | hsa-miR-342-5p | -9.184753 | MIMAT0004694 |
| 2 | hsa-miR-151a-3p | -5.3997445 | MIMAT0000757 |
| 3 | hsa-miR-361-3p | -4.302395 | MIMAT0004682 |
| 4 | hsa-miR-4298 | -3.877203 | MIMAT0016852 |
| 5 | hsa-miR-150-5p | -3.5215795 | MIMAT0000451 |
| 6 | hsa-miR-199a-5p | -3.4764502 | MIMAT0000231 |
| 7 | hsa-miR-374a-5p | -2.9588528 | MIMAT0000727 |
| 8 | hsa-miR-342-3p | -2.8622978 | MIMAT0000753 |

**APPENDIX E:** Significant dysregulated miRNAs and their predicted differentially expressed targets. Top 100 down-regulated and up-regulated miRNAs are indicated in red and blue, respectively

| miRNA-targets | Dyregulated microRNA |
|---|---|
| *CKAP2L* | MIMAT0019718,MIMAT0015052,MIMAT0016873,MIMAT0004693,MIMAT0018940,MIMAT0016876,MIMAT0019795,MIMAT0009447,MIMAT0019796,MIMAT0004910,MIMAT0016902,MIMAT0004912,MIMAT0015057,MIMAT0004185,MIMAT0003337,MIMAT0005953,MIMAT0018069,MIMAT0019057,MIMAT0019980,MIMAT0019884,MIMAT0019710,MIMAT0019713,MIMAT0019712,MIMAT0015065,MIMAT0015064,MIMAT0018082,MIMAT0015063,MIMAT0000264,MIMAT0015060,MIMAT0016865,MIMAT0004907,MIMAT0018954,MIMAT0016912,MIMAT0018122,MIMAT0015069,MIMAT0016914,MIMAT0018120,MIMAT0003887,MIMAT0019977,MIMAT0019067,MIMAT0000269,MIMAT0019720,MIMAT0018078,MIMAT0016869,MIMAT0017985,MIMAT0018075,MIMAT0019920,MIMAT0018447,MIMAT0019202,MIMAT0019922,MIMAT0000318,MIMAT0016891,MIMAT0005935,MIMAT0016921,MIMAT0019076,MIMAT0003290,MIMAT0018928,MIMAT0000762,MIMAT0019784,MIMAT0015081,MIMAT0005895,MIMAT0003225,MIMAT0018354,MIMAT0019911,MIMAT0003223,MIMAT0019789,MIMAT0001639,MIMAT0019004,MIMAT0019785,MIMAT0000102,MIMAT0019704,MIMAT0019917,MIMAT0019854,MIMAT0007888,MIMAT0015004,MIMAT0018935,MIMAT0018981,MIMAT0004953,MIMAT0019943,MIMAT0016845,MIMAT0019013,MIMAT0018989,MIMAT0005882,MIMAT0018988,MIMAT0002178,MIMAT0003238,MIMAT0019948,MIMAT0005889,MIMAT0019210,MIMAT0004812,MIMAT0020300,MIMAT0015019,MIMAT0019763,MIMAT0019832,MIMAT0019833,MIMAT0019767,MIMAT0005928,MIMAT0018990,MIMAT0015023,MIMAT0005875,MIMAT0016856,MIMAT0005874,MIMAT0019023,MIMAT0003243,MIMAT0000617,MIMAT0000756,MIMAT0018997,MIMAT0005828,MIMAT0019692,MIMAT0019220,MIMAT0002808,MIMAT0004803,MIMAT0019697,MIMAT0004802,MIMAT0019839,MIMAT0004807,MIMAT0017392,MIMAT0018084,MIMAT0018083,MIMAT0019735,MIMAT0019823,MIMAT0018199,MIMAT0018194,MIMAT0002878,MIMAT0019960,MIMAT0019732,MIMAT0003251,MIMAT0015039,MIMAT0018196,MIMAT0003307,MIMAT0014998,MIMAT0019968,MIMAT0003259,MIMAT0000721,MIMAT0005863,MIMAT0019233,MIMAT0014991,MIMAT0018969,MIMAT0017995,MIMAT0017992,MIMAT0000422,MIMAT0003300,MIMAT0005592,MIMAT0000426,MIMAT0019236,MIMAT0019811,MIMAT0019743,MIMAT0019048,MIMAT0014987,MIMAT0000730,MIMAT0004797,MIMAT0004798,MIMAT0019891,MIMAT0018114,MIMAT0005795,MIMAT0001536 |

| miRNA-targets | Dyregulated microRNA |
|---|---|
| *ASPM* | MIMAT0018083,MIMAT0019841,MIMAT0003251,MIMAT0005916,MIMAT0004676,MIMAT0001627,MIMAT0019803,MIMAT0005934,MIMAT0003393,MIMAT0017990,MIMAT0003270,MIMAT0018065,MIMAT0015065,MIMAT0015009,MIMAT0016860,MIMAT0005895,MIMAT0019741,MIMAT0000737,MIMAT0005874,MIMAT0000735,MIMAT0014981,MIMAT0004921,MIMAT0005941,MIMAT0004793,MIMAT0003285,MIMAT0002881 |
| *PCOLCE2* | MIMAT0019900,MIMAT0000271,MIMAT0019790,MIMAT0000081,MIMAT0000682,MIMAT0016903,MIMAT0003335,MIMAT0003232,MIMAT0019055,MIMAT0003275,MIMAT0011777,MIMAT0002170,MIMAT0019197,MIMAT0000719,MIMAT0000090,MIMAT0018081,MIMAT0000092,MIMAT0019760,MIMAT0019931,MIMAT0019065,MIMAT0019692,MIMAT0019976,MIMAT0003285,MIMAT0002805,MIMAT0019872,MIMAT0004773,MIMAT0019972,MIMAT0019225,MIMAT0004801,MIMAT0006778,MIMAT0002880,MIMAT0017984,MIMAT0017985,MIMAT0002883,MIMAT0017988,MIMAT0019877,MIMAT0005920,MIMAT0010364,MIMAT0016896,MIMAT0019039,MIMAT0016925,MIMAT0014998,MIMAT0019779,MIMAT0003312,MIMAT0018967,MIMAT0000720,MIMAT0019030,MIMAT0017999,MIMAT0019079,MIMAT0019230,MIMAT0000460,MIMAT0018200,MIMAT0002872,MIMAT0003218,MIMAT0019862,MIMAT0018092,MIMAT0000242,MIMAT0018933,MIMAT0015046,MIMAT0003161,MIMAT0002868,MIMAT0019812,MIMAT0016887,MIMAT0019746,MIMAT0000432,MIMAT0019048,MIMAT0000735,MIMAT0015088,MIMAT0019787,MIMAT0019004,MIMAT0000730,MIMAT0004922,MIMAT0011158,MIMAT0001630,MIMAT0018191,MIMAT0018192,MIMAT0018114 |
| *SHCBP1* | MIMAT0000274,MIMAT0019790,MIMAT0016876,MIMAT0018942,MIMAT0019792,MIMAT0018944,MIMAT0019797,MIMAT0001625,MIMAT0019803,MIMAT0004910,MIMAT0004692,MIMAT0019801,MIMAT0019054,MIMAT0003339,MIMAT0000715,MIMAT0019056,MIMAT0019909,MIMAT0002856,MIMAT0000717,MIMAT0000718,MIMAT0006764,MIMAT0018080,MIMAT0004983,MIMAT0004986,MIMAT0016863,MIMAT0000265,MIMAT0004907,MIMAT0018953,MIMAT0010251,MIMAT0003887,MIMAT0019069,MIMAT0003882,MIMAT0003287,MIMAT0000268,MIMAT0018078,MIMAT0000510,MIMAT0018957,MIMAT0017983,MIMAT0002843,MIMAT0002846,MIMAT0015072,MIMAT0004972,MIMAT0003215,MIMAT0000318,MIMAT0003311,MIMAT0016926,MIMAT0019776,MIMAT0005931,MIMAT0003393,MIMAT0019860,MIMAT0005930,MIMAT0019079,MIMAT0003315,MIMAT0003295,MIMAT0003292,MIMAT0002834,MIMAT0000242,MIMAT0004960,MIMAT0000074,MIMAT0018930,MIMAT0005897,MIMAT0018353,MIMAT0015085,MIMAT0000241,MIMAT0019787,MIMAT0003329,MIMAT0000101,MIMAT0015001,MIMAT0002826,MIMAT0015003,MIMAT0002825,MIMAT0002822,MIMAT0018937,MIMAT0018936,MIMAT0019851,MIMAT0019840,MIMAT0019756,MIMAT0013863, |

| miRNA-targets | Dyregulated microRNA |
|---|---|
| *SHCBP1* | MIMAT0005917,MIMAT0003948,MIMAT0000684,MIMAT0019941,MIMAT0018989,MIMAT0004765,MIMAT0004957,MIMAT0003238,MIMAT0019831,MIMAT0019029,MIMAT0000091,MIMAT0003248,MIMAT0005873,MIMAT0000617,MIMAT0019931,MIMAT0004948,MIMAT0005828,MIMAT0004774,MIMAT0005827,MIMAT0004775,MIMAT0005829,MIMAT0004777,MIMAT0004772,MIMAT0004801,MIMAT0019837,MIMAT0019362,MIMAT0005583,MIMAT0003150,MIMAT0019730,MIMAT0015037,MIMAT0000421,MIMAT0018195,MIMAT0000724,MIMAT0004677,MIMAT0003252,MIMAT0000726,MIMAT0019968,MIMAT0005863,MIMAT0019232,MIMAT0017997,MIMAT0019230,MIMAT0018969,MIMAT0017995,MIMAT0017990,MIMAT0005593,MIMAT0003301,MIMAT0013517,MIMAT0018200,MIMAT0018090,MIMAT0018106,MIMAT0002870,MIMAT0009451,MIMAT0018095,MIMAT0018094,MIMAT0019746,MIMAT0003260,MIMAT0005903,MIMAT0003265,MIMAT0019046,MIMAT0019047,MIMAT0003165,MIMAT0005791,MIMAT0005792,MIMAT0019897,MIMAT0019898,MIMAT0014982,MIMAT0019895,MIMAT0004799,MIMAT0018116,MIMAT0019819,MIMAT0005793,MIMAT0005794,MIMAT0019818,MIMAT0001536 |
| *NUF2* | MIMAT0018941,MIMAT0005917,MIMAT0005915,MIMAT0019795,MIMAT0004916,MIMAT0004692,MIMAT0018989,MIMAT0000089,MIMAT0003232,MIMAT0004185,MIMAT0004762,MIMAT0003274,MIMAT0003275,MIMAT0019907,MIMAT0018990,MIMAT0018954,MIMAT0000755,MIMAT0005874,MIMAT0019931,MIMAT0003241,MIMAT0019976,MIMAT0019222,MIMAT0004801,MIMAT0004987,MIMAT0016898,MIMAT0019736,MIMAT0003251,MIMAT0019038,MIMAT0003311,MIMAT0019961,MIMAT0019777,MIMAT0017997,MIMAT0018969,MIMAT0019076,MIMAT0000460,MIMAT0019709,MIMAT0015081,MIMAT0005895,MIMAT0019911,MIMAT0000735,MIMAT0003323,MIMAT0019955,MIMAT0019004,MIMAT0019785,MIMAT0014983,MIMAT0019819,MIMAT0018938,MIMAT0009978 |
| *RAD54L* | MIMAT0015037,MIMAT0019820,MIMAT0004605,MIMAT0018193,MIMAT0004692,MIMAT0016902,MIMAT0005881,MIMAT0019233,MIMAT0004766,MIMAT0005573,MIMAT0003339,MIMAT0002176,MIMAT0002835,MIMAT0017991,MIMAT0018200,MIMAT0018090,MIMAT0004780,MIMAT0019811,MIMAT0003225,MIMAT0005900,MIMAT0005872,MIMAT0018997,MIMAT0004777,MIMAT0019895,MIMAT0018110,MIMAT0000451,MIMAT0018192,MIMAT0007887 |
| *CTNNAL1* | MIMAT0019900,MIMAT0015037,MIMAT0016877,MIMAT0003311,MIMAT0016905,MIMAT0001627,MIMAT0004692,MIMAT0019801,MIMAT0005934,MIMAT0015057,MIMAT0016926,MIMAT0011778,MIMAT0017997,MIMAT0017991,MIMAT0002838,MIMAT0019926,MIMAT0002833,MIMAT0019830,MIMAT0019911,MIMAT0018182,MIMAT0000738,MIMAT0018358,MIMAT0016912,MIMAT0003244,MIMAT0003242,MIMAT0004777,MIMAT0003285,MIMAT0014983,MIMAT0019917,MIMAT0019918,MIMAT0019851 |

| miRNA-targets | Dyregulated microRNA |
|---|---|
| *CCNA2* | MIMAT0019718,MIMAT0004693,MIMAT0018942,MIMAT0000275,MIMAT0000276,MIMAT0019796,MIMAT0004916,MIMAT0003331,MIMAT0019798,MIMAT0004692,MIMAT0004912,MIMAT0019983,MIMAT0003275,MIMAT0011777,MIMAT0019884,MIMAT0007402,MIMAT0018065,MIMAT0019906,MIMAT0002859,MIMAT0018951,MIMAT0015065,MIMAT0018081,MIMAT0015062,MIMAT0000265,MIMAT0016919,MIMAT0015060,MIMAT0018954,MIMAT0004903,MIMAT0016912,MIMAT0015069,MIMAT0010251,MIMAT0019065,MIMAT0019977,MIMAT0003285,MIMAT0019067,MIMAT0000451,MIMAT0000268,MIMAT0019873,MIMAT0018074,MIMAT0001075,MIMAT0019725,MIMAT0019204,MIMAT0018447,MIMAT0018445,MIMAT0000318,MIMAT0019779,MIMAT0003311,MIMAT0016923,MIMAT0005935,MIMAT0005934,MIMAT0003310,MIMAT0003299,MIMAT0005930,MIMAT0019079,MIMAT0019076,MIMAT0018928,MIMAT0019865,MIMAT0000242,MIMAT0019689,MIMAT0005892,MIMAT0005894,MIMAT0015081,MIMAT0005895,MIMAT0018354,MIMAT0003225,MIMAT0015085,MIMAT0016883,MIMAT0003223,MIMAT0003323,MIMAT0005891,MIMAT0000102,MIMAT0019702,MIMAT0019916,MIMAT0018938,MIMAT0019842,MIMAT0005880,MIMAT0015016,MIMAT0005911,MIMAT0005912,MIMAT0015012,MIMAT0005916,MIMAT0019945,MIMAT0003235,MIMAT0014979,MIMAT0005887,MIMAT0019013,MIMAT0018988,MIMAT0019751,MIMAT0002814,MIMAT0002171,MIMAT0002817,MIMAT0004812,MIMAT0002890,MIMAT0019763,MIMAT0019832,MIMAT0019769,MIMAT0019833,MIMAT0018990,MIMAT0005928,MIMAT0018165,MIMAT0016856,MIMAT0005875,MIMAT0015021,MIMAT0005874,MIMAT0019761,MIMAT0000756,MIMAT0000617,MIMAT0005872,MIMAT0019931,MIMAT0004947,MIMAT0005827,MIMAT0004777,MIMAT0004949,MIMAT0004801,MIMAT0019224,MIMAT0004803,MIMAT0002880,MIMAT0005921,MIMAT0019361,MIMAT0019825,MIMAT0018083,MIMAT0015037,MIMAT0000727,MIMAT0019731,MIMAT0003306,MIMAT0018196,MIMAT0003251,MIMAT0003307,MIMAT0003255,MIMAT0018963,MIMAT0000721,MIMAT0010133,MIMAT0017997,MIMAT0019230,MIMAT0013517,MIMAT0005591,MIMAT0005592,MIMAT0005459,MIMAT0005457,MIMAT0001532,MIMAT0018094,MIMAT0019746,MIMAT0019743,MIMAT0018099,MIMAT0019742,MIMAT0000736,MIMAT0014987,MIMAT0003165,MIMAT0015041,MIMAT0014981,MIMAT0004923,MIMAT0004798,MIMAT0004799,MIMAT0018114,MIMAT0018190,MIMAT0018113,MIMAT0005795,MIMAT0000437,MIMAT0001536 |

| miRNA-targets | Dyregulated microRNA |
|---|---|
| *CYSLTR2* | MIMAT0015052,MIMAT0000274,MIMAT0018070,MIMAT0004693,MIMAT0000275,MIMAT0003330,MIMAT0016900,MIMAT0003337,MIMAT0019053,MIMAT0005953,MIMAT0019882,MIMAT0019057,MIMAT0019980,MIMAT0018065,MIMAT0015065,MIMAT0019727,MIMAT0019729,MIMAT0015063,MIMAT0015060,MIMAT0016917,MIMAT0016912,MIMAT0019072,MIMAT0019070,MIMAT0015066,MIMAT0003887,MIMAT0019977,MIMAT0018078,MIMAT0019204,MIMAT0004970,MIMAT0015072,MIMAT0004975,MIMAT0018445,MIMAT0019083,MIMAT0019200,MIMAT0005935,MIMAT0019201,MIMAT0016921,MIMAT0004979,MIMAT0000762,MIMAT0019709,MIMAT0004960,MIMAT0015087,MIMAT0018354,MIMAT0003223,MIMAT0019859,MIMAT0000241,MIMAT0003324,MIMAT0003321,MIMAT0005941,MIMAT0000771,MIMAT0019856,MIMAT0019854,MIMAT0019853,MIMAT0015016,MIMAT0005918,MIMAT0005916,MIMAT0016848,MIMAT0016846,MIMAT0004957,MIMAT0003238,MIMAT0004812,MIMAT0015019,MIMAT0010357,MIMAT0005924,MIMAT0005925,MIMAT0015025,MIMAT0005928,MIMAT0015023,MIMAT0003246,MIMAT0000753,MIMAT0003244,MIMAT0003243,MIMAT0000756,MIMAT0005828,MIMAT0005829,MIMAT0016853,MIMAT0016855,MIMAT0019699,MIMAT0004800,MIMAT0004803,MIMAT0004807,MIMAT0017392,MIMAT0015037,MIMAT0003251,MIMAT0015031,MIMAT0010133,MIMAT0004679,MIMAT0000423,MIMAT0002870,MIMAT0015046,MIMAT0005905,MIMAT0000736,MIMAT0005908,MIMAT0004920,MIMAT0019897,MIMAT0019895,MIMAT0019891,MIMAT0018119,MIMAT0018118,MIMAT0019900,MIMAT0018940,MIMAT0016870,MIMAT0018941,MIMAT0018942,MIMAT0019793,MIMAT0019794,MIMAT0019797,MIMAT0019796,MIMAT0004910,MIMAT0019802,MIMAT0002853,MIMAT0018949,MIMAT0018948,MIMAT0000441,MIMAT0018950,MIMAT0016864,MIMAT0001413,MIMAT0007348,MIMAT0004903,MIMAT0003289,MIMAT0000451,MIMAT0018959,MIMAT0018957,MIMAT0017985,MIMAT0001075,MIMAT0019920,MIMAT0019772,MIMAT0019921,MIMAT0019776,MIMAT0003291,MIMAT0019928,MIMAT0018928,MIMAT0003292,MIMAT0019784,MIMAT0019001,MIMAT0005895,MIMAT0019781,MIMAT0019780,MIMAT0005896,MIMAT0018930,MIMAT0016884,MIMAT0000075,MIMAT0000070,MIMAT0019004,MIMAT0019787,MIMAT0005890,MIMAT0019785,MIMAT0002829,MIMAT0019914,MIMAT0002827,MIMAT0015003,MIMAT0019916,MIMAT0007888,MIMAT0009978,MIMAT0005880,MIMAT0019844,MIMAT0019845,MIMAT0019013,MIMAT0000680,MIMAT0014978,MIMAT0000089,MIMAT0004766,MIMAT0019948,MIMAT0019210,MIMAT0002817,MIMAT0019214,MIMAT0019213,MIMAT0019217,MIMAT0019029,MIMAT0000091,MIMAT0019833,MIMAT0019769,MIMAT0018165,MIMAT0000093,MIMAT0018164,MIMAT0005875,MIMAT0005874,MIMAT0019021,MIMAT0019023,MIMAT0019931,MIMAT0005872,MIMAT0019939,MIMAT0019938,MIMAT0019838,MIMAT0002807,MIMAT0019824,MIMAT0003308,MIMAT0019734,MIMAT0019822, |

| miRNA-targets | Dyregulated microRNA |
|---|---|
| *CYSLTR2* | MIMAT0019736,MIMAT0018194,MIMAT0019730,MIMAT0019820,MIMAT0019821,MIMAT0003306,MIMAT0011162,MIMAT0019031,MIMAT0019966,MIMAT0019030,MIMAT0005869,MIMAT0019233,MIMAT0019232,MIMAT0014991,MIMAT0019230,MIMAT0017995,MIMAT0017993,MIMAT0003301,MIMAT0005593,MIMAT0018090,MIMAT0019812,MIMAT0018188,MIMAT0018187,MIMAT0019743,MIMAT0019744,MIMAT0011156,MIMAT0003164,MIMAT0019959,MIMAT0019050,MIMAT0011158,MIMAT0014984,MIMAT0018979,MIMAT000478 |
| *RASGRF2* | MIMAT0016870,MIMAT0004693,MIMAT0005911,MIMAT0004810,MIMAT0004764,MIMAT0019053,MIMAT0019212,MIMAT0019055,MIMAT0005577,MIMAT0019057,MIMAT0019198,MIMAT0019982,MIMAT0000441,MIMAT0002859,MIMAT0010357,MIMAT0019831,MIMAT0018081,MIMAT0000265,MIMAT0019767,MIMAT0016912,MIMAT0005872,MIMAT0000756,MIMAT0019070,MIMAT0003241,MIMAT0019065,MIMAT0019976,MIMAT0019972,MIMAT0000451,MIMAT0019224,MIMAT0020603,MIMAT0000268,MIMAT0019227,MIMAT0002882,MIMAT0005580,MIMAT0005920,MIMAT0019920,MIMAT0018083,MIMAT0019825,MIMAT0019820,MIMAT0019209,MIMAT0015039,MIMAT0016925,MIMAT0003253,MIMAT0019777,MIMAT0000722,MIMAT0019030,MIMAT0000423,MIMAT0003291,MIMAT0005459,MIMAT0004780,MIMAT0003292,MIMAT0018184,MIMAT0004613,MIMAT0018353,MIMAT0019708,MIMAT0019810,MIMAT0000735,MIMAT0015043,MIMAT0015041,MIMAT0019895,MIMAT0019856,MIMAT0019890,MIMAT0009978,MIMAT0000437 |
| *HKDC1* | MIMAT0019718,MIMAT0019793,MIMAT0016877,MIMAT0018944,MIMAT0019795,MIMAT0018945,MIMAT0016903,MIMAT0007892,MIMAT0019055,MIMAT0011777,MIMAT0019884,MIMAT0018065,MIMAT0003271,MIMAT0002858,MIMAT0019904,MIMAT0006764,MIMAT0000261,MIMAT0018952,MIMAT0016861,MIMAT0015063,MIMAT0016919,MIMAT0016866,MIMAT0010313,MIMAT0016912,MIMAT0016914,MIMAT0019872,MIMAT0003881,MIMAT0019870,MIMAT0000510,MIMAT0020601,MIMAT0018074,MIMAT0001075,MIMAT0019203,MIMAT0019208,MIMAT0019923,MIMAT0015078,MIMAT0019927,MIMAT0015378,MIMAT0005894,MIMAT0019782,MIMAT0016888,MIMAT0003225,MIMAT0019912,MIMAT0019005,MIMAT0019004,MIMAT0003328,MIMAT0002826,MIMAT0007885,MIMAT0019917,MIMAT0005880,MIMAT0015015,MIMAT0019846,MIMAT0019847,MIMAT0003948,MIMAT0018981,MIMAT0005884,MIMAT0000089,MIMAT0018988,MIMAT0004763,MIMAT0003238,MIMAT0019358,MIMAT0019357,MIMAT0019217,MIMAT0019830,MIMAT0019027,MIMAT0019834,MIMAT0015021,MIMAT0000754,MIMAT0000752,MIMAT0000758,MIMAT0019023,MIMAT0019931,MIMAT0019760,MIMAT0005878,MIMAT0019220,MIMAT0004773,MIMAT0019938,MIMAT0019363,MIMAT0019224,MIMAT0019837,MIMAT0019839,MIMAT0002806,MIMAT0004802,MIMAT0005920,MIMAT0019361,MIMAT0019824,MIMAT0018083,MIMAT0019823,MIMAT0019039,MIMAT0000728,MIMAT0018196,MIMAT0011162, |

| miRNA-targets | Dyregulated microRNA |
|---|---|
| *HKDC1* | MIMAT0019961,MIMAT0019033,MIMAT0005865,MIMAT0015031,MIMAT0019966,MIMAT0014991,MIMAT0010133,MIMAT0017995,MIMAT0018006,MIMAT0018004,MIMAT0019236,MIMAT0000428,MIMAT0005457,MIMAT0019746,MIMAT0015045,MIMAT0002867,MIMAT0000735,MIMAT0003264,MIMAT0015042,MIMAT0004922,MIMAT0004924,MIMAT0005791,MIMAT0005792,MIMAT0014985,MIMAT0014983,MIMAT0004799,MIMAT0019891,MIMAT0018113,MIMAT0018190,MIMAT0019816,MIMAT0005793,MIMAT0019815,MIMAT0019818 |